Coordination of neuronal proliferation and migration during corticogenesis : role of p27kip1

Élodie Gautier

▶ **To cite this version:**

Élodie Gautier. Coordination of neuronal proliferation and migration during corticogenesis : role of p27kip1. Neurons and Cognition [q-bio.NC]. Université Claude Bernard - Lyon I, 2011. English. ⟨NNT : 2011LYO10283⟩. ⟨tel-01127593⟩

HAL Id: tel-01127593

https://theses.hal.science/tel-01127593v1

Submitted on 7 Mar 2015

HAL is a multi-disciplinary open access archive for the deposit and dissemination of scientific research documents, whether they are published or not. The documents may come from teaching and research institutions in France or abroad, or from public or private research centers.

L'archive ouverte pluridisciplinaire **HAL**, est destinée au dépôt et à la diffusion de documents scientifiques de niveau recherche, publiés ou non, émanant des établissements d'enseignement et de recherche français ou étrangers, des laboratoires publics ou privés.

HAL Authorization

N° d'ordre 283- 2011 Année 2011

THESE DE L'UNIVERSITE DE LYON

Délivrée par

L'UNIVERSITE CLAUDE BERNARD LYON 1

ECOLE DOCTORALE
Biologie Moléculaire Intégrative et Cellulaire

DIPLOME DE DOCTORAT

(arrêté du 7 août 2006)

soutenue publiquement le 9 décembre 2011

par

M^{elle} GAUTIER Elodie

Coordination of neuronal proliferation and migration during corticogenesis: role of p27^{kip1}

Directeur de thèse: Dr DEHAY Colette

JURY: Dr. GAREL Sonia
Dr. MOLNAR Zoltan
Dr. NGUYEN Laurent
Dr. KENNEDY Henry
Dr. DEHAY Colette
Pr. GILLET Germain (Président du jury)

RESUME en français

Au cours du développement du néocortex, les précurseurs neuronaux prolifèrent dans les zones germinales bordant les ventricules. Les neurones post-mitotiques migrent ensuite radialement vers la surface du cortex. Par vagues successives, ils se positionnent dans la plaque corticale pour former six couches corticales. La cytoarchitecture du néocortex repose sur la coordination spatiotemporelle de deux processus: la production d'un nombre approprié de neurones -via la régulation du cycle cellulaire- et leur migration radiale.

La première partie de cette thèse caractérise la dynamique de migration radiale dans des aires présentant des taux de production neuronale différents: les aires visuelles adjacentes 17 et 18 du primate. Les couches supragranulaires de l'aire 17 sont plus développées que celles de l'aire 18, différence due à un taux de prolifération et de production neuronale plus élevés dans l'aire 17 aux stades embryonnaires E77-80 (Lukaszewicz et al., 2005). La cinétique de la migration radiale a été étudiée sur des neurones exprimant l'EGFP, après électroporation ex vivo et enregistrements en vidéomicroscopie bi-photonique sur des tranches organotypiques maintenues en culture jusqu'à 15 jours. La vitesse de migration est plus élevée dans l'aire 17 que dans l'aire 18, indiquant une congruence entre les variations aire-spécifiques des taux de prolifération et de migration neuronale.

La deuxième partie concerne l'étude des mécanismes cellulaires et moléculaires qui sous-tendent la régulation coordonnée de la prolifération et de la migration. La protéine $p27^{kip1}$est susceptible de jouer un rôle important puisque ce régulateur de la progression du cycle cellulaire promeut aussi la migration cellulaire et neuronale (Besson et al., 2004b; Nguyen et al., 2006a). Dans le cytoplasme, le domaine C-terminal de $p27^{kip1}$ inhibe la GTPase RhoA, induisant des modifications du cytosquelette d'actine. Cette double fonction prend toute son importance pendant la prolifération des précurseurs de la zone ventriculaire, dont les noyaux effectuent un mouvement stéréotypé de migration intercinétique (INM), synchronisé avec les phases du cycle cellulaire. Différentes formes mutantes de $p27^{kip1}$ ou des shRNA ont été électroporés dans des embryons murins à E14-15, pour modifier le niveau d'expression de $p27^{kip1}$ spécifiquement dans les neuroblastes. Sur des tranches organotypiques de cortex, des observations en vidéomicroscopie bi-photonique ont permis d'observer les divisions successives de différents types de précurseurs, la cinétique de l'INM et de la migration radiale des neurones produits. $p27^{kip1}$ affecte l'INM, promeut les divisions différenciatives et la migration radiale des neurones, via son domaine C-terminal.

$p27^{kip1}$ se place donc au sein d'un réseau d'acteurs moléculaires contrôlant conjointement, et de façon aire-spécifique, les cycles successifs de divisions des précurseurs corticaux, ainsi que le comportement migratoire des neurones qui en sont issus.

TITRE en anglais

Coordination of neuronal proliferation and migration during corticogenesis: role of $p27^{kip1}$

RESUME en anglais

During corticogenesis, neuronal precursors proliferate in the germinal zones lining lateral ventricules. Post-mitotic neurons then migrate radially towards the cortical surface. Through successive waves, they settle in the cortical plate to form the future 6-layered cortex. Cortical cytoarchitecture relies on the spatiotemporal coordination of neuronal production rate, cell-cycle control and neuronal radial migration.

In the first part of this PhD project, variations in the neuronal migration dynamics were characterized in cerebral areas displaying different rates of neuronal production: the adjacent visual areas 17 and 18 in the primate. In area 17, supragranular layers are more developed than in area 18, due to a higher proliferation and neuronal production rates in area 17 between E77-80 (Lukaszewicz et al., 2005). Radial migration kinetics of EGFP expressing neurons was recorded through two-photon videomicroscopy, after ex vivo electroporation and on organotypic slices maintained up to 15 days in culture. Migration velocity is higher in area 17 than 18, indicating that area-specific variations of proliferation and migration rates are congruent during corticogenesis.

The second part focused on the molecular mechanisms underlying the coordinated regulation of proliferation and migration. $p27^{kip1}$ is a candidate protein, as this cell-cycle regulator also promotes cellular and neuronal migration (Besson et al., 2004b; Nguyen et al., 2006a). In the cytoplasm, $p27^{kip1}$ C-terminal domain inhibits RhoA GTPase, leading to modifications of the actin cytoskeleton. This dual function could play a major role during the proliferation of the ventricular zone precursors cells, whose nuclei undergo a stereotyped Interkinetic Nuclear Migration (INM), synchronized with the cell-cycle phases. Several mutant forms of $p27^{kip1}$ or shRNA were electroporated in mice embryos at E14-15, in order to modify $p27^{kip1}$ expression level specifically into neuroblasts. Two-photon videomicroscopy recordings were performed on cortical organotypic slices, in order to observe successive divisions of different types of progenitors, the INM kinetics, as well as the radial migration dynamics of produced neurons. $p27^{kip1}$ affects INM, promotes differentiative divisions and neuronal radial migration, through its C-terminal domain.

$p27^{kip1}$ is thus part of a molecular network finely tuning the successive rounds of divisions of precursor cells, as well as the migratory behaviour of the newly born neurons.

DISCIPLINE

Biologie Moléculaire Intégrative et Cellulaire

MOTS-CLES

Corticogénèse, $p27^{kip1}$, primate, prolifération, migration radiale, Migration Nucléaire Intercinétique, couplage, RhoA

KEYWORDS

Corticogenesis, $p27^{kip1}$, primate, proliferation, radial migration, Interkinetic Nuclear Migration (INM), coupling, RhoA

INTITULE ET ADRESSE DE L'U.F.R. OU DU LABORATOIRE:

Unité INSERM U846,
Institut Cellule Souche et Cerveau
18 avenue du Doyen Lépine
69500 Bron

Work from this thesis has been presented in international meetings:

Poster presentations:

Gautier E, Cortay V, Betizeau M, Doerflinger N, Patti D, Kennedy H, Dehay C. *Area-specific dynamics of proliferation and migration during primate corticogenesis: role of the modular protein p27^{kip1}.* 40th SFN (Society for Neuroscience) Meeting, San Diego, USA, 13-17 Nov 2010

Gautier E, Cortay V, Betizeau M, Doerflinger N, Patti D, Kennedy H, Dehay C. *Area-specific dynamics of proliferation and migration during primate corticogenesis: role of the modular protein p27^{kip1}.* ENP Stem Cells Meeting, Abbaye des Vaux de Cernay, France, 17-19 June 2010

Gautier E, Cortay V, Betizeau M, Doerflinger N, Kennedy H, Dehay C. *Area-specific dynamics of proliferation and migration during primate corticogenesis: role of the modular protein p27^{kip1}.* 18thISDN (International Society for Development Neuroscience) Meeting, Estoril, Portugal, 6-9 June 2010
*Best Abstract Award

Gautier E, Doerflinger N, Cortay V, Huissoud C, Giroud P, Berland M, Kennedy H, Dehay C. *Role of p27^{kip1} in modulating radial migration in the neocortex.* 38th SFN (Society for Neuroscience) Meeting, Washington DC, USA, 15-19 Nov 2008

Gautier E, Doerflinger N, Cortay V, Huissoud C, Giroud P, Berland M, Kennedy H, Dehay C. *Role of p27^{kip1} in modulating radial migration in the neocortex.* 6thFENS (Forum of European Neuroscience) Meeting, Geneva, Suisse, 12-16 July 2008

Oral presentations:

Gautier E, Dehay C. *Coordination of neuronal proliferation and migrationduring corticogenesis: role of p27^{kip}.*SECO Meeting, Capocaccia, Sardignia, 27 Apr – 7 May 2011

Gautier E, Dehay C. *Coordinated rates of proliferation and migration in primate area 17 and 18.*SECO Meeting, Capocaccia, Sardignia, 6-9 May 2010

Author in:

Pilaz LJ, Patti D, Marcy G, Ollier E, Pfister S, Douglas RJ, Betizeau M, Gautier E, Cortay V, Doerflinger N, Kennedy H, Dehay C (2009) *Forced G1-phase reduction alters mode of division, neuron number, and laminar phenotype in the cerebral cortex.* Proc Natl Acad Sci USA 106(51): 21924-21929
Two-photon time lapse experiment to demonstrate the transfection of a synchronous cohort of precursor cells. Participation to discussion.

Abbreviation List

A17: area 17
A18: area 18
AP: apical progenitor
BP: basal progenitor
BrdU: Bromodeoxyuridine
CKI: cyclin-dependent kinase inhibitor
Cont: control
CP: cortical plate
E: embryonic day
EGFP: enhanced green fluorescent protein
GOF: gain of function
GZ: germinal zone
DM: downmodulation
INM: interkinetic nuclear migration
IP: intermediate precursor
IZ: intermediate zone
MAP: microtubule associated protein
MiV: migration velocity
MoI: motility index
MTS: microtubules
NSC: neural stem cells
OSVZ: outer subventricular zone
PFA: paraformaldehyde
RGC: radial glial cell
SP: subplate
SVZ: subventricular zone
VZ: ventricular zone

Table of contents

Introduction 9

I. Mammalian corticogenesis: an overview 10

Mouse corticogenesis 10

Cortical progenitor types 11

a. Radial Glial Cells (RGCs) or Apical Progenitors (APs) 11

b. Intermediate Progenitor Cells (IPCs) or Basal Progenitors (BPs) 12

c. Distinct types of division for apical and basal progenitors 12

Primate specific features 14

a. Anatomical organization of the primate developing cortex 14

b. Specific features of primate OSVZ precursors 16

II. Migration of cycling progenitors and post-mitotic neurons ... 17

Interkinetic Nuclear Migration (INM) 17

a. INM discovery 17

b. INM kinetics 18

c. INM regulation 20

Passive nuclei displacement 21

INM regulation by the actin cytoskeleton 21

INM regulation by the microtubule cytoskeleton 22

General model of INM regulation 28

d. INM role in neurogenesis 30

Impact of INM on neurogenesis 30

Links between INM and cell-cycle progression 32

Neuronal radial migration 32

a. Distinct phases during radial migration 33

b. Morphological remodelling during saltatory locomotion 34

III. Integration of rates of proliferation, neuronal production and radial migration 36

Structure and regulation of the cell-cycle 36

Control of neuron number 38

Cell-fate and laminar determination 39

Area-specific rates of neuron production and areal differences in migration rates 39

IV. Proliferation and migration coupling by p27^{kip1} 41

p27^{kip1}: a modular protein with multiple roles 41

a. p27^{kip1}: a well described cell-cycle inhibitor 41

b. Spatiotemporal regulation of p27^{kip1} expression 42

c. Cytoplasmic p27^{kip1}: an alternative function in cell migration 43

Crosstalk between CKI and Rho-GTPases 45

a. The Rho-GTPases family 46

b. Rho-GTPases role in the regulation of cell migration 47

c. Rho-GTPases role in the regulation of cell proliferation 50

Rho-GTPases role in G1 phase progression 50

Rho-GTPases role in mitosis and cytokinesis 52

d. Modulation of the RhoA pathway by Cip/Kip proteins 54

p27^{kip1} diverse roles in the cerebral cortex 55

a. p27^{kip1} inhibits neuronal progenitors proliferation 56

b. p27^{kip1} promotes neuronal differentiation 56

c. p27^{kip1} promotes radial migration 57

Coupling of proliferation and migration during corticogenesis 60

Chapter 1: Coordinated rates of proliferation and migration in primate area 17 and area 18 62

Chapter 2: p27^{kip1} influences the dynamics of interkinetic nuclear migration and radial migration in the developing cortex 83

General Conclusion 141

References 144

Introduction

I. Mammalian corticogenesis: an overview

The cerebral cortex is a highly specialized brain region derived from the dorsal telencephalon, which is responsible for higher order cognitive functions in mammals.

The cerebral cortex is organized into six horizontal cellular layers and is regionally subdivided into specialized areas. Each layer contains neurons that share common features including gene expression, birth date, morphologies and patterns of connectivity (for a review see (Hevner et al., 2003; Rash and Grove, 2006). The laminar organization of the cerebral cortex arises as a consequence of the sequential birth (Caviness, 1982) and orderly migration of neurons produced in the cortical germinal zones [reviewed in (Gupta et al., 2002)].

Mouse corticogenesis

In the mouse, corticogenesis lasts from embryonic day 11 (E11) to E19 (Fig. 1). The telencephalic primordium is composed of neuroepithelial stem cells which are elongated bipolar cells that form a homogeneous pseudo-stratified 'germinal epithelium'. This neuroepithelium lines the third ventricule of the emerging telencephalic vesicle, and is thus named the ventricular zone (VZ) (Fig. 1). Early proliferation, through proliferative symmetric divisions, increases the pool of neuroepithelial cells, as well as the surface area and thickness of the VZ. The onset of neurogenesis at E11 (Garcia-Moreno et al., 2007) is marked by the switch to an asymmetric mode of division (Chenn and McConnell, 1995; Rakic, 1995), giving rise to one progenitor cell and one neuron (Noctor et al., 2001; Takahashi et al., 1995b). The first generated neurons settle in a narrow zone above the neuroepithelium, termed the preplate (PP) (Caviness, 1982) (Fig. 1). The preplate contains early-appearing Cajal–Retzius cells, GABAergic neurons and pioneer neurons which are generated outside the cortex (Meyer et al., 2000). At E12-E13, some dividing cells appear at the basal border of the VZ (Smart, 1973), creating a new proliferative compartment above the VZ, named the subventricular zone (SVZ) (Fig. 1). Precursors within the SVZ are randomly organized, contrasting with VZ compact radial organization. In the emerging neocortex, neurons generated after E13 settle in the middle of the preplate to form the cortical plate (CP), thereby splitting the preplate into an outer marginal zone (MZ) and an inner sub-plate (SP) (Caviness, 1982; Marin-Padilla, 1978) (Fig. 1). The subplate is a transient compartment where thalamocortical and corticocortical fibres are found ((Hoerder-Suabedissen et al., 2009; Wang et al., 2010), for a review see (Molnar et al., 2006)). As corticogenesis proceeds, newly glutamatergic generated postmitotic neurons migrate radially from the germinal compartments, through the SP, to settle in the CP (Fig. 1). Neuronal migration occurs according to an inside-out pattern, with later born neurons bypassing earlier born neurons

and settling in more superficial layers (Angevine and Sidman, 1961; Sidman and Rakic, 1973).The five layers derived from the CP together with the MZ constitute the six-layered neocortex. The earliest-born neurons occupy the deep layer 6, and the last-born neurons become the superficial layer 2 (MZ becomes layer 1).

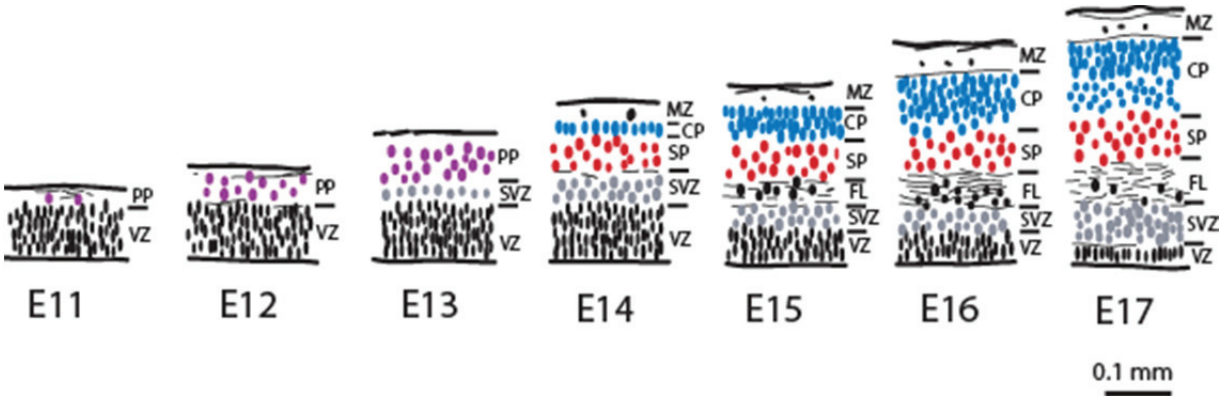

Fig. 1: Anatomical organization of the mouse embryonic cortex, during cortical neurogenesis that lasts 8 days. CP: cortical plate, FL: fibre layer, MZ: marginal zone, PP: preplate, SP: subplate, SVZ: subventricular zone, VZ: ventricular zone. Adapted from (Smart et al., 2002).

Cortical progenitor types

All pyramidal neurons of the mammalian neocortex derive, directly or indirectly, from two germinal zones (GZ), the ventricular zone (VZ) and the subventricular zone (SVZ). These two GZ contain two main types of precursors that differ in their morphology and proliferative features (Fig. 2).

a. Radial Glial Cells (RGCs) or Apical Progenitors (APs)

RGCs are derived from the original neuroepithelial (NE) cells, from which they inherit certain characteristic features. Both NE cells and RGCs undergo mitosis at the ventricular (apical) border of the VZ, and are named "apical progenitors» (APs). Like NE cells, RGCs exhibited a very elongated morphology, with a ‘‘pearl-on-a string’’ shape. They have two extremely thin radial processes (Rakic, 1988) and exhibit apical–basal polarity, with an apical end-foot at the ventricular surface and a basal end-foot at the basal lamina of the pia (Gotz and Huttner, 2005; Huttner and Brand, 1997; Miyata, 2008) (Fig. 2). The apical and basal plasma membranes constitute only a minor proportion of the cell surface [reviewed in (Farkas and Huttner, 2008)]. APs nevertheless exhibit a clear polarity with localized concentration of various transmembrane proteins, cell polarity proteins, tight junctions and adherens junctions at the apical pole, and receptors for constituents of the basal lamina at the basal pole [reviewed in (Gotz and Barde, 2005; Gotz and Huttner, 2005)]. An important subcellular component found in the apical end-foot is the centrosome, crucial for mitosis at

the apical border. Of note, the basal process maintains its contact with the pia and hence lengthens concomitant with the thickening of the neuronal layers. The very long processes of RGCs, spanning the entire cortical wall, have led RGCs to be considered for many years as a major scaffold for neuronal radial migration (Rakic, 1971). Later, RGCs have been shown to be the early precursors of both neurons and glial cells (Malatesta et al., 2000; Noctor et al., 2001). Despite their extremely elongated morphology, RGCs cell bodies are restricted to the VZ (Heins et al., 2002; Miyata et al., 2004; Noctor et al., 2001). Their nuclei perform a characteristic cell-cycle-dependent up and down movement, called interkinetic nuclear migration (INM) (Sauer, 1935; Takahashi et al., 1993). RGCs undergo S phase with their nuclei at the basal side of the VZ and M phase at the apical side. INM will be described more in detail p17. Virtually all APs are positive for Pax6, a transcription factor specifically expressed by neuroepithelial and radial glial cells and involved in their proliferation and neurogenesis (Gotz et al., 1998; Sansom et al., 2009).

Besides RGCs, a second type of APs: the short neural precursors (SNPs) have also been described. SNPs possess a ventricular end-foot and a basal process of variable length that is retracted during mitotic division (Gal et al., 2006; Stancik et al., 2010) (Fig. 2).

b. Intermediate Progenitor Cells (IPCs) or Basal Progenitors (BPs)

BPs are a secondary class of progenitor cells that originate from APs from which they differ in many respects. BPs are not located in the VZ but further basally, in the SVZ. Born at the ventricular border, they delaminate to translocate their nucleus to the basal region of the VZ. Then they lose the bipolar structure, retracting both their apical and basal process while moving towards the basal VZ (Attardo et al., 2008; Miyata et al., 2004). Subsequently, their centrosome is observed in the perinuclear area [reviewed in (Farkas and Huttner, 2008)]. Accordingly, BPs lack markers of apical-basal polarity (Attardo et al., 2008). BP divisions are typically located in the basal VZ and SVZ (Haubensak et al., 2004; Miyata et al., 2004; Noctor et al., 2004) (Fig. 2b). Not attached to the ventricular surface, BPs do not undergo INM (Takahashi et al., 1995b). However, they are not completely static as they extend and retract multiple very short processes, resulting in a multipolar morphology (Noctor et al., 2004; Noctor et al., 2008). Virtually all BPs are positive for the transcription factor Tbr2 (Englund et al., 2005; Kowalczyk et al., 2009) that controls the production of pyramidal neurons (Arnold et al., 2008; Sessa et al., 2008).

c. Distinct types of division for apical and basal progenitors

Several studies using time-lapse imaging of precursor cells, clonally labelled with GFP-expressing virus, revealed that APs have greater proliferative capacities than BPs. Early APs undergo symmetrical proliferative divisions (both daughter cells return into the cell-cycle)

(Noctor et al., 2001; Noctor et al., 2004; Noctor et al., 2008) thus amplifying the progenitor pool (Fig. 2a). Then, as corticogenesis proceeds, the RGCs undergo increasing numbers of asymmetrical division (Gotz and Huttner, 2005; Huttner and Kosodo, 2005). One daughter gives rise to another RGC, while the other gives rise to either a neuron (asymmetric differentiative division) (Malatesta et al., 2000; Miyata et al., 2001; Noctor et al., 2001) or to another precursor cell, a BP (asymmetric proliferative division) (Chenn and McConnell, 1995; Haubensak et al., 2004; Miyata et al., 2004) (Fig. 2b). SNPs differ from RGCs in that they undergo mostly neurogenic divisions (Stancik et al., 2010) (Fig. 2a,b).

By contrast, the vast majority of BPs (90%) undergo one terminal symmetric differentiative division, producing two neurons that quit the cell-cycle and migrate out to the cortical plate (Attardo et al., 2008; Haubensak et al., 2004; Noctor et al., 2004) (Fig. 2b). Only a small proportion of BPs is able to self-amplify by proliferative symmetric division (Kowalczyk et al., 2009; Noctor et al., 2004; Wu et al., 2005). Of note, once cortical neurogenesis is completed, most RGCs retract their pia-attached processes and ascend to the CP where they differentiate into astrocytes (Schmechel and Rakic, 1979;Noctor et al., 2004).

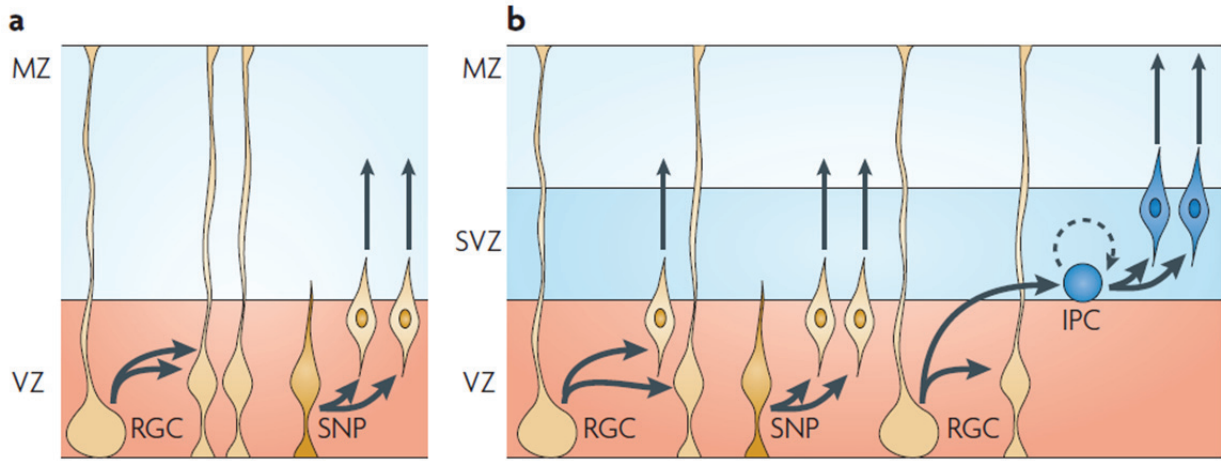

Fig. 2: Different types of cortical precursors divisions.
Schematic transects of the mouse cortex at embryonic day 13 (E13) (a) and E15 (b). Three types of progenitors: radial glial cells (RGCs), short neural precursors (SNPs) and intermediate progenitor cells (IPCs) are represented. RGCs and SNPs divide at the ventricular surface (a,b) and undergo symmetrical self-renewing divisions, symmetrical neurogenic divisions, as well as asymmetrical divisions giving rise to a RGC, a neuron or an intermediate precursor cell (IPC). IPCs divide in the SVZ (b), where they undergo mostly symmetric neurogenic divisions. A small fraction undergoes symmetrical proliferative divisions (dotted arrow). Adapted from (Dehay and Kennedy, 2007)

In the rodent, the SVZ is continually seeded by the VZ, and SVZ is seen as the major site of neurogenesis (Haubensak et al., 2004; Noctor et al., 2004). Furthermore, the spatial separation of two proliferative compartments could contribute to increasing neural complexity. Indeed, it enables different environmental influences (e.g. transcription factors and growth factors) to act in specific manners in order to generate diverse neural subtypes (Guillemot et al., 2006; Hevner, 2006; Molnar and Cheung, 2006).

Primate specific features

While considerable progress has been made in understanding corticogenesis in the rodent, recent findings in primates show that there are a number of unique primate specific features [reviewed in (Dehay and Kennedy, 2007; Jones, 2009; Kennedy et al., 2007; Molnar et al., 2006)]. The adult primate cortex is characterized by greatly expanded and differentiated supragranular layers (2,3 and 4), hosting neurons that connect different areas of the cortex or project locally (Peters and Jones, 1985). It is considered that this expansion underlies the unique computational features of the primate cortex. During primate corticogenesis, supragranular layers expansion relies on the proliferative activity of a supplementary GZ: the outer subventricular zone (OSVZ) (Lukaszewicz et al., 2005; Smart et al., 2002).

a. Anatomical organization of the primate developing cortex

The organization, developmental timing and relative dimensions of the germinal and postmitotic compartments of the primate cortex differ from those of rodents (Smart et al., 2002) (Fig. 3). In the monkey, cortical neurons are produced over a 60-day period from E40 to E100 (Rakic, 1974). Formation of the cortical plate (CP) is initiated relatively early (E46), before the appearance of the subplate (Fig. 3). The CP neurons in place by E65 are destined to constitute the deep layers V and VI of the mature cortex (Smart et al., 2002). At E55, a fibre layer appears between the developing subplate and the germinal zones (Smart et al., 2002) (Fig. 3). By contrast, no corresponding fibre layers at a comparable developmental stage can be observed in rodents (Miller, 1985; Smart, 1984). After E65, the growth of the subplate accelerates and cells continue to accumulate in this compartment up to mid-corticogenesis at E78. The subplate becomes much thicker than in the mouse developing cortex (Kostovic and Rakic, 1990; Smart et al., 2002) (Fig. 3). After E65, the ventricular zone (VZ) declines progressively while another proliferative compartment expands: the SVZ (Fig. 3). By E72, the SVZ is divided into an inner subventricular zone (ISVZ) and outer subventricular zone (OSVZ) by an intruding inner fibre layer (IFL) (compared with the outer fibre layer (OFL) that separate the GZs from the subplate) (Fig. 3). The OSVZ, which is not found in rodents, exhibits a number of unique features (Smart et al., 2002; Zecevic et al., 2005). Contrasting with the randomly organized SVZ of rodents, OSVZ has a compact radial organization. OSVZ progenitors are characterized by a bipolar morphology with radially oriented processes (Lukaszewicz et al., 2005; Smart et al., 2002).

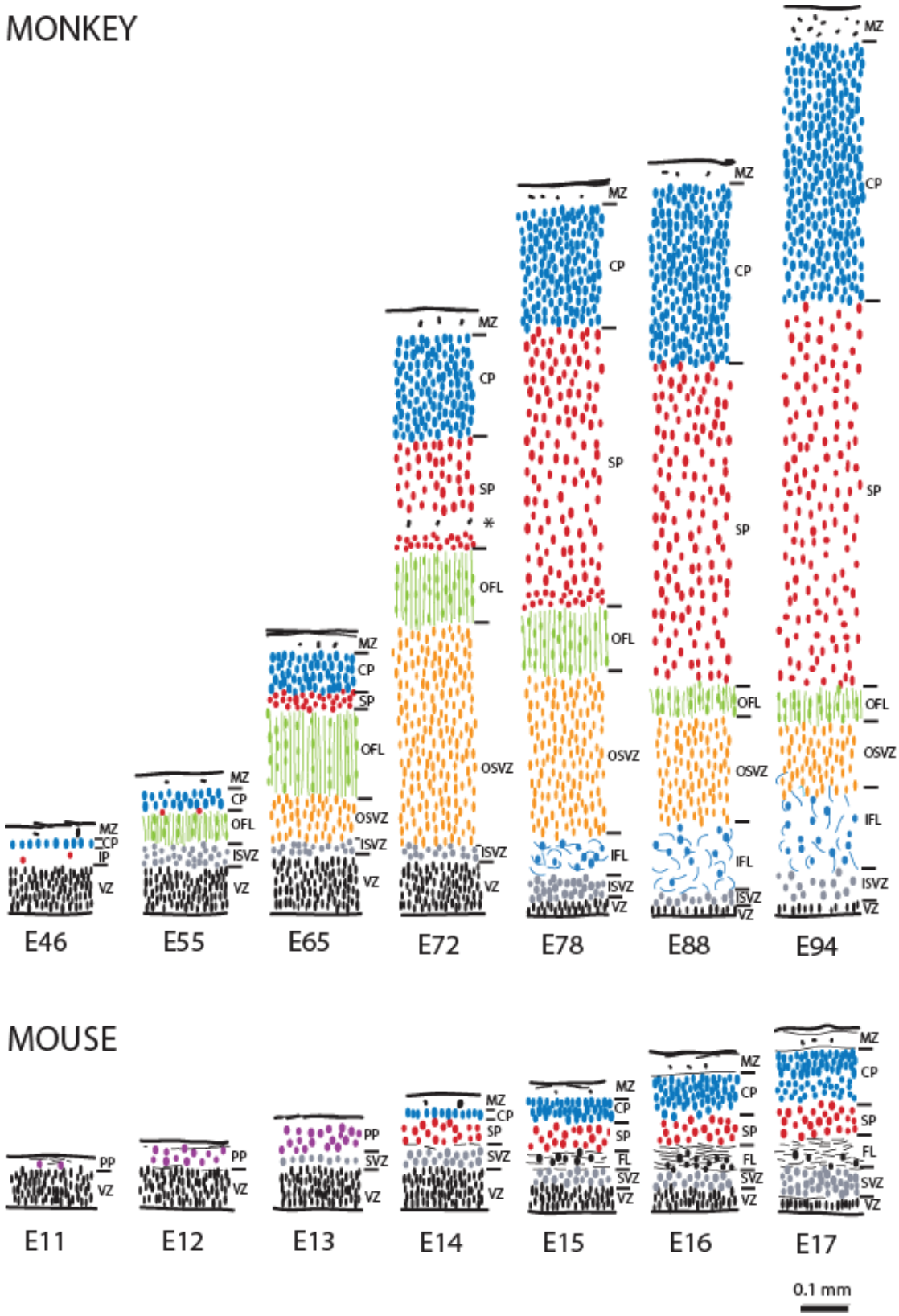

Fig. 3: Differences in the anatomical organization of the rodent and primate embryonic cortex. Schematic transects through the embryonic cortex in mouse (a) and monkey (b) at comparable developmental stages. The thickness of each layer is drawn to a common scale. Gestation period is 19 days in the mouse and 165 days in the monkey. Cortical neurogenesis lasts 8 days in the mouse and 60 days in the primate. CP: cortical plate, FL: fibre layer, IP: inner plexiform layer, IFL: inner fibre layer, ISVZ: inner subventricular zone, MZ: marginal zone, OFL: outer fibre layer, OSVZ: outer subventricular zone, PP: preplate, SP: subplate, SVZ: subventricular zone, VZ: ventricular zone. Adapted from (Smart et al., 2002).

b. Specific features of primate OSVZ precursors

The OSVZ is the main proliferative compartment and its expansion in the primate is considered to be an evolutionary adaptation underlying brain expansion and the increased complexity of cortical circuitry (Fish et al., 2008; Lukaszewicz et al., 2005; Rakic, 2005). The OSVZ progenitor cell population is more heterogeneous and complex than in the rodent SVZ. OSVZ contain progenitor cells that are either epithelial cells resembling RGCs (Fish et al., 2008) or cells resembling BPs (Kriegstein et al., 2006). Besides this diversity in the morphological features, OSVZ progenitors display varying molecular phenotypes, expressing markers typical of RGCs or BPs in a mosaic fashion (Fietz et al., 2010; Hansen et al., 2010). Further investigations are required to describe more precisely these different progenitor types and to determine whether they are associated with particular laminar cell fates. The OSVZ progenitors have a higher proliferative capacity than rodent SVZ progenitors. Whereas the rodent SVZ is only partially self-sustaining, requiring a constant supply of precursors from the VZ (Haubensak et al., 2004; Miyata et al., 2004; Noctor et al., 2004; Reznikov et al., 1997), OSVZ self-renewal is considerably more pronounced in primates (Lukaszewicz et al., 2005; Smart et al., 2002).One possible factor responsible for this enhanced proliferative ability in the primate OSVZ is the presence of the embryonic thalamic fibres, that are located next to the GZ in primates. Previous work of the team has shown that the thalamic axons release a diffusible factor that promotes proliferation of cortical precursors, through modification of cell-cycle parameters (Dehay et al., 2001). Compared with rodents, the length of the cell-cycle in primate cortical precursors is considerably extended (Kornack and Rakic, 1998; Lukaszewicz et al., 2005; Smart et al., 2002). All these features, plus the finding that OSVZ precursors produce supragranular layers neurons (Kornack and Rakic, 1998; Lukaszewicz et al., 2005; Smart et al., 2002), provide explanatory developmental mechanisms for the huge expansion of the upper layers in primate cortices.

II. Migration of cycling progenitors and post-mitotic neurons

Interkinetic Nuclear Migration (INM)

a. INM discovery

In the mouse cerebral cortex, the INM is a dynamic oscillation characteristic of cycling APs -either neuroepithelial cells during early developmental stages (E8-11) or RGCs at later stages (E11-17). APs undergo mitosis exclusively at the ventricular apical surface, due to the primary cilium and the centrosome being located at the apical plasma membrane (Dubreuil et al., 2007). Of note, INM of neuroepithelial cells span the entire thickness of the neuroepithelium, whereas INM of RGCs is restricted to the VZ (Gotz and Huttner, 2005). The APs nuclei move within the elongated cytoplasm, up and down along the apicobasal axis, in a stereotypic manner synchronized with the cell-cycle phases (Baye and Link, 2007; Frade, 2002; Takahashi et al., 1995a, 1996) (Fig. 4). After mitosis, the nuclei of the newborn precursor cells ascend away from the ventricule, migrating basally during G1-phase. The nuclei subsequently linger at the basal region of the VZ during S-phase. Finally, during G2 phase, the nuclei descend back toward the apical side to undergo M-phase upon reaching the ventricular surface (Fig. 4). Of note, INM is an evolutionary conserved process of nuclear migration and positioning (Morris et al., 1998; Reinsch and Gonczy, 1998), that occurs in the majority of neuroepithelial precursors of the central nervous system (dorsal telencephalon, retina) (Sauer, 1935; Takahashi et al., 1999) as well as in some non-neuronal epithelial tissues (Bort et al., 2006; Meyer et al., 2011).

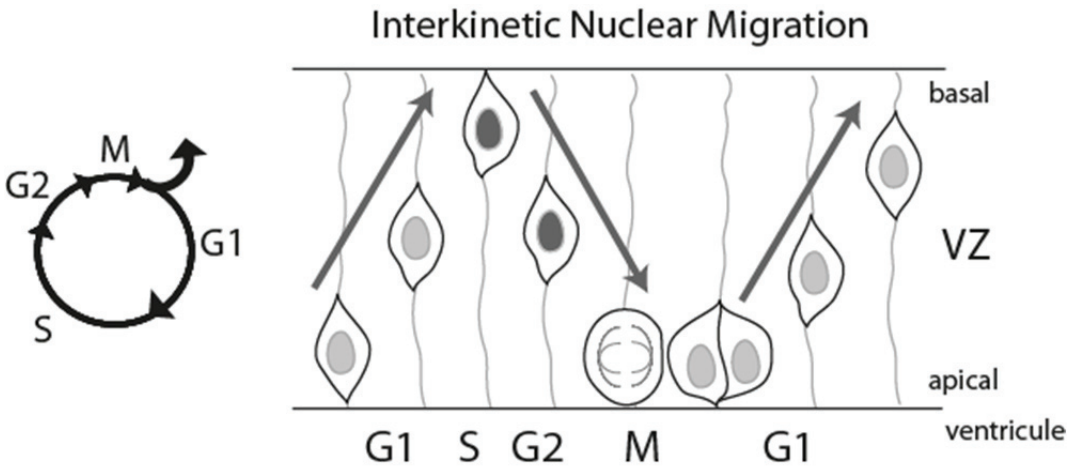

Fig. 4: Schematic representation of the Interkinetic Nuclear Migration performed by apical progenitors in the VZ, during the progression of the cell-cycle phases (G1, S, G2 and M).

The varying positions of APs nuclei along the apical-basal axis are responsible for the pseudostratified (multilayered) appearance of the neuroepithelium and the VZ which was described as early as 1935 by Sauer (Baye and Link, 2008; Miyata, 2008; Sauer, 1935). Before the beginning of the twentieth century, Alfred Schaper was the first to suggest that different cells morphologies close to the ventricule were representative of different cell-cycle phases (Schaper A, 1897). His studies were rediscovered by Sauer several decades later. Through observations of histological sections of embryonic chick neural tube and pig neural plate, Sauer found a correlation between the size, structure, and position of the nucleus relative to the ventricule (Sauer, 1935). Hence he proposed that the pseudostratification is facilitated by nuclear movements (Sauer, 1935), named it Interkinetic Nuclear Migration. Subsequently, DNA labelling techniques allowed to track the changes in the position of nuclei throughout the thickness of the neuroepithelium (Fujita, 1960; Hayes and Nowakowski, 2000; Langman et al., 1966; Sauer and Walker, 1959; Sidman et al., 1959; Takahashi et al., 1995a). Studies using cell-cycle inhibitors that arrest cells in S or G2/M phase showed that nuclear positioning movements are correlated with cell-cycle phases (Kallen, 1962; Watterson RL, 1956). Recently, live imaging studies combined with gene manipulation enabled to monitor nuclear movements in real time, leading to important progress in the understanding of the biological significance of the INM during corticogenesis as well as in the underlying mechanisms [reviewed in (Reiner et al., 2011; Taverna and Huttner, 2010)].

b. INM kinetics

Time-lapse videomicroscopy analysis has allowed to characterise the INM kinetics. The first detailed observations were made in the retina. In the early chick embryonic retina, the speed of movement was similar for nuclei moving toward and away from the ventricular zone (mean velocity of 21µm/h) (Pearson et al., 2005). However, nuclear movements were not linear but characterized by phases of movement interspersed by periods in which nuclei move only slowly or are stationary (Pearson et al., 2005). Recordings in zebrafish retina revealed two distinct types of motion (Norden et al., 2009). Stochastic movements with direction changing frequently and randomly represent 90% of the cell-cycle duration. Rapid but unfrequent movements are observed both soon after division (carrying nuclei over a distance corresponding to 40% of the epithelium thickness) and prior to division (carrying nuclei over a distance corresponding to 30% to 70% of the epithelium thickness). Here, INM is described as a stochastic process, similar to the Brownian motion, punctuated with transient directed movements surrounding cell division (Norden et al., 2009). In an another study conducted in zebrafish, the velocity for basal nuclear migration was slower than nuclear migration in the opposite direction (Baye and Link, 2007).

In the rodent embryonic cortex, recordings revealed that apical and basal movement exhibit distinct kinetics (Kosodo et al., 2011; Tsai et al., 2010). Nuclear movement away from the ventricular surface was unidirectional and continuous, with rare or no pauses but very

slow (mean basal velocity is 3.8µm/h) (Tsai et al., 2010). Recordings at a higher sampling frequency revealed that during G1-phase, the nucleus moves toward the basal side by nuclear 'ratcheting', a forward and backward motion. Nuclear movements toward the apical surface were found to be unidirectional but very intermittent, with bursts of fast nuclear translocation (30-60 µm/h) interrupted by pauses of 0.5-2 h (mean apical velocity is 8.4µm/h) (Tsai et al., 2010). Slower G1 associated movement is consistent with the longer duration estimated for G1 than G2 phase (Takahashi et al., 1993). This was also observed in ferret, where cortical progenitor cells move basally with an average speed of 5.6µm/h whereas they move apically at a mean rate of 18.3µm/h, and sometimes moved at rates exceeding 40µm/h (Chenn and McConnell, 1995).

Of note, during S-phase some nuclei show slow basal-to-apical migration although most remain stationary (Kosodo et al., 2011), undergoing minute random movements (Leung et al., 2011). These features of S-phase nuclei have been reported in other studies using histological methods (Hayes and Nowakowski, 2000; Takahashi et al., 1993).

The largely stochastic nuclear movement observed in the zebrafish or chick retina is clearly different from the directed nuclear movement reported in the developing rodent cortex (Attardo et al., 2008; Haubensak et al., 2004; Miyata et al., 2004; Noctor et al., 2004). These divergent observations could be explained by differences related to the cytoarchitecture of the different systems. In the retina at the developmental stage studied, the apical-to-basal extension of the neuroepithelium corresponded to 3-4 nuclear diameters, which is less than in the rodent cortex (Attardo et al., 2008; Haubensak et al., 2004; Miyata et al., 2004; Noctor et al., 2004). It is thus possible that certain parameters of tissue architecture such as cell elongation or volume ratio of nucleus to surrounding cytoplasm determine whether INM is rather largely stochastic or directed (Taverna and Huttner, 2010). Another difference relies on the proportion of the cell-cycle phases: whereas S phase is largely predominant in retinal precursor cell-cycle (Leung et al., 2011), it represents on average 30% of cell-cycle duration in cortical precursors (Takahashi et al., 1999). Therefore, assuming that stochastic nuclear movements typically occur during S phase whereas directed nuclear movements are characteristic of G1 and G2 phase, the global INM movement in the retina is seen as mainly stochastic (Norden et al., 2009).

Time lapse videomicroscopy studies have also revealed that nuclei of cortical progenitors are elongated during migration, and rounds up on approach to the ventricular zone, before division (Haubensak et al., 2004). Tear-drop shaped nuclei during INM are consistent with the nucleus being pulled or push by cytoskeletal motors attached to the nuclear envelope.

c. INM regulation

Like many migration processes, INM is dependent both on forces involving cytoskeletal dynamic changes as well as on the action of molecular motors associated with microtubules and/or actin [reviewed in (Baye and Link, 2008; Reiner et al., 2011; Taverna and Huttner, 2010)]. However, the nuclear movement occurring during INM differs strikingly from the one occurring in radially migrating neurons. One major difference concerns the centrosome which is the main microtubule organizing center. During classic nucleokinesis, the centrosome is tightly associated with the nucleus, moves forward into the leading process and is then closely followed by the nucleus (Farkas and Huttner, 2008; Higginbotham and Gleeson, 2007; Marin et al., 2006; Reinsch and Gonczy, 1998; Solecki et al., 2004; Tsai and Gleeson, 2005). In cycling APs, the centrosome is maintained in the apical end-foot adjacent to the ventricular surface throughout the different phases of INM, independently from nuclear position ((Astrom and Webster, 1991; Hinds and Ruffett, 1971), [reviewed in (Higginbotham and Gleeson, 2007)]. Thus, the distance between the nucleus and the centrosome dynamically changes during INM. More, nuclear movement during G1 is directed away from the centrosome, and that during G2 is directed toward the centrosome. This suggests that the microtubules coupling the nucleus and the centrosome must be dynamically regulated. Nevertheless, as is the case in radial migration nucleokinesis, directional actomyosin contractility could also underlie the INM associated nuclear movement.

Hence, recent studies have identified three major forces driving the nuclei during INM: (i)passive push of nuclei towards the basal side by nearby nuclei (Kosodo et al., 2011; Norden et al., 2009), (ii) actomyosin constriction at the apical side for movement in the opposite direction basally (Schenk et al., 2009), and (iii) kinesin and dynein-mediated movement towards the apical and basal sides, respectively (Del Bene et al., 2008; Gambello et al., 2003; Tsai et al., 2005)(Tsai et al., 2010) (see Fig. 10).

Of note, the cytoskeletal machinery involved in the apically directed nuclear translocation during G2 phase has been extensively studied, mainly implicating microtubule relating proteins. By contrast, the mechanisms regulating the basally directed nuclear movement, away from the centrosome in G1, have received less attention, mainly because of two reasons. First, studying the basal INM movement, occurring during G1 phase, requires to manipulate the cytoskeleton without impairing mitosis and cytokinesis. Second, whereas APs are the only VZ cell subtype to undergo apically directed migration, basal directed nuclear migration also occurs in BPs and newborn neurons, all delaminating from the ventricular surface to exit the VZ. This adds difficulty to follow basal nuclear movement specific of INM (Taverna and Huttner, 2010).

Passive nuclei displacement

Decades ago, cell nuclei were thought to be passively displaced away from the ventricular surface, by the mitotic divisions increasing cell density at the ventricular surface (Langman et al., 1966; Zwaan et al., 1969). Real-time studies in mouse described the basal movement as extremely slow (Tsai et al., 2010), even seen as a stochastic movement, similar to Brownian motion, with frequent and random changes in the direction of movement in the zebrafish retina (Norden et al., 2009). A recent study claims that this basal migration in G1-phase occurs mainly through passive, non-autonomous displacement (Kosodo et al., 2011). Magnetic fluorescent microbeads incorporated into the VZ of cultured mouse brain slices were observed to progressively translocate to the basal region, through intercellular space. Beads showed a 'ratcheting' back and forth movement, as observed during nuclei G1 migration. Finally, beads exhibited a unidirectional translocation, did not show the return apically directed movement but remained stationary and never entered the neuronal layer (Kosodo et al., 2011). Decreasing the number of apically migrating nuclei during G2, by blocking the cell-cycle at S-phase, resulted in a reduced distance and velocity of basal migration for both the majority of the nuclei and the microbeads (Kosodo et al., 2011). Computational modelling suggests that basal nuclear migration in G1-phase is mainly driven by a collective displacement effect generated by other nuclei migrating in the opposite direction during G2 phase (Kosodo et al., 2011). Nevertheless, the implication of a "passive mechanism" in regulating the basal INM movement does not exclude the occurrence of active, autonomous mechanisms.

INM regulation by the actin cytoskeleton

The role of actin cytoskeleton in INM has been shown decades ago, by using pharmacological inhibitors (Webster and Langman, 1978). This led to defects in nuclear positioning and INM. However, recent studies on the role of myosin II in INM are controversial.

In the zebrafish retinal neuroepithelial cells, inhibition of myosin II has been reported to interfere with both directed movements (Norden et al., 2009). This study claims that INM is mainly driven by actomyosin dependent forces, and that microtubule cytoskeleton is not necessary for INM to proceed. Of note, retinal INM does not occur within the same environmental constrains as in the cortex, where the neuroepithelium is thicker and more complex, as mentioned above.

In the developing mouse neocortex, inhibition of myosin II has been reported to interfere only with basally directed movement (Schenk et al., 2009). INM was indirectly analysed, via the analysis of the distribution of BrdU labelled nuclei in the VZ at different time points (from 0 to 14h) after a 15-min BrdU pulse labelling. The actomyosin system was weakened using the myosin II inhibitor Blebbistatin at low concentration, which impaired

the redistribution of nuclei from the apical to the basal side, during the G1 phase (Schenk et al., 2009). F-actin was seen to be enriched at the apical cell cortex, where it can generate contractile force to push the nucleus basally (Schenk et al., 2009) (Fig. 5). The authors claim that their low-blebbistatin treatment does not impair progression through cytokinesis but failed to substantiate it by direct examination. This makes it difficult to reject the possibility that blebbistatin treatment has interfered with proper division and that cells accumulating at the apical border are blocked into mitosis (Murthy and Wadsworth, 2005).

A third recent study appear to invalidate these findings and show, using real rime imaging that either myosin II inhibition or knockdown has no effect on the basal or apical movements in E17 organotypic rat slices (Tsai et al., 2010). Application of blebbistatin while cells were undergoing either apically or basally directed nuclear movement did not interrupt the normal nuclear trajectory, with velocities in both directions being similar to those in control cells.

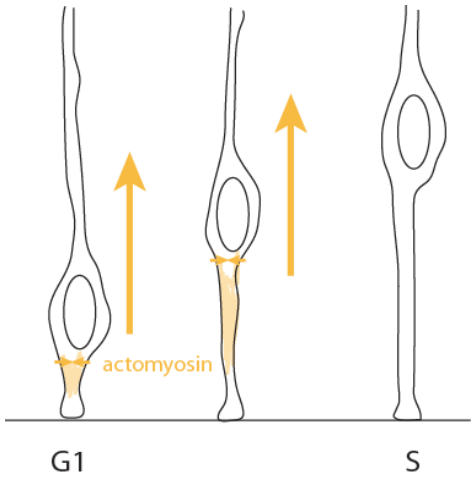

Fig. 5: Schematic representation of the putative action of actomyosin contraction, into the ventricular process, to promote the basal movement during INM.

INM regulation by the microtubule cytoskeleton

Microtubules have been shown to exert pulling forces for nucleokinesis in yeast (Tran et al., 2001), as well as during granule cell migration in the cerebellum and radial neuronal migration in the cortex (Solecki et al., 2004; Xie et al., 2003).

Organisation and dynamics of the microtubule (MT) network through the cell-cycle of APs was analyzed in videomicroscopy on E18 rat brain slices (Tsai et al., 2010). Throughout interphase, GFP-tubulin is distributed in bundles extending throughout both the basal and apical processes, parallel to the long axis of the cell. The nucleus is surrounded by a perinuclear MT ‘‘cage’’ structure, adjacent to the nuclear membrane (Xie et al., 2003). Assembly behaviour and orientation of individual microtubules was analyzed via the labelling of growing MT plus-ends by GFP-EB3 (Norden et al., 2009; Tsai et al., 2010). ‘Comet tail’–like streaks of EB3 emerge from the centrosome at the apical end-feet and extend throughout the processes, curve around the nucleus and enter in the basal process (Tsai et al., 2010). Microtubules grow with a uniform orientation, with the plus end orientated towards the pial surface (Norden et al., 2009; Tsai et al., 2010). Of note, during mitosis, both GFP-tubulin and GFP-EB3 labelling was clearly detected on the mitotic spindle, but not anymore in the basal process, which becomes very thin throughout mitosis (Tsai et al.,

2010). The process is reinvaded by MTs after mitosis at rates similar to the advance of EB3 streaks, suggesting that restoration of microtubules may be driven primarily by reassembly.

INM requires factors that link the nucleus to the MTs, to allow the nucleus to be moved as a cargo along the microtubule tracks, towards and away from the centrosome, thanks to minus-end-directed motor such as dynein, and plus-end directed motor proteins such as kinesin (see Fig. 10).

- **Anchoring of the nucleus to the centrosome**

Pax6 stabilizes the centrosome at the apical side of RGCs

The Pax6 transcription factor is predominantly expressed in neuroepithelial cells dividing in the VZ (Englund et al., 2005). Small eye mutant rodents (Sey/Sey) that lack Pax6 function show an abnormal laminar formation of the cortex (Fukuda et al., 2000).The VZ seems to expand, and *in vivo* studies on rodents brains at various developmental stages revealed that Pax6 dysfunction induced cell-cycle kinetics defects (Quinn et al., 2007), with a lengthening of S phase (Estivill-Torrus et al., 2002). This is accompanied by abnormal patterns of nuclear migration toward the apical: a premature descent of S phase nuclei, that tottered up and down during the G2 phase, did not reach the ventricular surface and divide ectopically at the basal side of the VZ (Tamai et al., 2007). Time-lapse imaging also revealed a frequent loss of the apical process of RGCs, associated with a modification of centrosomal localization. In some cases, centrosomes are unstable during the S to G2 phase, moving up and down inside the apical process, but staying near to the ventricular surface. Centrosomes also frequently translocate basally within apical process, such as in newborn BPs or neurons delaminating from the ventricular surface (Tamai et al., 2007). Pax6 is thus required for normal INM during the S to M phase progression, where it stabilizes the centrosome at the apical side (Tamai et al., 2007). However, the molecular mechanisms by which Pax6 regulates the centrosomal position and INM are still unclear.

Cep120 and TACCs promote growth of the microtubule-network from the centrosome towards the nucleus

Cep120 and transforming acidic coiled-coil proteins (TACCs) are Microtubule Associated Proteins (MAPs) associated with the centrosome and the microtubule lattice that links the centrosome and nucleus during INM (Xie et al., 2007) (Fig. 6). In mouse developing neocortex, Cep120 is highly expressed in neural progenitors at early and mid-embryonic stages, colocalizes with centrosomal markers along the ventricular surface, and interacts with a number of established centrosomal proteins in a yeast two-hybrid system (Xie et al., 2007). Transforming acidic coiled-coiled proteins (TACCs) associate with both the centrosome and MTs (Gergely, 2002), and are important for the growth or stabilization of centrosome-associated MTs (Bellanger and Gonczy, 2003; Gergely et al., 2000; Srayko et al., 2003). TACCs are expressed during mouse cortical development and co-immunoprecipitate with Cep120 in embryonic mouse brain (Xie et al., 2007). Cep120 is important for the

recruitment of TACC3 to the centrosome in neural progenitors *in vivo* (Shu et al., 2004; Tanaka et al., 2004; Xie et al., 2007). Cep120 or TACC interference impairs the apical INM movement on E11.5 organotypic brain slices. Under these conditions, APs display less elongated nuclei and fewer nuclei are observed to migrate toward the ventricule, along a shorter distance (Xie et al., 2007). In dissociated neocortical cells, Cep120 or TACC silencing decreases the size of the prominent MT bundles that form the microtubule ''fork'' coupling the centrosome and the nucleus. Under these conditions, the shortened bundles not longer reach the nucleus (Xie et al., 2007). These defects were accompanied by an increase in nucleus-centrosome distance in the VZ progenitor cells, sign of a defect in nucleus-centrosome coupling (Shu et al., 2004; Tanaka et al., 2004). To summarize, Cep120 interacts with TACC and recruits it to the centrosome. Cep120 and TACC act cooperatively to promote the assembly of long microtubules emanating from the centrosome and reaching the nucleus (Fig. 6). This microtubule-dependent coupling between the centrosome and the nucleus allows the transport or the pulling of the nucleus toward the ventricular surface.

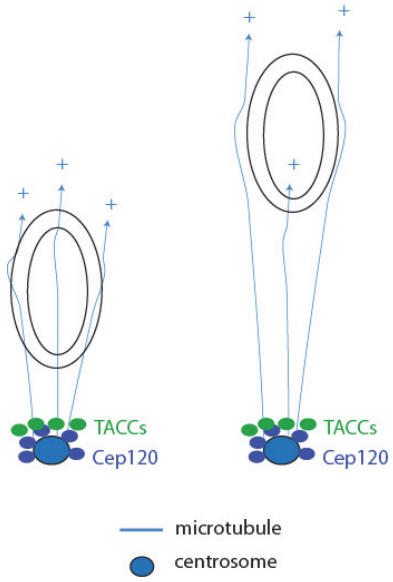

Fig. 6: Schematic representation of the action of Cep120 and TACCs on microtubule growth. Cep120 recruits TACCs at the centrosome, and together they promote the elongation of microtubules towards the nucleus.

SUN1/2 and Syne/Nesprin-1/2 complexes bridges the nucleus with the cytoskeleton

SUN and Syne nuclear envelope proteins act in nuclear migration and anchorage in a variety of eukaryotic cells from fungi to mammals, maintaining the connection between the nuclear envelope (NE) and the cytoskeleton (Starr and Fischer, 2005). In the developing mouse cortex SUN-domain proteins SUN1/2 and KASH-domain proteins Syne-1/2 bridge the centrosomal microtubule network to the nucleus (Zhang et al., 2009) (Fig. 7). SUN-domain proteins (SUN1 and SUN2) are transmembrane proteins localized to the inner nuclear membrane. Their N-terminal domain interacts with nuclear lamins in the nucleoplasm and their conserved C-term SUN domain is located inside the perinuclear space. Here, they interact with KASH-domain proteins (Syne-1/Nesprin-1 and Syne-2/Nesprin-2) (Worman and Gundersen, 2006). These giant proteins also have a conserved transmembraneous C-term KASH domain, localized to the outer nuclear membrane. Syne has a long spectrin repeats and a large N-terminal domain, located into the cytoplasm, and containing actin and MT-binding sites. In the developing mouse cortex, Syne-2 interacts with (i) the dynein

intermediate chain on the NE, (ii) the dynactin subunit p150 and (iii) kinesin on the NE in the VZ (Zhang et al., 2009) (Fig. 7). Moreover, SUN1, SUN2, and Syne-2 also colocalize with α-Tubulin not only at the NE but also on the ‘‘fork’’ structures, thus connecting microtubule to the NE (Zhang et al., 2009). In Sun1/2 or Syne-1/2 mutant brains, videomicroscopy observations revealed a disruption of the apical INM movement and of post-mitotic radial migration. In both cases, the nuclei failed to catch up to centrosome (Zhang et al., 2009). To summarize:SUN1 and SUN2 recruit Syne-2 to the NE. Syne-2 interacts with the dynein/dynactin and kinesin complexes at the NE. SUN/KASH protein complexes bridge the nucleus and cytoskeleton, allowing both nuclear anchorage and movement by transducing the pulling force from the microtubule network to the nucleus (Fig. 7).

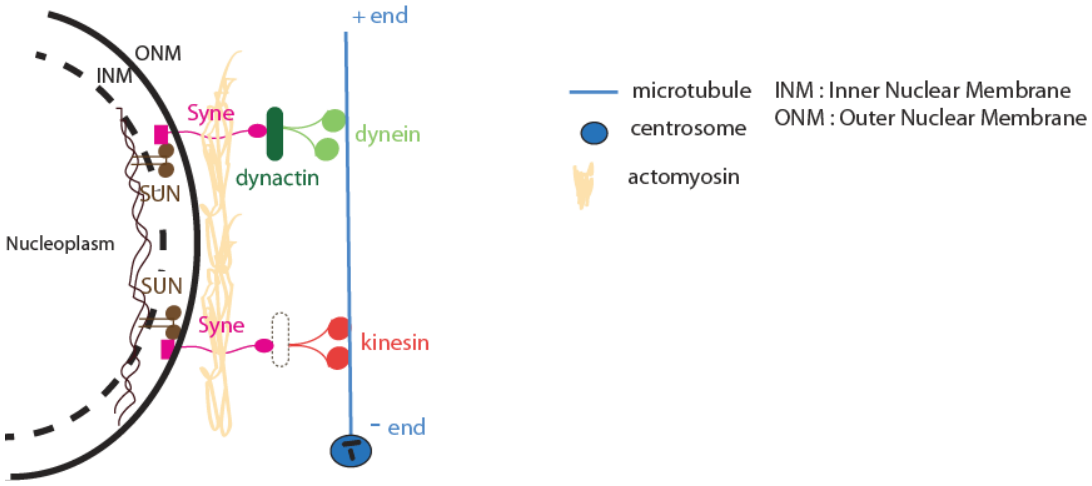

Fig. 7: Schematic representation of the linking between nucleus and microtubules, mediated by Syne and SUN proteic complexes. These complexes link the nuclear membrane to the motor proteins associated with the microtubule network, and thus allow to transduce the applied forces to the nucleus.

- **Travelling along microtubules, toward the apical side**

Tpx2 promotes microtubule bundling and alignment in the apical process

Driving forces of nuclear movement may come from polymerization and depolymerisation of microtubules connected to the nucleus. Tpx2 is a MT-nucleating/bundling protein (Schatz et al., 2003). Its expression is regulated by the cell-cycle in HeLa cells (Gruss et al., 2002) as well as in mouse AP cells (Kosodo et al., 2011). Tpx2 is absent in G1-phase, accumulates in nuclei during S/G2-phase and localizes at the spindle pole during M-phase before being degraded in early G1 (Gruss et al., 2002). In G2-phase, Tpx2 redistributes in the apical process, as bundled fibre extending toward centrosomes on the apical surface (Kosodo et al., 2011). Tpx2 interference via E13.5 utero electroporation leads to a decreased velocity in the apical movement. This is associated with an increased number of abventricular mitotis as well as a mitotic arrest and abolishment of mitotic spindle. Tpx2 interference impaired the sharp distribution of growing microtubules plus end inside the apical process (Kosodo et al., 2011). The regulation of Tpx2 distribution during

S/G2 transition is thus part of the mechanism that determines the timing of apical nuclear migration. Upon entry into G2-phase, Tpx2 redistributes into the apical process, promote the apical microtubules packing and alignment critical for the nuclear transport, along microtubule, towards the apical surface (Kosodo et al., 2011).

Lis1 associates with the centrosome and interacts with the dynein motor protein

Lis1 is a MAP that associates with centrosomes and interacts with the microtubule minus end-directed motor cytoplasmic dynein and its regulatory complex dynactin (Faulkner et al., 2000; Smith et al., 2000; Tanaka et al., 2004) (Fig. 8). Lis1 was shown to be essential for nuclear migration and nuclear orientation in fungi (Xiang et al., 1995). In human, Lis1 mutation is responsible for type I lissencephaly, characterized by a nearly complete absence of gyri, an abnormally thickened four-layered cortex, and enlarged ventricules (Vallee et al., 2001). In rodents, LIS1 interference leads to severe neuronal migration defects, due to a block in the conversion of multipolar to bipolar migratory state, as well as an impairment in nucleokinesis (Tsai et al., 2007; Tsai et al., 2005; Yingling et al., 2008). A defect in neuroblast proliferation was suggested by a thinner VZ than in control, and an overall reduction in the number VZ neuronal precursors (Gambello et al., 2003). In Lis1 mutant mice embryo cortices, a defect in INM movement was suggested by the ectopic position of M phase nuclei in the VZ, away from the ventricular surface (Gambello et al., 2003). Videomicroscopy analysis on embryonic rat brain slices after Lis1 interference revealed an abolishment of INM over substantial distances and no cell divisions were detected (Tsai et al., 2005). The direction of movement in which Lis and dynein participate remained undetermined, because of the complete immobilization of RGCs nuclei by Lis1 RNAi (Tsai et al., 2005). However, dynein interference leads to slower apically directed nuclear movement whereas basally directed nuclear migration is not affected (Tsai et al., 2010). Hence, Lis1 can regulate INM via its interaction with dynein, a minus-end-directed motor which is the force generator allowing nuclear movement in the apical direction, consistent with the orientation of minus-end MTs towards the centrosome (Fig. 8).

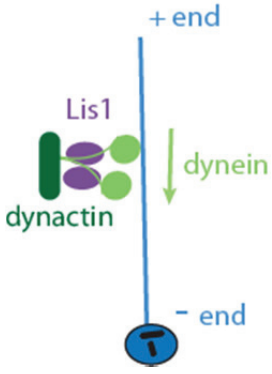

Fig. 8: Schematic representation of the LIS/dynein/dynactin motor complex, generating forces that allow the transport towards the minus-end microtubules at the centrosome.

Dynactin-1 interacts with dynein microtubule motor protein

Dynactin is a multiprotein complex that interacts with and activates cytoplasmic dynein. Dynactin mediates interaction of dynein with numerous cargoes and allows dynein to go through the microtubule lattice over long distances by increasing its processivity (King

and Schroer, 2000) (Fig. 8). In the zebrafish retina, Dynactin-1 is expressed through cytoplasmic punctuates enriched at the apical surface of RGCs (Del Bene et al., 2008). In zebrafish mikre oko (mok) mutants, in which the motor protein Dynactin- 1 is disrupted, videomicroscopy analysis revealed that RGCs nuclei migrate faster and further basally while moving more slowly to the apical side. Under this condition, RGC frequently enter mitosis before reaching the ventricular surface (Del Bene et al., 2008). Dynamitin overexpression- which inhibits dynactin function- leads to a complete arrest of RGCs nuclei far from the ventricular surface (Tsai et al., 2010), as it was the case after dynein RNAi (Tsai et al., 2010) or Lis1 inhibition (Tsai et al., 2005). Hence, dynactin associates with the dynein complex, which is implicated in cross linking microtubules to the nuclear envelope and mediate apically directed nuclear movement (Tsai et al., 2010) (Fig. 8).

- **Travelling along the microtubules, towards the basal side: role of Kinesin 3**

A plus end-directed MT-based motor of the kinesin type may be involved in the basal INM for two reasons. First, the outer nuclear envelope protein Syne2 interacts not only with dynein complexes (Del Bene et al., 2008) but also with kinesin complexes (Zhang et al., 2009). Second, the microtubules in APs are uniformly oriented with the plus ends directed away from the centrosome (Norden et al., 2009), thus providing a possible track to move the nucleus basally via a plus end-directed motor.

A functional shRNA screen has led to the identification of a nonconventional kinesin, that specifically mediates basal INM in rodent cortical APs (Tsai et al., 2010). Interference with Kif1a, member of the kinesin-3 family, leads to defects in basally directed INM. In this case, RGC display a normal apical movement and undergo mitosis at the ventricular surface. However, the velocity and the amplitude of the basal movement are markedly decreased, with no alteration of the centrosome behaviour or microtubule orientation. Kinesin 3 is thus implicated in INM as a basal nuclear transport motor (Fig. 9). Of note, Kif1a contains a C-terminal pleckstrin homology domain that is known to interact with membrane lipids (Klopfenstein and Vale, 2004), and might thus help to recruit Kif1a to the nuclear surface. Furthermore, INM kinetics are consistent with kinesin being implicated in basal movement: unlike cytoplasmic dynein, which is a very fast minus end– directed microtubule motor (Paschal et al., 1987), Kif1a is plus-end–directed and moves slowly and processively as a monomer (Okada and Hirokawa, 1999).

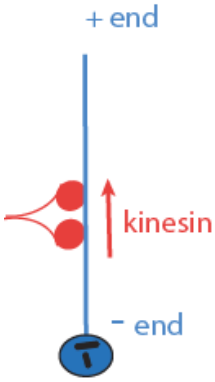

Fig.9: Schematic representation of the kinesin motor generating forces that allow the transport towards the plus-end microtubules away from the centrosome.

General model of INM regulation

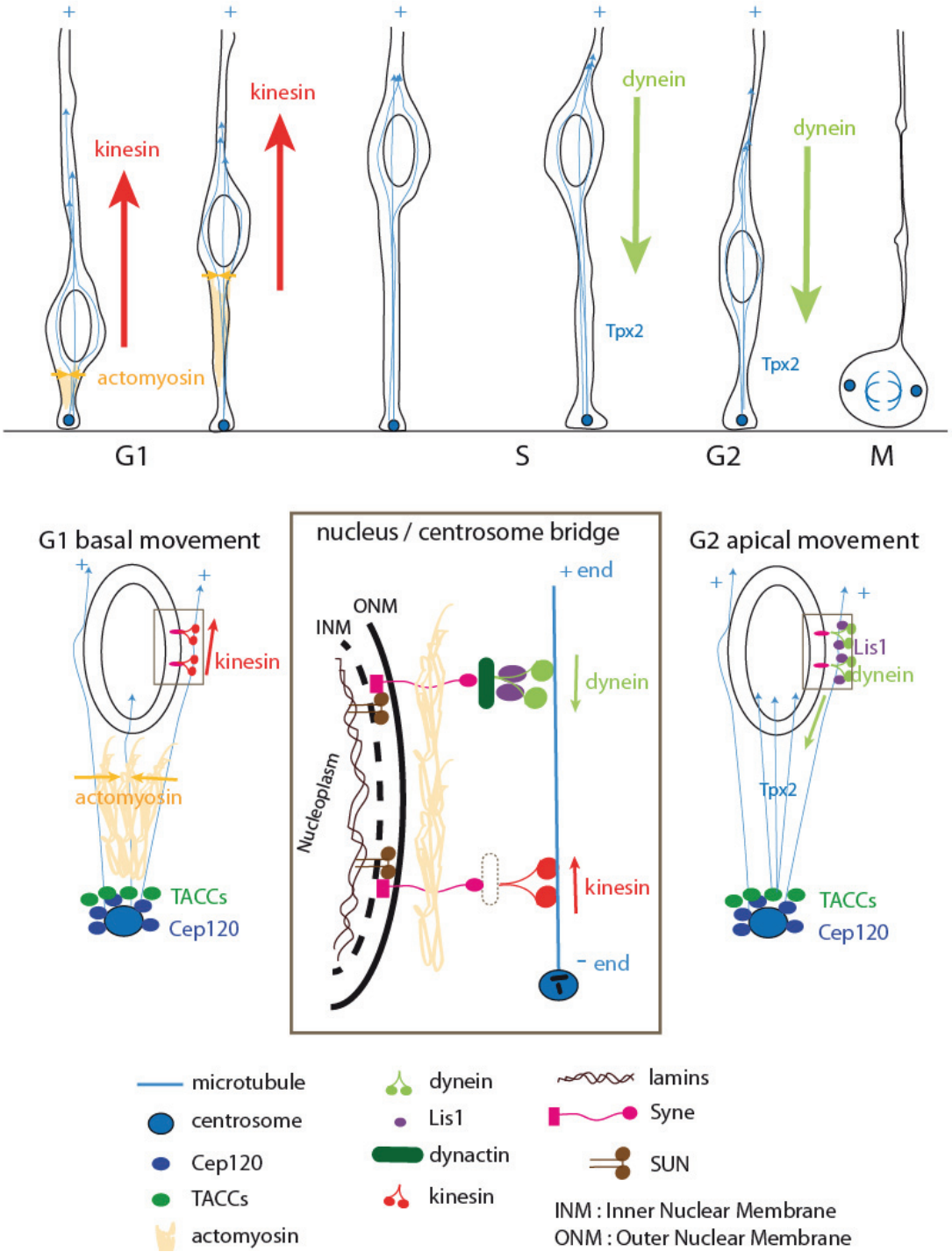

Fig. 10: Schematic representation of the regulation of INM movements.
The nuclear movement, which occurs during progression in the cell-cycle phases G1, S G2 and M, is finely regulate by a combination of microtubules and actin related proteins (upper panel). Actin is thought to be enriched in the ventricular process, microtubules growth is promoted by the cooperative action of Cep120 and TACCs at the centrosome, and lastly, microtubule alignment is potentiated by Tpx2. The basal nuclear movement during G1 may rely on both actomyosin activity and kinesin transport away from the centrosome (lower left panel). The apical movement in G2 phase is promoted by microtubules alignment (Tpx2) and subsequent transport towards the centrosome thanks to Lis1/dynactin/dynein motor complex (lower right panel). During the whole nuclear migration, the nucleus and the centrosome are linked together by the SUN/Syne complexes, interacting with both the nuclear envelope, actin fibres and the microtubule motor complexes (lower middle panel).

INM movement, away and towards the centrosome, strongly relies on the coupling between the nucleus and the microtubules (Fig. 10). First, the centrosomal protein Cep120 interacts with TACC and recruits it to the centrosome. Cep120 and TACC both promote together the assembly of long microtubules from the centrosome to the nucleus (Xie et al., 2007). Efficient coupling and linking of the nucleus to the cytoskeleton relies on the nuclear envelope associated proteins SUN1/2 and Syne-1/2 (Zhang et al., 2009). These complexes transmit forces of microtubule motor proteins, cytoplasmic dynein, or kinesin, to the nucleus. Of note, Syne proteins are also able to bridge microtubule and actin cytoskeleton (Starr and Han, 2003). Syne2 may thus constitute a point of convergence between actomyosin and the dynein/kinesin system. More, the large N-terminal domains of Syne proteins may have other binding partners that can provide further levels of regulation and other functions (Koizumi and Gleeson, 2009).

G1 phase basal movement could be driven in part passively, by apically migrating G2-phase nuclei (Kosodo et al., 2011). Nevertheless, other data support alternative hypothesis including a microtubule/ kinesin-mediated mechanism, pushing the nucleus away from the centrosome (Tsai et al., 2010), as well as an actomyosin-driven nuclear migration (Schenk et al., 2009) (Fig. 10). This apparent controversy will need to be addressed in detail, although it is possible that all three mechanisms contribute to a certain extent to proper nuclear movement. The observed differences may result from specific experimental differences. It might also be that during the evolution of the mammalian cortical neuroepithelium, the pronounced increase in the neuroepithelium thickness and the denser packing of nuclei may have compromised the ability of actomyosin to drive nuclei towards the apical side, which would then require the help of the microtubule system (Leung et al., 2011).

Of note, a common mechanism has been proposed to control basal nuclear migration during G1 phase and delamination of BPs towards the basal side of the VZ. Consistent with this, myosin II inhibition also impaired translocation of delaminating BPs (Schenk et al., 2009), leading to the suggestion that the directional myosin II-mediated constriction of the apical process could push the nucleus in the basal direction. In this context, it is interesting to note that newborn BPs retain their apical process during basal nuclear translocation and retract it only after its completion (Miyata et al., 2004; Noctor et al., 2004).

During G2 phase, the apical movement is mainly driven by the microtubule motor system (Fig. 10). Tpx2 relocalizes to the apical process, where it facilitates microtubule packing and alignment (Kosodo et al., 2011). This promotes apically directed nuclear migration through enhancement of dynein-dependent motor activity, shown to carry organelles more efficiently where microtubules are uniformly orientated (Ross et al., 2008). Lis1 may sustain the migration of the nucleus by regulating the activity of dynein/dynactin, pulling the nucleus toward the centrosome (Del Bene et al., 2008; Tsai et al., 2005; Tsai et al., 2010).

Thus, the emerging model is that both microtubule-based motors and actomyosin participate to INM, although to a different extent. Bidirectional nuclear transport is mainly achieved by a dual microtubule motor system (Fig. 10). The maintenance of nuclear

migration may depend on a balance of plus-end and minus-end-directed microtubule motor function (Whited et al., 2004).

d. INM role in neurogenesis

Impact of INM on neurogenesis

INM oscillations allow the extensive proliferation of AP cells together with maintenance of their apical–basal polarity. The movements of interphase nuclei away from the apical ventricular zone avoid overcrowding of diving cells and thus provide space for other mitotis to occur (Frade, 2002). It also allows to maintain the APs apical and basal attachments throughout the cell-cycle (Frade, 2002), as well as the localisation of protein signalling complexes such as adherens- and tight junction-associated protein complexes, which were shown to have essential roles in cell fate decisions related to cell-cycle exit, cell type choice, and laminar positioning (Gotz and Huttner, 2005). Hence, INM serves to maximize the number of AP mitoses per unit area of apical surface, while maintaining the pseudostratified structure, and thus promoting the expansion of APs (Fish et al., 2008).

INM can also induce cell fate differences between neural progenitors, by mediating differential exposure to environmental cues as shown in the retina (Baye and Link, 2007; Del Bene et al., 2008; Latasa et al., 2009; Murciano et al., 2002). Because a cell competence to respond to extrinsic cues varies with progression through the cell-cycle, nuclei movements through signalling gradients along the apical–basal axis of the epithelium, and according to specific cell-cycle phases, may establish heterogeneity among progenitor cells. Consistent with this model, both the extent of basally directed nuclear migration and the cell-cycle length vary in a seemingly homogeneous population of neuroepithelial cells (Baye and Link, 2008). Interfering with INM amplitude and velocity leads to a progressive depletion of the AP progenitor pool. Perturbation of apical INM by downregulation of centrosomal (Cep120 and TACCs) (Xie et al., 2007), microtubule motor-associated proteins dynein/dynactin (Del Bene et al., 2008), or SUN-domain and KASH-domain proteins (Zhang et al., 2009) caused enhanced neurogenesis at the expense of neural progenitor cells. In the developing zebrafish retina, the more basal the AP nucleus moves, the more likely it is to undergo a neurogenic division (Baye and Link, 2007). Furthermore, slowing-down of basal INM by myosin II inhibition has been found to increase neurogenic BPs at the expense of proliferative APs, and thus more basal mitoses at the expense of apical mitoses (Schenk et al., 2009).

INM can balance the exposure of progenitor nuclei to neurogenic versus proliferative signals, such as the Notch signalling pathway. The Notch pathway has a well-characterized role during neurogenesis, preventing progenitors from leaving the cell-cycle and differentiating prematurely (Del Bene et al., 2008; Latasa et al., 2009; Mizutani et al., 2007). Upon binding to its ligand, Notch receptor undergoes a proteolytic cleavage, its cytosolic

fragment translocates to the nucleus where it modulates the transcription of target genes. Components of the Notch pathway have been shown to be expressed in an apical-to-basal gradient in the developing retina of chick and zebrafish neuroepithelium (Murciano et al., 2002). Notch mRNA is enriched on the apical side, whereas Delta (one of the Notch ligands) mRNA and protein are enriched basally. Notch signalling is activated in the developing retina as the nuclei move toward the apical surface and downregulated in nuclei that move in the opposite direction (Del Bene et al., 2008). In the mouse cortex, however, Notch-active nuclei are found in the basal region of the VZ (Kawaguchi et al., 2008). Further studies are necessary to clarify how Notch signals are transduced during INM progression. Nevertheless, it is conceivable that the cell fate diversification among progenitor cells is influenced by INM, which determine the time the AP nucleus spends at any given location along the apical-basal axis during the cell-cycle.

Furthermore, in the densely packed population of VZ progenitors, neighbouring cells can exchange developmentally relevant signals to facilitate synchronized entry into the different phases of the cell-cycle and to harmonize the INM movements (Pearson et al., 2005; Weissman et al., 2004). Cells can communicate via gap junctions directly linking the cytoplasm of two neighbouring cells or indirectly by the release of substances through unopposed connexons, known as hemichannels. In both the embryonic retina and cortex, gap junction channels couple progenitor cells into radial columnar clusters that exclude differentiated neurons (Bittman et al., 1997; Owens and Kriegstein, 1998). Connexins and gap junctions expression vary according to the cell-cycle phases and to the developmental stage (Bittman et al., 1997; Oyamada et al., 2005). Connexin 43 (Cx43) is the major connexin in the mouse VZ precursors and is responsible for the gap junction coupling in the neuroepithelium (Pearson et al., 2005). This coupling allows the passage of signalling molecules, such as Ca2+ waves, that can spread between neighbouring cells and play pivotal roles in the regulation of both cell movement and proliferation (Owens and Kriegstein, 1998; Pearson et al., 2005; Weissman et al., 2004). In migrating neurons, the speed of movement is positively correlated with both the frequency and amplitude of Ca2+ transients (Komuro and Rakic, 1996; Nadarajah et al., 2001), spreading through Cx43 hemichannels (Elias et al., 2007). In the chick retinal neuroepithelial cells, basal and apical INM movements are preceded by elevated bursts of Ca2+ (Pearson et al., 2005). In chick retina and mice brain slices, chelation of these Ca2+ transients, blocking of gap junctions/hemichannels, transfection of cells with shRNA or dominant-negative constructs of connexin 43 slowed down the apical movement, as well as the basal one but to a lesser extent (Liu et al., 2010; Pearson et al., 2005). Actomyosin contractility is involved in INM (Schenk et al., 2009) and calcium regulates this contractility (Marston, 1995). Hence, gap junction-mediated calcium signals could contribute to harmonize INM movements within the AP population, and consequently the cell-cycle progression and cell fate choices.

Links between INM and cell-cycle progression

Several studies have indicated that INM is not required for cell-cycle progression. Blocking or delaying the nuclear movement does not alter cell-cycle length (Murciano et al., 2002; Schenk et al., 2009). Numerous studies also show that interfering with INM impairs divisions at the ventricular surface (Del Bene et al., 2008; Gambello et al., 2003; Tamai et al., 2007; Tsai et al., 2005; Zhang et al., 2009). In these studies, the ectopic mitosis occurring basally in the VZ could correspond to BPs, which divide at a basal location. Although INM is dispensable for progression into the cell-cycle, INM alteration may lead to changes in progenitor cell fate.

By contrast, INM movement requires cell-cycle progression. When the cell-cycle of retinal neuroepithelium is lengthened by genetic mutations or pharmacological manipulations, INM is proportionally slowed (Baye and Link, 2007; Pearson et al., 2005). Pharmacological treatments inducing S phase or G2/M arrest resulted in concomitant inhibition of INM in the basal and apical region of the VZ, respectively (Baye and Link, 2008; Ueno et al., 2006). G1 phase blockade of cell-cycle progression after p18Ink4c overexpression caused nuclear accumulation at the basal side of the VZ, suggesting that entry into S-phase is a prerequisite for apical nuclear migration (Kosodo et al., 2011).

Together, these data support the concept that nuclear migration is not essential for cell-cycle progression but that the master regulators of cell-cycle progression could exert a tight control upon INM (Taverna and Huttner, 2010). It will be important to dissect the pathway(s) via which this control is achieved.

Neuronal radial migration

Glutamatergic projection neurons (as well as a substantial fraction of inhibitory neurons in the primate, (Jones, 2009; Letinic et al., 2002; Petanjek et al., 2009; Zecevic et al., 2011)) are generated from precursor cells of the GZ lining the ventricules deep within the embryonic brain [reviewed in (Gorski et al., 2002; Gupta et al., 2002)]. Consequently, they have to migrate long distances from their birthplace to reach their final destination in the CP. During mid and late corticogenesis, projection neurons migrate in the radial direction along radial glial guides (Hatten, 1990; Rakic, 1978), to undergo the so-called gliophilic or glia-guided migration, also called locomotion (Nadarajah et al., 2001; Noctor et al., 2004; Tabata and Nakajima, 2003) (Fig. 11).

Of note, inhibitory interneurons, mainly produced in the ventral ganglionic eminence, undergo a tangential migration to reach the dorsal cortex. This tangential migration follow several routes, and its regulatory mechanisms are different from that of radial migration [reviewed in (Nakajima, 2007)]. Tangentially migrating interneurons establish a permissive corridor essential for the development of the thalamocortical projection (Lopez-Bendito et al., 2006).

In this work, we shall focus on the radial migration of cortical projection neurons.

a. Distinct phases during radial migration

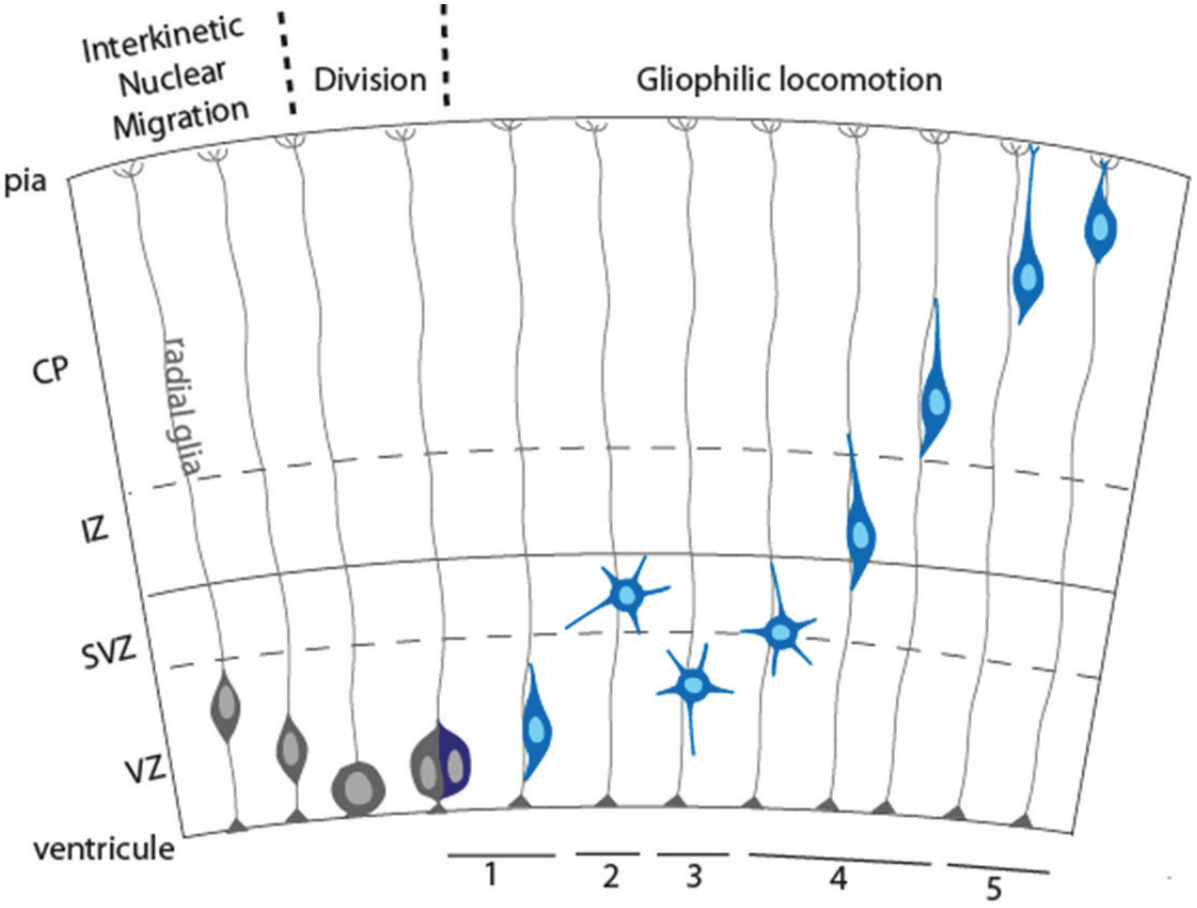

Fig. 11: Successive phases of neuronal migration by locomotion.
After division at the ventricular surface, the newborn neuron adopts a bipolar morphology and delaminates away from the ventricular surface (1). The neuron settles in the SVZ where it adopts a multipolar morphology (2) and frequently changes its orientation (3). The neuron finally grows a leading process towards the pia and initiates radial migration to the CP (4), terminating its migration by a small somal translocation (5). Adapted from (Kriegstein and Noctor, 2004)

Studies using time-lapse imaging in slice cultures have demonstrated that radial migration of pyramidal neurons does not progress smoothly from the GZ to the CP. Instead, neurons go through a series of spatially and temporally distinct changes in both cell shape and movement direction (Noctor et al., 2004; Tabata and Nakajima, 2003) [reviewed in (Kriegstein and Noctor, 2004)] (Fig. 11). These observations have led to a model where of radial migration can be divided into four distinct phases (Noctor et al., 2004; Tabata and Nakajima, 2003): (i) neurons generated at the ventricular surface move relatively rapidly and directly into the SVZ, (ii) neurons pause in the SVZ for 24 h or longer and convert to a multipolar non-migratory phase (Noctor et al., 2004; Rakic, 1974; Tabata and Nakajima,

2003). At this stage, they are still highly dynamic and extend and retract processes. Because they are not tightly adhering to radial glial guide fibres, neurons can move tangentially within the SVZ over a distance equivalent to the width of several cell bodies (Noctor et al., 2004; Tabata and Nakajima, 2003). (iii) Many, but not all neurons pass through a third phase, involving retrograde motion toward the ventricule. Some neurons extend a process towards the ventricule and are often observed to translocate their cell body back into the VZ (Noctor et al., 2004; Tabata and Nakajima, 2003). (iv) Finally, neurons extend a pia-directed short leading process (100–200 μm) (Nadarajah et al., 2001; Noctor et al., 2004), thus converting to the bipolar morphology of migrating neurons. Neurons ascend to the CP along radial glial fibres, undergoing the so-called gliophilic or glia-guided migration (Noctor et al., 2004; Tabata and Nakajima, 2003). The progression of neurons migrating along radial glial fibres is characterized by stasis interspersed with short periods of rapid movement, resulting in a saltatory locomotion (Nadarajah et al., 2001; Noctor et al., 2004). Once connecting the pia, neurons undergo a final nuclear translocation to settle at their appropriate position in the CP.

b. Morphological remodelling during saltatory locomotion

During each migratory cycle, neurons reiterate a four-step process (Tsai and Gleeson, 2005) (Fig. 12). (i) First, the leading edge of the neuron extends along the radial glial fibre, in the direction of migration. Extension of the highly polarized leading process requires protrusion forces exerted by actin polymerization, microtubules growth and establishment of adhesion complexes that link the extracellular substrate to the actin cytoskeleton (Marin et al., 2006). (ii) Then a swelling of the plasma membrane forms in the leading process, immediately ahead of the nucleus. The microtubule network is then pulled forward, and the centrosome moves steadily into the swelling. Despite the distance between the nucleus and the centrosome, they are constantly attached together through a fork-like network of microtubules that enwraps the nucleus in a cage-like fashion (Xie et al., 2003). Microtubules extend from the centrosome into the leading process, and F-actin and actomyosin motors are enriched in the proximal portion of the leading process. (iii) Nucleokinesis then relocates the nucleus forwards into the cytoplasmic dilatation (Schaar and McConnell, 2005). Nuclear movement involves the participation of microtubules pulling forces, through LIS1/dynein activity (Tanaka et al., 2004; Tsai et al., 2007; Tsai et al., 2005).Polymerisation and stabilization of microtubules also relies on DCX (Francis et al., 1999; Friocourt et al., 2007; Tanaka et al., 2004; Vreugdenhil et al., 2007). Actomyosin activity at the rear of the nucleus provide a pushing force that squeezes the nucleus forward (Schaar and McConnell, 2005; Solecki et al., 2009) [reviewed in (Vallee et al., 2009)]. (iv) Finally, rupture of cell adhesions at the back of the cell allows the neuron to glide forward and the trailing cytoplasmic region to retract. Subsequent to the forward movement of the nucleus and the soma, a new

interstitial adhesion junction forms and the migration cycle starts again so that migration continues in a cyclical, saltatory manner.

Each step of this complex morphological remodelling is finely regulated by an extensive network of protein interactions and signalling pathways, reviewed in (Heng et al., 2010; Huang, 2009; Kawauchi and Hoshino, 2008; Marin et al., 2006).

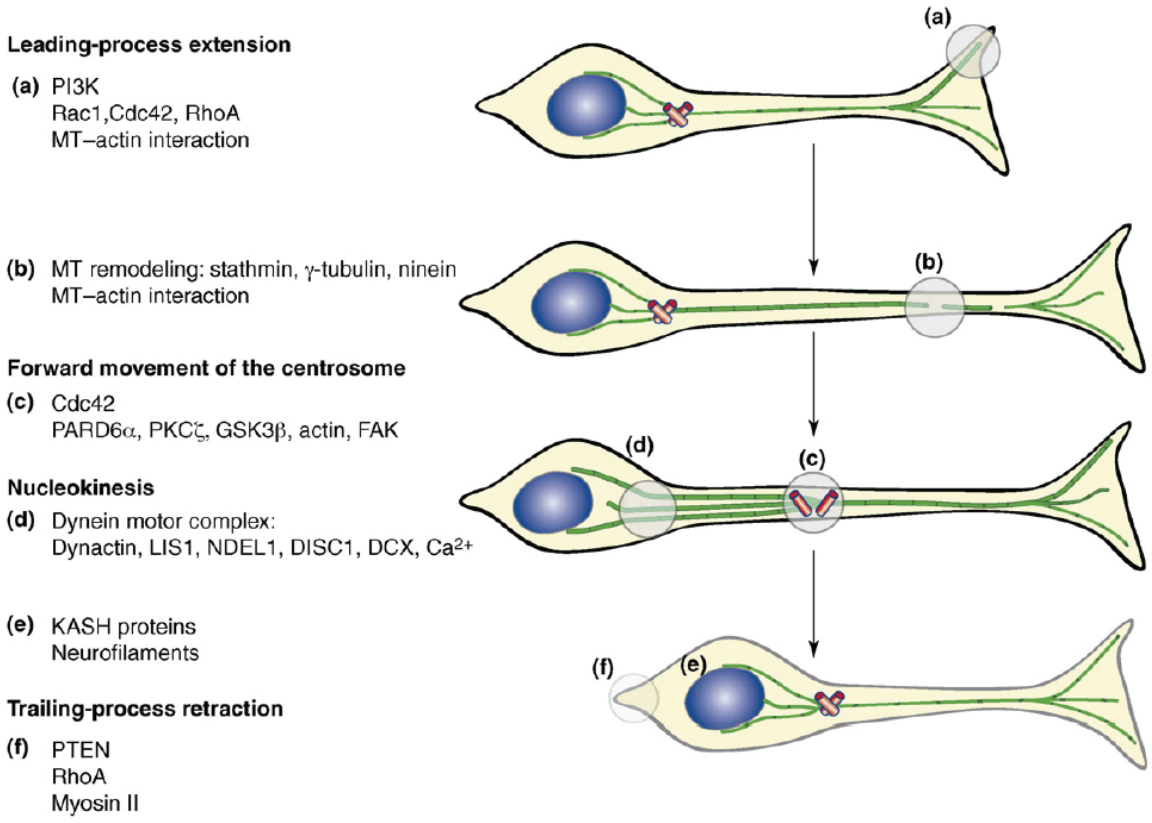

Fig. 12: Schematic representation of the four-step process undergone by radially migrating neurons. Main molecular factors implicated in each phase are listed on the left panel. Adapted from (Marin et al., 2006)

III. Integration of rates of proliferation, neuronal production and radial migration

Each cortical area is characterized by specific cytoarchitectonic properties that are determined by the thickness and cell density of each of the six cortical layers. During corticogenesis, the area-specific cytoarchitecture relies on the spatiotemporal regulation of the rate of proliferation of GZ precursors, through the control of G1/S phase transition, and of the timing of the last mitosis [reviewed in (Dehay and Kennedy, 2007)].

Structure and regulation of the cell-cycle

In cortical progenitors, as in other somatic cells, proliferation and growth arrest are regulated by a balance of extrinsic and intrinsic signals that modulate entry, progression into and exit from the cell-cycle [reviewed in (Cunningham and Roussel, 2001)]. Work on mutant mice has shown that the overall size of the brain is governed by the molecular machinery of the cell-cycle (Ferguson et al., 2002; Nakayama et al., 1996).

The complex regulatory and signalling pathways that regulate cell-cycle progression are highly conserved in eukaryotes. The cell-cycle is comprised of four successive phases: DNA synthesis S phase and mitosis M phase are separated by two gap phases G1 and G2 [reviewed in (Cunningham and Roussel, 2001; Frank and Tsai, 2009)] (Fig. 13). The unidirectional progression of the cell-cycle is ensured by checkpoints that ensure that all phases of the cell-cycle are executed in the correct order. G1 phase is a critical time window during which the cell can respond to extracellular cues that induce or not progression through the restriction point (Mummery et al., 1987). Beyond this first checkpoint, the cell will either commit to a further round of cell division or leave the cell-cycle to enterG0 and embark on a differentiation pathway (Zetterberg et al., 1995). Of note, terminally differentiated neurons cannot undergo cell-cycle re-entry. Another important feature of G1 phase is the control of DNA integrity and preparation of DNA replication origins. After the cells have passed the restriction point, they commit to DNA replication, during S phase. Once the entire genome is duplicated, cells enterG2 phase, during which cells check the completion and fidelity of DNA replication prior to progress further into mitosis. If genome integrity is confirmed, cells undergo mitosis, equally dividing the DNA content, the nucleus and the cytoplasm in two daughter cells. The last checkpoint occurs during mitosis, ensuring that chromosomal kinetochores are properly attached to the mitotic spindle, allowing the sister chromatid to segregate in each daughter cell [reviewed in (Frank and Tsai, 2009)].

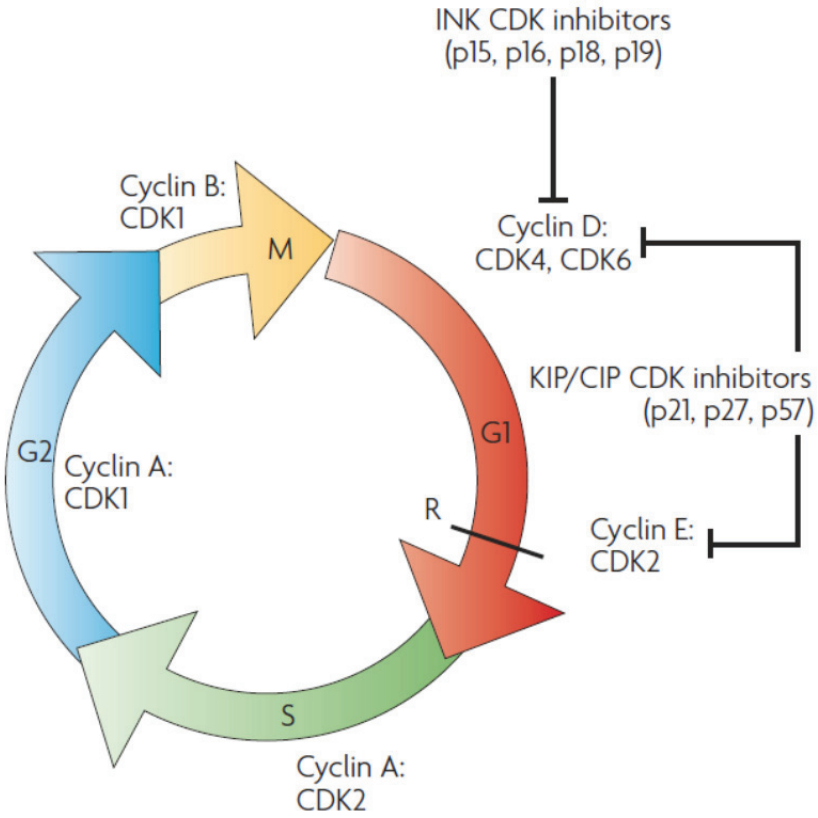

Fig. 13: Structure and regulation of the cell-cycle. Progression in each cell-cycle phases (G1, S, G2 and M) is controlled by different Cyclin/CDK complexes and CDK inhibitors of the INK4 and KIP/CIP family, reviewed in (Dehay and Kennedy, 2007)

Proper timing of progression from one phase of the cell-cycle to the next is tightly regulated by oscillating expression, activation, and inhibition of positive and negative regulators [reviewed in (McClellan and Slack, 2006; Murray, 2004; Sherr and Roberts, 1999)] (Fig. 13).

Cyclin-dependent kinase (CDK) and their activating partners, the cyclins, form complexes that positively drive progression of the cell-cycle, whereas by binding to and inactivating cyclin–CDKs, CKIs negatively regulate progression through the cell-cycle. G1 progression is promoted by CDK4/cyclin D and CDK6/cyclin D activation, in early to mid G1, followed by cyclin E/CDK2 complexes in late G1 (Fig. 13). The cyclins and CDKs associate to phosphorylate the retinoblastoma tumour suppressor protein, Rb. This derepresses E2F transcription factors, thus able to induce downstream target genes required for subsequent cell-cycle progression. Cyclin A/CDK2 complexes and are active in the G1-S phase boundary and throughout S phase (Fig. 13). Cyclin A/CDK1 drives the cell through G2 phase (Fig. 13). At the G2/M transition, cyclin A is degraded and CDK1 associates with newly synthesized cyclin B, to trigger mitosis entry (Fig. 13).

Nevertheless, to ensure that cell-cycle progression occurs only under the appropriate environmental conditions, cyclin–CDK activity is tightly regulated at several levels: through control of cyclin synthesis and degradation; assembly of cyclin and CDK subunits, inhibitory and activating phosphorylation and dephosphorylation events of the CDK subunit;

subcellular localization; and inhibition by association with CDK inhibitors (CKIs) [reviewed in (Sherr and Roberts, 1999)]. CKI prevent CDK from binding to ATP, and hence block their catalytic activity (Sherr and Roberts, 1999). There are two families of CKIs: INK4 and Cip/Kip (Elledge and Harper, 1994; Sherr and Roberts, 1999). CKIs of the Ink4 family (p15Ink4b, p16Ink4a, p18Ink4c and p19Ink4d) are specific inhibitors of CDK4 and CDK6 but not to other CDKs or to D-type cyclins, and are therefore specific for early G1 phase (Fig. 13). CKIs of the Cip/Kip family (p21Cip1, p27kip1and p57Kip2) have a broader specificity, able to bind both to cyclin and CDK subunits, of all cyclin–CDK complexes, thus not specific for a particular phase (Fig. 13). By binding to cyclin/CDK complexes they modulate their activity: at low levels they promote assembly and nuclear localization of active cyclin/CDK complexes but at higher levels can inhibit them (Sherr and Roberts, 1999). Downregulation of p27kip1accompanies progression through G1 phase and is permissive for the periodic activation of cyclin E-CDK2 and cyclin A-CDK2, which drive S phase. Conversely, G1 progression can be stopped by p21 and p27kip1, following anti-mitogenic signals or DNA damage for example, leading to cell-cycle arrest.

Control of neuron number

The production of the correct number and relative proportion of each neuronal type in individual layers relies on a tight spatiotemporal control of the rate of neuron production through cell-cycle regulation (Polleux et al., 1997a; Polleux et al., 1997b) [reviewed in (Dehay and Kennedy, 2007)]. Two cell-cycle parameters determine neuron number: the rate of cell-cycle progression and the balance between cell-cycle re-entry or exit (Caviness et al., 2003; Lukaszewicz et al., 2005; Polleux et al., 1997b). The mode of division, which is correlated to G1-phase regulation is the major player in determining the size of the precursor pool and neuron number (Pilaz et al., 2009).

During mouse corticogenesis, the progressive increase in neuron production, linked to the increased frequency of differentiative divisions, is correlated with a slowing down of cell-cycle progression, mainly due to a lengthening of the G1 phase (Caviness et al., 1995; Dehay et al., 2001; Polleux et al., 1997b; Takahashi et al., 1995a). Different studies revealed that a long G1 phase is associated with differentiative divisions whereas short G1 is linked to proliferative divisions (Calegari et al., 2005; Calegari and Huttner, 2003; Lukaszewicz et al., 2005; Lukaszewicz et al., 2002; Pilaz et al., 2009; Polleux et al., 1997b). A prolonged G1 phase could facilitate the integration of extrinsic differentiation signals that influence cell fate (Mummery et al., 1987) and/or allow an unequally inherited cell-fate determining factor(s) to act over a sufficient time period (Calegari and Huttner, 2003; Gotz and Huttner, 2005).

Cell-fate and laminar determination

Laminar commitment relies on the timing of the terminal mitosis. The earliest-born neurons form the deep layers of the cortex and later-generated neurons occupy successively higher layers, according to the stereotypic inside-out mode of corticogenesis (Angevine and Sidman, 1961; Caviness, 1982). The cell fate seems to be determined during the S phase of the last progenitor cell division in the GZ (McConnell and Kaznowski, 1991). Thus, timing of cell-cycle exit influences neuronal fate and that fate is determined within a precise window during the cell-cycle. This process of neuronal fate specification is also regulated by the interaction of cell-intrinsic programs of transcriptional regulation (Shen et al., 2006) with extrinsic patterning signals according to time and region of the proliferative zone in which the final mitotic cycle occurs (Fishell, 1995; McConnell and Kaznowski, 1991).

Area-specific rates of neuron production and areal differences in migration rates

Neuronal production and laminar cell fate determination are regulated in an area-dependent fashion. Areal differences in cytoarchitecture and laminar neuron number are general features of the cortex across species (Rockel et al., 1980; Skoglund et al., 1996). Area-specific differences in the rate of cell-cycle progression, mode of division (Polleux et al., 1997b) and cell fate (Polleux et al., 2001) show that cortical areas originate from a mosaic of distinct proliferative programs in the various germinal compartments in rodents. In the primate, area 17 and 18 of the primate visual cortex were used as a model system to shed light upon the developmental mechanisms that contribute to the specification of distinct cytoarchitectonic areas. In the adult, area 17 has twice more neurons in the upper layers with respect to its neighbouring area, area 18, from which it is separated by a sharp border (Rockel et al., 1980) (Fig. 14B). During mid corticogenesis, the GZ that generate area 17 are thicker than the one generating area 18, especially the OSVZ (Fig. 14A). More, area-specific differences in cell-cycle kinetics occur selectively at the time of upper layer neuron production (Dehay et al., 1993; Lukaszewicz et al., 2005). Area 17 OSVZ precursors are characterized by both a shorter G1 phase and increased rates of cell-cycle re-entry compared with area 18 OSVZ precursors. These differences in cell-cycle regulation are underlined by differences in the levels of expression of the CKI p27kip1 and cyclin E, important regulators of S-phase entry (Lukaszewicz et al., 2005). Modelling the observed differences in both rates of cell-cycle re-entry and in the length of the G1 phase shows that the combined variation of these two parameters is sufficient to generate the enlarged supragranular layers that distinguish area 17 from the adjacent area 18.

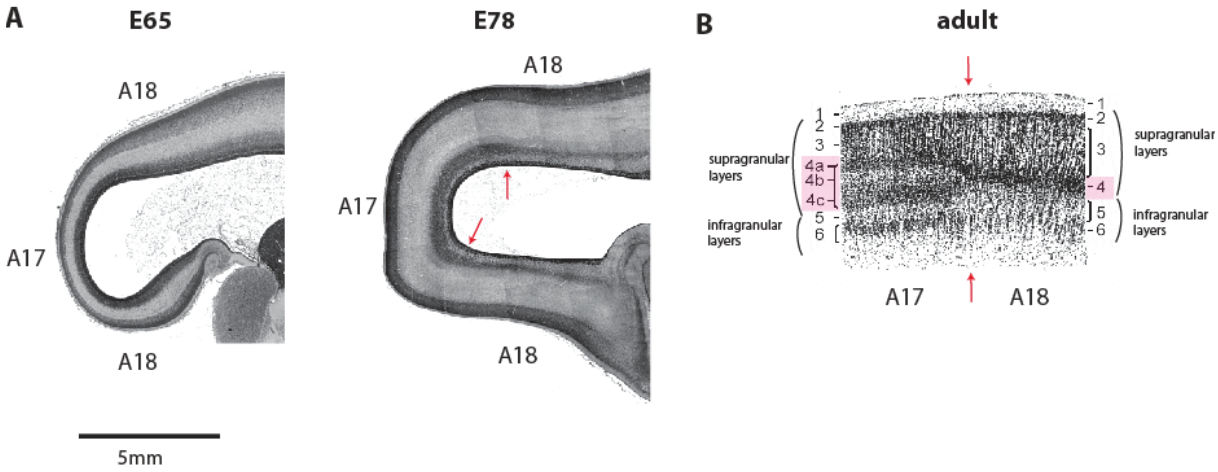

Fig. 14: Microphotographs of Nissl stained parasagittal sections of developing (A) and adult (B) primate area 17 and area 18.
A: Parasagittal sections of the primate developing occipital lobe at E65 (time of production of infragranular layer neurons) and E78 (time of production of supragranular layer neurons). At E78, note the increased thickness of GZ in area 17 (due to the OSVZ enlargement), which is not seen in area 18. Red arrows represent the border between the two areas. Adapted from (Smart et al., 2002)
B: Nissl stained section cutting through the border (red arrows) between area 17 and area 18 in the adult primate cortex. Note the increased thickness of the supragranular layer in area 17, in particular layer 4.

The proper development of the cortex requires a tight spatiotemporal orchestration of multiple fine-tuned developmental processes. In particular, there is the need for a precise regulation and coordination of the developmental programs governing neuron production and migration. For instance, increased rates of neuron production might be correlated to increased rates of migration so as to avoid congestion in the migratory pathways. Preliminary *in vivo* results based on tritiated-thymidine pulse injections combined with one to two weeks survival times suggest that, during the production of supragranular layer neurons, cohorts of area 17 and 18 neuroblasts migrate out of the GZ to the CP with different rates of progression (Lukaszewicz et al., 2006). These data show that a cohort of labelled migrating neuroblasts reach the CP earlier in area 17 than in area 18. However, the interpretation of these in vivo data is made complex by the fact that the radial progression is not continuous and instead there are clearly defined horizontal compartments (Smart et al., 2002) where migrating neurons may pause (Altman and Bayer, 1990).

The possibility of a coupling between proliferation/ neuron production rates and migration rates in the developing cortex is therefore an important open question which remains to be explored, as well as the underlying mechanisms.

In the first part of this thesis, I have addressed this question at the system level. Using area 17 and area 18 of the primate as a model, I have shown, using real-time imaging that rates of proliferation and radial migration are coordinated and regulated in an area-specific manner. I have also shown that the modular protein p27kip1-which expression level is differentially regulated in the GZ of area 17 and area 18 (Lukaszewicz et al., 2006; Lukaszewicz et al., 2005)- is a likely candidate to mediate this area-specific coupling of rates

of neuron production and rates of migration. In the second part, I have used the developing mouse cortex to further explore the p27kip1-related cellular and molecular mechanisms that contribute to coordinate neuron proliferation and migration during corticogenesis. I have largely focused my investigation on the interkinetic migration (INM) of the cycling APs in the VZ, where cell-cycle progression and migration are integrated. Therefore, the subsequent sections of this bibliographic introduction will review the pleiotropic role of p27kip1in cell-cycle control, differentiation and migration as well as the regulatory mechanisms of the INM.

IV.Proliferation and migration coupling by $p27^{kip1}$

$p27^{kip1}$: a modular protein with multiple roles

Before describing the role of p27kip1in key stages of corticogenesis, I shall first review recent findings showing that p27kip1regulates multiple cellular processes that are critical for the histogenesis of various tissues. In particular, I shall focus on the migration promoting role of p27kip1via its interaction with the Rho pathway.

a. $p27^{kip1}$: a well described cell-cycle inhibitor

The protein p27kip1was first identified as a cell-cycle inhibitor almost 20 years ago (Polyak et al., 1994).p27kip1is a member of the Cip/Kip family of CKIs (Cyclin-dependent Kinase Inhibitors) and is a well characterized negative regulator of G1-phase cell-cycle progression (Sherr and Roberts, 1999). Homozygous deletion of the p27kip1 gene in mice causes a general rise in cell proliferation in various organs, leading to increased body and organ size (including the brain), as well as increased tumorigenesis (Fero et al., 1998; Fero et al., 1996).

When p27kip1was cloned, it was first identified as an inhibitor of cyclin–CDK complexes (Polyak et al., 1994; Slingerland et al., 1994; Toyoshima and Hunter, 1994). Through its N-terminal domain, p27kip1 tightly associates with both cyclin (residues 25 to 52) and CDK (residues 52 to 93) (Russo et al., 1996) (Fig. 15A). Structural studies showed that p27kip1 binds to cyclin/CDK complexes in three steps: an α-helix of p27kip1 initiates a first contact with a conserved cyclin box; a second helix binds the N-terminal lobe of the CDK subunit and inserts itself deep inside the catalytic cleft, mimicking ATP binding mechanism (Russo et al., 1996). This prevents the cyclin–CDK complexes from binding to ATP and thereby blocks their catalytic activity (Russo et al., 1996). Of note, p27kip1 also facilitates both the assembly and the nuclear import of cyclinD1-CDK4 complexes (Cheng et al., 1999; LaBaer et al., 1997).

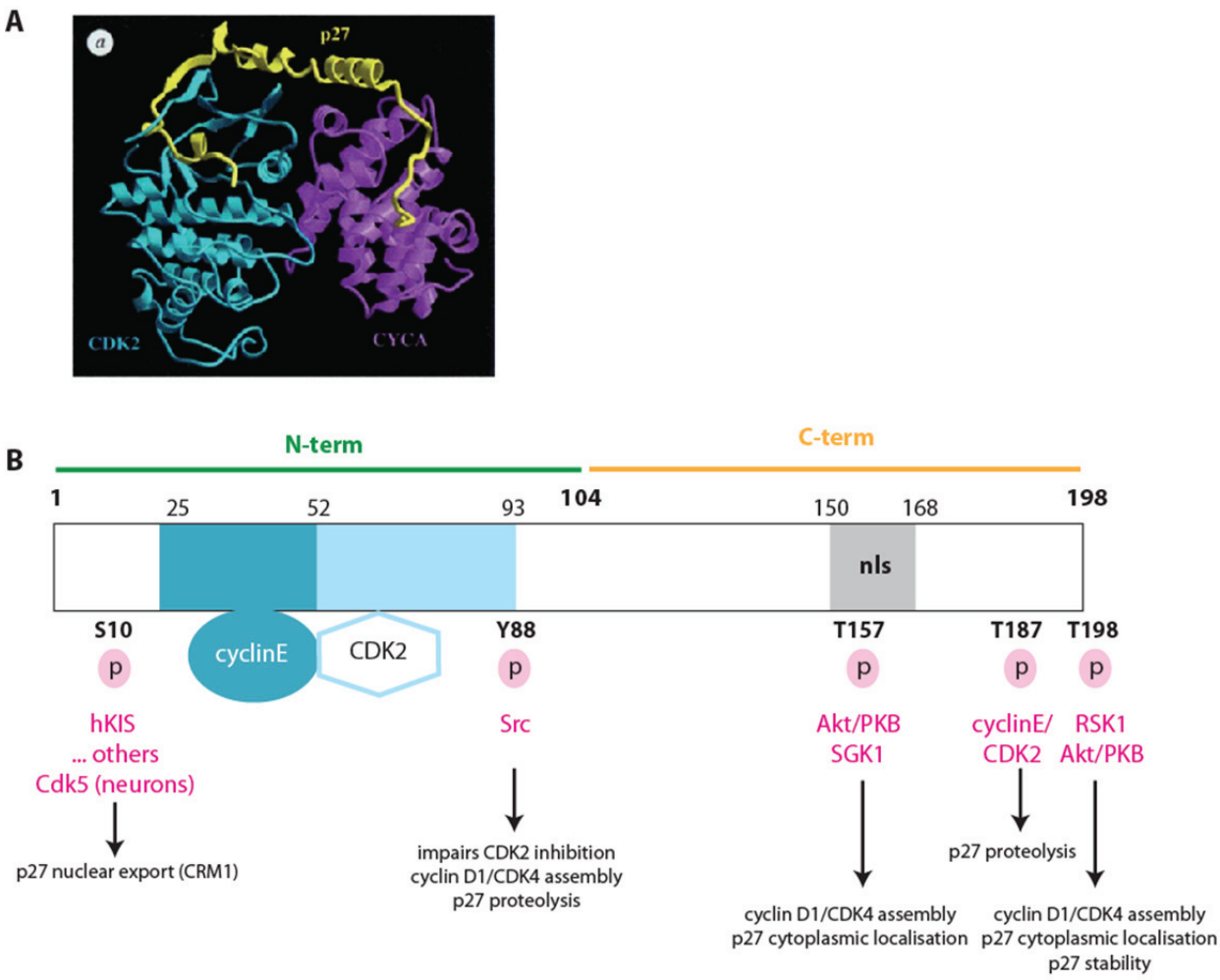

Fig. 15: Structure of the p27kip1 protein, its main domains and phosphorylation sites.
A: Crystal structure of p27kip1N-term domain bound to the CyclinA/CDK2 complex. p27kip1 binds the complex as anextended structure interacting with both cyclin A and CDK2 (Russo et al., 1996).
B: p27kip1N-term and C-term domains and phosphorylation sites. The binding domain with the Cyclin/CDK complexes is represented in blue. Phosphorylation sites are in pink. Kinases that phosphorylate p27kip1at specific sites are listed, as well as the resulting effects on p27kip1function. Adapted from (Russo et al., 1996) and (Larrea et al., 2009b)

b. Spatiotemporal regulation of $p27^{kip1}$expression

p27kip1protein levels are highest during G0 and early G1 phases, then rapidly fall in late G1 and S phases (Nourse et al., 1994; Reynisdottir et al., 1995). p27kip1downregulation is controlled by a decline in translation (Hengst and Reed, 1996) and mainly by ubiquitin-mediated proteolysis which is phosphorylation-regulated (Pagano et al., 1995). Of note, microRNAs may also regulate p27kip1 synthesis (Gillies and Lorimer, 2007).

To function as a CDK inhibitor (CKI), p27kip1 needs to be localized in the nucleus. p27kip1 contains a nuclear localization signal (NLS) harboured in the C terminus (residues 153-166) (Zeng et al., 2000) (Fig. 15B). p27kip1 requires association with the nuclear pore-associated protein mNPAP60 to be imported in the nucleus (Hammond et al., 2009).

The regulation of p27kip1 protein level, function and localization involves several signalling pathways, relying on p27kip1 phosphorylation events. To date, five different phosphorylation sites on p27kip1 have been characterized (Fig. 15B).

- S10 is phosphorylated by the serine-threonine kinase KIS (Kinase Interacting Stathmin), mediating p27kip1 nuclear export in early G1 by binding to the carrier protein CRM1 (Boehm et al., 2002; Connor et al., 2003; Ishida et al., 2002; Ishida et al., 2000; McAllister et al., 2003; Rodier et al., 2001). Other kinases, such as Mirk/dyrk1B (Deng et al., 2004) and PKB/Akt and ERK2 (Fujita et al., 2002; Ishida et al., 2000), were also reported to phosphorylate p27kip1 on Ser10 *in vitro*. Of note, the atypical cyclin-dependent kinase Cdk5 phosphorylates p27kip1on Ser10 in neurons (details p58-59).

- Y74, Y88, Y89 are phosphorylated by the Src-family kinase in early G1, leading to a loss of p27kip1inhibitory action towards Cyclin/CDK complexes. Tyrosine phosphorylation by Src is also required for activation of assembled cyclin D1/CDK4 complexes, to promote G1 progression (Chu et al., 2007; Grimmler et al., 2007; James et al., 2008; Larrea et al., 2008).This subsequently facilitates cyclinE-CDK2-mediated T187 phosphorylation and SCF Skp2-dependent p27kip1proteolysis (Chu et al., 2007; Grimmler et al., 2007).

- T187 is phosphorylated in the S and G2 phases of the cell-cycle by active cyclin E and A-CDK2. This targets p27kip1for degradation via the SCF Skp2 ubiquitin proteasome pathway (Carrano et al., 1999; Nakayama and Nakayama, 2006; Sheaff et al., 1997; Sutterluty et al., 1999; Tsvetkov et al., 1999; Vlach et al., 1997).

- T157 is phosphorylated by a downstream PI3K effector kinase, Akt (or PKB, Protein kinase B), which sequesters p27kip1in the cytoplasm by impairing nuclear import (Liang et al., 2002; Shin et al., 2002; Viglietto et al., 2002) and activates the assembly function of p27kip1for cyclin D1-CDK4 (Larrea et al., 2008). SGK1 (Serum and Glucocorticoid-regulated Kinase 1) also contributes to T157 phosphorylation and cytoplasmic mislocalization of p27kip1 (Hong et al., 2008).

- T198 is phosphorylated by RSK1 (or p90 ribosomal S6 kinase), a kinase activated downstream of both MAPK and PI3K. This mislocalizes and stabilizes p27kip1 in the cytoplasm (Fujita et al., 2002; Larrea et al., 2009a). T198 can also be phosphorylated by PKB/Akt, inducing its export to the cytoplasm (Fujita et al., 2002) and activating the assembly function of p27kip1 for cyclin D1-CDK4 (Kossatz et al., 2006; Larrea et al., 2008; Liang et al., 2007). T198 phosphorylation also regulates p27kip1 stability by preventing its ubiquitin-dependent degradation (Kossatz et al., 2006; Liang et al., 2007).

c. Cytoplasmic $p27^{kip1}$: an alternative function in cell migration

Cancer studies have uncovered a new cyclin–CDK inhibition independent function of p27kip1 when localized in the cytoplasm. In numerous human cancers, p27kip1 protein expression deregulation occurs mostly via relocation to the cytoplasm, rather than via mutation as is the case for most of the tumour suppressors. This cytoplasmic localization of

p27kip1 is associated with an increased tumour aggressiveness and a poor clinical outcome (Bloom and Pagano, 2003; Philipp-Staheli et al., 2001; Ponce-Castaneda et al., 1995; Slingerland and Pagano, 2000). Several influential studies [reviewed in (Besson et al., 2004a)] have analysed the underlying mechanisms and showed that, in addition to its growth-inhibitory function when located in the nucleus, p27kip1 is a regulator of cytoskeletal structure and cell migration when located in the cytoplasm.

The involvement of p27kip1 in the promotion of migration was first reported in hepatocellular carcinoma cells, in which delivery of a transducible form of p27kip1(TAT-p27kip1) led to high cytoplasmic p27kip1 levels and promoted cell migration (Nagahara et al., 1998). Further analysis showed that fibroblasts from p27-/-mice present a motility defect, rescued by re-expression of p27kip1 (Besson et al., 2004b; McAllister et al., 2003).

The importance of p27kip1 cytoplasmic localization in the regulation of cell migration was illustrated in numerous cancer studies. Expressing cytosolic mutant forms of p27kip1 in melanoma, breast cancer, glioma cell lines and metastatic hepatocellular carcinoma cells increased their motility *in vitro* (Denicourt et al., 2007; Larrea et al., 2009a; Wang et al., 2008; Wu et al., 2006). Moreover, p27kip1 knock-down reduced tumorigenicity and invasion in a xenograft model (Wu et al., 2006), while expression of cytoplasmic p27kip1 greatly enhanced the metastatic and invasive properties of melanoma cells *in vivo* (Denicourt et al., 2007).

The increased cell migration resulting from cytoplasmic p27kip1 was shown to be independent from its cell-cycle role. Indeed, expression of the N-terminal half of p27kip1, containing the functional cyclin-CDK binding domain (Fig. 15B), fails to induce cell migration (McAllister et al., 2003). Moreover, re-expression of a p27kip1 mutant that cannot bind to cyclin–CDK complexes (p27CK-) was able to restore migration of p27 -deficient cells (Besson et al., 2004b). p27kip1 role in promoting migration relies on a C-terminal “scatter domain” (residues 118 to 158) (McAllister et al., 2003) (Fig. 15B). A SQx7AxI motif (residues 140 to 151) was shown to be critical to promote migration. This motif is also found in the yeast cell-cycle inhibitor homolog Far1p C-terminal region involved in actin rearrangement (McAllister et al., 2003).

In the cytoplasm, p27kip1 colocalizes with F-actin at both the membrane and in areas of organized actin filaments (McAllister et al., 2003). Some actin-related structures, such as stress fibres and focal adhesions, were found to be more numerous in p27-/- fibroblasts, thus exercising a negative effect on cell motility (Besson et al., 2004b). These cellular features are indicative of high RhoA GTPase activity (Besson et al., 2004b). The RhoA pathway has been shown to be involved in the remodelling of the actin cytoskeleton, which plays a crucial role in migration (Narumiya et al., 2009). Inhibition of the RhoA pathway by Y27632 rescued the migration defect (Besson et al., 2004b). Furthermore, p27kip1 and RhoA can interact both *in vitro* and in cells transfected with RhoA (Besson et al., 2004b), binding which subsequently interferes with RhoA activation (details p54). p27kip1 co-immunoprecipitate with RhoA via its C-terminal half (Besson et al., 2004b; Larrea et al., 2009a). Moreover, it appears that phosphorylation of the last residue of p27kip1 (Thr-198)

by RSK1, in addition to promoting p27kip1 cytoplasmic localisation and stabilization, enhances RhoA-p27 binding (Besson et al., 2004b; Larrea et al., 2009a).

To summarize, p27kip1promotes migration in several cell types, independently from its cell-cycle function. p27kip1 binds to RhoA, through its C-term domain, and prevents RhoA pathway activation, which in turn allows a dynamic remodelling of the actin cytoskeleton necessary for cell migration.

However, while some studies show that p27kip1 cytoplasmic localization promotes cell motility, others show the opposite. For instance, in cells of mesenchymal origin such as fibrosarcomas (Baldassarre et al., 2005), endothelial cells (Goukassian et al., 2001), mesangial cells (Daniel et al., 2004) or smooth muscle cells (Diez-Juan and Andres, 2003; Sun et al., 2001), p27kip1 acts as an inhibitor of cell migration. One possible source of discrepancy between these studies appears to come from cell type dependent differences in the signalling pathways. For instance, in sarcoma cells, p27kip1was shown to bind and inhibit stathmin, a microtubule destabilizing protein that promotes microtubule depolymerisation (Baldassarre et al., 2005). Another source of variability in the results is linked to the type of motility assay. For instance, different tumour cell lines can move in either an amoeboid or an elongated mode, with distinct requirements for the GTPases Rho and Rac. The elongated mode is associated with Rac dependent protrusions that are rich in actin filaments, whereas the amoeboid migration is dependent on RhoA signalling (Sahai and Marshall, 2003). In fibroblasts migrating in a 3D matrigel matrix, p27kip1 was found to inhibit elongated migration, whereas it was promoting amoeboid migration (Berton et al., 2009).

Lastly, the effect of p27kip1 can also vary depending on the degree of the Rho pathway inhibition. Indeed, efficient migration requires a tightly balanced activation and deactivation of Cdc42, Rac and RhoA both spatially and temporally (Ridley et al., 2003). Insufficient levels of Rho–GTP will inhibit migration by preventing cells from achieving sufficiently strong adhesion and traction to move forward (Nobes and Hall, 1999; Worthylake et al., 2001). Conversely, excessive Rho activity can inhibit cell migration by increasing adhesion to the substrate and preventing focal adhesion turnover (Arthur and Burridge, 2001; Cox et al., 2001; Ren et al., 1999; Sahai et al., 2001). Increased Rac-mediated cell-to-cell interactions also prevent migration (Malliri and Collard, 2003).

Crosstalk between CKI and Rho-GTPases

As mentioned above, the CKI p27kip1binds to RhoA, through its C-term domain, and prevents RhoA pathway activation, which in turn allows a dynamic remodelling of the actin cytoskeleton necessary for cell migration.

a. The Rho-GTPases family

The Rho-GTPases are low molecular weight guanine nucleotide binding proteins tethered to the cellular membrane. In this area, they can be activated by various upstream signals, including receptor tyrosine kinases (RTK), integrins (αβ) and G-protein-coupled receptors (GPCR) (Fig. 16). Rho-GTPases are binary molecular switches that control multiple signalling events regulating functions such as cell movement, gene transcription, cell growth and proliferation, as well as cell-cycle progression.

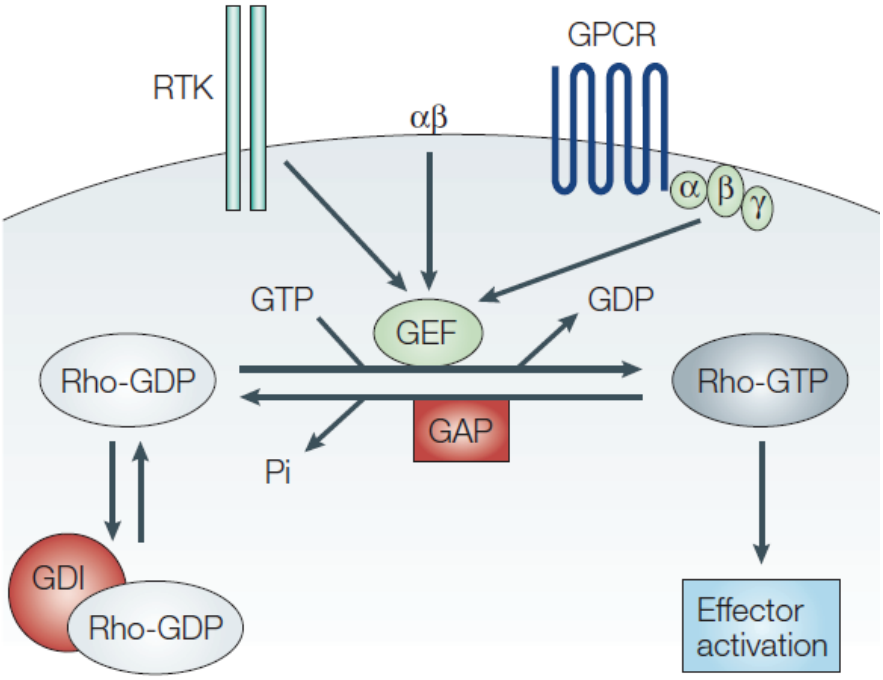

Fig. 16: Regulation cycle of Rho-GTPases activity.
Rho-GTPases are sequestered in the cytoplasm in their inactive GDP-bound state by guanine nucleotide dissociation inhibitors (GDIs). After reception of upstream signals coming from receptor tyrosine kinases (RTK), integrins (αβ) and G-protein-coupled receptors (GPCR), guanine nucleotide exchange factors (GEFs) exchange GDP for GTP, thus activating Rho-GTPases. Rho-GTPases can return to their inactive state by GTPase activating proteins (GAPs) that stimulate the slow hydrolysis of bound GTP. Issued from (Besson et al., 2004a)

Rho-GTPases alternate between an inactive GDP-bound state and an active GTP-bound state (Fig. 16). In the active state, they transduce upstream signals by interacting with various downstream effectors proteins. Their activity is promoted by guanine nucleotide exchange factors (GEFs) (Zheng, 2001) that promote the exchange of GDP for GTP (Schmidt and Hall, 2002) (Fig. 16). The return to the inactive state is facilitated by GTPase activating proteins (GAPs) (Moon and Zheng, 2003) that stimulate the slow hydrolysis of bound GTP (Bernards and Settleman, 2004; Zalcman et al., 1999) (Fig. 16). Rho proteins can also be sequestered in the cytoplasm in their GDP-bound form by guanine nucleotide dissociation inhibitors (GDIs) until the cell receives a positive signal (DerMardirossian and Bokoch, 2005; Zalcman et al., 1999) (Fig. 16).

There are currently 20 identified members of the Rho family (Burridge and Wennerberg, 2004; Etienne-Manneville and Hall, 2002; Jaffe and Hall, 2005). Approximately 60 GEFs, 80 GAPs and 3 GDIs have been identified so far, as well as over 60 downstream effectors proteins, providing a wide variety of mechanisms for regulating Rho-family GTPase activities.

Three of the most studied Rho-GTPases are RhoA, Cdc42 and Rac1. The main functions of these proteins are the regulation of actin and microtubule cytoskeletons, cell morphogenesis, polarity, adhesion, migration as well as cell-cycle progression and cytokinesis (Burridge and Wennerberg, 2004; Etienne-Manneville and Hall, 2002; Jaffe and Hall, 2005).

b. Rho-GTPases role in the regulation of cell migration

Cell migration involves polarization of the cell in the direction of the movement, extension of protrusions, formation of new adhesions at the leading edge and forward translocation of the cell body (Ridley et al., 2003; Vicente-Manzanares et al., 2009). Adhesions are subsequently disassembled at the rear of the cell to allow detachment. This cycle of events enables cells to migrate to their destination. The actin cytoskeleton and microtubules (MTs) are critical elements for these events. Actin polymerization at the leading edge drives membrane protrusion. The association of the actin cytoskeleton with integrins regulates their binding to extracellular matrix. The actomyosin motors and integrin-based adhesion receptors provide the force and traction needed to pull the cell body forward and retract the tail. MTs are also polarized in migrating cells and are essential for the directed migration, possibly by delivery of signalling molecules and membrane components (Ridley et al., 2003).

Signals that induce cell migration originate from cell surface receptors, including integrins, growth factor receptors and G-protein-coupled receptors. These signals converge to modulate the activity of Rho-family GTPases (Burridge and Wennerberg, 2004; Etienne-Manneville and Hall, 2002; Ridley et al., 2003). In turn, Rho-GTPases control the cytoskeletal reorganizations that are required for migration (Moon and Zheng, 2003; Narumiya et al., 2009).

Cdc42 is active at the cell front (Itoh et al., 2002), establishing the centrosome polarity that defines the direction of movement. Cdc42 acts in orienting the MT organizing center (MTOC) as well as the Golgi apparatus in front of the nucleus toward the leading edge (Nobes and Hall, 1999), through a Cdc42/Par6/aPKC pathway (review in (Narumiya et al., 2009)). Cdc42 also induces the formation of filopodia, spike-like membrane protrusions containing long parallel actin bundles, that serve as sensors to explore the local environment (Ridley et al., 2003). MRCK, a ROK-related target of Cdc42, is involved in the formation of focal complexes and filopodia (Leung et al., 1998).

Rac1 is active at the front of migrating cells (Itoh et al., 2002). It promotes actin polymerization at the cell edges and the extension of the lamellipodia, made of a meshwork of short branches of actin filaments. Rac1 activates the p21-activated kinases (PAKs), leading to lamellipodia formation and disassembly of stress fibres and focal adhesions (Frost et al., 1998; Manser et al., 1997). Rac1 induces membrane protrusion by stimulating actin polymerization through activation of the WAVE-Arp2/3 complex pathway (Cory and Ridley, 2002; Miki et al., 1998).

RhoA promotes the formation of 'stress fibres' - actomyosin bundles composed of anti-parallel actin filaments cross-liked by myosin- and enhances integrin-based focal adhesions (Riento and Ridley, 2003). Downstream effectors of RhoA are ROCK (Rho-associated coiled-coil forming kinase) (Amano et al., 1997; Ishizaki et al., 1996; Leung et al., 1995; Matsui et al., 1996) and mDia (mammalian homolog of Drosophila diaphanous) (Watanabe et al., 1997) (Fig. 17). ROCK is a serine/threonine kinase that can phosphorylate a variety of substrates (Riento and Ridley, 2003). ROCK can directly phosphorylate myosin light chain (MLC-P) (Amano et al., 1996) (Fig. 17). Otherwise, ROCK phosphorylates and inhibits the myosin-binding subunit of myosin phosphatase (Kimura et al., 1996; Uehata et al., 1997) (Fig. 17). These two actions increase myosin light chain phosphorylation, stimulate cross-linking of actin by myosin and enhance actomyosin contractility. ROCK can also phosphorylate and activate LIM domain-containing protein kinase (LIMK), which in turn phosphorylates and inhibits the actin depolymerisation factor cofilin, regulating actin filament turnover (Maekawa et al., 1999). The phosphatase slingshot dephosphorylates cofilin, which inhibits actin polymerization (Fig. 17). Thus, ROCK and LIMK activity result in an increase in actin stress fibre polymerization and stability, which both promote integrin clustering and focal adhesion assembly (Burridge and Wennerberg, 2004; Ridley et al., 2003) (Fig. 17). The Rho-ROCK signalling is also involved in tail retraction by negative regulation of integrin-mediated adhesions in the tail (Worthylake and Burridge, 2003). The other RhoA effector, mDia, produces actin filaments by catalyzing actin nucleation and polymerization through actin-binding protein profiling (Burridge and Wennerberg, 2004) (Fig. 17). This induces long thin stress fibres along the cell (Goode and Eck, 2007; Higashida et al., 2004; Li and Higgs, 2003). mDia also regulates microtubule dynamics locally, promoting their alignment and stabilization (Ishizaki et al., 2001; Palazzo et al., 2001) (Fig. 17).

Of note, Rho and Rac have antagonistic and complementary functions during migration, implying that a careful balance between their activities is needed for efficient cell migration [reviewed in (Narumiya et al., 2009)].

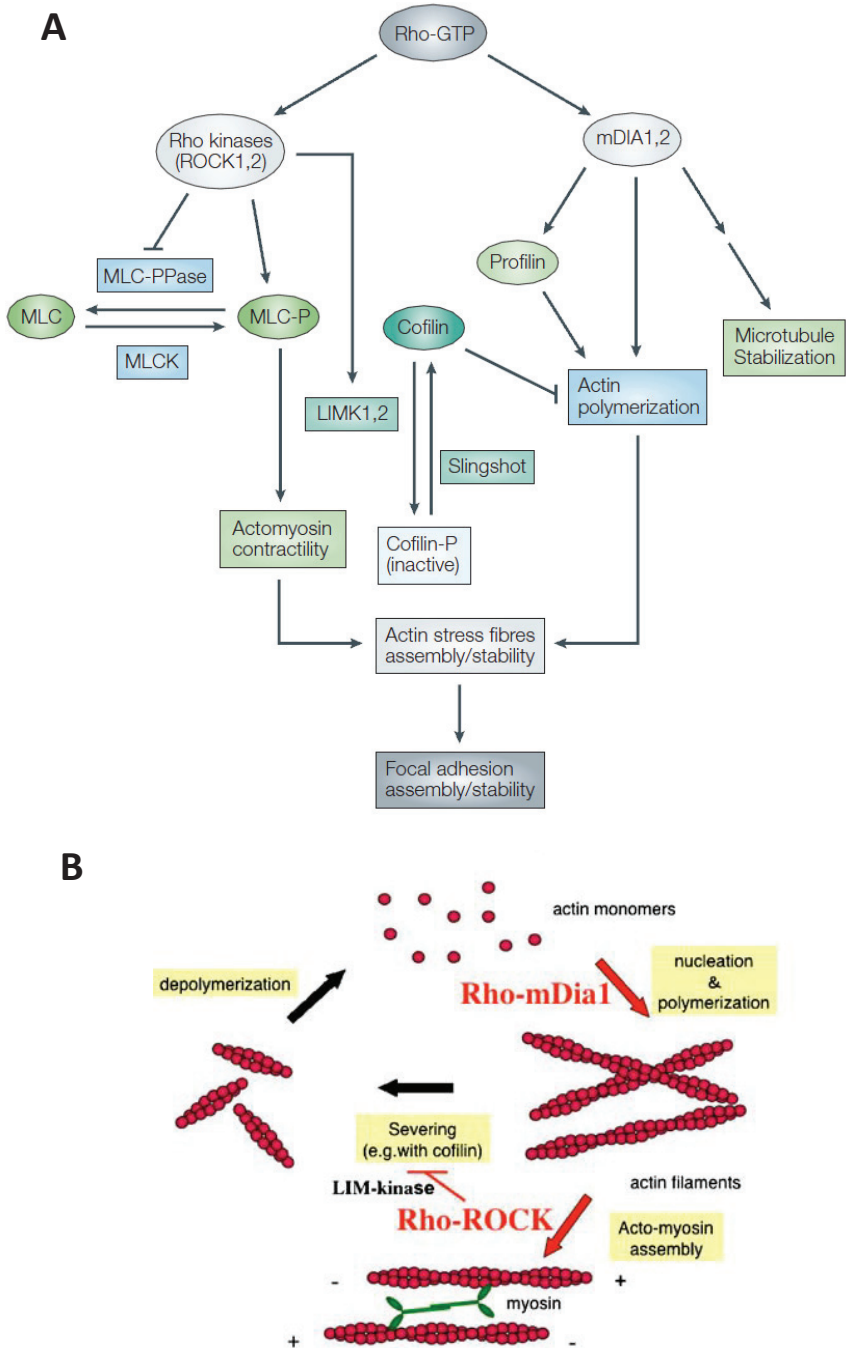

Fig. 17: Regulation of the cytoskeleton by Rho signalling pathway.

A: Diagram showing the main signalling pathways implicating Rho-GTPases in the regulation of both actin and microtubule cytoskeleton. RhoA activates its effector proteins ROCK and mDia. Activation of mDia by Rho facilitates actin nucleation and polymerization as well as the formation and orientation of stable microtubules. ROCK directly phosphorylates myosin light chain (MLC-P) and inhibit MLC-phosphatase (MLC-PPase), increasing the contractility of myosin. ROCK also activates LIM domain-containing protein kinase (LIMK), which phosphorylates and inhibits the actin depolymerisation factor cofilin. This increases actin polymerization, stabilization of actin stress fibres and actomyosin contractility, all promoting integrin clustering, focal adhesion assembly and cell adhesion.

B: Schematic representation of the regulation of actomyosin bundles assembly by Rho.mDia1 catalyzes actin nucleation and polymerization to form actin filaments. ROCK activates myosin to cross-link them. ROCK also inactivates cofilin through LIM-kinase, inhibiting its actin severing and depolymerisation.

Issued from (Besson et al., 2004a) and (Narumiya et al., 2009).

c. Rho-GTPases role in the regulation of cell proliferation

In addition to their role in regulating cell motility, Rho-family GTPases control cell proliferation and transformation. Rho-GTPases act as integrators of extracellular signals responsible for cell-cycle progression and in particular for the G1/S transition (Fig. 18) [reviewed in (Villalonga and Ridley, 2006)].

Rho-GTPases role in G1 phase progression

The first indications of the role of Rho-GTPases in the cell-cycle came from studies using the bacterial exo enzymeC3 transferase. C3 transferase ADP-ribosylates Rho proteins, inhibiting their downstream signalling, and was found to prevent G1 progression in Swiss-3T3 fibroblasts (Yamamoto et al., 1993). The contribution of Rho-GTPases to mitogen-induced G1 progression was further demonstrated by studies using dominant-negative constructs or constitutively active mutants of RhoA, Rac1 and Cdc42 (Olson et al., 1995). The specific molecular events linking Rho-GTPases with the G1 cell-cycle machinery are progressively better understood, in particular involving the regulation of cyclin and CKI expression (Fig. 18).

The Rho-GTPases Rac1, RhoA and RhoE (also known as Rnd3) act together to affect cyclin D1 expression level. They regulate cyclin D1 transcription and/or translation depending on the cellular context (Fig. 18).

Rac1 is an important downstream target of Ras in cyclin D1 transcriptional regulation (Gille and Downward, 1999). Rac and, to a lesser degree CDC42, have been reported to stimulate the expression of cyclin D1 mRNA in both fibroblasts and epithelial cells (Roovers and Assoian, 2003; Welsh and Assoian, 2000), or to promote the translation of cyclin D1 mRNA in human umbilical vein endothelial cells (Mettouchi et al., 2001). Rac1 induction of cyclin D1 transcription involves activation of NF-kB (Boyer et al., 2004) (Fig. 18).

RhoA regulation of cyclin D1 expression is more complex than that of Rac1. In certain cell types, such as mammary epithelial cells, RhoA activation is associated with activation of the cyclin D1 promoter (Liberto et al., 2002). In NIH3T3 cells plated on fibronectin, but not other substrates, cyclin D1 expression and G1 progression were induced through the activation of RhoA (Danen et al., 2000). RhoA indirectly regulates cyclin D1 gene expression in mid-to-late G1 phase, through a pathway involving the kinases ROCK and LIMK and modulating integrin-dependent signalling. RhoA promotes ROCK/LIMK-mediated stress fibre assembly and focal adhesion formation, which, in turn, allows for the sustained clustering of integrins and therefore the sustained activation of ERKs (extracellular-signal-regulated kinases) (Roovers and Assoian, 2003; Roovers et al., 2003; Swant et al., 2005) (Fig. 18). However, a number of studies fail to report such a direct link between RhoA and cyclin D1 induction. Upon RhoA inhibition, cyclin D1 expression is not blocked, and is observed much earlier than usual in G1, through a Rac dependent pathway (Welsh et al., 2001) (Fig. 18).

Thus, RhoA inhibits Rac-dependent cyclin D1 expression and this inhibition requires the nuclear translocation of activated LIMK (Roovers and Assoian, 2000). Therefore, through its stimulatory effect on ERK signalling and its inhibitory effect on Rac signalling, the Rho kinase–LIMK pathway determines whether cyclin D1 is expressed and whether the expression is mediated by ERK or Rac.

Another Rho GTP-binding protein that can affect cyclin D1 translation is RhoE. RhoE expression leads to cell-cycle arrest in fibroblasts and inhibits Ras induced transformation (Villalonga et al., 2004) (Fig. 18).RhoE-expressing cells fail to accumulate cyclin D1 protein, although signalling pathways leading to cyclin D1 transcription are activated normally (Villalonga et al., 2004). Thus, RhoE inhibits cyclin D1 translation (Fig. 18).

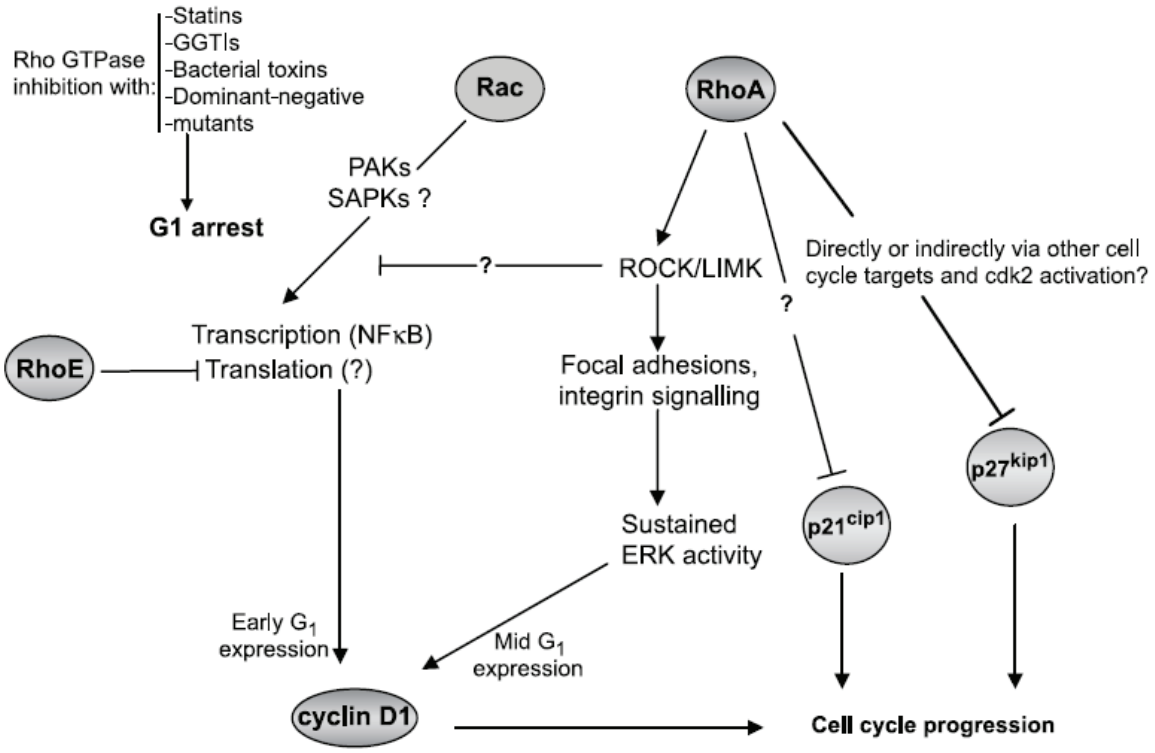

Fig. 18: Rho-GTPases action on G1 phase progression.
Diagram showing the main signalling pathways and molecular events where different members of the Rho family act on both G1 cyclin/CDK complexes and CDK inhibitors. Issued from (Villalonga and Ridley, 2006)

The CKIs p21cip1 and p27kip1 are other major targets of Rho-GTPase signalling within the cell-cycle machinery. In many systems, inhibition of Rho proteins induces up-regulation of these proteins, although the mechanisms underlying this effect are still poorly understood (Fig. 18).

Dominant-negative RhoA increases p21cip1 levels and, conversely, activated RhoA mutants prevent p21 up-regulation in response to geranylgeranyl transferase inhibitors (GTIs) (Adnane et al., 1998). Rho inhibits p21cip1 expression at the transcriptional level, by preventing the increase in p21cip1 levels in response ERK activation by Ras (Olson et al.,

1998; Roovers and Assoian, 2000) (Fig. 18). So, whereas Ras and Rho play opposite roles in the regulation of p21, they have complementary roles in regulating cell proliferation: ERK signalling in Ras-transformed cells precludes cell proliferation unless RhoA downregulates p21.

RhoA activation has been linked to inhibition of p27 mRNA translation efficiency (Vidal et al., 2002). However, the prevailing view is that RhoA is important for p27kip1 degradation. The best characterized proteolytic pathway is mediated by cyclin E–CDK2-dependent phosphorylation of p27kip1 on Thr187, which targets p27kip1 for degradation by the F-Box protein SKP2 (Malek et al., 2001; Slingerland and Pagano, 2000) (cf p43). RhoA stimulates p27kip1 degradation through the activation of cyclinE/CDK2, as evidenced by the observation that dominant-negative CDK2 completely prevents the down-regulation of p27kip1 in response to the expression of an activated RhoA mutant (Hu et al., 1999). RhoA-mediated activation of ROCK and mDia promotes G1 progression via Skp2-mediated degradation of p27kip1 (Mammoto et al., 2004). When spread on fibronectin, endothelial cells required RhoA activity for cell-cycle re-entry to induce SKP2 expression and the subsequent downregulation of p27kip1 (Mammoto et al., 2004).

Rho-GTPases role in mitosis and cytokinesis

Although Rho-GTPases act as essential mediators of G1 phase progression in numerous cell types, some observations indicate that these proteins also control mitosis and cytokinesis (Fig. 19). For instance, in Rat2 fibroblasts, expression of a dominant negative version of Rac1 induces cell-cycle arrest with cells accumulating in G2/M (Moore et al., 1997). In hepatocytes, the Rho effector Citron Kinase (Citron-K) is also required for G2/M progression (Liu et al., 2003). Rho-GTPases regulate actin polymerization and contractility, which are required for cytokinesis, but they also regulate local dynamics of microtubules, crucial for the orientation of the centrosome and the mitotic spindle (Fig. 19).

The RhoA effectors of the mDia family stabilize and align microtubules in interphase cells, and may function during both spindle orientation and chromosome congression (review in (Narumiya and Yasuda, 2006)) (Fig. 19). Centrosome separation occurs early in mitosis in two steps. Separation first occurs around the nuclear envelope, but following nuclear envelope breakdown, separation becomes dependent upon aster MTs attachment to the cell cortex. Some studies indicate a role for Rho in the interaction of aster MTs at the cortex. Lfc is a Rho GEF that associates with MTs in interphase cells and concentrates on spindle MTs in mitosis (Benais-Pont et al., 2003). The Lfc–Rho–mDia1 pathway may regulate aster MTs attachment to the cortex (Bakal et al., 2005; Rosenblatt et al., 2004), as well as MTs attachment to the kinetochore and thus promote spindle assembly in early mitosis (Bakal et al., 2005)(Fig. 19). The Cdc42-mDia3 pathway also plays a role in regulating the attachment of MTs to kinetochores (Fig. 19). This is important for ensuring proper chromosome alignment during metaphase, which contributes to their correct segregation during anaphase (Yasuda et al., 2004).

Rho family proteins are also crucial mediators of cytokinesis (cytoplasmic division), generating two daughter cells at the end of the cell division cycle. During cytokinesis, an actomyosin-based ring forms and contracts, leading to the physical cleavage of the cell body. Since the contractile ring composition is similar to that of stress fibres, cooperation of the Rho effectors, mDia, ROCK and Citron-K, promotes the formation and the contractility of the actomyosin bundles in the cytokinesis ring (Kosako et al., 2000; Watanabe et al., 2008)(Fig. 19).

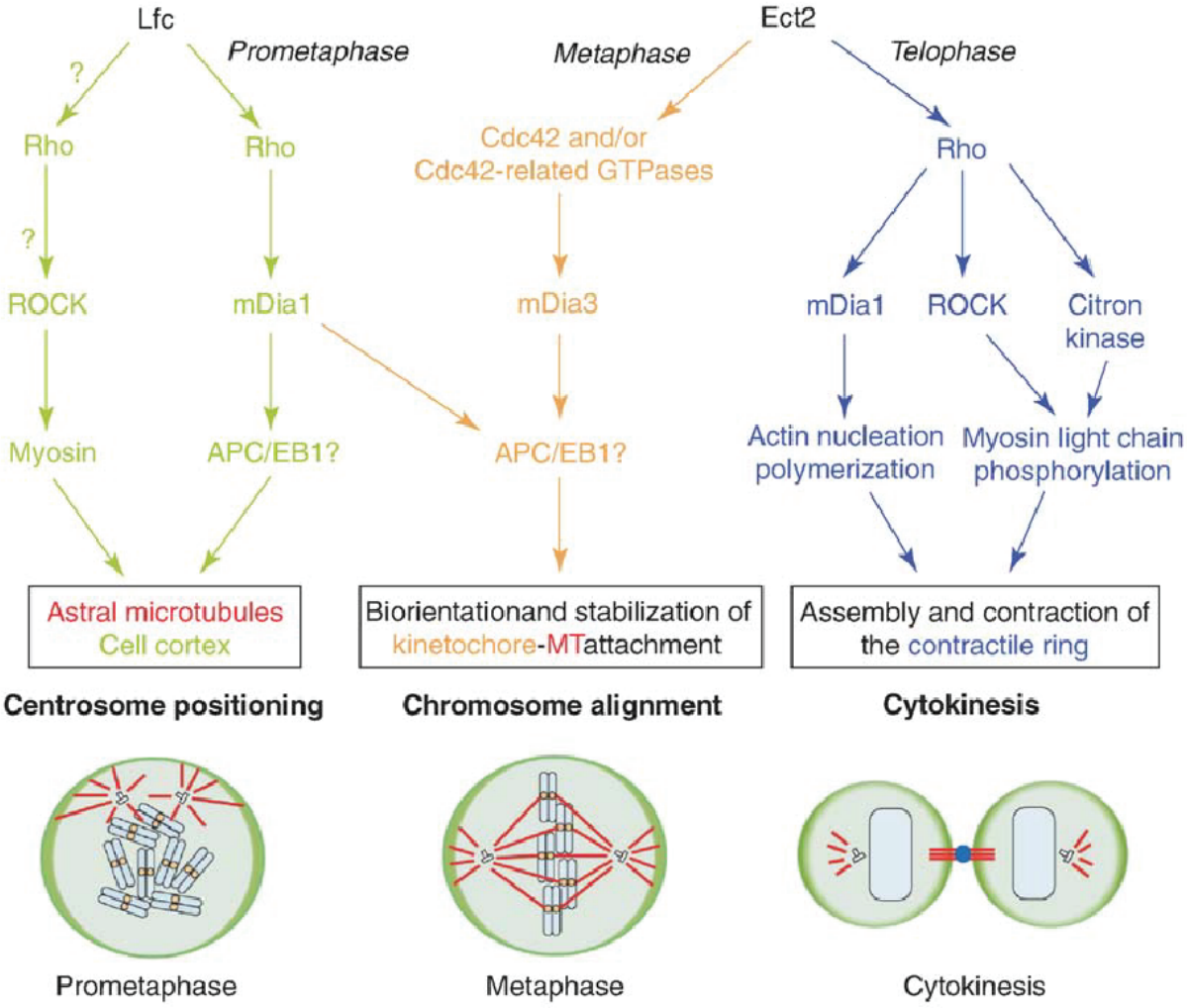

Fig. 19: Roles of Rho-GTPases in mitosis and cytokinesis.
(i) The Rho GEF Lfc is activated in prophase. In prometaphase, RhoA/ROCK and RhoA/mDia activations are implicated in the attachment between aster microtubules and the cell cortex for centrosome separation and spindle orientation. (ii) The Rho GEF Ect2 activates Cdc42 in metaphase. mDia3 activation facilitates bi orientation and stabilization of attachment of the spindle microtubules (MTs) to the kinetochore, to ensure correct chromosomal alignment at the metaphase plate and segregation in anaphase. (iii) The Rho GEF Ect2 also activates Rho in telophase, leading to Rho accumulation in the cleavage furrow, and recruitment of mDia1, ROCK and citron kinase, working together to assemble and contract the actin ring. Issued from (Narumiya and Yasuda, 2006)

d. Modulation of the RhoA pathway by Cip/Kip proteins

Not only does Rho signalling regulate the levels and timing of expression of cell-cycle regulators, but cytoplasmic Cip/Kip CKIs can also inhibit the activity of various components of the Rho-signalling pathway (Fig. 20). This negative feedback loop allows the coordinated control of cellular proliferation with cytoskeletal reorganization and cell migration (Besson et al., 2004a).

In the cytoplasm, p21cip1 binds to and inhibits ROCK1, impairing ROCK-mediated LIMK activation and modulation of actin cytoskeleton organization (Lee and Helfman, 2004)(Fig. 20). This promote neurite extension in neuroblastoma cells and hippocampal neurons cells (Lee and Helfman, 2004; Tanaka et al., 2002), and lead to loss of actin stress fibres and decreased phosphorylated cofilin in NIH3T3 cells (Lee and Helfman, 2004; Tanaka et al., 2002). However, in mouse fibroblasts, the loss of p21cip1 had no effect on their migratory ability (Besson et al., 2004b).

On the contrary, cytoplasmic p27kip1 is able to promote cell migration by binding to and inhibiting RhoA (Besson et al., 2004b; Larrea et al., 2009a) (cf p44-45). ROCK inhibition rescued the migration of p27−/− cells, indicating that p27kip1affected the Rho pathway upstream of ROCK (Besson et al., 2004b)(Fig. 20). Furthermore, p27kip1does not interfere with RhoA binding to its effectors, becausep27kip1 has been shown to inhibit the activation of wild-type RhoA but not of a constitutively active RhoA mutant (RhoA-63L; always bound to its effector)(Besson et al., 2004b). However, further dominant negative experiments revealed that p27kip1interaction with RhoA interfere with its activation by two Rho-specific GEFs, p115-RhoGEF and Lbc (Besson et al., 2004b). p27 -deficient cells had a significantly higher level of active RhoA-GTP and an increased level of phospho-cofilin, compared to wild-type cells (Besson et al., 2004b). As a reminder, cofilin regulates actin filament turnover, and is inactivated by phosphorylation by LIMK, itself activated by the Rho/ROCK pathway (Maekawa et al., 1999) (cf p48). Thus, p27kip1promotes cell migration by binding to RhoA, preventing its activation and thus reducing RhoA–GTP levels as well as the subsequent activation of the ROCK effectors. Inhibition of the RhoA/ROCK pathway in turn allows cofilin activity for a dynamic remodelling of the actin cytoskeleton(Besson et al., 2004b)(Fig. 20).

Cytoplasmic p57kip2 is able to interact with the effector LIMK of the RhoA-pathway. This induces LIMK translocation and sequestration in the nucleus, where it cannot inactivate cofilin to regulate the actin cytoskeleton (Yokoo et al., 2003). This inhibition by p57kip2, shown in osteoblasts, leads to a loss of LIMK1-associated stress fibres (Fig. 20).

Overall, Cip/Kip proteins inhibit the Rho pathway at distinct points, leading to a net decrease in Rho-induced formation of actin stress fibres and focal adhesion (Fig. 20).

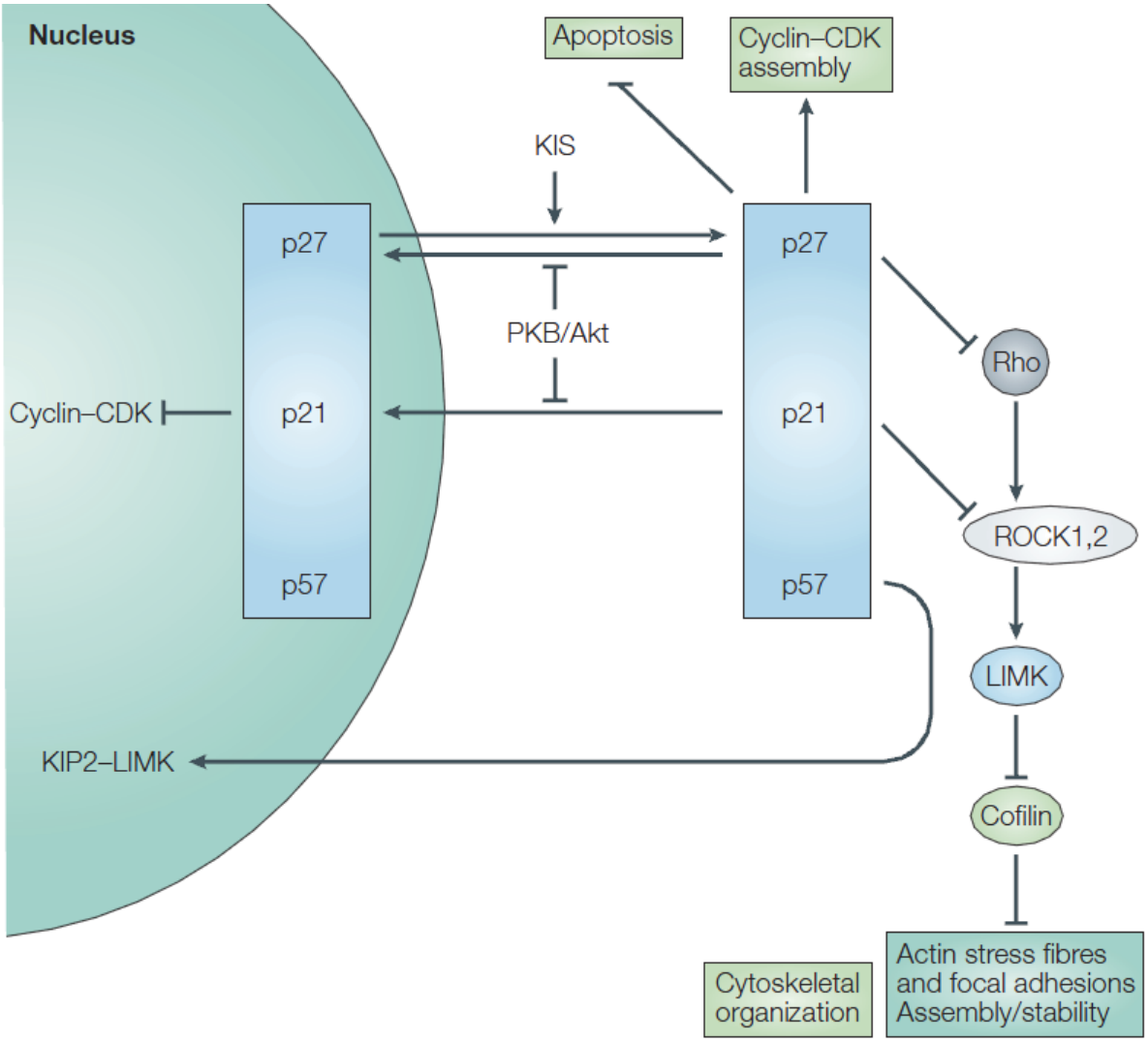

Fig. 20: Regulation of the Rho pathway and the cytoskeleton by CDK inhibitors.
Phosphorylation events regulate the shuttling of p21 and p27between the cytoplasm and the nucleus. When localized in the cytoplasm, p27, p21 and p57 inhibit the Rho-signalling pathway at different levels, affecting cytoskeletal organization and cell motility. Issued from (Besson et al., 2004a)

$p27^{kip1}$ diverse roles in the cerebral cortex

p27kip1 is the most important CKI for cerebral cortex development. Indeed, while p21Cip1 and p57Kip2 are expressed in neurons of the cortical plate, p27kip1is expressed in all layers of the developing cerebral cortex (Nguyen et al., 2006a). In addition to its well documented role in the control of cell proliferation, p27kip1has been shown to influence other developmental processes in the nervous system, including cell fate choices and differentiation (Baldassarre et al., 1999; Munoz-Alonso et al., 2005; Nguyen et al., 2006a; Ohnuma et al., 1999; Sasaki et al., 2000; Vernon et al., 2003), as well as radial migration (Kawauchi et al., 2006; Nguyen et al., 2006a; Nguyen et al., 2006b)(see Fig. 21).

a. $p27^{kip1}$ inhibits neuronal progenitors proliferation

In cortical progenitors, p27kip1expression levels influence two cell-cycle parameters, the cell-cycle length and the probability of cell-cycle exit (Lukaszewicz et al., 2005). p27kip1 overexpression in cortical progenitors induces a premature lengthening of their cell-cycle, mostly resulting from an extension of G1 phase duration (Lukaszewicz et al., 2005; Mitsuhashi et al., 2001). p27kip1 modification of the cell-cycle length duration also impacts on the birth date of cortical projection neurons (Caviness et al., 2003). Accordingly, p27-/-cortices show an enlargement of upper cortical layers, resulting from the reduction in neuronal production during mid-corticogenesis followed by an increase in production of late born neurons (Goto et al., 2004). Conversely, overexpression of p27kip1in cortical progenitors results in a reduced number of upper layer neurons (Tarui et al., 2005). Moreover, p27kip1is involved in areal differences in neuronal production in the primate, where p27kip1 expression levels differ significantly between cortical areas (Lukaszewicz et al., 2005).

b. $p27^{kip1}$ promotes neuronal differentiation

In the mouse neocortex, p27kip1also promotes neuronal differentiation (Nguyen et al., 2006a; Nguyen et al., 2006b). Analysis of post-mitotic neuronal markers in Bromodeoxyuridine (BrdU) birth-dating cells in p27-/-embryos, or after utero electroporation of p27kip1siRNA, revealed a decreased differentiation into neurons, whereas overexpression of p27kip1promoted the differentiation (Nguyen et al., 2006a). Of note, overexpression of other Cip/Kip genes, p21Cip1 or p57Kip2, did not affect neuronal differentiation (Nguyen et al., 2006a). Neurogenic activity is not abolished by the suppression of the cell-cycle regulatory function of p27kip1in cortical progenitors. Bypassing of the cell-cycle function of p27kip1was performed by replacing the coding sequence of p27kip1by p27 CK- (a mutant version that no longer binds to cyclins and CDKs(Besson et al., 2004b)).p27kip1therefore regulates cell-cycle exit and neuronal differentiation through distinct molecular mechanisms.

p27kip1 promotes the differentiation of cortical progenitors by up-regulating Neurogenin2 expression(Nguyen et al., 2006a)(Fig. 21). Ngn2 is a proneural basic Helix-Loop-Helix (bHLH) protein that promotes the selection of neuronal precursors from neuroepithelial cells and drives their differentiation into specific subsets of neurons(Parras et al., 2002). Ngn2 is the main proneural factor expressed by cortical progenitors(Fode et al., 2000)and it regulates both their differentiation into projection neurons and their laminar destination(Schuurmans et al., 2004).Interestingly, Ngn2 and p27kip1are extensively coexpressed in cortical VZ and SVZ cells(Kawaguchi et al., 2004; Nguyen et al., 2006a).Strikingly, there was a significant reduction in the number of VZ/SVZ cells expressing

Ngn2 in p27knockout cortices that was not observed in p27CK-cortices(Nguyen et al., 2006a).

p27kip1 stabilises Ngn2 protein in cortical progenitors by a mechanism that depends on the integrity of its N-terminal half (Fig. 21) but does not require interactions with cyclin and CDKs (Nguyen et al., 2006a). p27kip1 may interact and sequestrate specific ubiquitin ligases (Laman et al., 2005) that target Ngn2 to the proteasome for degradation, or may mask some residues that are important for Ngn2 ubiquitination (Reynaud et al., 2000). p27kip1 could also influence neuronal differentiation by regulating the expression of other factors or by extending the cell-cycle duration and providing a time window for the accumulation of specific cell fate determinants in VZ cells, during G1.

Of note, in Xenopus, p27Xic1 promotes the differentiation of Müller glial cells in the retina (Ohnuma et al., 1999) and is required in combination with the proneural protein X-NGNR1 for the formation of primary neurons (Vernon et al., 2003). Separate domains in the N-terminal region are independently responsible for driving progenitors out of the cell-cycle and controlling their fate determination (Ohnuma et al., 1999; Vernon et al., 2003). p27kip1 additional role in neuronal differentiation, through its N-terminal domain and Ngn2 activity, hence seems to be an evolutionary conserved mechanism.

c. $p27^{kip1}$ promotes radial migration

p27kip1 promotes cell migration through regulation of the actin cytoskeleton dynamics in several *in vitro* models (Besson et al., 2004b; Diez-Juan and Andres, 2003; Goukassian et al., 2001; McAllister et al., 2003; Sun et al., 2001; Supriatno et al., 2003) (cf p44-45). More, p27kip1 is expressed in migrating cortical projection neurons (Nguyen et al., 2006a), and was shown to contribute to the cytoskeletal changes that also underlie radial migration in the cerebral cortex (Itoh et al., 2007; Kawauchi et al., 2006; Nguyen et al., 2006a).

In p27-/- cerebral cortices, birth-dating analysis revealed a reduced proportion of newly born neurons reaching the CP (Nguyen et al., 2006a). p27 knock down by siRNA electroporation also lead to neurons mispositioning (Itoh et al., 2007; Nguyen et al., 2006a), whereas overexpression of p27kip1, but not other Cip/Kip genes, promoted the migration of newly born neurons away from the germinal zones (Nguyen et al., 2006a). In contrast, cortices expressing p27CK-, a cell-cycle mutant form of p27kip1 (Besson et al., 2004b), did not show significant migration defect (Nguyen et al., 2006a). This confirms that p27kip1 promotes neuronal migration independently of its cell-cycle function, as it was the case in fibroblasts (Besson et al., 2004b; McAllister et al., 2003).

In cortical progenitors, p27kip1 is able to stabilize Ngn2 (Nguyen et al., 2006a), which can control radial migration. Ngn2 can regulate the transcription of genes important for cell migration (Ge et al., 2006) and its phosphorylation on a tyrosine residue in its C-terminal domain specifies the morphology and polarity of radially migrating pyramidal neurons (Hand et al., 2005). However, coelectroporation of Ngn2 was not able to rescue the migration

defect induced by p27kip1 knock-down, showing that p27kip1 regulates neuron migration through a mechanism that does not involve Ngn2 (Nguyen et al., 2006a).

Cortical neuron migration requires the inhibition of the activity of RhoA (Hand et al., 2005; Kholmanskikh et al., 2003). In the developing rodent neocortex, RhoA mRNA expression is high in the premigratory cortical VZ and SVZ, and low in cells migrating in the IZ (Ge et al., 2006; Nguyen et al., 2006a; Olenik et al., 1999). Electroporation of the VZ of embryonic mouse cortex with RhoA or DN-RhoA, followed by slice culture, shows that ectopic expression of RhoA blocks radial migration, whereas interfering with RhoA function promotes migration. Taken together, these findings suggest that downregulation of RhoA activity is required for the radial migration of neurons. Mechanisms of RhoA regulation involving Ngn1 and 2, Par6, FilaminA or Semaphorin 3A are reviewed in (Govek et al., 2010). They allow to draw a more complete picture, in which a reduction in RhoA levels and activity are required to commence migration, and persistently low levels may regulate actin reorganization, actomyosin contractility, and transcription required to drive motility and the cessation of movement.

Studies analyzing p27kip1 effect on radial migration revealed that the mechanism by which p27C-terminal domain promotes the migration of fibroblasts, by blocking the activation of the small GTPase RhoA (Besson et al., 2004b), also operates for the migration of cortical neurons (Nguyen et al., 2006a)(Fig. 21). Indeed, coelectroporation of a dominant negative version of RhoA with p27siRNA rescued the neuronal migration defect caused by p27knock-down (Nguyen et al., 2006a).

Another study has shed light on the upstream and downstream events that explain how p27kip1 promotes radial migration (Kawauchi et al., 2006). First, the atypical cyclin-dependent kinase Cdk5, whose activity is restricted to post-mitotic neurons (Dhavan and Tsai, 2001), was shown to phosphorylate p27kip1 at Serine 10 (Kawauchi et al., 2006) (Fig. 21). This allows the stabilization of p27kip1 in the cytoplasm, hence promoting the migration of cortical neurons. In the cerebral cortex, it was already shown that Cdk5 associate with its coactivator p35 to promote radial migration, through phosphorylation of several targets that influence microtubule stability, dynein motor complex activity and actin cytoskeleton dynamics (Gupta et al., 2002). Immunohistochemistry analysis revealed that p27kip1 and Cdk5 were colocalized in the perinuclear region as well as in punctuate cytoplasmic inclusions in the tips of neuronal processes, colocalizing with F-actin (Kawauchi et al., 2006). Cdk5 and p27kip1 participate in regulating the multipolar morphology of neurons, as both dominant negative Cdk5 and p27kip1 shRNA expressing cells in the lower IZ are round with thin processes instead of multipolar (Kawauchi et al., 2006).

Second, these authors confirmed that p27-mediated inhibition of the RhoA pathway in neurons promotes actin reorganization by activating cofilin, an actin depolymerising /severing protein (Kawauchi et al., 2006), as is the case in fibroblasts (Besson et al., 2004b) (cf p48) (Fig. 21). As a reminder, the RhoA effector ROCK phosphorylates and activates LIMK, which in turn phosphorylates and inactivates cofilin (Maekawa et al., 1999) (Fig. 17). Inhibiting Cdk5 activity or p27kip1 activity individually both resulted in increased cofilin

phosphorylation, lower F-actin amount in neurons, hence resulting in impaired cortical migration (Kawauchi et al., 2006). The importance of cofilin phosphorylation to radial migration is further highlighted by the arrest of neuronal precursors in the IZ after electroporation of a phosphorylation deficient cofilin mutant (Kawauchi et al., 2006).

To summarize, Cdk5 increases the amount of cytoplasmic p27kip1 via Ser 10 phosphorylation, which subsequently inhibits the RhoA/ROCK/LIMK pathway, thus suppressing the phosphorylation of cofilin. Non-phosphorylated active cofilin can finally promote the actin cytoskeleton remodelling necessary for neuronal migration (Fig. 21).

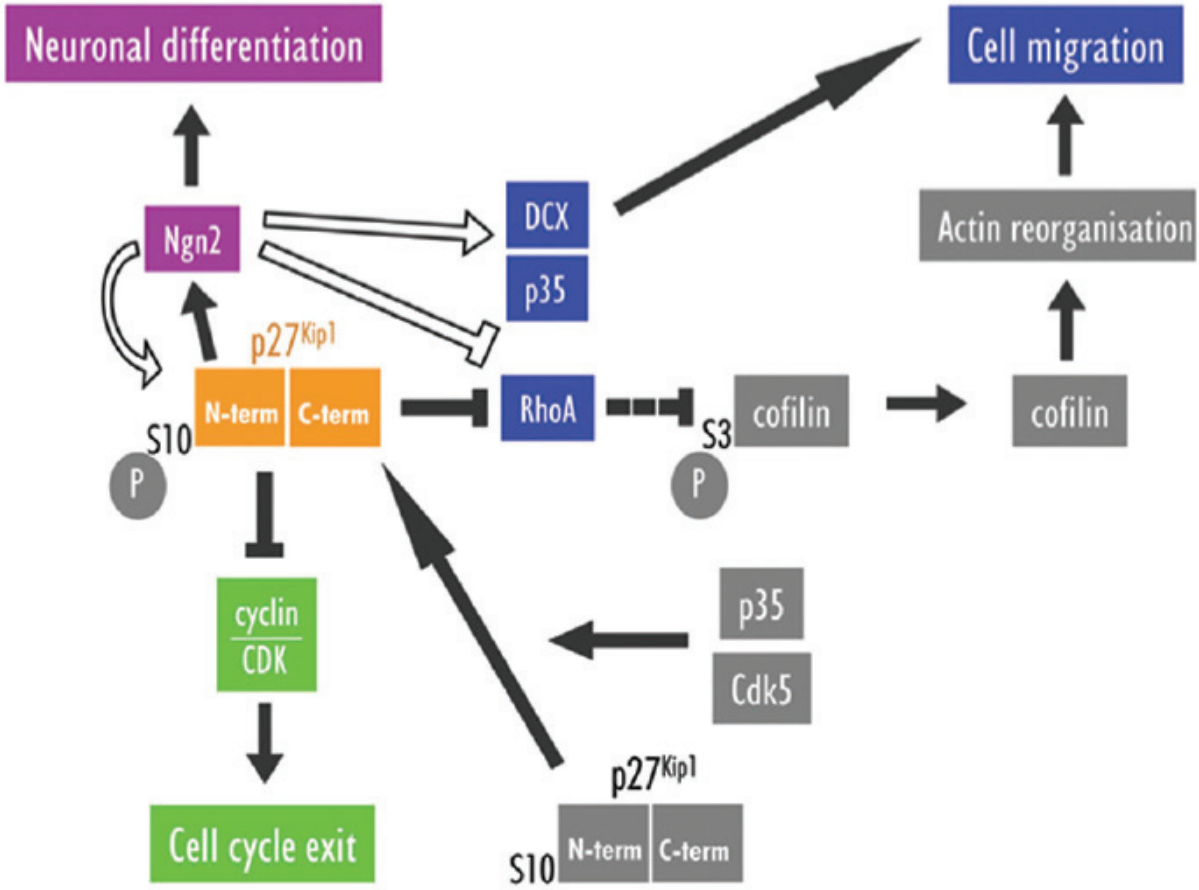

Fig. 21: Coupling of neuronal proliferation, differentiation and migration signalling pathways by p27kip1.

p27kip1 binds to CDK/cyclins complexes through its N-term domain, in the nucleus, leading to cell-cycle exit (molecular pathway in green). p27kip1 also stabilises Ngn2 in the nucleus through its N-term domain, promoting neuronal differentiation (molecular pathway in purple).

Cdk5 phosphorylates p27kip1 to Ser10, regulating its stability and promoting its cytoplasmic distribution. In the cytoplasm, p27 C-term domain binds to and inhibits RhoA, promoting radial migration (molecular pathway in blue). A downstream target of p27kip1activity on the RhoA pathway is cofilin, an actin-binding protein with actin-severing activity (molecular pathway in grey). Black arrows represent nontranscriptional interactions and white arrows represent transcriptional interactions. Issued from (Nguyen et al., 2006b)

Coupling of proliferation and migration during corticogenesis

The generation of cerebral cortex neurons requires that progenitor cells leave the cell-cycle and initiate specific differentiation genetic programs. Subsequently, postmitotic neurons migrate radially to reach their final destination in the CP, before their terminal maturation into functional neurons. Although a lot of progress has been made in the understanding of the cellular and molecular regulation of these basic events, how proliferation, differentiation and migration are integrated into a coherent developmental program during corticogenesis has yet to be elucidated.

Multifunctional proteins like p27kip1, that regulate both cell-cycle exit, differentiation and migration are likely to be major players in orchestrating the major steps of cortical development (Ohnuma et al., 2001). The modular protein, p27kip1 promotes both cell-cycle exit, neuronal differentiation and radial migration of cortical neurons, through the regulation of distinct molecular pathways (Kawauchi et al., 2006; Nguyen et al., 2006a), reviewed in (Nguyen et al., 2006b) (Fig. 21). Its N-terminal domain activity is implicated in the promotion of cell-cycle exit, by an inhibitory association with CDK/cylins complexes. Its N-terminal domain also stabilizes Ngn2, leading to neuronal differentiation (Nguyen et al., 2006a). When located into the cytoplasm, p27C-term domain has been shown to promote radial migration of cortical neurons, through inhibition of the RhoA pathway (Besson et al., 2006; Kawauchi et al., 2006; Nguyen et al., 2006a).The resulting modulation of ROCK effector activity leads to increase of non-phosphorylated activated cofilin, leading to actin cytoskeletal reorganization in migrating neurons processes (Kawauchi et al., 2006).The p27-related signalling network is made complex by feedback loops (Fig. 21). Ngn2 is thought to promote the transcription of p27kip1 in cortical progenitors (Farah et al., 2000). Ngn2 also activates the transcription of genes regulating radial migration (Ge et al., 2006).Lastly, the direct crosstalk between p27kip1 and components of the Rho pathway might provide a mechanism for coordinating proliferation and the cytoskeleton reorganization during migration.

In this thesis, I have first examined how proliferation and migration rates are coordinated during corticogenesis using a system level approach in the developing primate visual cortex. This model provides the unique possibility to explore whether and how area-specific changes in rates of proliferation are correlated with changes in rates of radial migration. In a second step, using the mouse model, I have embarked on exploring the role of p27kip1 in regulating progenitor cells behaviour (including Interkinetic Nuclear Migration, cell-cycle progression, mode of division and progenitor cell fate), and in controlling radial migration of post-mitotic neurons (Fig. 22).

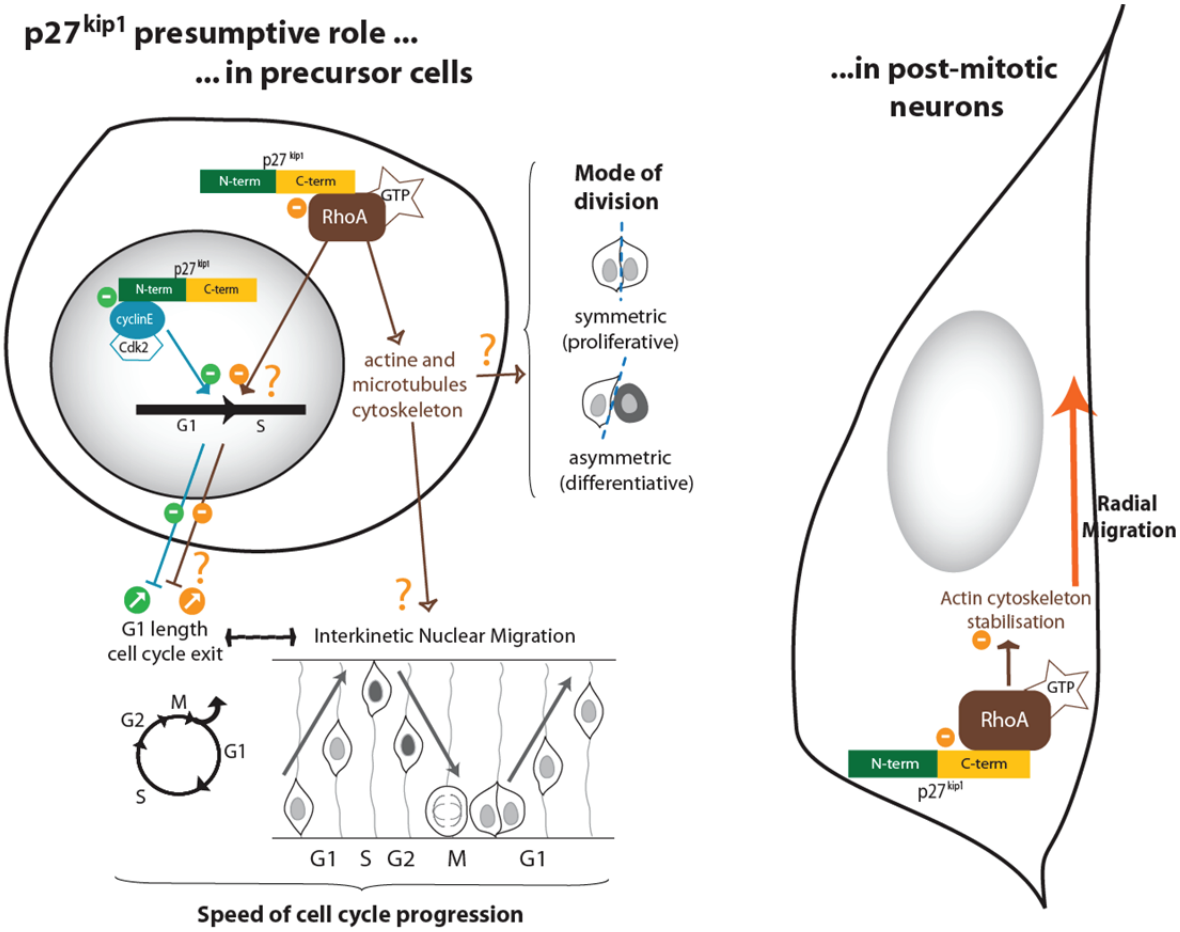

Fig. 22: Schematic representation of the putative role of p27kip1in the neuronal progenitor cells and in neurons of the cerebral cortex, focusing on its action on the RhoA pathway.
When located in the nucleus of progenitor cells, p27 N-terminal domain inhibits CDK/cyclins complexes. This results in (i) slowing down S phase, (ii) lengthening cell-cycle duration,(ii) altering INM kinetics,(iii) altering progenitor fate or (iv) promoting cell-cycle exit. In the cytoplasm, p27C-term domain can inhibit RhoA, thereby leading to reorganization of the cytoskeleton as well as potentially impacting on the INM movement and the orientation of the plane of division. More, RhoA can also modify cell-cycle regulators level of expression. In post-mitotic neurons, p27C-terminal mediated RhoA inhibition leads to remodelling of the actin cytoskeleton which promotes radial migration.

Chapter 1: Coordinated rates of proliferation and migration in primate area 17 and area 18

Manuscript in preparation

Abstract

Proper cortical lamination and cytoarchitecture rely on the spatiotemporal coordination of cell-cycle and neuronal production rates in the germinal zones, as well as of kinetics of neuronal radial migration. Here, using area 17 and area 18 of the primate as a model study, we show for the first time that area-specific rates of proliferation are coupled with area-specific rates of radial migration of postmitotic neurons. p27kip1 is known to promote cell cycle exit and differentiation when located into the nucleus, as well as radial migration when located into the cytoplasm. Bi-photonic real time imaging on organotypic embryonic slices coupled with quantitative immunohistochemistry revealed that p27kip1 cytoplasmic expression in GFP expressing migrating neurons was higher in area 17 than in area 18 at E78, congruent with the higher migration kinetics measured in area 17. This points to p27kip1 contributing to the area-specific coordination of proliferation and radial migration dynamics during the development of the primate cortex.

Introduction

The cytoarchitecture of the cerebral cortex is largely determined by variation of the number and density of neurons in individual layers. Cortical cytoarchitecture requires the fine spatiotemporal control of neuron production in the germinal zones and its coordination with radially directed migration. These two processes orchestrate the emergence of cortical layers and ultimately cortical circuitry.

A number of studies have revealed a fate map of distinct proliferative programs in the germinal zones, that are spatially and temporally coordinated to generate the layout of cortical areas. In rodents and primates, mathematical modelling of results of birth-dating experiments has shown that variations in rates of proliferation are correlated to the neuron numbers in cortical layers, and that adjacent areas showing different neuron number are generated by differences in the cell-cycle parameters during corticogenesis. This area-specific modulation of rates of neuron production raises the question of whether rates of radial migration of postmitotic neurons are also area-specifically regulated, as suggested by static *in vivo* observations in the developing primate visual cortex (Lukaszewicz et al., 2006).

p27kip1 (p27), a Cip/Kip member, has recently been shown to regulate actin dynamics and cell migration, in postmitotic radially migrating pyramidal neurons and tangentially migrating interneurons, via inhibition of the RhoA signalling (Nguyen et al., 2006a) and binding to the microtubules (Labouesse et al., unpublished).

Until recently, Cip/Kip members were viewed as nuclear proteins with a principal function of inhibiting cyclin/CDK dependent kinase (CDK inhibitor). Multiple phosphorylation events on p27 regulate its shuttling between the nucleus and the cytoplasm. Phosphorylation on Ser10 induces its export from the nucleus. While cytoplasmic localization results in the loss of the cyclin–CDK inhibitory function of p27(Nter domain), p27 can, via its Cter domain, bind to the GTPase RhoA, and prevent its activation, thereby regulating the actin cytoskeleton and cell migration and other aspects of RhoA signalling. Importantly, p27has been shown to regulate the cell-cycle progression of cortical precursors via its CDK inhibitor activity (Caviness et al., 2003; Goto et al., 2004; Lukaszewicz et al., 2005; Tarui et al., 2005) and its level of expression in the germinal zones varies in an area-specific manner (Lukaszewicz et al., 2005)(Lukaszewicz et al., 2006), making it a putative candidate to coordinate proliferation and migration.

In order to explore the mechanisms that coordinate proliferation and migration in the embryonic cortex, we have examined the dynamics of radial migration in visual area 17 (A17) and area 18 (A18) of the developing primate. These two adjacent areas are characterised by strikingly distinct cytoarchitectural features: area 17 exhibits enlarged and densely packed supragranular layers as well as a highly developed granular layer (layer 4) compared to area 18. These cytoarchitectural differences have been shown to stem from distinct proliferative programs and rates of neuron production observed during the generation of supragranular layers (E75-E85) (Dehay et al., 1993; Lukaszewicz et al., 2005). No difference in proliferation could be detected during the generation of infragranular layer neurons (between E55 and E70) (Dehay et al., 1993; Lukaszewicz et al., 2005).

Real time imaging of EGFP expressing cortical precursors and newborn neurons on organotypic slices allowed us to monitor several parameters of cell motility during radial migration in area 17 and area 18, including movement speed and amplitude, as well as pause number and duration.

Material and methods

Animals

Foetuses from timed-pregnant rhesus monkeys (Macaca fascicularis) were delivered by caesarian section according to protocols described in Lukaszewicz et al (Lukaszewicz et al., 2005). All experiments were performed in compliance with the national and European laws as well as with institutional guidelines concerning animal experimentation.

Plasmids

The pCAGGS-IRES-EGFP vector was generously provided by J. Briscoe (National Institute for Medical Research London, U.K.), where a [cDNA]-nlsIRES-EEGFP cassette is under the control of aCMV enhancer and a chicken beta-actin promoter. cDNAs encoding full-length human p27 WT were provided by L. Nguyen (GIGA-Neurosciences, University of Liège, Belgium).

Ex vivo electroporation

In E65 and E75 primate embryos, we have implemented *ex vivo* electroporation targeted to the occipital cortex, so as to label precursors from area 17 and area 18. Each dissected hemisphere was embedded in 1% low gelling agarose (Sigma) in PBS at 37°C. 100µl of plasmid solution (0.2-0.4 µg/µl) colored with Fast Green (0.01 mg/mL; Sigma) are microinjected by pressure into the lateral ventricule of the hemisphere, via a Hamilton syringe. 3 pulses of current (50 ms on/1000 ms off) were delivered (voltages: 70-120V for E66; 100-150V for E78) using a pair of gold electrodes (Genepaddles Model 543, Harvard Apparatus, dimensions: 5x7mm). The electrodes were oriented with the anode caudally and the cathode rostrally, so as to target the occipital pole, corresponding to presumptive area 17. To target area 18, the electrodes were positioned with the anode laterally and the cathode on the interhemispheric fissure.

Focal electroporation on slices

Embryonic primate brain slices (300µm thick) fragment was immersed in 20 µl of plasmid solution (0.4 µg/µl). 3-5 pulses of current (10-20V, 50 ms on/1000 ms off) were delivered using a pair of gold electrodes (Genetrode BTX Model 514, Harvard Apparatus). The electrodes were positioned with the anode on the pial surface and the cathode on the ventricular surface, so as to target specifically the VZ precursor cells. The slice fragment was then mounted on a Millicell culture insert system on a drop of type I collagen.

Retroviral infection on slices

pCMV-EGFP retrovirus were produced by M. Afanassieff (Stem Cell and Brain Research Institute, INSERM U846 Bron, France). Embryonic primate brain slices (300µm thick) were incubated floating in GMEM culture medium containing pCMV-EGFP retrovirus (1 to 5.10^5 pi/mL), for 2 to 3h at 37°C. The slice was then mounted on a Millicell culture insert system on a drop of type I collagen.

Organotypic slice culture

Anesthetized primate foetuses were perfused through the heart with cold HBSS (Gibco) supplemented with glucose 18%, MgSO4 and CaCl2 (Sigma). Primate brain hemispheres were embedded in 3% low gelling agarose (Sigma) in HBSS (Gibco) supplemented with glucose 18%, MgSO4 and CaCl2 (Sigma) at 37°C. The sample was then put on ice, and acute brain slices were prepared thanks to a vibratome (Leica VT1000S). Embryonic occipital lobes slices (300µm) were cut in the parasagittal plane. Slices were then transferred into laminin/poly-lysine (Sigma) coated 0.4µm Millicell culture insert (Millipore) on a drop of type I collagen (BD Biosciences) (diluted to 2.7mg/mL with DMEM and neutralizing buffer). Slices were cultured at 37°C and 7.5% CO_2, in a 6-well plate (Falcon) on 1.2mL of Glasgow minimum essential medium (GMEM) medium supplemented with 1% sodium pyruvate, 7.2µM beta-mercaptoethanol, 1% nonessential amino acids, 2 mM glutamine, 1% penicillin/streptomycin, and 10% fetal calf serum (FCS). Culture medium was renewed twice a day.

Brain cryosections

At E66 and E78, primate foetuses were perfused through the heart with buffered 4% PFA during 30min. After cryoprotection in 10% then 20% sucrose (in phosphate buffer), brains are embedded in Tissue-Tek with a specific orientation allowing cutting them following a parasagittal plane. Cryosections (20 µm) were performed with a cryostat (Microm HM500), then mounted on superfrost glass slides (Superfrost Plus, Thermo Scientific) and stored at -20°C.

Organotypic slices cryosections

At the end of one experiment, organotypic brain slices (300µm thickness) are fixed by immersion in cold buffered 2% paraformaldehyde (PFA) in 120 mM phosphate buffer overnight. They are conserved in PB supplemented with Sodium Azide 0.1%. After cryoprotection in 10% then 20% sucrose (in phosphate buffer), slices are embedded in Tissue-Tek, with an orientation conserving the parasagittal plane of section. Cryosections (20 µm) were performed with a cryostat (Microm HM500), then mounted on superfrost glass slides (Superfrost Plus, Thermo Scientific) and stored at -20°C.

Immunofluorescence and antibodies

Cryosections were air-dried for 30 min and hydrated in Tris-buffered saline (TBS) for 30min. Glass slides were rinsed three times in TBS Triton (0.5%) and incubated in normal goat serum

(10%, Gibco, 16210-064) BSA (1%, Sigma, A7906) in TBS for 30 min. Primary antibodies were coincubated overnight in BSA (1%) in TBS at 4°C, at the following concentrations: chicken anti-EGFP (Invitrogen, A10262, 1:1000), mouse anti-p27 (BD Biosciences, 610241, 1/400), Secondary antibodies were coincubated in Dako Diluent (Dako, S3022) 1h at RT, at the following concentrations: Alexa Fluor 488 goat anti-chicken IgG (Invitrogen, A110039, 1/1000), Alexa Fluor 555 goat anti-mouse IgG (Invitrogen, A21422, 1/800), Alexa Fluor 647 goat anti-rat IgG (Invitrogen, A21247, 1/200). Nuclear staining was performed using Topro3 (Invitrogen, T3605, 1µM in TBS) or Dapi (Invitrogen, D1306, 3µM in TBS), for 10min at RT. Mounting was realized in Fluoromount G medium (Southern Biotech) or in Mounting medium (Sigma M1289) supplemented with p-Phenylene diamine (Sigma, P6001, 1mg/mL) to reduce photobleaching and optimize long-term storage.

Confocal imaging

Confocal examination of the fluorescent labelling was carried out on a LEICA DM 6000 CS, equipped with an Argon laser tuned to 488nm, a HeNe laser 543nm, a HeNe laser 633nm and a diode 405nm. Acquisition were performed using an oil 20x/0.70 objective, thanks to the LAS AF software (Leica)

Confocal measurements of p27expression levels

p27protein expression levels were quantified by means of confocal microscopy analysis of immunofluorescent labelling (Durand et al., 1997; Lukaszewicz et al., 2002; Tokumoto et al., 2002). After confocal images acquisition on several focal plane (5 optical sections spaced at 3µm intervals), the expression levels were analyzed at the single cell level. In non-electroporated primate cortices, cytoplasmic outline was based on the p27staining. Quantitative analysis of alexa 555 fluorescence (p27staining), in the cytoplasm and nuclei, was performed using ImageJ. The boundaries between different compartments were based on cytological cues.

Two-photon videomicroscopy

Two-photon time-lapse video recordings were performed by using an inverted Axio-Observer Z1 (Zeiss) two-photon microscope, equipped with Zeiss optics and a Chameleon system Ultra (I) Titane Sapphire 80 Mhz laser. The recording system is equipped with a Microscope Cage Incubation System (Okolab) maintaining temperature at 37°C and CO_2 at 7.5% during the whole recording session. Milicell inserts were imaged in a 6-well glass bottom plate (Iwaki), where the medium was changed twice a day thanks to a tubing system. Laser was tuned to 880 nm for EGFP imaging, with a power between 12 and 20%. Observations were performed using a plan apochromatic dry objective 10x/0.45. Time lapse analysis was usually started 24 hrs after EGFP labelling. By using the Multi Time Series macro of Zeiss Zen software, 4D stacks were acquired on a 95µm thickness (20 optical sections spaced at 5µm intervals), which allows following the 4D migration pattern of precursors and postmitotic neurons. Recording was performed using a single scanning run at 1024x1024

pixels resolution with a scanning speed of 6 µsec/pix. Images were acquired every 2 or 3 hours during up to 15 days.

Manual tracking on video recordings

Tracking of cell movements and divisions was done manually by the experimenter thanks to the ImageJ software, by using the plugin MTrackJ (a java program developed by Erik Meijering at the Biomedical Imaging Group Rotterdam of the Erasmus MC). Although manual tracking is time-consuming, it appears to be the only reliable analytical procedure. MTrackJ facilitate manual tracking of moving objects in image sequences and the measurement of basic statistics of travelled distances and velocities. It can handle 4D (x, y, z, time) image sequences of any type supported by ImageJ, which allows reliable 4D tracking. The tracking data are then filled in a spreadsheet.

In a next step, we developed an Excel Visual Basic Program which allows to extract all the relevant parameters of the videorecordings, so as to improve the quantitative analysis of the spatiotemporal characteristics of proliferation and migration. Migration parameters are related to (i) timing of migration (departure time, final destination time, trajectory duration, pause duration, etc); (ii) speed of migration (migration velocity, motility index, etc). A neuron is considered to pause if it covers a distance less than 3.5µm during over a 6 hour period. Proliferation parameters are related to INM movement of AP cells (basal and apical movement kinetics).

Western blot analysis

Different cortical areas (VZ, SVZ, SP and CP) were dissected and transferred in the lysis buffer implemented with 450mM NaCl. Proteins were extracted by centrifugation (10,000g) 10 minutes at 4°C, separated by SDS-PAGE and transferred to 0.45µm PVDF membranes (Millipore, Billerica, USA). Membranes were blocked 1 hour in a solution containing non-fat milk then incubated with specific antibodies O/N at 4°C, followed by HRP-conjugated antibodies applied for 1 hour at RT (HRP-conjugated anti-mouse IgG, anti-rabbit 1:10000-GE Healthcare, Waukesha, USA). Membranes were developed with the ECL chemiluminescent reagent (Thermo scientific, Rockford, USA) using hyperfilm ECL (GE Healthcare, Waukesha, USA). The following antibodies were used for western blot: rabbit anti-p27 (1:1000, Santa Cruz, USA), rabbit anti-RhoA (1:500, Newest Biosciences, Malvern, USA).

Co-immunoprecipitations

Proteins were extracted by centrifugation (10,000g) for 10 minutes at 4°C, and immunoprecipitations were carried out using specific antibodies O/N at 4°C, followed by 1 hour incubation with protein A-agarose beads or G plus-agarose beads (Santa Cruz, USA). Anti-HA immunoprecipitation was carried out as negative control. Immunoprecipitates were washed twice with the basic lysis buffer and four times with another lysis buffer (Tris-HCL 50mM pH7.5, EDTA 1mM, NP40 1%, 500mM NaCl, proteases inhibitors, Roche). The following antibodies were used: mouse anti-HA (1:250, Santa Cruz, USA), mouse anti-RhoA

(1:250, Santa Cruz, USA). Immunoprecipitates were then subjected to SDS-PAGE for subsequent Western blot analysis.

Statistical analysis

Quantitative data are presented as the mean +/- SEM from representative experiments. Statistical tests and p values are indicated in the figure legends. Student t tests were performed with the Excel software. $p < 0.05$ was considered statistically significant.

Results

Area-specific rates of radial migration in area 17 and area 18

We have monitored the migratory behaviour of EGFP expressing newborn neurons, using two photon Time Lapse Videomicroscopy (TLV), following *ex vivo* electroporation of VZ precursors with pCAG-IRES-EGFP or retroviral mediated gene transfer of pCMV-EGFP. Whole hemisphere *ex vivo* electroporation allows to selectively target the VZ precursors whose progeny maintains high level of EGFP expression over several weeks *in vivo* (Pilaz et al., 2009). 300 µm thick embryonic monkey cortex organotypic slices were maintained for two weeks (Gautier E, 2010b). TLV recordings of cytoplasmic EGFP expressing postmitotic neurons have been obtained on E66 (electroporation and retroviral infection) and E78 embryonic occipital cortex (retroviral infection), in both A17 and A18.

Upon exit from the OSVZ, 5 days post electroporation, newborn postmitotic neurons typically exhibit a multipolar morphology, with a round soma and numerous short processes emanating from it, before initiating radial migration (Fig. 1A). Radially migrating neurons are characterised by an elongated morphology of the nucleus and the soma, with a very long and thick leading process, directed toward the pia, and a short trailing process (Fig. 1B). The migratory behaviour was analysed in the depth of the subplate (SP), ranging from the exit of OSVZ to the upper part of the SP before entry in the cortical plate (CP). A substantial fraction (70 %) of the observed neurons pauses at least once during their radial trajectory, in agreement with the saltatory locomotion described in the mouse (Nadarajah, 2003; Nadarajah et al., 2003; Nadarajah and Parnavelas, 2002; Noctor et al., 2004). (Movie 1)

Several parameters were monitored: (i) migration velocity, defined as the distance with respect to the time, in µm/h; (ii) the number of pauses, (iii) the individual pauses duration, in h and (iv) the motility index, defined as the distance with respect to time, minus the pause(s) duration.

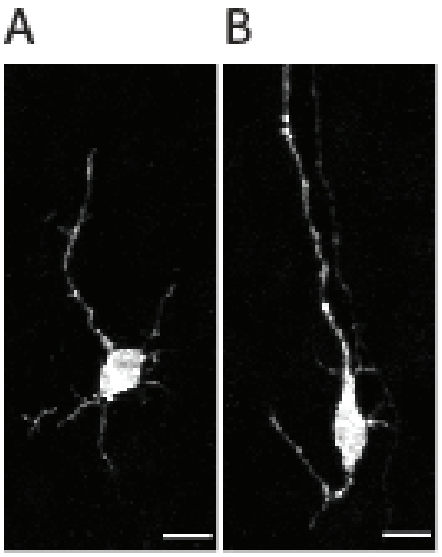

Fig. 1: Morphology of EGFP neurons in the primate subplate.

A: Microphotograph of a multipolar neuron, before radial migration.
B: Microphotograph of a radially migrating bipolar neuron.
(scale bars: 10µm)

At E66, radially migrating neurons cover a distance ranging from700µm (in area 17) to 1000 µm (in area 18) before reaching the bottom region of the CP, as measured on parasagittal organotypic slices of embryonic visual cortex. At this stage, a fraction of neurons were observed to migrate over the whole trajectory during the 2 weeks. The average radial migration duration is 44.7 h, with a maximum of 146 h (6 days). Recordings of EGFP labelled postmitotic neurons did not reveal differences between area 17 (n= 174) and area 18 (n=157) migration velocity (6.91 and 7.35 µm/h respectively) and motility index (9.53 and 10.06 µm/h respectively) (Fig. 2A). Other parameters were also found not to differ between the two areas. Mean pause duration (10.80 and 12.94 h, with maximum of66 and 70 h for area 17 and area 18 respectively) and number (1.63 and 2.06, with a maximum of 9 for A17 and A18 respectively) did not vary significantly between the two areas (Fig. 2B). These data show that, at E66, the different parameters of the migratory behaviour of postmitotic neurons exiting the GZ are identical in area 17 and area 18.

At E78, radially migrating neurons have to migrate over a distance of 1100µm (in area 17) to 1250 µm (in area 18) before reaching the bottom region of the CP, as measured on parasagittal organotypic slices. The maximum migration distance (800µm) measured over the 14 days recording period was observed in the first cohort of postmitotic neurons exiting the GZ. Subsequent cohorts of later newborn neurons could only be observed for shorter migration distances (183 µm for A17 neurons and 165 µm for A18 neurons). At this stage, area 17 postmitotic neurons showed statistically higher values of migration velocity than area 18 postmitotic neurons (10.94 vs.9.19 µm/h, n= 253 vs. n=260) (Fig. 2C). This areal difference in average migration speed was accompanied by an increase in both the number and duration of pauses which were more frequent and statistically longer (2.06 h vs.3.88 h) in area 18 than in area 17 (Fig. 2D). However the increased migration velocity in area 17 migration is not entirely attributable to less pausing since area 17 postmitotic neurons exhibited a significantly higher motility index than area 18 neurons (11.21 vs.9.64 µm/h respectively) (Fig. 2C).

These results reveal area-specific variations in the migratory behaviour and point to the dynamics of proliferation and migration being coordinated. Migration rates variations appear to be congruent with proliferation variations: faster radial migration velocities are observed in area 17 where proliferation rates are high while slower migration velocities are found when proliferation rates are slower, in area 18.

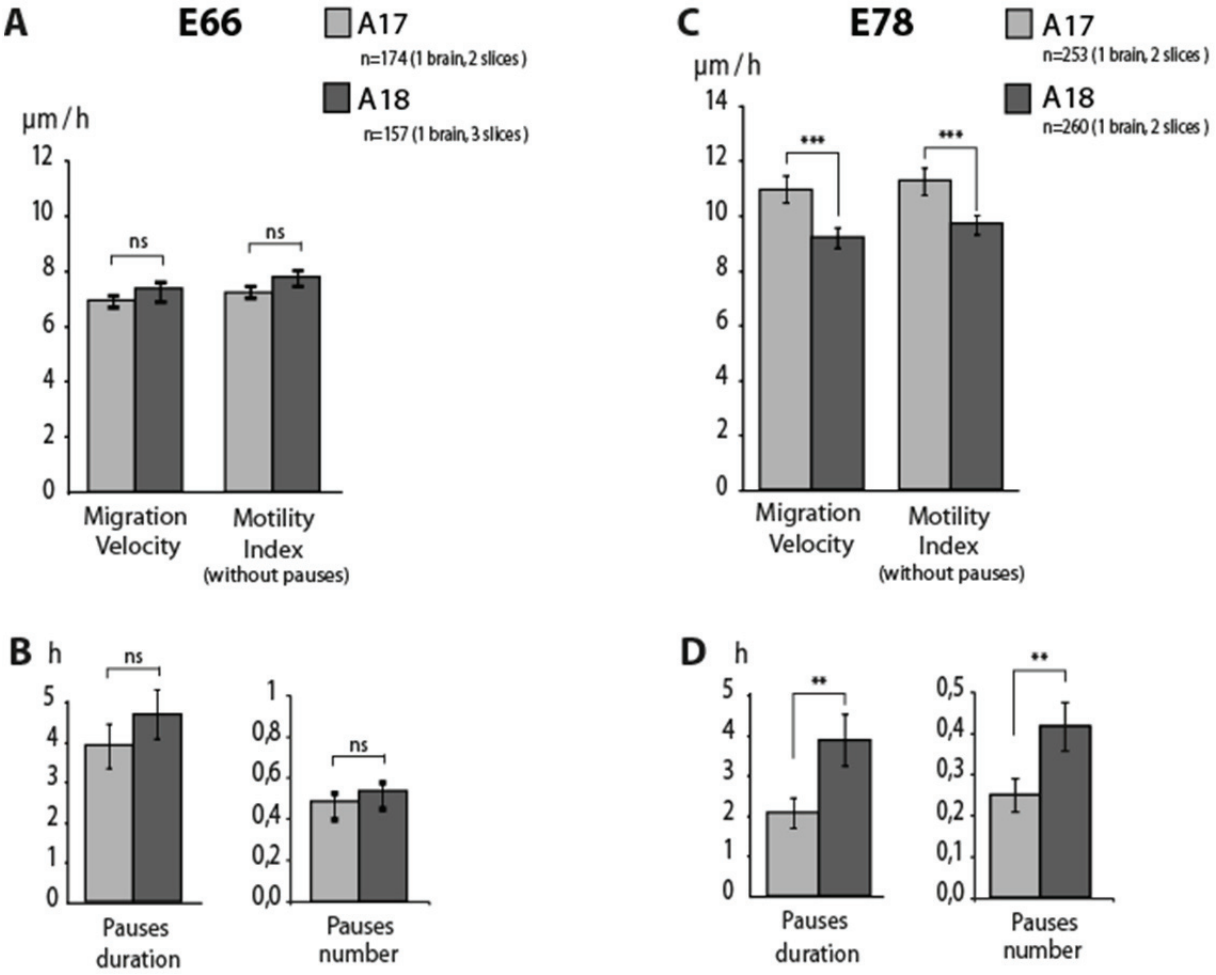

Fig. 2: Radial Migration is faster in area 17 than area 18 of embryonic primate cortex at E77, but not at E66.

A-B: Migration kinetics calculated on A17 or A18 post-mitotic neurons in the SP compartment of E66 primate brain, then averaged on the total population.

C-D: Migration kinetics calculated on A17 or A18 post-mitotic neurons in the SP compartment of E78 primate brain, then averaged on the total population.

Migration Velocity (µm/h) represents the total migrated distance (µm) on to the total migration duration (h).

Motility Index (µm/h) represents the total migrated distance (µm) with respect to the migration duration, without the pause duration (h).

Pause Duration (h) represents the cumulated duration of every pauses that a neuron can make. A neuron is considered to pause if it covers a distance less than 3.5µm during at least 6 hours.

Error bars represent SEM. Student's t tests p values: < 0.05 *, < 0.01 **, < 0.005 ***.

Interkinetic Nuclear Migration rates in area 17 and area 18 ventricular zone

Next, we have analyzed Interkinetic Nuclear Migration (INM) in the VZ of A17 and A18. INM corresponds to the stereotyped nucleokinesis behaviour of proliferating progenitors throughout the cell-cycle in the neuroepithelium of the VZ (Sauer and Walker, 1959), reviewed in (Reiner et al., 2011) (Fig. 3B). Interphase progenitor cells span the neuroepithelium, moving apically toward the ventricular surface just before mitosis. During G1, the nucleus of the cycling progenitor cells moves basally away from the apical ventricular surface. During the S phase of the cycle, the nucleus is located close to the basal surface, and moves back toward the apical, ventricular surface just before entering mitosis (Sauer and Walker, 1959), reviewed in (Reiner et al., 2011) (Fig. 3B). The INM therefore provides a valuable model to explore coordination between proliferation and migration.

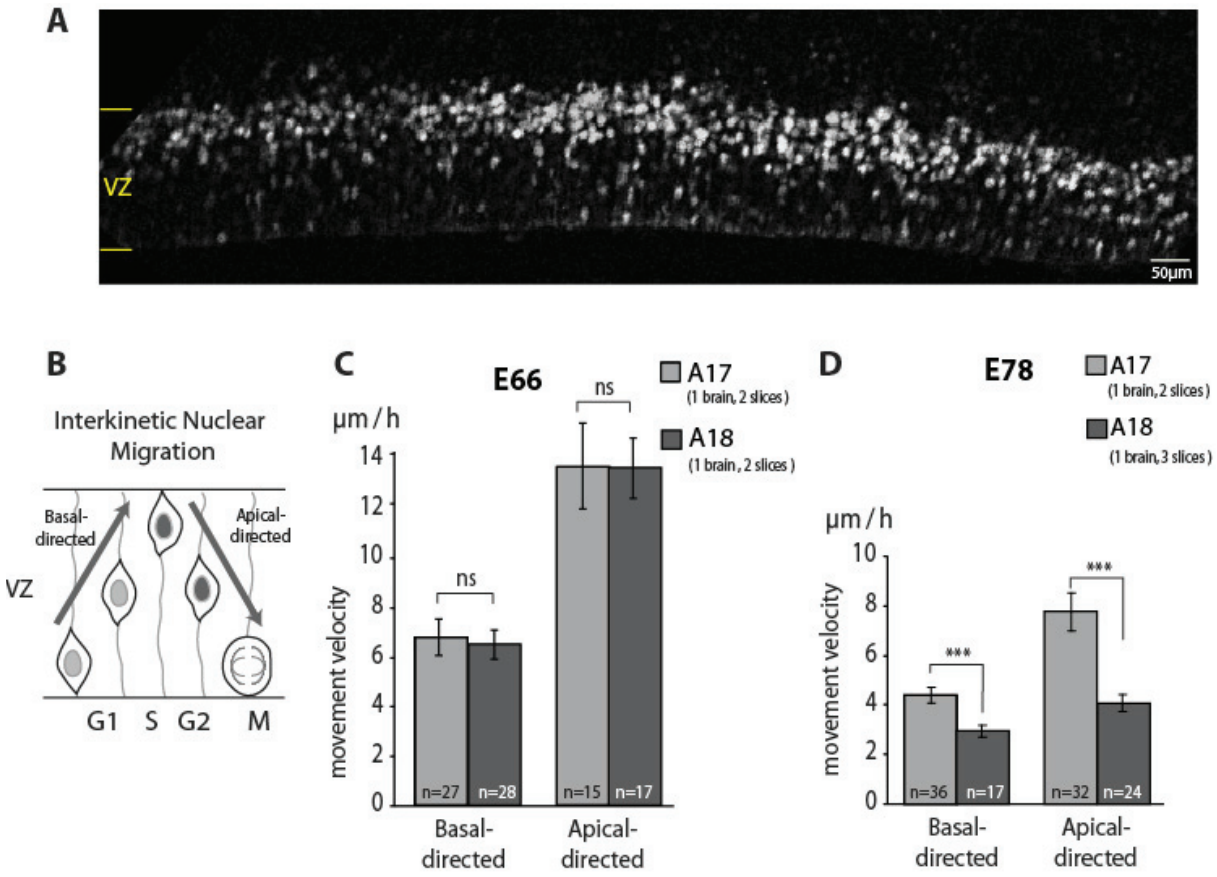

Fig. 3: INM kinetics is faster in area 17 precursors compared to area 18 at E78.
A: Two-photon microphotograph of EGFP-electroporated progenitor cells in the VZ of the primate at E78 (24h after *ex vivo* electroporation).
B: Schematic representation of the Interkinetic Nuclear Migration.
C: INM kinetics (µm/h) measured on A17 or A18 EGFP radial glial cells at E66.
D: INM kinetics (µm/h) measured on A17 or A18 EGFP radial glial cells at E78.
Velocities of both basal- and apical-directed movements are averaged in each population.
Error bars represent SEM. Student's t tests p values: < 0.05 *, < 0.01 **, < 0.005 ***.

We have monitored the INM of EGFP expressing precursors following whole hemisphere *ex vivo* electroporation, to target specifically the VZ RGCs (Fig. 3A) (Movie 2A), or following retroviral mediated gene transfer, on primate organotypic slices (Movie 2B). Using optimal infection rates, this latter procedure makes use of cytoplasmic EGFP labelling which, together with the targeting of a smaller population, allows a substantially improved resolution, compared to electroporation-mediated gene transfer. Two-photon TLV imaging was performed on E66 and E77 embryonic cortex, in area 17 and 18 VZ.

In most cases, it was difficult to follow the precursor during the entire duration of the trajectory At E66, the mean duration of the basal-directed movement was 19h (average trajectory length:98µm) vs. 9 h for the apical-directed movement (average trajectory length: 102µm). Measurements did not reveal any difference in migration velocity between A17 and A18 cycling precursors, neither for the basal-directed nor for the apical-directed movement (Fig. 3C) (6.56 µm/h and 13.17 µm/h in area 17 respectively ; 6.28 µm/h and 13.17 µm/h in area 18 respectively). The similar velocities observed in these two areas are consistent with the comparable proliferation rates observed at this developmental stage (Dehay et al., 1993; Lukaszewicz et al., 2005).

At E78, the average trajectory length in area 17, is 66µm. The average duration of the basal-directed movement is 16.7 h versus 10.9 h for the apical-directed movement. In area 18, the average trajectory length is 55µm, with an average duration of 22.5 h for the basal-directed movement and 13.8 h for the apical-directed movement. At E78, measurements revealed a higher migration velocity of progenitors in area 17, for both the basal-directed movement (4.39 vs.2.96 µm/h) and the apical-directed movement (7.77 vs.4.10 µm/h) (Fig. 3D). These results indicate that during both the basal and apical-directed movements of VZ precursors, corresponding respectively to the G1 and G2 phase, precursor motility is higher in area 17 than in area 18. At this stage, which corresponds to the production of supragranular layer neurons, rates of proliferation in the OSVZ are higher in area 17 than in area (Dehay et al., 1993; Lukaszewicz et al., 2005). However, no direct correlation between rates of INM and cell-cycle kinetics can be made at this point.

Of interest, at both E66 and E78 stages, the apical-directed movement, occurring during G2 phase, is always faster than the basal-directed movement, occurring during G1 phase (which is the longest one during cell-cycle) (Fig. 3C and 3D), as observed in the rodent (see Chapter 2, Fig. 15 page 110 and (Kosodo et al., 2011; Tsai et al., 2010)).

Cytoplasmic p27 expression variations are congruent with proliferation and migration kinetics at E78

p27 cytoplasmic localization results in the loss of its cyclin–CDK inhibitory function (mediated via the Nter domain).p27 can, via its Cter domain, bind to the GTPase RhoA, and prevent its activation, thereby regulating the actin cytoskeleton and cell migration (Nguyen et al., 2006a). To gain insight in the role of p27 in the control of radial migration and INM, we

have analysed its level of cytoplasmic expression in primate area 17 and area 18 migrating postmitotic neurons and precursors.

Confocal quantification of the intensity of the fluorescent p27 immunolabelling showed that OSVZ A17 cycling precursors (PCNA+) exhibit lower levels of nuclear p27 expression than A18 cycling precursors, consistent with the increased rates of proliferation of A17 precursors (Lukaszewicz et al., 2005).

Using confocal microscopy, we have examined the subcellular location of p27 as well as its level of expression in migrating postmitotic neurons from areas 17 and 18 at E78, when differences in migration rates between these two areas are observed (cf Fig. 2C). Confocal quantification of the immunofluorescent labelling against p27 was performed either on fixed organotypic slices in EGFP positive migrating neurons (Fig. 4A,B) or in situ (Fig. 4C,D) in migrating neurons which showed an elongated morphology (Fig. 4A,C). This analysis returned a statistically higher level of cytoplasmic p27 expression, in area 17 compared to area 18 at E78 (Fig. 4B,D) but not at E66 (Fig. 4B).

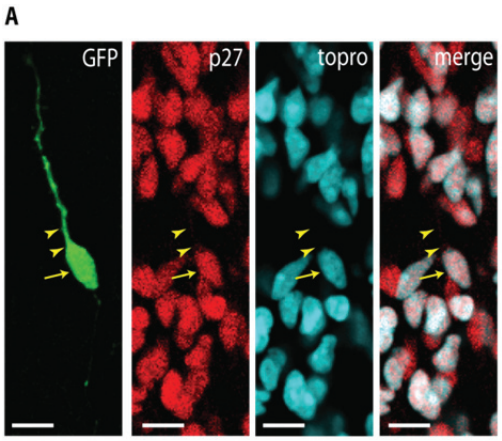

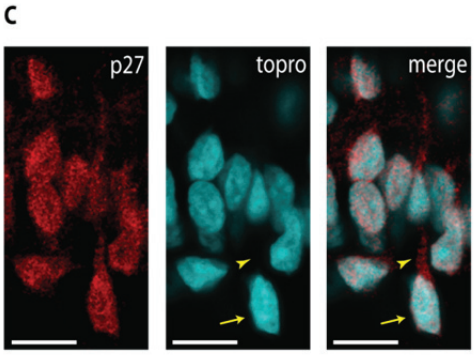

B p27 expression level in GFP migrating cells

A17/ A18 difference	E66	E78
nucleus	+3% ns	+2% ns
cytoplasm	+5% ns	+28% ***
n cells	458	860

D p27 expression level in OFL and SP cells at E78

A17/ A18 difference	OFL	inner SP	outer SP
cytoplasm	+25% ***	+22% ***	+30% ***
n cells	316	404	290

Fig. 4: p27 expression level variations in the primate visual areas A17 and A18

A: Confocal microphotograph of GFP (green) expressing postmitotic neuron showing p27 protein expression (red) in the nucleus (labelled by topro blue staining) (arrow) and the cytoplasm (arrowhead).Scale bar: 10µm

B: Quantification of p27 subcellular expression level in the nucleus and the cytoplasm of GFP migrating cells in primate areas 17 and 18, at E78 and E66. The percentage of difference between area 17 and area 18 is represented.

C: Confocal microphotograph of p27 immunolabelling (red) and nuclear staining (cyan), showing both nuclear (arrow) and cytoplasmic (arrowhead) expression of p27 protein in migrating neurons of the subplate. Scale bar: 10µm

D: Quantification of p27 cytoplasmic expression level in the cells of the OFL and SP compartments in primate E78 areas 17 and 18.

Student's t tests p values: < 0.05 *, < 0.01 **, < 0.005 ***.

p27 promotes radial migration of primate cortical precursor cells

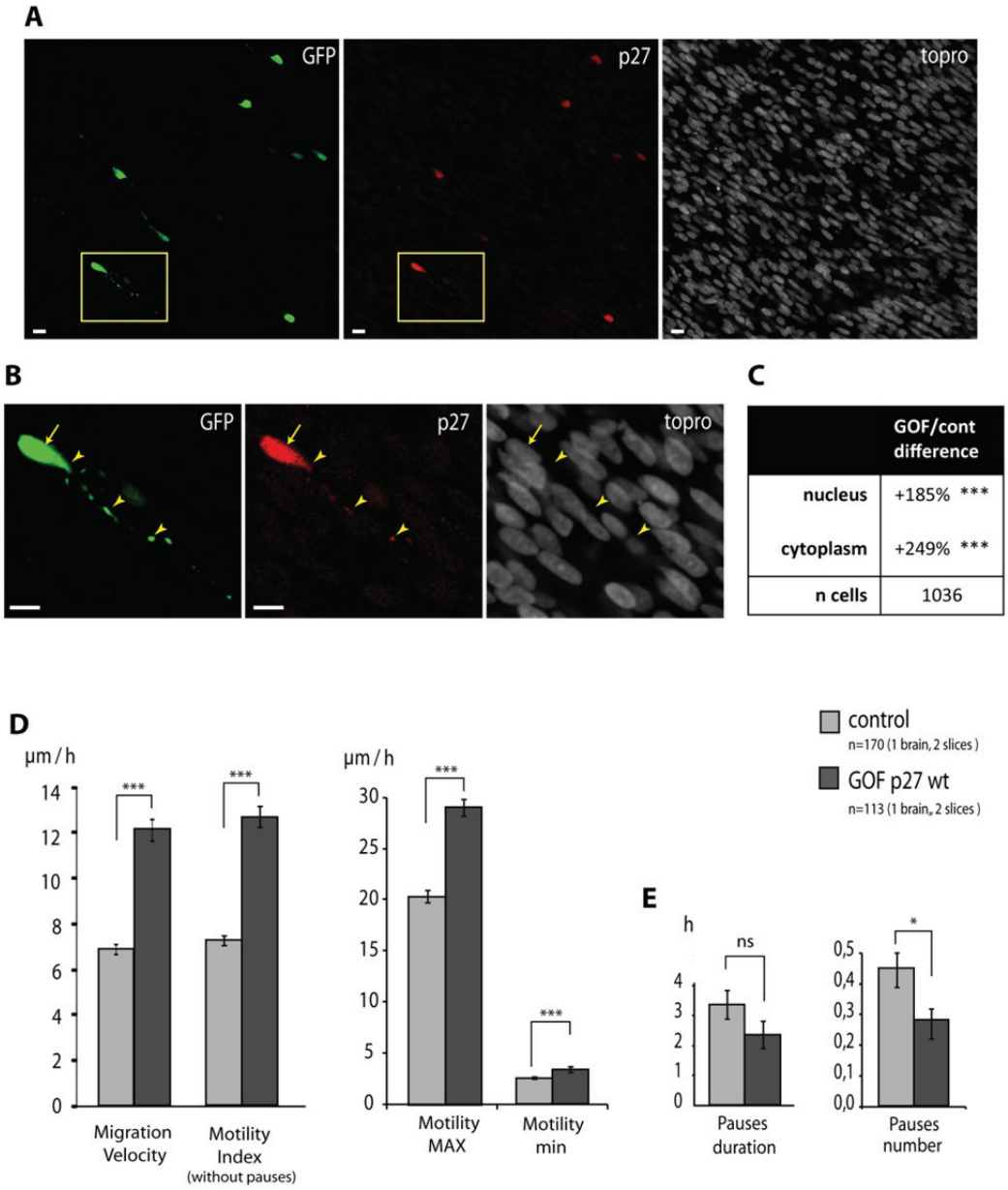

Fig. 5: p27 overexpression increases the radial migration velocity of post-mitotic cells in primate.
A: Confocal microphotograph of GFP (green) and p27 (red) immunolabelling, and nuclear staining (gray), showing p27 overexpression in GFP electroporated post-mitotic neurons. Scale bar:10µm
B: High magnification of the confocal microphotograph, showing both nuclear (arrow) and cytoplasmic (arrowhead) overexpression of p27 protein in a migrating neuron. Scale bar:10µm
C: Quantification of p27 subcellular expression level in the nucleus and the cytoplasm of GFP migrating cells electroporated with a p27GOF expression vector, compared to control electroporated cells, in primate area 17 at E66.
D: Migration kinetics calculated on E66 primate post-mitotic neurons of A17, after electroporation with a control EGFP vector or after p27GOF. Values are averaged on the total population.
Migration Velocity (µm/h): total migrated distance (µm) reported to the total migration duration (h).
Motility Index (µm/h): total migrated distance (µm) reported to the migration duration, without the pause duration (h).
Motility MAX and min: maximum and minimum velocity between two measurements time points.
E: Pause Duration (h) represents the cumulated duration of every pauses that a neuron can make. A neuron is considered to pause if it covers a distance less than 3.5µm during at least 6 hours.
Error bars represent SEM. Student's t tests p values: < 0.05 *, < 0.01 **, < 0.005 ***.

So as to directly explore the role of p27 in migration, we have assessed the effect of its overexpression in primate cortical precursors, in area 17 at E66.

We have monitored the migration velocities of postmitotic radially migrating neurons, born from precursors overexpressing p27 via whole hemisphere *ex vivo* electroporation of the bicistronic plasmid construct pCAG-p27 WT-ires-nls-EGFP, at E66. 5 days post electroporation, EGFP expressing postmitotic neurons exiting the OSVZ were tracked during their radial migration in area 17. Our observations show that, compared to control EGFP expressing neurons, p27 overexpressing neurons exhibit a statistically significant increase in the migration velocity (12.2 µm/hr vs. 6.9 µm/hr for GOF and control respectively) (Fig. 5D). This difference was paralleled by an increase in the expression level of cytoplasmic p27 in neurons originating from p27GOF precursors (Fig. 5A,B,C). In a shorter time (35h vs. 45h, mean values), p27GOF neurons cover a greater distance (384µm vs. 277µm) than control cells, showing their higher migratory capacity. They also exhibit a higher maximum motility (28.9 µm/h vs. 20.3 µm/h) (Fig. 5D). The mean pause number (0.28 vs. 0.46 for GOF and control respectively) was decreased as well as the pauses duration (2.35 vs. 3.36) (Fig. 5E). Values range from a maximum of 24 h for GOF neurons, and 42 h for control neurons. This increase in migration velocity, upon p27 overexpression, confirms and extends observations in mouse precursor cells ((Nguyen et al., 2006b), and see Chapter 2 Fig. 5 and 6 p97-98)

p27 interacts with RhoA in primate cortical precursors and postmitotic neurons

So as to make progress in the understanding of p27 role in cortical precursors and postmitotic neuron migration, we have investigated whether p27 interacts with RhoA in the GZ (VZ and OSVZ) as well as in the SP and CP. Co-immunoprecipitation assays were performed on freshly isolated tissue, through a collaborative work with Sophie Laguesse and Laurent Nguyen (University of Liege).Co-immunoprecipitation assays revealed a specific interaction between p27 and RhoA in the GZ (both VZ and OSVZ), as well as a strong interaction in the SP compartment, whereas no interaction is observed in CP cells (Fig. 6).

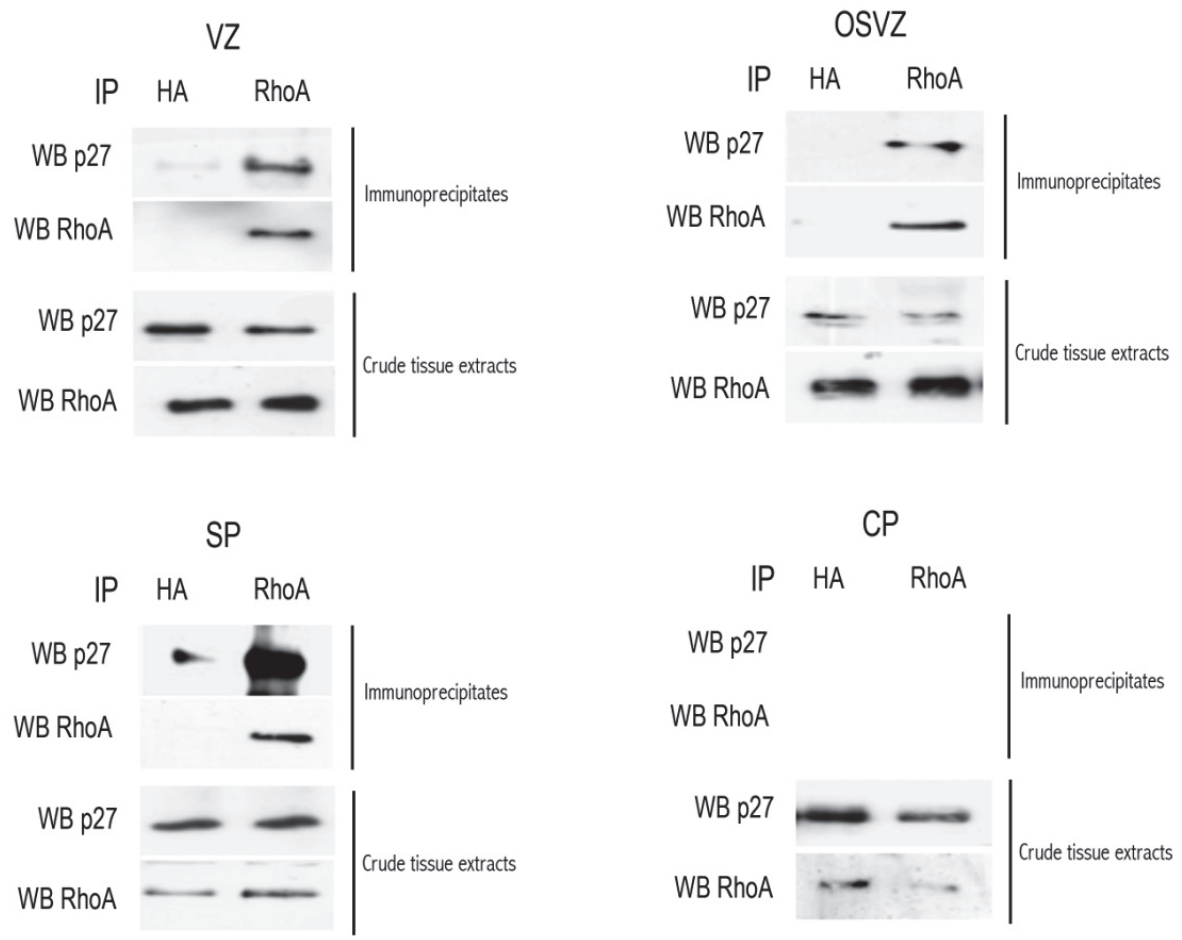

Fig. 6: p27 interacts with RhoA in the primate embryonic cortex.
Western Blot and immunoprecipitations have been performed by S. Labouesse in Laurent Nguyen team. Immunoprecipitates from microdissected E71 primate cortex. Protein extracts from VZ, OSVZ, SP and CP tissue samples were subjected to anti-p27 or anti-RhoA western-blot analyses. Western blot were performed on crude tissue extracts, as indicated.

Discussion

Technical considerations

Because cell-cycle duration is significantly longer in primate than in rodents cortical precursors (Caviness et al., 1995; Kornack and Rakic, 1998; Lukaszewicz et al., 2005; Takahashi et al., 1995a), it is necessary to make observations over 10 to 14 days in order to monitor migration of infected or electroporated precursors. Embryonic cortex organotypic slices were maintained in culture for up to two weeks, without significant degradation of the cytoarchitecture. Under the present culture conditions, optimal rates of proliferation were maintained as shown by computation of LI values of BrdU labelled cells at different time points (Lukaszewicz et al., 2005)(Betizeau et al, unpublished). Cell-cycle duration of OSVZ EGFP expressing precursors in organotypic slices was observed to be in the range of *in vivo* data (Lukaszewicz et al., 2005)(Betizeau et al, unpublished). Bi-photonic confocal time-lapse

video-recording allows ultra-precise point scanning and spectral imaging, as well as Z-stack images in a fraction of a second. Besides providing a better resolution and precision than conventional confocal video-microscopy, this technique allows to image the tissue for longer periods with limited phototoxicity.

In the present study, we did not detect any significant change in migration parameters over time during the 10 to 14 days recording session.

Stage- and area-specific differences in INM kinetics

At E66 and E78, the apical directed movement velocity -corresponding to the G2 motion-is significantly faster than the basal directed movement of G1 phase, in agreement with the published data in other species (Kosodo et al., 2011; Tsai et al., 2010). The migration velocity of both the apical- and basal-directed movements is higher at E66 than at E78. However, the VZ is 2.5 times thicker at E66 (170 µm) than at E78 (70 µm) (data not shown), which means that the E66 cycling VZ precursors have to cover significantly longer trajectories in both the ascending and descending legs of INM. Given that the velocities at E66 are 1.5 faster than at E78, this longer distance (x2.5) in both the G1 and G2 movements at E66 could result in longer cell-cycle duration than that at E78. Although one would need to measure the entire cell-cycle duration in the VZ to draw a firm conclusion, these observations appear to agree with *in vivo* (Kornack and Rakic, 1998) and *ex vivo* (Betizeau et al, unpublished) data. Using S phase cumulative labelling the *in vivo* study showed that, contrarily to what has been reported during mouse corticogenesis, the cell-cycle duration of VZ precursors in the primate cortex lengthens until E60 and then shortens at E80(Kornack and Rakic, 1998). This is confirmed by *ex vivo* analysis on monkey organotypic slices where the cell-cycle duration of EGFP labelled VZ precursors has been measured (Betizeau et al, unpublished).

Area-specific differences in the migration velocities of the INM were observed at E78. These area-specific variations are observed in both G1 and G2 movements, suggesting that the cell-cycle duration of area 17 VZ precursors is shorter than that of area 18 precursors. However, there is no available *in vivo* data on the areal differences in cell-cycle duration of VZ precursors -the previous studies have focused on the areal-differences in the OSVZ cell-cycle duration (Dehay et al., 1993; Lukaszewicz et al., 2005). Although preliminary and incomplete, the present data may indicate area-specific differences in cell-cycle kinetics of VZ precursors, reminiscent of what has been reported in OSVZ precursors (Dehay et al., 1993; Lukaszewicz et al., 2005).

Supragranular layer neurons exhibit area-specific radial migration kinetics linked to area-specific proliferation rates

Studies on radial migration have been mostly carried out in the embryonic rodent cortex (Kriegstein and Noctor, 2004; Nadarajah and Parnavelas, 2002) where the identification of individual presumptive cortical areas is not possible. Earlier work in the primate visual cortex -where area 17 and area 18 can be readily identified during early stages of corticogenesis- pointed to areal differences in radial migration rates between area 17 and area 18 (Lukaszewicz et al., 2006). However this study was not completely conclusive. It was based on static observations where the position of tritiated thymidine labelled neurons (following a pulse injection at E65 and E78) was plotted in the depth of the SP and CP. The uneven distribution of tritiated thymidine labelled neurons suggested that there are compartments where migration is hindered and others where it is more rapid. Here, by using real time imaging we have been able to directly quantify the actual velocity of migrating neurons in the primate.

The present work in the primate visual cortex uncovers for the first time the existence of area-specific radial migration kinetics. These area-specific radial migration kinetics are stage-specific and are selectively observed in supragranular neurons, which are generated by OSVZ precursors during the second half of corticogenesis. Infragranular neurons, generated earlier by VZ precursors, radially migrate with similar kinetics in both area 17 and area 18.

Interestingly, these area-specific variations in rates of radial migration appear to be correlated with area-specific proliferation kinetics. Previous work has shown that while cell-cycle kinetics did not differ between area 17 and area 18 during the generation of infragranular layers (E60 to E72), area 17 precursors showed increased cell-cycle kinetics compared to area 18during the production of the supragranular neurons (E76 to E90) (Dehay et al., 1993; Lukaszewicz et al., 2006; Lukaszewicz et al., 2005). This increased proliferation rate in area 17 precursors was shown to result in higher rates of neuron production (Lukaszewicz et al., 2005).

Therefore, postmitotic neurons issued from a precursor pool showing a high rate of proliferation exhibit increased radial migration kinetics compared to neurons generated by precursors with lower proliferation rates. These coordinated area-specific variations in proliferation and migration could serve as a way to avoid cell crowding in regions of high neuron production.

Radial migration kinetics variations are congruent with cytoplasmic p27 level expression variations

Cytoplasmic p27 level of expression was quantified in EGFP migrating labelled neurons using confocal quantification of the immunofluorescent labelling according to established procedures (Durand et al., 1997; Lukaszewicz et al., 2006; Lukaszewicz et al., 2005).We

observed stage-specific areal variations in cytoplasmic p27 level of expression. At E66, no significant difference was observed between area 17 and area 18 radially migrating neurons whereas at E78, radially migrating neurons in area 17 were characterised by significantly higher levels of cytoplasmic p27 level than their area 18 counterparts.

Therefore, these result show congruent variations in the expression level of cytoplasmic p27 and radial migration velocities, suggesting that p27 exerts a promigratory effect as shown by previous studies in the mouse (Kawauchi et al., 2006; Nguyen et al., 2006a). This is further supported by the GOF experiments where p27 overexpression in area 17 significantly increases the radial migration velocity.

In the mouse, p27 impact on the actin cytoskeleton is mediated by the inactivation the Rho pathway via p27Cterdomain (Nguyen et al., 2006a). The immunoprecipitation data, obtained in collaboration with Laurent Nguyen confirms an interaction between p27 and RhoA in the SP of the developing monkey cortex, where radial migration takes place.

Of note, we need to perform the analysis of cytoplasmic p27 expression in VZ precursor to determine whether it correlates with the area-specific INM variations that are observed at E78. The immunoprecipitation experiments have shown for the first time, that p27-RhoA interaction also takes place in VZ precursors. However, given that the G1 and G2 movements of the INM rely on different cytoskeleton regulatory mechanisms (Del Bene et al., 2008; Gambello et al., 2003; Kosodo et al., 2011; Norden et al., 2009; Schenk et al., 2009; Tsai et al., 2005)(Tsai et al., 2010), the p27-mediated RhoA inactivation may affect INM in complex ways. Further experiments aimed at exploring the potential p27 mediated RhoA action on INM during cell-cycle progression have been implemented in the mouse cortex (see Chapter 2, Fig 13 and 15, p107 and 110).

Together these results indicate that p27 contributes to the coordination of cytoskeletal changes that occur during cell-cycle and migration.

Significance of area-specific coordinated rates of migration and proliferation

Our observations in the primate show stage- and area-specific coordinated changes in rates of proliferation and radial migration. The increased rates of proliferation and radial migration of area 17 supragranular neurons are accompanied by a greater rate of tangential expansion than that observed in the neighbour area 18. This suggests that areal dimensions are determined by both the rates of neuron production and migration (Lukaszewicz et al., 2006). The cerebral cortex has undergone massive tangential expansion during evolution, so that one could hypothesize that the coordination of cell-cycle rates and radial migration rates might represent a critical mechanism for primate corticogenesis.

Of note, both areal differences in rates of proliferation between area 17 and area 18 are maintained *in vitro* in dissociated cultures (Lukaszewicz et al., 2005) as well as in organotypic slices (Lukaszewicz, Kennedy and Dehay, unpublished). Likewise, area 17 and area 18 differences in rates of migration at E78 were maintained on the organotypic slices.

Besides intrinsic cell autonomous mechanisms, several extrinsic factors have been reported to influence the radial migration rates of postmitotic neurons. The *in vitro* work of Edgar and Price showed that coculture of cortical slices with thalamic explants enhances the directed migration of E16 mouse cortical precursors (Edgar and Price, 2001). The developing thalamus could be the source of trophic factors (Lein et al., 2000) and neurotransmitters (Ding and Casagrande, 1998; Montero, 1990) that may influence the migration of cortical precursors. Brain-derived neurotrophic factor, which is expressed in the developing lateral geniculate nucleus (Lein et al., 2000), has been shown to be anterogradely transported in axons (Altar et al., 1997) and to stimulate migration of dissociated cortical neurons (Behar et al., 1997). Interestingly the embryonic thalamic axons have also been shown to regulate proliferation in an area-specific manner in the primate visual cortex [reviewed in (Dehay and Kennedy, 2007)].

Perspectives

This analysis at the system level has uncovered a concerted regulation of rates of proliferation and rates of radial migration, which might play a critical role in the building of the primate cortex. So as to explore how this coupling between proliferation and migration impact on area formation and cytoarchitecture, the team has undertaken collaboration with the group of R. Douglas at the Institute of Neuroinformatics in Zurich (SECO project -short for Self Construction). The goal is to explore the developmental process of cell division and migration and the resulting primate neocortical lamination, by experimental observation, modelling, and simulation in 3D. Using the CX3D software designed by Zubler and Douglas (Zubler and Douglas, 2009), it will be possible to integrate experimentally observed migration rates with proliferative rates so as to build a quantitative dynamic model of corticogenesis. The modelling of these data will provide powerful insight towards the understanding of the developmental processes that underlie the unique features of the primate cerebral cortex and in particular the drastic enlargement of the supragranular layer compartment in this order. Work has already been done to model the building of two distinct areas in the mouse cortex (areas 3 and 6). Future improvement will be to model the primate areas 17 and 18, and to reproduce the striking cytoarchitectonic differences between these two areas as well as the sharp border which is formed between them.

References

Altar, C.A., Cai, N., Bliven, T., Juhasz, M., Conner, J.M., Acheson, A.L., Lindsay, R.M., and Wiegand, S.J. (1997). Anterograde transport of brain-derived neurotrophic factor and its role in the brain. Nature *389*, 856-860.

Behar, T.N., Dugich-Djordjevic, M.M., Li, Y.X., Ma, W., Somogyi, R., Wen, X., Brown, E., Scott, C., McKay, R.D., and Barker, J.L. (1997). Neurotrophins stimulate chemotaxis of embryonic cortical neurons. Eur J Neurosci *9*, 2561-2570.

Caviness, V.S., Goto, T., Tarui, T., Takahashi, T., Bhide, P.G., and Nowakowski, R.S. (2003). Cell output, cell cycle duration and neuronal specification: a model of integrated mechanisms of the neocortical proliferative process. Cerebral cortex (New York, NY : 1991) *13*, 592-598.

Caviness, V.S., Jr., Takahashi, T., and Nowakowski, R.S. (1995). Numbers, time and neocortical neuronogenesis: a general developmental and evolutionary model. Trends Neurosci *18*, 379-383.

Dehay, C., Giroud, P., Berland, M., Smart, I., and Kennedy, H. (1993). Modulation of the cell cycle contributes to the parcellation of the primate visual cortex. Nature *366*, 464-466.

Dehay, C., and Kennedy, H. (2007). Cell-cycle control and cortical development. Nat Rev Neurosci *8*, 438-450.

Del Bene, F., Wehman, A.M., Link, B.A., and Baier, H. (2008). Regulation of neurogenesis by interkinetic nuclear migration through an apical-basal notch gradient. Cell *134*, 1055-1065.

Ding, Y., and Casagrande, V.A. (1998). Synaptic and neurochemical characterization of parallel pathways to the cytochrome oxidase blobs of primate visual cortex. J Comp Neurol *391*, 429-443.

Durand, B., Gao, F.B., and Raff, M. (1997). Accumulation of the cyclin-dependent kinase inhibitor p27/Kip1 and the timing of oligodendrocyte differentiation. Embo J *16*, 306-317.

Edgar, J.M., and Price, D.J. (2001). Radial migration in the cerebral cortex is enhanced by signals from thalamus. Eur J Neurosci *13*, 1745-1754.

Gambello, M.J., Darling, D.L., Yingling, J., Tanaka, T., Gleeson, J.G., and Wynshaw-Boris, A. (2003). Multiple dose-dependent effects of Lis1 on cerebral cortical development. J Neurosci *23*, 1719-1729.

Gautier E, C.V., Betizeau M, Doerflinger N, Patti D, Kennedy H, Dehay C (2010). Area-specific dynamics of proliferation and migration during primate corticogenesis: role of the modular protein p27kip1. 40th SFN (Society for Neuroscience) Meeting, San Diego, USA.

Goto, T., Mitsuhashi, T., and Takahashi, T. (2004). Altered patterns of neuron production in the p27 knockout mouse. Dev Neurosci *26*, 208-217.

Kawauchi, T., Chihama, K., Nabeshima, Y., and Hoshino, M. (2006). Cdk5 phosphorylates and stabilizes p27kip1 contributing to actin organization and cortical neuronal migration. Nat Cell Biol *8*, 17-26.

Kornack, D.R., and Rakic, P. (1998). Changes in cell-cycle kinetics during the development and evolution of primate neocortex. Proc Natl Acad Sci U S A *95*, 1242-1246.

Kosodo, Y., Suetsugu, T., Suda, M., Mimori-Kiyosue, Y., Toida, K., Baba, S.A., Kimura, A., and Matsuzaki, F. (2011). Regulation of interkinetic nuclear migration by cell cycle-coupled active and passive mechanisms in the developing brain. Embo J *30*, 1690-1704.

Kriegstein, A.R., and Noctor, S.C. (2004). Patterns of neuronal migration in the embryonic cortex. Trends Neurosci *27*, 392-399.

Lein, E.S., Hohn, A., and Shatz, C.J. (2000). Dynamic regulation of BDNF and NT-3 expression during visual system development. J Comp Neurol *420*, 1-18.

Lukaszewicz, A., Cortay, V., Giroud, P., Berland, M., Smart, I., Kennedy, H., and Dehay, C. (2006). The concerted modulation of proliferation and migration contributes to the specification of the cytoarchitecture and dimensions of cortical areas. Cereb Cortex *16 Suppl 1*, i26-34.

Lukaszewicz, A., Savatier, P., Cortay, V., Giroud, P., Huissoud, C., Berland, M., Kennedy, H., and Dehay, C. (2005). G1 phase regulation, area-specific cell cycle control, and cytoarchitectonics in the primate cortex. Neuron *47*, 353-364.

Lukaszewicz, A., Savatier, P., Cortay, V., Kennedy, H., and Dehay, C. (2002). Contrasting effects of basic fibroblast growth factor and neurotrophin 3 on cell cycle kinetics of mouse cortical stem cells. The Journal of neuroscience : the official journal of the Society for Neuroscience *22*, 6610-6622.

Montero, V.M. (1990). Quantitative immunogold analysis reveals high glutamate levels in synaptic terminals of retino-geniculate, cortico-geniculate, and geniculo-cortical axons in the cat. Vis Neurosci *4*, 437-443.

Nadarajah, B. (2003). Radial glia and somal translocation of radial neurons in the developing cerebral cortex. Glia *43*, 33-36.

Nadarajah, B., Alifragis, P., Wong, R.O., and Parnavelas, J.G. (2003). Neuronal migration in the developing cerebral cortex: observations based on real-time imaging. Cereb Cortex *13*, 607-611.

Nadarajah, B., and Parnavelas, J.G. (2002). Modes of neuronal migration in the developing cerebral cortex. Nat Rev Neurosci *3*, 423-432.

Nguyen, L., Besson, A., Heng, J.I.-T., Schuurmans, C., Teboul, L., Parras, C., Philpott, A., Roberts, J.M., and Guillemot, F. (2006). P27Kip1 Independently Promotes Neuronal Differentiation and Migration in the Cerebral Cortex. Genes & development *20*, 1511-1524.

Noctor, S.C., Martinez-Cerdeno, V., Ivic, L., and Kriegstein, A.R. (2004). Cortical neurons arise in symmetric and asymmetric division zones and migrate through specific phases. Nat Neurosci *7*, 136-144.

Norden, C., Young, S., Link, B.A., and Harris, W.A. (2009). Actomyosin is the main driver of interkinetic nuclear migration in the retina. Cell *138*, 1195-1208.

Pilaz, L.-J., Patti, D., Marcy, G., Ollier, E., Pfister, S., Douglas, R.J., Betizeau, M., Gautier, E., Cortay, V., Doerflinger, N.*, et al.* (2009). Forced G1-phase reduction alters mode of division, neuron number, and laminar phenotype in the cerebral cortex. Proceedings of the National Academy of Sciences of the United States of America *106*, 21924-21929.

Reiner, O., Sapir, T., and Gerlitz, G. (2011). Interkinetic Nuclear Movement in the Ventricular Zone of the Cortex. J Mol Neurosci.

Sauer, M.E., and Walker, B.E. (1959). Radioautographic study of interkinetic nuclear migration in the neural tube. Proc Soc Exp Biol Med *101*, 557-560.

Schenk, J., Wilsch-Brauninger, M., Calegari, F., and Huttner, W.B. (2009). Myosin II is required for interkinetic nuclear migration of neural progenitors. Proc Natl Acad Sci U S A *106*, 16487-16492.

Takahashi, T., Nowakowski, R.S., and Caviness, V.S., Jr. (1995). The cell cycle of the pseudostratified ventricular epithelium of the embryonic murine cerebral wall. J Neurosci *15*, 6046-6057.

Tarui, T., Takahashi, T., Nowakowski, R.S., Hayes, N.L., Bhide, P.G., and Caviness, V.S. (2005). Overexpression of p27 Kip 1, probability of cell cycle exit, and laminar destination of neocortical neurons. Cerebral cortex (New York, NY : 1991) *15*, 1343-1355.

Tokumoto, M., Tsuruya, K., Fukuda, K., Kanai, H., Kuroki, S., and Hirakata, H. (2002). Reduced p21, p27 and vitamin D receptor in the nodular hyperplasia in patients with advanced secondary hyperparathyroidism. Kidney Int *62*, 1196-1207.

Tsai, J.W., Chen, Y., Kriegstein, A.R., and Vallee, R.B. (2005). LIS1 RNA interference blocks neural stem cell division, morphogenesis, and motility at multiple stages. J Cell Biol *170*, 935-945.

Tsai, J.W., Lian, W.N., Kemal, S., Kriegstein, A.R., and Vallee, R.B. (2010). Kinesin 3 and cytoplasmic dynein mediate interkinetic nuclear migration in neural stem cells. Nat Neurosci *13*, 1463-1471.

Zubler, F., and Douglas, R. (2009). A framework for modeling the growth and development of neurons and networks. Front Comput Neurosci *3*, 25.

Chapter 2: $p27^{kip1}$ influences the dynamics of interkinetic nuclear migration and radial migration in the developing cortex

Manuscript in preparation

Abstract

During corticogenesis, the spatio-temporal coordination of the cell-cycle regulation and neuronal differentiation of precursors in the germinal zones, with the radial migration dynamics of postmitotic neurons to the cortical plate, is crucial for determining the adult cortical cytoarchitecture. Although the complex molecular network underlying the coordinated regulation of these ontogenetic events is not elucidated, p27kip is a candidate player. Nuclear p27kip1 negatively regulates G1 cell-cycle progression through its N-terminal domain. In the cytoplasm, p27kip1 C-terminal domain inhibits RhoA GTPase, leading to modifications of the actin cytoskeleton, thus promoting migration. Here, we have explored this dual function of p27kip 1 during the proliferation of the ventricular zone precursors cells. The precursor nuclei undergo the Interkinetic Nuclear Migration (INM) in synchrony with the cell-cycle phases. p27kip1 expression levels were modified in ventricular zone precursors by electroporation of several mutant forms of p27kip1 or shRNA in mice embryos at E14-15. Two-photon videomicroscopy recordings were performed on cortical organotypic slices, allowing to observe in real-time at the single cell level the behavior of EGFP expressing precursors. We have analysed the successive divisions of different types of progenitors, the INM kinetics, and the radial migration dynamics of neurons generated by the transfected precursors. This revealed that p27kip1 affects INM, promotes differentiative divisions and neuronal radial migration, through its C-terminal domain. p27kip1 is thus part of a molecular network finely tuning the successive rounds of divisions of precursor cells, as well as the migratory behaviour of the newly born neurons.

Introduction

During development, cell proliferation, differentiation and migration must be tightly coordinated and temporally linked, so as to ensure the proper construction of the neocortex. Cortical neurons are generated in the germinal zones, where neural precursor cells undergo massive expansion before they exit the cell-cycle to enter differentiation. Newborn postmitotic neurons leave the GZ and move toward the cortical pial surface in a highly ordered process of neuronal migration [reviewed in (Ayala et al., 2007)]. Cortical neurons settle into six layers in an inside-out manner, with the earliest-generated neurons positioned in the deepest layers and later-generated neurons occupying the more superficial layers. The precise temporal coupling between proliferation, cell-cycle exit, differentiation and migration is crucial for determining the cytoarchitectural organization of the cortex.

The mechanisms that coordinate proliferation and migration during corticogenesis are still incompletely understood. One putative candidate to couple proliferation and migration is p27kip1 (p27). p27 is a member of the cyclin-dependent kinase (CDK) interacting protein/kinase inhibitor protein (Cip/Kip) family of the CDK inhibitors. Nuclear p27 negatively regulates G1 cell-cycle progression, by sequestering and inactivating cyclin E or A-CDK2 complexes. p27 protein levels are increased upon induction of neuronal differentiation, and p27 is implicated in the cell-cycle arrest of cortical precursors (Caviness et al., 2003; Goto et al., 2004; Lukaszewicz et al., 2005; Tarui et al., 2005). Recent data have uncovered a role for cytoplasmic p27 in the regulation of cell migration, independent of cyclin-CDK inhibition. For example, mouse embryonic fibroblasts deficient in p27 exhibited impaired cell motility, whereas expression of p27 has been shown to promote migration of HepG2 hepatocellular carcinoma, embryonic fibroblasts, endothelial cells, and vascular smooth muscle cells (Diez-Juan and Andres, 2003; Goukassian et al., 2001; Mcallister et al., 2003; Sun et al., 2001). The C-terminal domain of p27 is capable of rescuing the migration defect of p27-deficient fibroblasts and thus appears to be responsible for the regulation of cell motility (Besson et al., 2004a; Besson et al., 2004b).

A migration promoting role of p27, via its C-terminal domain, has been demonstrated in murine cortical neurons (Kawauchi et al., 2006; Nguyen et al., 2006a).

Our work in the primate has shown that proliferation and radial migration are coordinated and regulated in an area-specific manner (Gautier E, 2010a, b)(see chapter 1 of the thesis) and point to p27 being a likely candidate to mediate this area-specific coupling. Because the influential studies of Nguyen et al. (Nguyen et al., 2006a) and Kawauchi et al. (Kawauchi et al., 2006) relied on static observations, their work did not allow to dissect the respective impact of migration alteration from that of changes in differentiation rates. Nor did these studies explore the underlying cellular mechanisms involved in migration dynamics, such as intrinsic motility properties. Here, using real time imaging at the single cell-level, we examine the role of p27 on the migration kinetics of radial migration of postmitotic neurons. We then turn to analyse p27 putative role in coordinating migration and proliferation of cycling precursors in the VZ, with a focus on the interkinetic nuclear migration (INM) as a model system for proliferation and migration coupling.

Material and methods

Animals

Wild-Type OF1 mice were kept under a 12-h light/12-h dark schedule. Mating was programmed during the night, and E1 is the day of vaginal plug detection. Animal protocols were approved by the University of Lyon.

Plasmids and siRNA

Purification of plasmid DNA was processed by precipitation with polyethylene glycol. cDNAs encoding full-length human p27 WT, p27 CK- (a mutant p27 that can no longer bind to cyclins and CDKs (Besson et al., 2004b; Vlach et al., 1997), p27 WT Cter, p27 WT Nter and p27 CK- Nter, were provided by L. Nguyen (GIGA-Neurosciences, University of Liège, Belgium) (Nguyen et al., 2006a). The pCAGGS-IRES-EGFP vector was generously provided by J. Briscoe (National Institute for Medical Research London, U.K.), where a [cDNA]-nlsIRES-EGFP cassette is under the control of a CMV enhancer and a chicken beta-actin promoter (Nguyen et al., 2006a). The pHpCAG expression plasmid (Niwa et al., 1998) was provided by Hitoshi Niwa. p27 cDNAs were amplified by PCR from pCAGGS-p27-IRES-EGFP and inserted between the two XhoI sites of the pHpCAG expression plasmid, or between the NheI and XhoI sites of the pCAGGS-IRES-EGFP vector to form bicistronic vectors. All constructs were verified by sequencing.

p27 siRNA were purchased from Ambion (Ref 118712), and the sequences were as follows: GCUUGCCCGAGUUCUACUAtt (sense) and UAGUAGAACUCGGGCAAGCtg (antisense). The extent of mRNA knockdown elicited was compared to cells transfected with a nonsense control siRNA: the Silencer Negative Control #1 from Ambion (Ref 4611). Three sequences for p27 shRNA were designed. sh1-p27 (GCTTGCCCGAGTTCTACTA) was derived from the sequence of the p27 siRNA from Ambion (Ref 118712), and is effective on both murine and primate p27 RNA sequences. sh2-p27 (GGTCAATCATGAAGAACTA) and sh3-p27 (GGCCAACAGAACAGAAGAA) were designed with the updated scoring algorithm of Dharmacon (siDesign Center) and are specific for the murine p27 sequence. The extent of mRNA knockdown elicited was compared to cells transfected with an irrelevant shRNA sequence from pBS as nonsense control shRNA (TTCGATATCAAGCTTATCG) (Kim 03, Antisense Nucleic Acid Drug Dev). All these shRNA sequences were linked by PCR amplification to the mU6 promoter and inserted into the SpeI unique site of the pCAG-ires-nls-EGFP vector. The rescue for one shRNA experiment was performed by electroporating plasmid encoding the full length mouse p27 with 6 silent mutations on the AA 66 to 68 and 70 to 72 corresponding to the mouse sh3-p27 shRNA target.

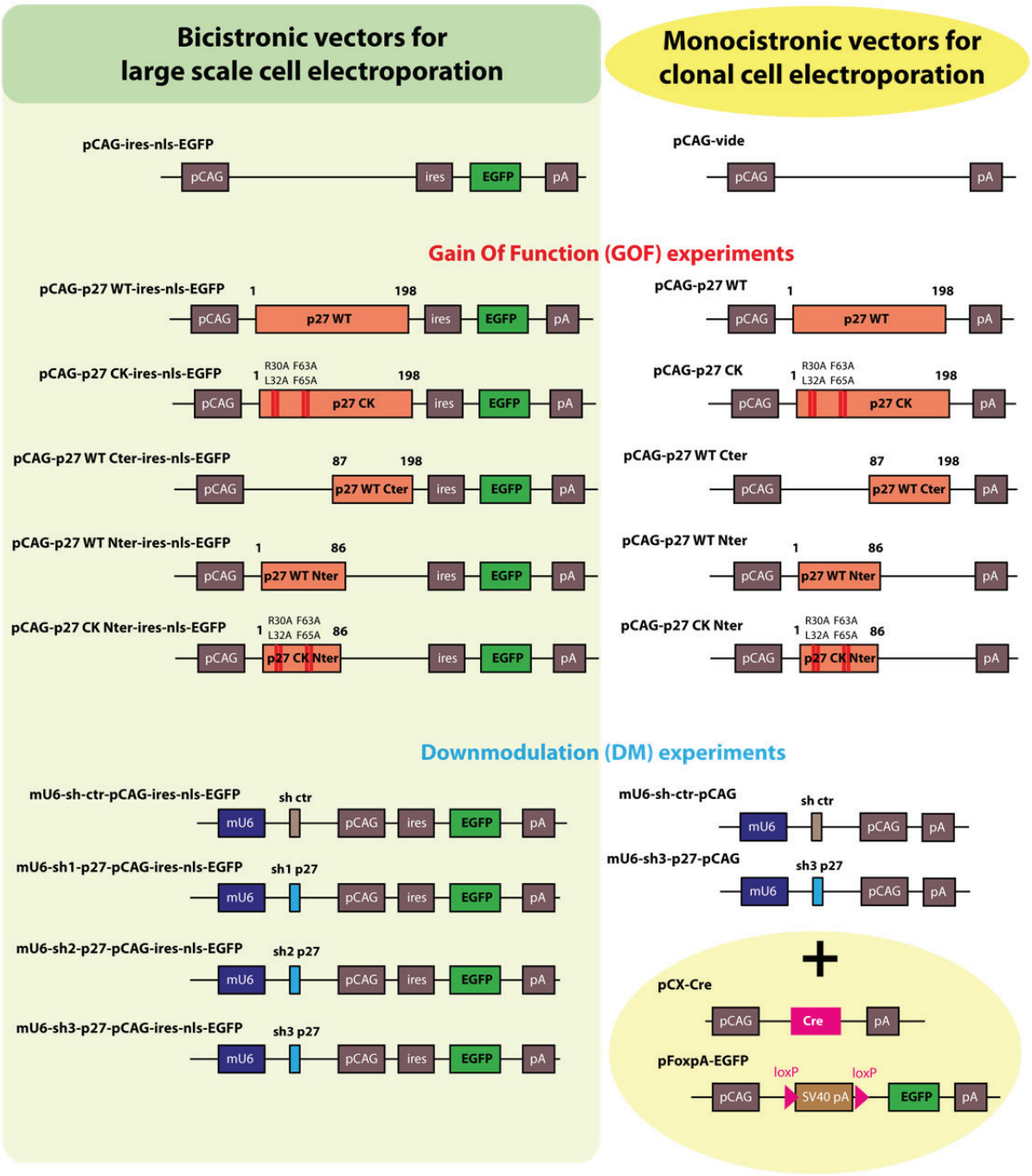

Fig. 1: Plasmidic vectors used for mouse brain electroporation.

For large-scale cell electroporation (left panel), bicistronic vectors with a CAG promoter allow the expression of both nuclear EGFP and the protein p27 or shRNA against p27. For GOF experiments, 5 different forms of p27 are overexpressed: the full-length p27 WT, the full-length p27 CK- (mutated on its interaction site with cyclin/CDKs), the C-terminal part of p27 WT, the N-terminal part of p27 WT and the N-terminal part of p27 CK-. For downmodulation experiments, 4 different shRNA sequences are expressed, under the control of mU6 promoter. sh-ctr is a nonsense control shRNA, sh1-p27 targets the sequence of both murine and primate p27, whereas sh2-p27 and sh3-p27 are specific for the murine p27 sequence.

For clonal cell electroporation (right panel), different monocistronic vectors with a CAG promoter allow the expression of the different forms of p27 protein or the different shRNA against p27. EGFP is expressed through the clonal conditional system, where SV40-PolyA is flanked by two loxP sites, in front of EGFP sequence, allowing EGFP expression through Cre excision.

For the clonal cell electroporation strategy, pCX-Cre and pFloxpA-EGFP were provided by X Morin (Morin et al., 2007) (Ecole Normale Supérieure, Institut de Biologie de l'ENS, IBENS, Paris, France).

In utero electroporation

A xylazin/ketamin mix was used to anesthetize E14 or E15 pregnant mice. Plasmid solution (0.5–2 µg/µL) was colored with Fast Green (0.01 mg/mL; Sigma) to monitor the injection site. The uterine horns were exposed, and plasmid solution (2–3 µL) was pressure microinjected through the uterine wall into the lateral ventricules of embryos, via pulled glassed capillaries. Five pulses of current (60 V, 50 ms on/1,000 ms off) were delivered by using a pair of tweezertrodes (BTX Harvard Apparatus, diameter 0.7 or 1 cm, for E14 and E15 embryos respectively). The electrodes were pinching the whole body of each embryo through the uterine wall, and placed with the anode on the injected hemisphere to target the VZ of the dorsomedial cortex. The uterine horns were replaced back into the mouse abdomen, finally sutured.

Ex vivo electroporation

In E15 mouse embryos, *ex vivo* electroporation was performed on the whole head dissected in 1× phosphate buffered saline (PBS). 1.5 µL of plasmid solution (1-2 µg/µl) colored with Fast Green (0.01 mg/mL; Sigma) were microinjected by pressure into each lateral ventricule, via a Hamilton syringe. Five pulses of current (30V, 50 ms on/1000 ms off) were delivered using a pair of gold electrodes (Genetrode BTX Model 514, Harvard Apparatus). The electrodes were oriented with the anode dorsally and the cathode ventrally, so as to target the VZ of the dorsomedial cortex of both hemispheres.

Clonal cell electroporation

Classic in utero or *ex vivo* electroporation allows a selective and large-scale targeting of the VZ precursor cells, having a membranous contact with the ventricular surface. This results in a strong EGFP expression in numerous precursors, sometimes difficult to follow in real-time experiments (Fig. 2A-B).

In order to track more easily VZ precursor cells and their progeny, we used a clonal technique (Morin et al., 2007), through in utero electroporation in E14 mouse embryos. A conditional EGFP reporter vector (pFlox-pA-EGFP, 0.5 µg/µL) was introduced in VZ cells together with a control, GOF or shRNA construct (0.5-2 µg/µL), and a Cre recombinase expression vector (pCX-Cre) added at a very low concentration (0.2 ng/µL) to clonally activate EGFP expression in individual neural progenitors (Fig. 2C). Vector concentrations of 1–2 µg/µL result in transfection of multiple plasmids per cell. The 2500-fold dilution of the Cre expression vector ensures that excision of the SV40-PolyA, flanked by two loxP sites, will result in high EGFP expression in clonally dispersed cells (Fig. 2D).

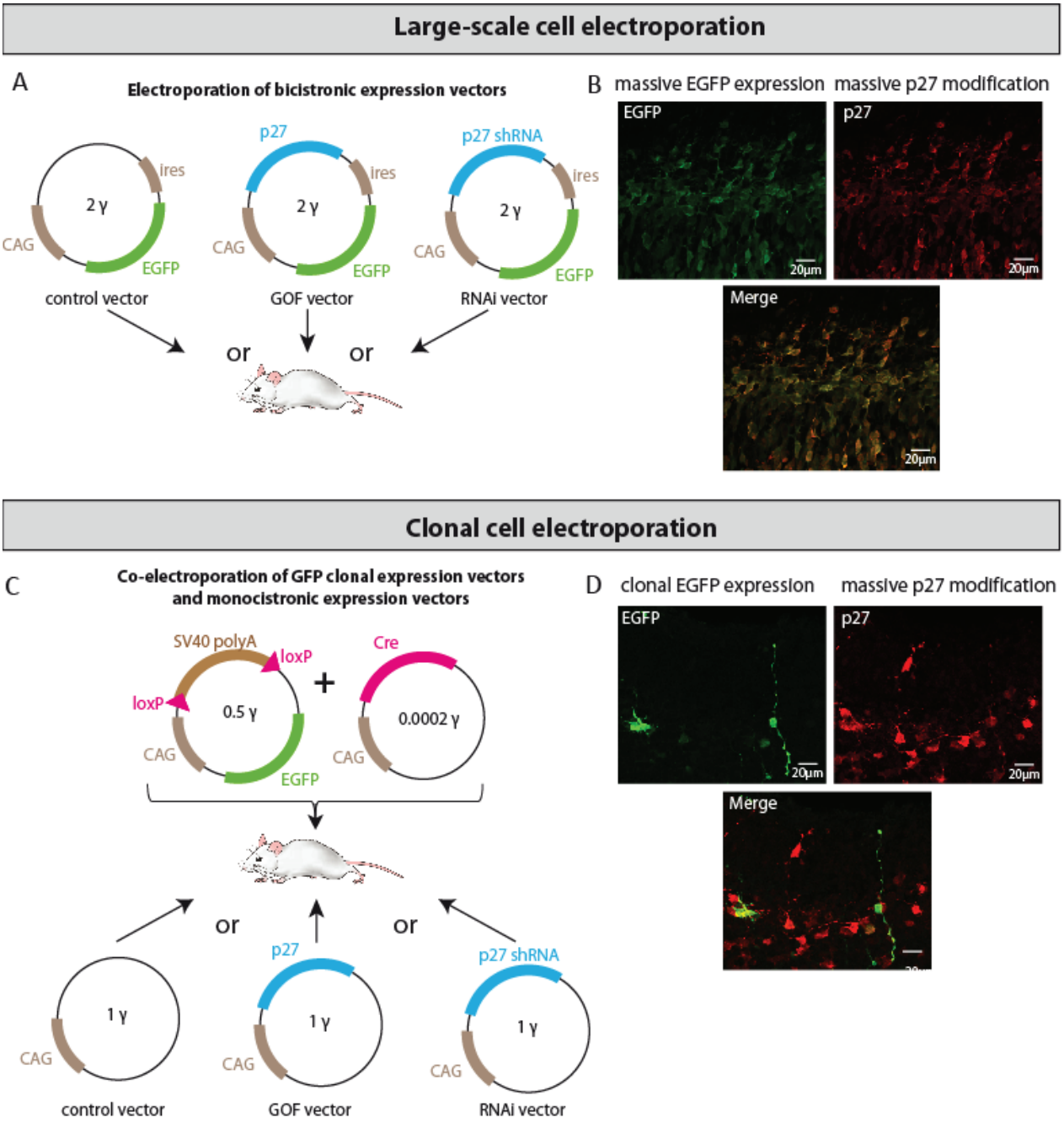

Fig. 2: Large-scale and clonal electroporation strategies used for VZ precursor cells targeting.
A,B: Large-scale cell electroporation is aimed at targeting and labelling a large population of precursors.
A: Bicistronic expression vectors are electroporated, so that both EGFP and the protein of interest (p27) or shRNA (against p27) are expressed in a large number of precursors.
B: Confocal microphotograph of EGFP (green) and p27 immunolabelling (red), showing a large population of cells where EGFP is expressed and p27 expression is modified.
C,D: Clonal cell electroporation aims to label a sparse population of precursors.
C: 3 monocistronic vectors are co-electroporated, so that both a conditional EGFP reporter (where loxP sites are flanked by SV40-PolyA) and the protein of interest (p27) or shRNA (against p27) are expressed. The Cre expression vector is introduced in weak quantity, in order to clonally activate EGFP expression in individual neural progenitors.
D: Confocal microphotograph of EGFP (green) and p27 immunolabelling (red), showing a massive population of cells where p27 expression is modified, but only few of them are labelled with EGFP.

BrdU labelling

For *in vivo* labelling of S phase cells, a single i.p. injection of BrdU (50 µg/g, diluted in PBS) was performed 30min before sacrifice. BrdU-positive cells were detected by immunohistochemistry as described later.

Organotypic slice culture

Mice uterine horns were isolated and embryos head were dissected in cold phosphate buffered saline (PBS). Mice brain hemispheres were embedded in 3% low gelling agarose (Sigma) in HBSS (Gibco) supplemented with glucose 18%, MgSO4 and CaCl2 (Sigma) at 37°C. The sample was then put on ice, and acute brain slices were prepared thanks to a vibratome (Leica VT1000S). Mouse embryonic brains slices (150 or 200 µm for E15 and E14 embryos respectively) were cut in the coronal plane. Slices were then transferred into laminin/poly-lysine (Sigma) coated 0.4µm Millicell culture insert (Millipore) on a drop of type I collagen (BD Biosciences) (diluted to 2.7mg/mL with DMEM and neutralizing buffer). Slices were cultured at 37°C and 7.5% CO_2, in a 6-well plate (Falcon) on 1.2mL of Glasgow minimum essential medium (GMEM) medium supplemented with 1% sodium pyruvate, 7.2µM beta-mercaptoethanol, 1% nonessential amino acids, 2 mM glutamine, 1% penicillin/streptomycin, and 10% fetal calf serum (FCS). Culture medium was renewed twice a day.

Pharmacological inhibition of the RhoA pathway

The pharmacological ROCK blocker Y27632 (10 µM, Tocris, Bristol, UK) was added to cultured organotypic slices 48h after electroporation, for a duration of 7 or 24h during time-lapse recordings.

Brain cryosections

24h, 48h or 72h after in utero electroporation, mice embryonic brains were dissected in PBS and fixed by immersion in cold buffered 2% paraformaldehyde (PFA) during 2h. After cryoprotection in 10% then 20% sucrose (in phosphate buffer), brains are embedded in Tissue-Tek with a specific orientation allowing cutting them following a coronal plane. Cryosections (20 µm) were performed with a cryostat (Microm HM500), then mounted on superfrost glass slides (Superfrost Plus, Thermo Scientific) and stored at -20°C.

Organotypic slices cryosections

At the end of one experiment, organotypic brain slices (150 to 200µm thickness) are fixed by immersion in cold buffered 2% paraformaldehyde (PFA) in 120 mM phosphate buffer during 1h. They are conserved in PB supplemented with Sodium Azide 0.1%. After cryoprotection in 10% then 20% sucrose (in phosphate buffer), slices are embedded in Tissue-Tek, with an orientation conserving the coronal plan of section. Cryosections (20 µm) were performed with a cryostat (Microm HM500), then mounted on superfrost glass slides (Superfrost Plus, Thermo Scientific) and stored at -20°C.

Immunofluorescence and antibodies

Cryosections were air-dried for 30 min and hydrated in Tris-buffered saline (TBS) for 30min. Glass slides were rinsed three times in TBS Triton (0.5%) and incubated in normal goat serum (10%, Gibco, 16210-064) BSA (1%, Sigma, A7906) in TBS for 30 min. Primary antibodies were coincubated overnight in BSA (1%) in TBS at 4°C, at the following concentrations: chicken anti-EGFP (Invitrogen, A10262, 1:1000), rabbit anti-p27 (SantaCruz C19, sc-528, 1/1000), mouse anti-Pax6 (Developmental Studies Hybridioma, concc, Bank, 1:1000), rabbit anti-Tbr2 (Abcam, ab23345, 1:1000), rat anti-Ki67 (Dako, clone TEC-3, 1:50), rabbit anti-phosphorylated histone H3 (pH3, Ser-28, Upstate, 07-145, 1:600), rat anti-BrdU (Abcam, ab6326, 1:500), mouse anti-Nestin (Cell Signaling, Rat 401, 1:50), mouse anti-NeuN (Chemicon MAB371, 1:200). For BrdU staining, sections were incubated in 2 N HCl for 30 min at 37°C, followed by incubation in sodium borate (pH 8.5) for 15 min. Secondary antibodies were coincubated in Dako Diluent (Dako, S3022) 1h at RT, at the following concentrations: Alexa Fluor 488 goat anti-chicken IgG (Invitrogen, A110039, 1/1000), Alexa Fluor 555 goat anti-mouse IgG (Invitrogen, A21422, 1/800), Alexa Fluor 405 goat anti-rabbit IgG (Invitrogen, A31556, 1/400), Alexa Fluor 555 goat anti-rabbit IgG (Invitrogen, A21428, 1/800), Alexa Fluor 647 goat anti-rabbit IgG (Invitrogen, A21244, 1/200), Alexa Fluor 586 goat anti-rat IgG (Invitrogen, A11077, 1/200), Alexa Fluor 647 goat anti-rat IgG (Invitrogen, A21247, 1/200). Nuclear staining was performed using Topro3 (Invitrogen, T3605, 1µM in TBS) or Dapi (Invitrogen, D1306, 3µM in TBS), for 10min at RT. Mounting was realized in Fluoromount G medium (Southern Biotech) or in Mounting medium (Sigma M1289) supplemented with p-Phenylene diamine (Sigma, P6001, 1mg/mL) to reduce photobleaching and optimize long-term storage.

Confocal imaging

Confocal examination of the fluorescent labelling was carried out on a LEICA DM 6000 CS, equipped with an Argon laser tuned to 488nm, a HeNe laser 543nm, a HeNe laser 633nm and a diode 405nm. Acquisition were performed using an oil 20x/0.70 or 40x/1025-0.75 objective, thanks to the LAS AF software (Leica)

Counting of cell types

After confocal images acquisition on one focal plane, brightness and contrast were adjusted and the cells were counted using the Cell Counter Plugin in ImageJ software. The boundaries between different compartments were based on cytological cues and differential immunoreactivity to different proteins (Pilaz et al., 2009).

Confocal measurements of p27 expression levels

p27 protein expression levels were quantified by means of confocal microscopy analysis of immunofluorescent labeling (Durand et al., 1997; Lukaszewicz et al., 2002; Tokumoto et al., 2002). Care was taken to compare p27 levels of expression in different experimental conditions on sections that were simultaneously processed for immunostaining in strictly

identical conditions. Confocal picture acquisition and quantification were implemented using strictly identical parameters (laser intensity, gain and offset). After confocal images acquisition on several focal plane (5 optical sections spaced at 3µm intervals), the expression levels were analyzed at the single cell level. In electroporated mouse cortices, quantification was performed in the targeted EGFP precursor cells. For quantification of p27 downmodulation, the experimenter chooses the optimal focal plane for each EGFP cell and delineates the EGFP staining and the nuclear staining outline, corresponding respectively to the cytoplasmic and nuclear compartments. For quantification of p27 overexpression, we have used an automatic detection of the EGFP staining outline. Quantitative analysis of alexa 555 fluorescence (p27 staining), in the cytoplasm and the nucleus, was performed using ImageJ software. The boundaries between different compartments were based on cytological cues.

Two-photon videomicroscopy

Two-photon time-lapse video recordings were performed by using an inverted Axio-Observer Z1 (Zeiss) two-photon microscope, equipped with Zeiss optics and a Chameleon system Ultra (I) Titane Sapphire 80 Mhz laser. The recording system is equipped with a Microscope Cage Incubation System (Okolab) maintaining temperature at 37°C and CO_2 at 7.5% during the whole recording session. Milicell inserts were imaged in a 6-well glass bottom plate (Iwaki), where the medium was changed twice a day thanks to a tubing system. Laser was tuned to 880 nm for EGFP imaging, with a power between 12 and 20%. Observations were performed using a plan Apochromatic dry objective 10x/0.45. Time lapse analysis was usually started between 8 and 24 hrs after EGFP labelling. By using the Multi Time Series macro of Zeiss Zen software, 4D stacks were acquired on a 95µm thickness (20 optical sections spaced at 5µm intervals), which allows following the 4D migration pattern of precursors and postmitotic neurons. Recording was performed using a single scanning run at 1024x1024 pixels resolution with a scanning speed of 6 µsec/pix. Images were acquired every 30 min or every hour, during 48 to 72 h.

Manual tracking on video recordings

Tracking of cell movements and divisions was done manually by the experimenter thanks to the ImageJ software, by using the plugin MTrackJ (a java program developed by Erik Meijering at the Biomedical Imaging Group Rotterdam of the Erasmus MC). Although manual tracking is time-consuming, it appears to be the only reliable analytical procedure. MTrackJ facilitate manual tracking of moving objects in image sequences and the measurement of basic statistics of travelled distances and velocities. It can handle 4D (x, y, z, time) image sequences of any type supported by ImageJ, which allows reliable 4D tracking. The tracking data are then filled in a spreadsheet.

In a next step, we developed an Excel Visual Basic Program which allows to extract all the relevant parameters of the videorecordings, so as to improve the quantitative analysis of the spatiotemporal characteristics of proliferation and migration. Proliferation parameters are

related to (i) timing of division (division rank in the lineage; division time; cell-cycle length); (ii) type of division (cell type of the mother cell; cell type of the two daughter cells, and their position with respect to the apico-basal axis after division); (iii) INM movement of AP cells (basal and apical movement kinetics; G1, S and G2 movement duration). Migration parameters are related to (i) timing of migration (departure time, final destination time, trajectory duration, pause duration, etc); (ii) speed of migration (migration velocity, motility index, etc). A neuron is considered pausing if it moves less than 4 µm during at least 2 consecutive hours.

Statistical analysis

Quantitative data are presented as the mean +/- SEM from representative experiments. Statistical tests and p values are indicated in the figure legends. Student t tests were performed with the Excel software, and Generalized Linear Model (GLM) analysis with the R software. $p<0.05$ was considered statistically significant.

Results

Efficient GOF and DM strategy

In order to explore the consequences of upregulating (GOF) or downmodulating (DM) p27 expression level in embryonic mouse cortical precursors, we have implemented in utero electroporation mediated gene transfer, which specifically targets VZ precursor cells (Pilaz et al., 2009). We have overexpressed the wild-type protein (p27 WT), mutated and truncated forms of p27 (Fig. 1), as well as siRNA and shRNA expression vectors targeting p27. Both GOF and shRNA expression vectors express concomitantly EGFP, a reporter gene which allows to follow the behaviour of targeted modified precursor cells and their progeny (Pilaz et al., 2009) in a preserved cortical environment.

So as to dissect the relative contribution of the N and Cter regions of p27, we have used the following mutants: (i) p27 CK- which is a mutant p27 that can no longer bind to cyclins and CDKs (Besson et al., 2004b; Vlach et al., 1997). (ii) p27 WT Nter corresponds to the N-terminal portion of p27, able to inhibit the cyclins/CDKs complexes (Nguyen et al., 2006a). (iii) p27 WT Cter corresponds to the C-terminal portion of p27, able to act on the RhoA pathway (Nguyen et al., 2006a). (iv) p27 CK- Nter is restricted to the N-terminal portion of the p27 CK- form, acting neither on the cyclins/CDKs complexes, nor on the RhoA pathway. To downmodulate p27 expression, we used both siRNA and shRNA expression vectors targeting p27. (Fig. 1)

Our strategy was to explore the radial migratory behaviour of postmitotic neurons with modified levels of p27 expression in a normal micro environment on organotypic slices of mouse embryonic cortex. Neuronal migration can be affected by radial scaffolds (radial

fibres of VZ precursor cells) that support neuronal migration in a non-cell autonomous manner. Immunolabelling of radial fibres with an antibody against Nestin, a marker of neural precursor cells, revealed no distinguishable differences between the radial fibres of neuroepithelial cells overexpressing expressing p27 protein or p27 shRNA and those of normal neuroepithelial cells, indicating a cell autonomous role for p27 in radial migration (Fig. S1).

In a first step, we verified, using confocal quantification of the intensity of the fluorescent p27 immunolabelling, that the plasmidic constructions and electroporation conditions were efficient to modulate, positively or negatively, p27 level of expression. In all conditions, when a p27WT or a mutant form expressing plasmid was introduced into E15 VZ precursors, via in utero electroporation, p27 immunoreactivity was observed to be significantly increased in all the EGFP-positive postmitotic neurons at E16 (Fig. S2) and E18 (Fig. S3). Similarly, upon forced expression of p27 shRNA, p27 immunoreactivity was significantly reduced in all the EGFP-positive cells at E16 and E18 (Fig. S4 C,D,E). Electroporation of siRNA and shRNA vectors was able to significantly diminish p27 expression level in both the nucleus and the cytoplasm (Figure S4 D,E). GOF vectors raised both nuclear and cytoplasmic p27 level (Figure S4 A,B). Each plasmidic construction of the mutants (p27 CK-, p27 CK- Nter, p27 WT Nter, p27 WT Cter), showed an efficient overexpression (Fig. S2, S3 and S4A,B). The induced increase or decrease in p27 level was maintained during the whole duration of the experiment, and was found to persist 72h after electroporation, in both proliferative precursors and post-mitotic neurons (Figure S3 and S4B,E).

Dynamics of the radial migratory behaviour at E16.5

Until now, a few publications based on observations collected on several tens of neurons (Noctor et al., 2004; Noctor et al., 2008; Tabata and Nakajima, 2003) have described radial migration in a rather qualitative manner. Recent time-lapse imaging of migrating cerebral cortex neurons have identified specific phases in radial neuronal migration (Noctor et al., 2004; Noctor et al., 2008; Tabata and Nakajima, 2003). After their final division in the GZ, immature neurons transiently become multipolar, with multiple neurites within the subventricular zone (SVZ) and lower intermediate zone (IZ).Then, neurons change their shape from multipolar to bipolar - with a leading process, a thick neurite extending toward the pial surface- just before migrating along radial glial fibres (Rakic, 1972) from the premigratory zone to the cortical plate (CP).

Here, the examination of several hundreds of migrating neurons on more than 40 organotypic slices provides a population analysis which allows to extract characteristic features of the tempo and dynamics of radial migration.

Brains were electroporated *ex vivo* at E15.5 with the CAG-EGFP plasmid, in which EGFP was used for the visualization. Slices were imaged at 1 hour intervals for 48 hours from 1 day

after electroporation. As electroporation results in a synchronised cycling cell population expressing the transgene (Pilaz et al., 2009), cohorts of EGFP expressing cells were observed to leave the GZ (Fig. 3) (Movie 1).

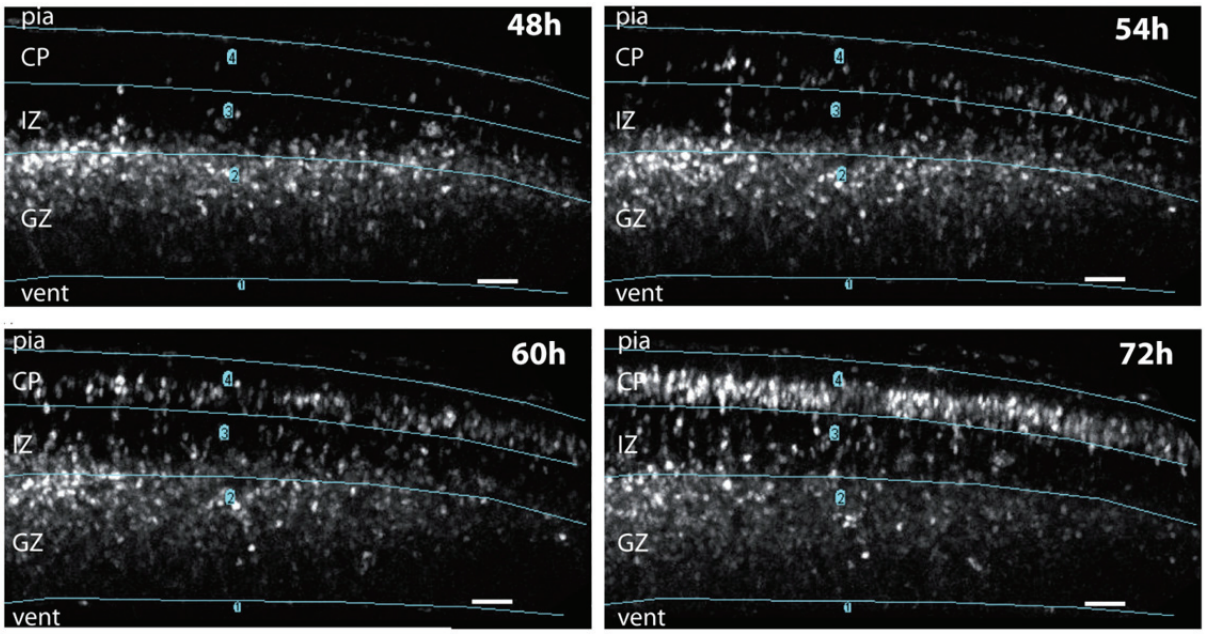

Fig. 3: Radial migration of successive cohorts of EGFP electroporated cells.
Microphotographs of two-photon recordings, 48h, 54h, 60h and 72h after *ex vivo* electroporation. Scale bars:50µm

Typically, newborn postmitotic neurons migrate during about 10h over a distance of circa 90 µm before reaching the CP (Fig. 4A). Nearly half of the neurons pause at least once during their trajectory (Fig. 4A), a behaviour characteristic of the saltatory locomotion (Nadarajah et al., 2001; Nadarajah and Parnavelas, 2002).

Four parameters were monitored: (i) migration velocity defined as the distance with respect to the time in µm/h; (ii) the number of pauses, (iii) the individual pauses duration in h and (iv) the motility index, defined as the distance with respect to the time, minus the pause(s) duration.

The mean Migration Velocity at E16.6is 10.6µm/h, and the mean Motility Index is 12.8 µm/h (Fig. 4A). In order to further characterize the migration kinetics of newborn neurons through the different postmitotic compartments of the embryonic cortical wall, we subdivided the cortex thickness into 10 horizontal bins. This compartmental analysis reveals a 3-phase migration profile which can be broken down as follows: (i) an acceleration during migration initiation, (ii) maximum velocity reached at the top of IZ, where cell density is low, (iii) deceleration at the entry in CP, where the substrate becomes denser (Fig. 4B).

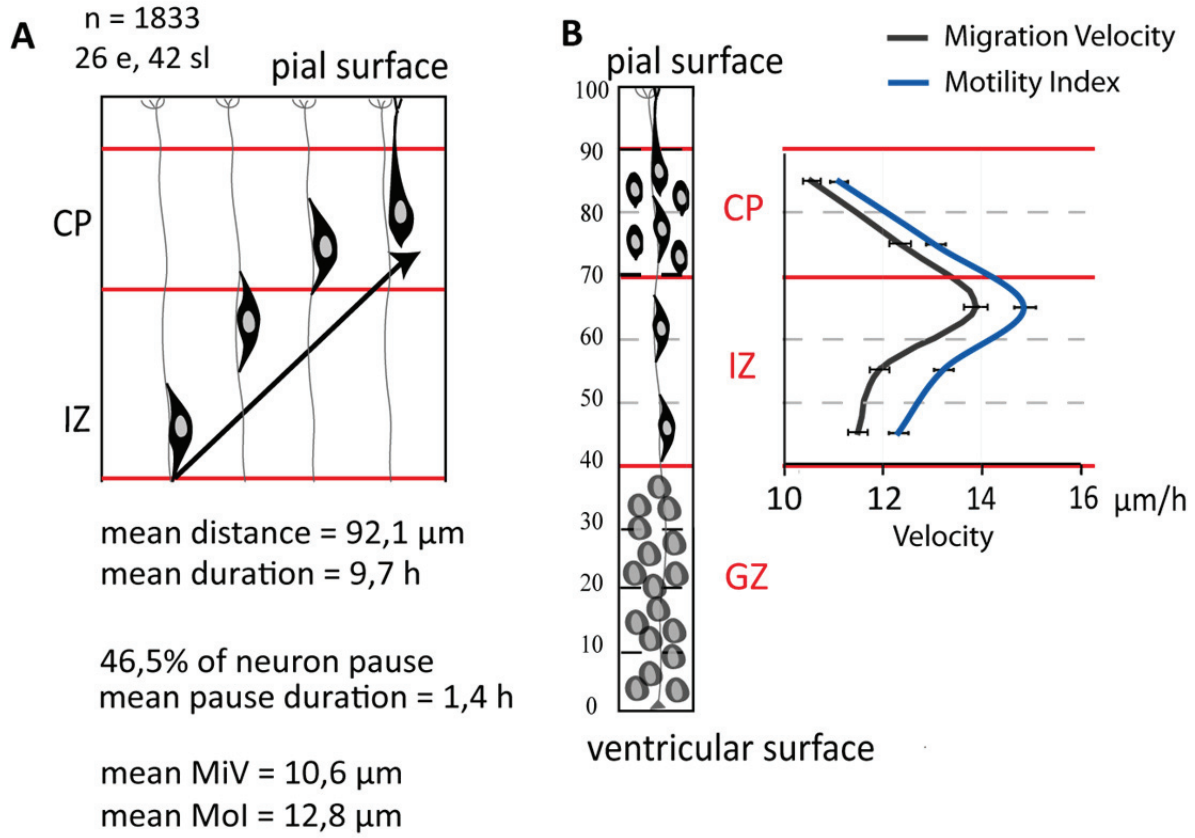

Fig. 4: Dynamics of the radial migratory behaviour of control neurons at E16.5.
A: Radial migration kinetics were measured on more than 1800 post-mitotic neurons. The mean Migration Velocity (MiV) is defined as the migrated distance with respect to the time in µm/h. The mean Motility Index (MoI) is defined as the migrated distance with respect to the time, minus the pause(s) duration.
B: Spatial profile of the mean MiV and MoI in the thickness of cortical wall, subdivided into 10 bins parallel to the ventricular surface.
Kinetics values are averaged on the total population of neurons. Error bars represent SEM.

p27 promotes radial migration of post-mitotic neurons

Two studies reported a promoting effect of p27 on radial migration, based on static observations (Kawauchi et al., 2006; Nguyen et al., 2006a). The conclusions were drawn from the fact that a few days after *in vivo* electroporation, less cells were found in the cortical CP after p27 overexpression. However, these indirect observations do not allow to accurately distinguish migration defects from neuronal production perturbations. Here we investigate how p27 forced expression influence the single cell behaviour using real time live imaging.

A dozen of independent experiments carried out on 64 brains (47 slices) have been implemented (Fig. 5E,F). So as to be able to reliably compare the results from different experiments, the values of the migration parameters have been normalized (control migration velocity: 10µm/h, control motility index: 12µm/h and control pause duration: 0.5h) (Fig. 5 and Fig. S5).

In a first instance, we have analysed the consequence of p27 overexpression (GOF) on the radial migration kinetics of E16.5 newborn postmitotic neurons. Brains were electroporated *ex vivo* at E15.5 with a control pCAG-ires-nls-EGFP or a GOF vector, pCAG-p27 WT-ires-nls-EGFP, and organotypic slices were prepared. EGFP post-mitotic neurons were imaged at 1 hour intervals for 48 hours, starting 1 day after electroporation.

No impairment of the transformation from a multipolar to bipolar shape upon p27 GOF was observed. No obvious delay in migration initiation was observed.

In p27 GOF experiments, videomiscrocopy analysis revealed that the wild-type protein is able to significantly increase the migration kinetics of post-mitotic neurons. In particular, we observe an increased migration velocity (+12%, Fig. S5A). This increase in migration velocity is underlined by a higher motility index (+11%, Fig. 5A), and is therefore not attributable to less pausing in GOF neurons. No significant decrease in pause duration is observed (Fig. 5C). Conversely p27 DM, via siRNA or shRNA electroporation, has the reverse effect. In these conditions, we observe a significant decrease of the migration velocity compared to controls, electroporated with control siRNA or shRNA (Fig. S5B). The pauses duration is also significantly increased (average increase of 200%) (Fig. 5D).However, the decreased migration velocity is not entirely attributable to more pausing since DM neurons exhibit a significantly lower motility index than controls (average decrease of 12%) (Fig. 5B). Despite their migration defect, DM neurons are able to reach the CP. Of note, shRNA p27 #1, which was derived from the siRNA sequence and is compatible for both murine and human p27 sequence, has no significant effect on migration kinetics (Fig. 5B). The others shRNA (# 2 and #3), which specifically target the murine sequence, result in an increased efficiency of the DM. Only shRNA p27 # 2 and #3 were kept for further studies.

To determine which domain of p27 protein is responsible for the promotion of radial migration, we analysed the migration kinetics after overexpression of different p27 mutants. Two mutated forms of p27 are able to increase the migration kinetics: p27 CK- and p27 WT Cter (Fig. S5A). Their common characteristic is the integrity of the C-terminal domain, which allows the interaction with the RhoA pathway. Of note, they both appear to increase the motility index (average increase of 13.5%, Fig. 5A) and decrease pauses duration (average decrease of 68%, Fig. 5B), which makes them more efficient than p27 WT GOF in promoting radial migration. On the contrary, p27 WT Nter and p27 CK- Nter GOF neurons did not show changes in their kinetics, compared to controls (Fig. S5A and Fig. 5A).

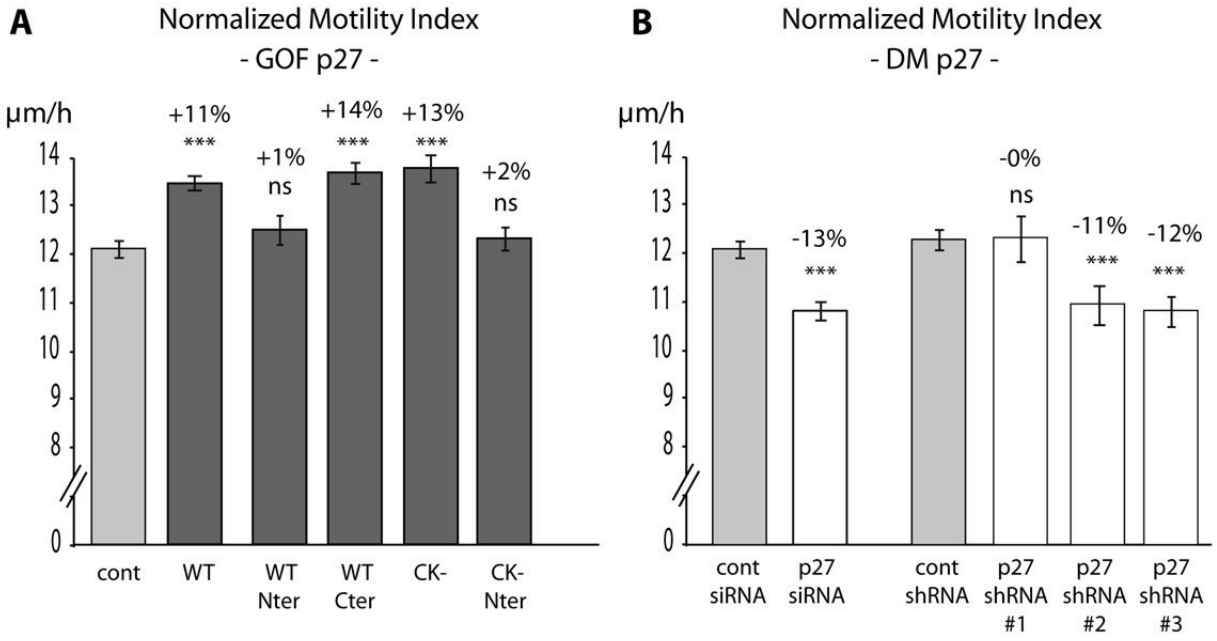

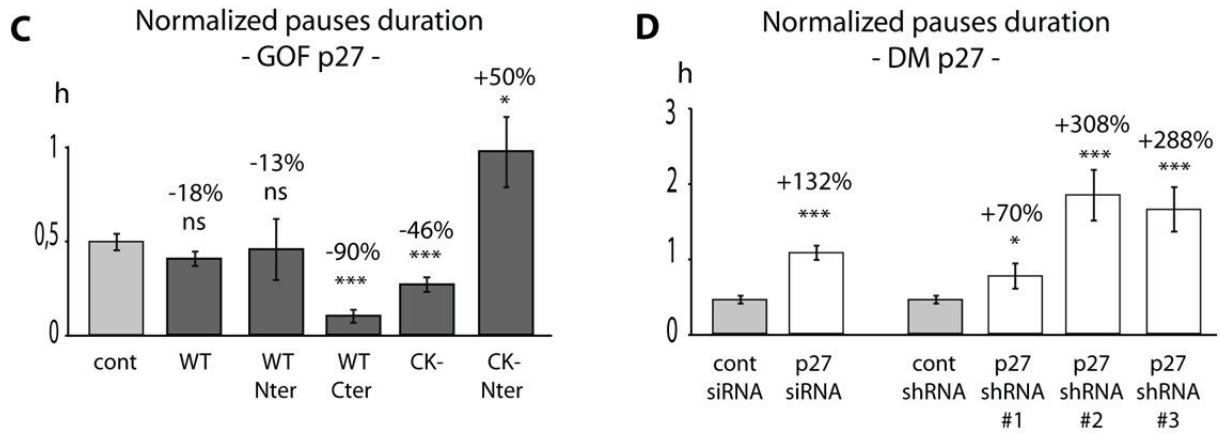

E

	cont	WT	WT Nter	WT Cter	CK-	CK- Nter
n neurons	626	505	143	228	223	158
n slices	7	6	1	2	3	1
n embryos	5	5	1	2	1	1

F

	cont siRNA	p27 siRNA	cont shRNA	p27 shRNA #1	p27 shRNA #2	p27 shRNA #3
n neurons	250	212	165	78	67	87
n slices	7	9	3	3	3	4
n embryos	5	5	2	2	2	3

Fig. 5: p27 promotes radial migration of post-mitotic cells at E15.5.

A,B: Motility index (µm/h) calculated on radially migrating cells after overexpression of different forms of p27 (A), or after p27DM by RNAi (B). Control motility index was normalized to 12µm/h.

C,D: Total pause duration (h) of migrating cells make after overexpression of different forms of p27 (C), or after p27DM by RNAi (D). Control pause duration was normalized to 0.5h.

E,F: Tables compiling the number of embryos, brain slices and neurons analysed in each conditions, after overexpression of different forms of p27 (E), or after p27DM by RNAi (F).

Kinetics values are averaged on the total population of neurons. Error bars represent SEM.

Student's t tests ; p values: < 0.05 *, < 0.01 **, < 0.005 ***, compared to control, control siRNA or control shRNA.

In a refined analysis, we measured migration kinetics through the different postmitotic compartments of the embryonic cortical wall, subdivided into 10 horizontal bins (Fig. 6). This revealed that p27 wt, p27 WT Cter and p27 CK- GOF promote migration kinetics mostly in the CP where control neurons begin their deceleration. Of note, they also slightly accelerate the motility index during migration initiation in the lower IZ. By contrast, p27DM induces a motility index decrease in the IZ, where control neurons accelerate. Thus, p27 may impact on migration kinetics to a different extent depending on the extracellular context met in the different post-mitotic compartments.

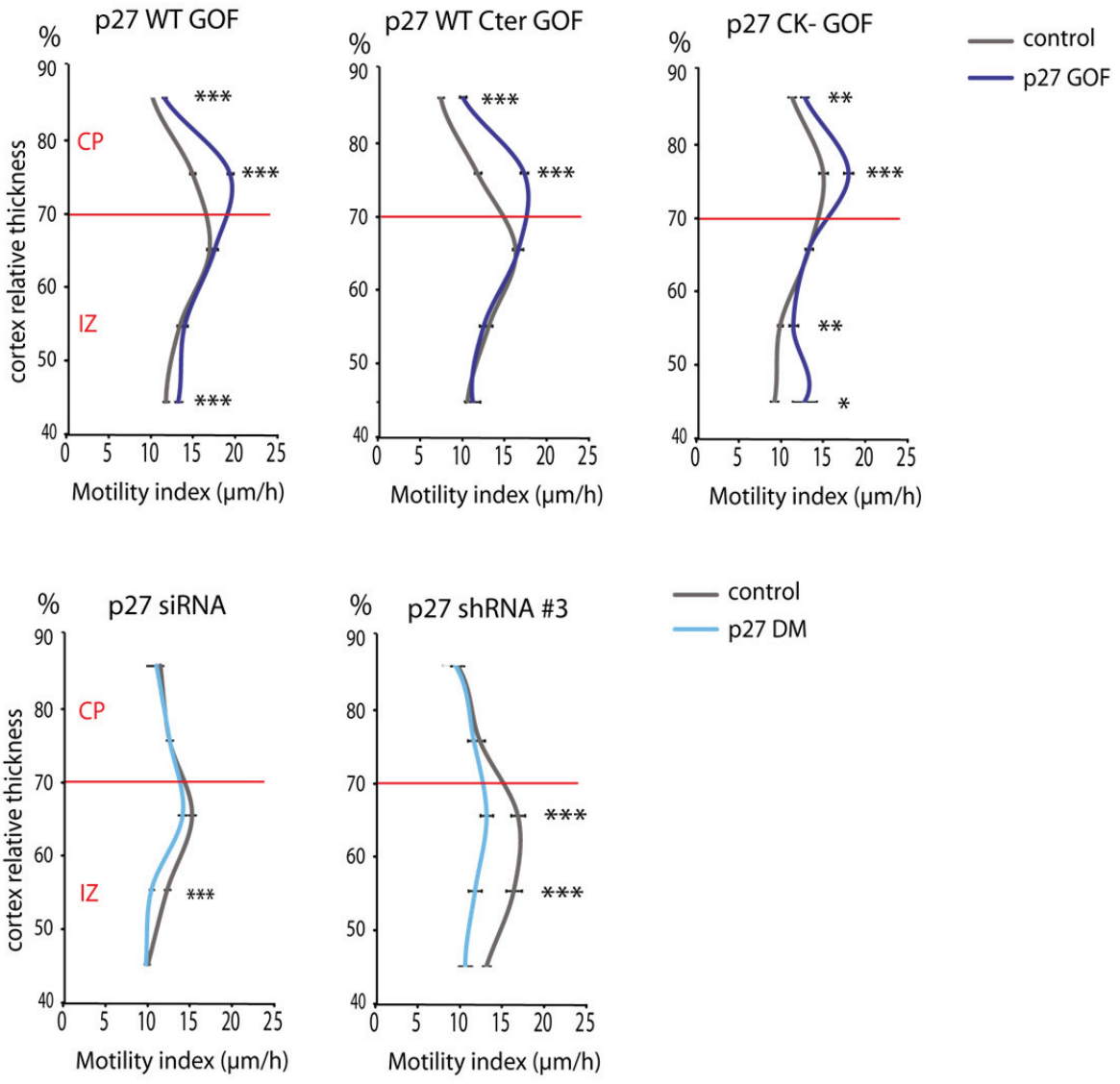

Fig. 6: p27 spatial specific effect on neuronal radial migration in E15.5 post-mitotic compartments.
Spatial profile of the mean Motility Index in the thickness of the cortical wall, subdivided into 10 horizontal bins, parallel to the ventricular surface, after p27 GOF or DM.
Kinetics values are averaged on the total population of neurons. Error bars represent SEM.
Student's t tests ; p values: < 0.05 *, < 0.01 **, < 0.005 ***, compared to control, control siRNA or control shRNA conditions.

p27 promotes migration through the RhoA pathway

The real-time observations confirm that p27 promotes the radial migration of post-mitotic neurons in the cortex. They show that p27 effect on cell motility relies on its C-terminal domain, probably through inhibition of the RhoA pathway (Nguyen et al., 2006a; Nguyen et al., 2006b).

To verify that p27 effect on radial migration is mediated by inhibition of the RhoA pathway, we examined the consequences of an inhibitor of one RhoA effector, the ROCK kinase. We implemented a rescue experiment using shRNA p27 #3 (the most efficient shRNA construct to decrease migration kinetics). The inhibitor Y27632 (10µM) (Narumiya et al., 2000) was added to the organotypic slices culture medium, just before the beginning of radial migration of the electroporated cohort (48h after electroporation), during 7 or 24h (Fig. 7). The analysis of the migration kinetics shows a gradual rescue of the migration defect.

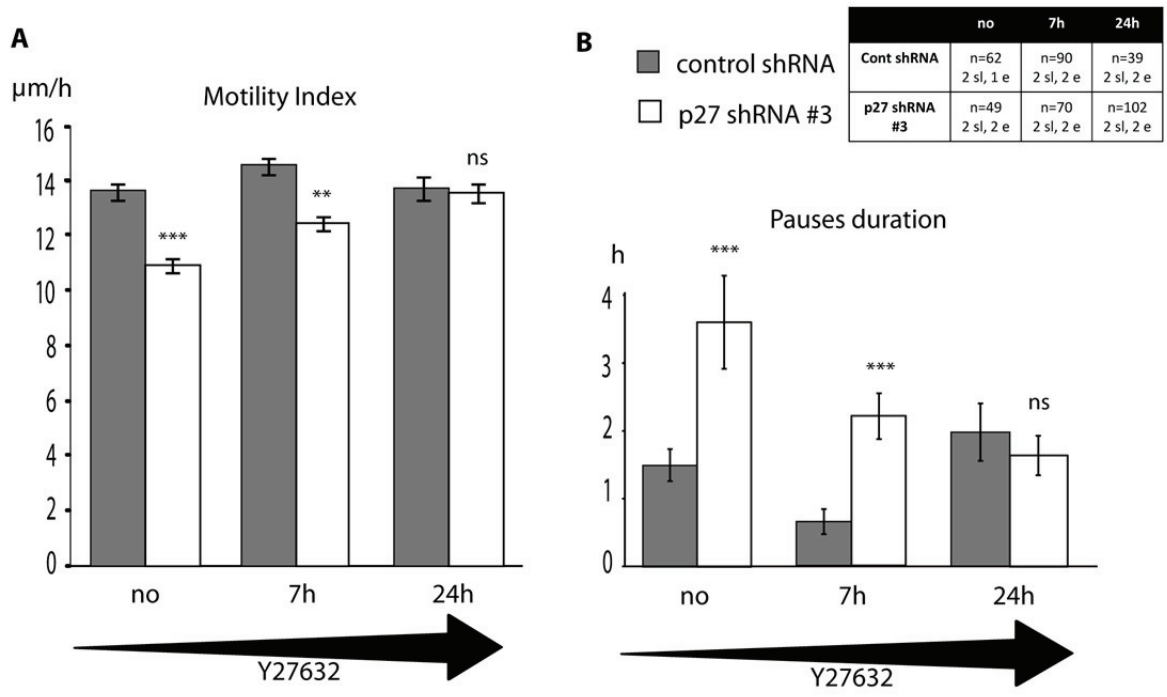

	no	7h	24h
Cont shRNA	n=62 2 sl, 1 e	n=90 2 sl, 2 e	n=39 2 sl, 2 e
p27 shRNA #3	n=49 2 sl, 2 e	n=70 2 sl, 2 e	n=102 2 sl, 2 e

Fig. 7: Inhibition of the RhoA pathway rescues the radial migration defects after p27 DM at E15.5.
A: Migration velocity (µm/h) calculated on radially migrating cells after p27 DM by shRNA at E15.5, and application or not of the RhoA inhibitor Y27632 (10µM) in the culture medium for 7 or 24h during the migration of post-mitotic cells.
Kinetics values are averaged on the total population of neurons. Error bars represent SEM.
Student's t tests ; p values: < 0.05 *, < 0.01 **, < 0.005 ***, compared to control shRNA conditions.

After 7h of inhibitor exposure, the kinetics of both control and shRNA electroporated cells are increased, compared to the condition without inhibitor. After 24h of inhibitor exposure, the shRNA electroporated cells display the same migration kinetics values than

control cells (Fig.7). Furthermore, observations of the spatial profile of motility index confirms that Y27632 inhibitor rescues the migration defects of p27 shRNA expressing neurons during their entire trajectory towards the pia (Fig. 8).

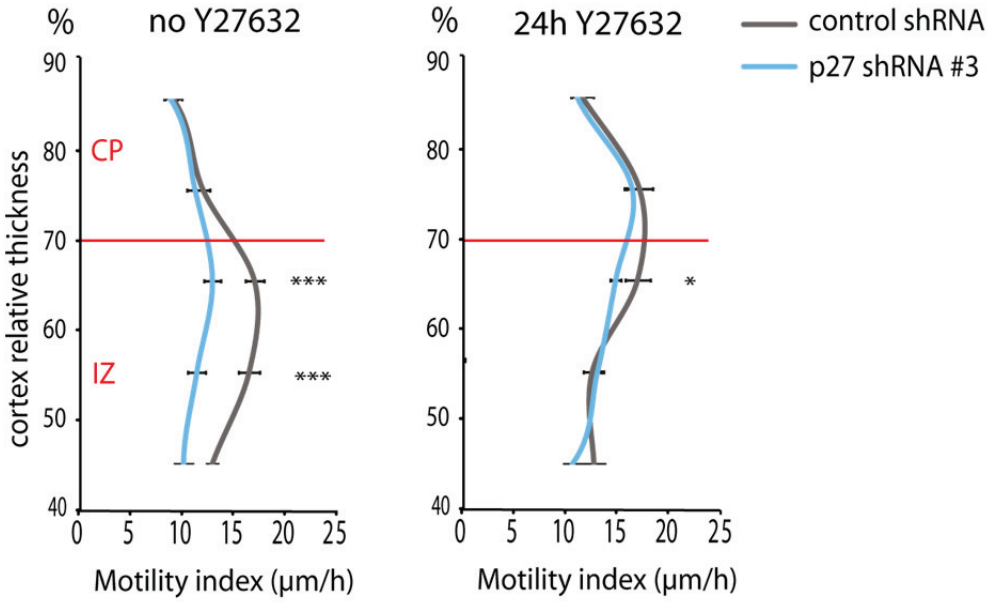

Fig. 8: Inhibition of the RhoA pathway restores the spatial profile of migrating neurons, impaired after p27 DM at E15.5

Spatial profile of the mean Motility Index in the thickness of the cortical wall, subdivided into 10 bins parallel to the ventricular surface, in neurons expressing p27 shRNA, cultured in presence or not of the ROCK inhibitor Y27632 (10µM).

Kinetics values are averaged on the total population of neurons. Error bars represent SEM.

Student's t tests ; p values: < 0.05 *, < 0.01 **, < 0.005 ***, compared to control shRNA conditions.

These observations show that RhoA pathway inhibition is sufficient to rescue the migration defect of p27 DM neurons. Counteracting the lack of RhoA pathway inhibition by p27 brings back the migration kinetics values to normal. These results confirm that p27 acts on radial migration kinetics through inhibition of the RhoA pathway.

p27 negatively regulates cortical precursor cells proliferation

p27 is a well-known regulator of the cell-cycle progression, inhibiting cyclin E or A-CDK2 complexes through its N-terminal domain (Sherr and Roberts, 1999). p27 has been implicated in the cell-cycle arrest of cortical precursors (Caviness et al., 2003; Goto et al., 2004; Lukaszewicz et al., 2005; Tarui et al., 2005). RhoA is highly expressed in the VZ and SVZ (Nguyen et al., 2006a). In the VZ, the RhoA signalling could influence the motion of cycling APs during the INM which has been shown to be coupled with cell-cycle progression (Kosodo et al., 2011). Here, we explore the relative contribution of the N and C-terminal domains of p27 on the regulation of cell-cycle progression in cortical progenitors.

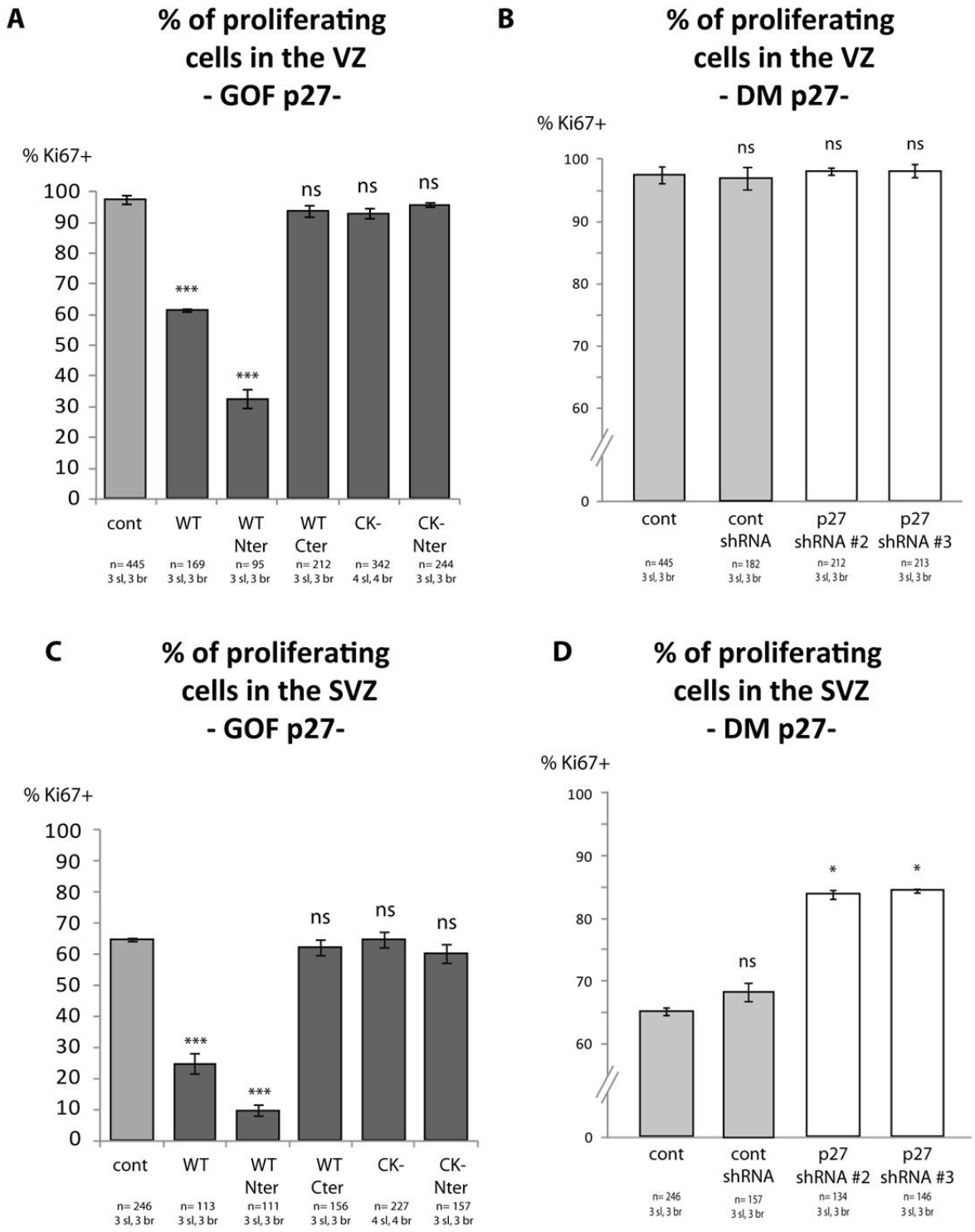

Fig. 9: Effect of p27 GOF and DM on the proportion of cycling cells in the VZ and the SVZ, 48h after in utero electroporation at E15.5.

A,B: Proportion of Ki67+ cells among the EGFP+ cells in the VZ, in GOF (A) and DM (B) conditions.
C,D: Proportion of Ki67+ cells among the EGFP+ cells in the SVZ, in GOF (C) and DM (D) conditions.
Proportion values are averaged on the total number of repeated observations (number of EGFP cells (n), brain slices (sl) and embryos (e) analyzed). Error bars represent SEM.
GLM tests ; p values: < 0.05 *, < 0.01 **, < 0.005 ***, compared to control condition

In a first step, we examined the consequences of p27 GOF and DM on the cycling status of cortical precursors in the VZ and SVZ, by computing the proportion of Ki67 expressing EGFP cells (Ki67+) (Fig. S6 and S7). In control conditions, nearly all the EGFP cells in the VZ are cycling (97.5% are Ki67+) (Fig. 9A), whereas in the SVZ almost half of the EGFP cells have exited the cell-cycle (64.9% are Ki67+) (Fig. 9C), confirming that the VZ is the main proliferating compartment. 48h after p27 WT GOF, more than 40% of the VZ EGFP cells have exited the cell-cycle (61.5% Ki67+ vs. 97.5% in control) (Fig. 9A). A 3-fold decrease of cycling cells (25% Ki67+ vs. 64.9% in control) was observed in the SVZ (Fig. 9C). p27 WT Nter GOF leads to a more drastic effect, with a 3-fold and 6-fold decrease of cycling cells in the VZ and the SVZ, respectively (32.6% and 9.9% of Ki67+ cells respectively) (Fig. 9A,C). The overexpression of p27 mutants unable to interact with Cyclin/CDK complexes (WT Cter and CK-) does not influence proportions of cycling cells in both germinal zones (Fig. 9A,C).

p27 DM results in an increase of the cycling cell proportion in the SVZ (84% vs. 64.9% for control) (Fig. 9D). No significant changes are observed in the VZ (where nearly more than 95% of precursors are Ki67+ in control condition) (Fig. 9B).

These results confirm that p27 promotes cell-cycle exit of cortical progenitors through its N-terminal domain.

The proportion of cells in M phase at E17, 48h after GOF or DM, was measured using phospho-Histone3 (pH3) immunolabelling (Fig. S8 and S9). Few mitotic cells are found in the control condition in the VZ (3.8%) and in the SVZ (1.1%) (Fig. 10 A,C). In the VZ, all mitotic cells are found lining the ventricular border, whereas they are scattered in the SVZ (Figure S8 and S9), as previously described (Takahashi et al., 1996). As mitosis is the shortest cell-cycle phase, lasting about one hour, the proportion of cells in M phase at any given time point is low. This minute fraction of mitotic cells was nevertheless significantly decreased after p27 WT and p27 WT Nter GOF in the VZ (Fig. 10 A). A similar trend of decreased rates of mitotic cells was also observed in the SVZ (Fig. 10 C). p27 DM was not found to significantly impact on mitotic cell proportions, probably due to the moderate modification of p27 expression. (Fig. 10 B,D). Again, the p27 mutants unable to interact with Cyclin/CDK complexes do not exert a significant effect on M phase cells proportion (Fig. 10 A,C). All together, these results confirm that p27 inhibits cell-cycle progression through its N-terminal domain.

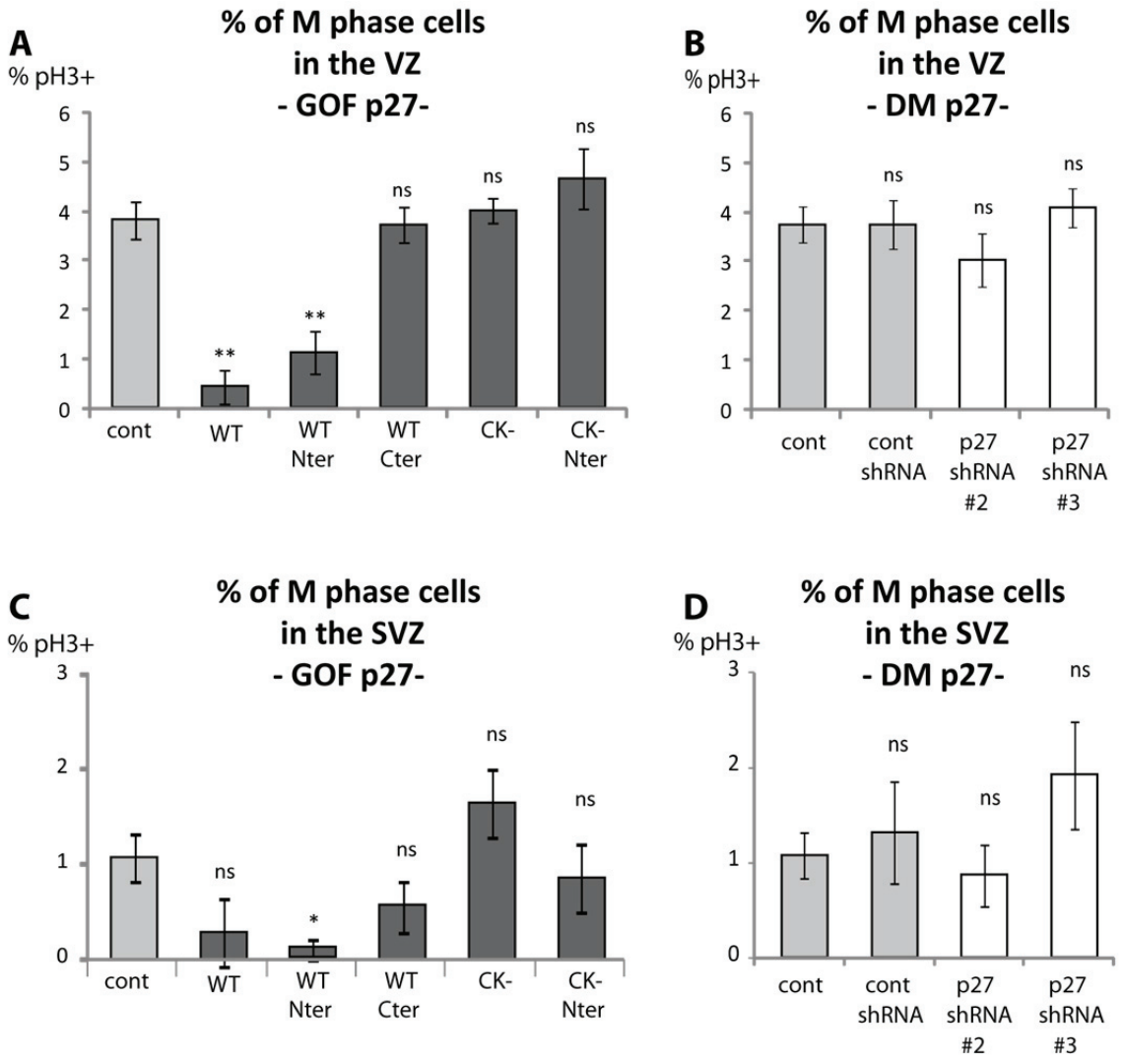

E

	cont	WT	WT Nter	WT Cter	CK-	CK- Nter
n VZ cells	1215	493	730	1215	877	1083
n SVZ cells	840	362	951	1088	729	939
n slices	9	8	10	9	6	8
n embryos	5	4	4	5	3	5

F

	cont	cont shRNA	p27 shRNA #2	p27 shRNA #3
n VZ cells	1215	924	1078	774
n SVZ cells	840	608	810	522
n slices	9	10	8	6
n embryos	5	5	4	3

Fig. 10: Effect of p27 GOF and DM on the proportion of M-phase (pH3+) cells, in the VZ and the SVZ, 48h hours after in utero electroporation at E15.5.

A,B: Proportion of pH3+ cells among the EGFP+ cells in the VZ, in GOF (A) and DM (B) conditions.
C,D: Proportion of pH3+ cells among the EGFP+ cells in the SVZ, in GOF (C) and DM (D) conditions.
E,F: Tables showing the number of embryos and brain slices that have been analysed, as well as the number of precursor cells counted in each conditions, after GOF of different forms of p27 (E), or after p27 DM (F).
Proportion values are averaged on the total number of repeats. Error bars represent SEM.
GLM tests ; p values: < 0.05 *, < 0.01 **, < 0.005 ***, compared to control conditions.

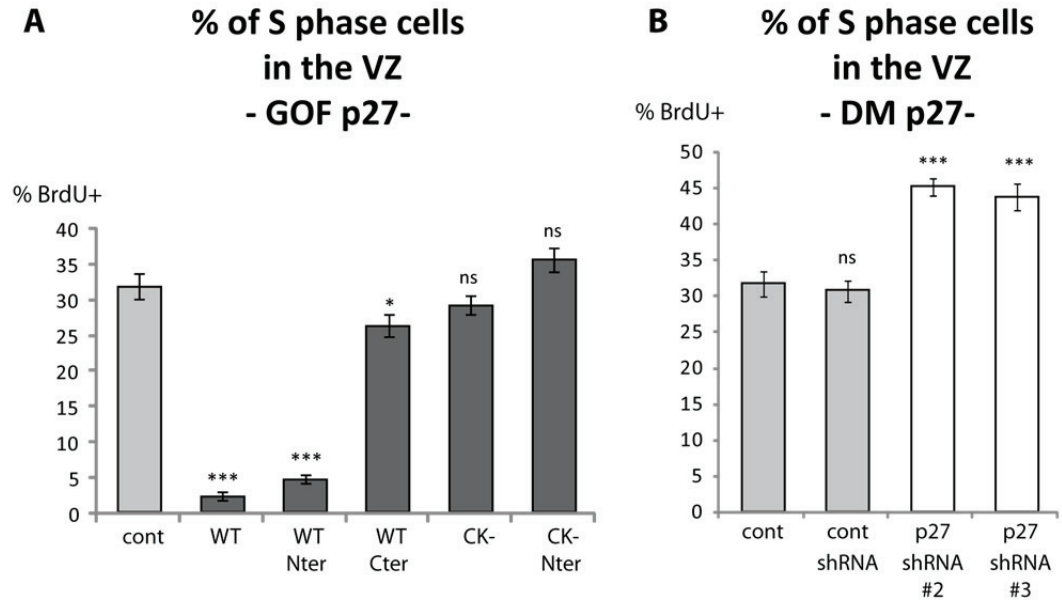

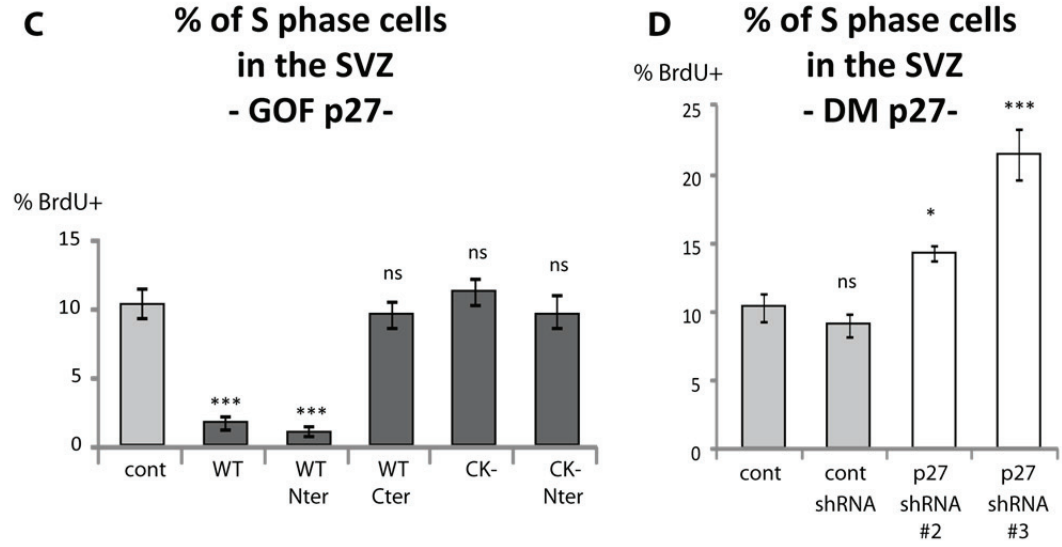

E

	cont	WT	WT Nter	WT Cter	CK-	CK- Nter
n VZ cells	1215	493	730	1215	877	1083
n SVZ cells	840	362	951	1088	729	939
n slices	9	8	10	9	6	8
n embryos	5	4	4	5	3	5

F

	cont	cont shRNA	p27 shRNA #2	p27 shRNA #3
n VZ cells	1215	924	1078	774
n SVZ cells	840	608	810	522
n slices	9	10	8	6
n embryos	5	5	4	3

Fig. 11: Effect of p27 GOF and DM on the proportion of S-phase (BrdU+) cells, in the VZ and the SVZ, 48h hours after in utero electroporation at E15.5. A 30 min BrdU pulse was performed before sacrifice at E17.5.

A,B: Proportion of BrdU+ cells among the EGFP+ cells in the VZ, in GOF (A) and DM (B) conditions.
C,D: Proportion of BrdU+ cells among the EGFP+ cells in the SVZ, in GOF (C) and DM (D) conditions.
E,F: Tables showing the number of embryos and brain slices that have been analysed, as well as the number of precursor cells counted in each conditions, after GOF of different forms of p27 (E), or p27DM (F).
Proportion values are averaged on the total number of repeats. Error bars represent SEM.
GLM tests; p values: < 0.05 *, < 0.01 **, < 0.005 ***, compared to control conditions.

We checked that p27 blocks the progression in S phase, by measuring the proportion of BrdU labelled EGFP cells at E17, after GOF or DM through electroporation at E15 (Fig. S8, S9). BrdU was injected to the electroporated embryos 30 min before sacrifice at E17, in order to precisely label cells which are in S phase. In control condition, 31.7% of the EGFP+ VZ cells are in S phase 48h after electroporation, whereas only 10.4% of the EGFP+ SVZ cells are in S phase, confirming that the VZ is the main proliferating compartment (Fig. 11 A,C). Precursor cells overexpressing p27 WT or p27 WT Nter show a drastic decrease of BrdU labelling, both in the VZ and the SVZ, compared to control condition (Fig. 11 A,C). Of note, the proportion of S-phase cells is barely higher in the VZ than in the SVZ. Conversely p27 DM has the reverse effect (Fig. 11 B,D), although less drastic, due to the moderate modification of p27 expression. These results confirm that p27 inhibits S phase progression, through its N-terminal domain. The other p27 mutants, unable to interact with Cyclin/CDK complexes, do not exert a significant effect on S phase cells proportion (Fig. 11 A,C). One exception was observed in the case of p27 WTCter GOF condition which returned slightly lower proportions of cells having incorporated BrdU in the VZ. This could result from (i) a decreased number of cells in S phase, or (ii) a shorter S phase, diminishing the time window for BrdU incorporation. Real time experiments described further are in favor of a shortening of G1+S phase in p27 WT Cter GOF precursors (see Fig. 15).

p27 role in cell-cycle duration

Because classical methods to measure cell-cycle phases duration (eg cumulative BrdU labelling and computation of the percentage of labelled mitotic figures) are not appropriate to study cell-cycle kinetics of electroporated cells (Pilaz et al., 2009), we turned to time-lapse videomicroscopy analysis to analyse cell-cycle duration of normal, GOF and DM precursors.

We performed clonal cell electroporation of EGFP (Morin et al., 2007), in order to reliably track individual VZ precursor cells and their progeny (Movie 2 and 3, Fig. 12, for a magnification, see Fig. S11). In utero electroporation of control, GOF or DM expression vectors was performed at E14.5, organotypic slices were prepared at E15 and maintained in culture during 3 days. Using two-photon videorecording of the EGFP cells we were able to reconstruct cell lineages up to 4 successive divisions. At E14.5 the majority of the targeted precursors undergo 2 or 3 rounds of divisions, before exiting the cell-cycle. This strategy allowed to track several hundreds of cells and divisions, in the different GOF and DM conditions (Table 1). Because p27 shRNA#3 was the most efficient p27 shRNA to decrease p27 levels (Fig. S4 D,E) and to modify progenitors cell-cycle dynamics (Fig. 11D), we focused on this construct to study the DM effects. p27 WT and WT Nter GOF lead to a complete arrest of the cell-cycle and the INM, and all the electroporated precursors stop their progression in the cell-cycle before becoming neurons which migrate out of the GZ. We therefore focused on the effect of p27 WT Cter and p27 CK-. Of note, the CK- Nter GOF did

not lead to significant differences in the division pattern (Fig. S10), consistent with the absence of the domains acting on cell-cycle progression and cytoskeleton.

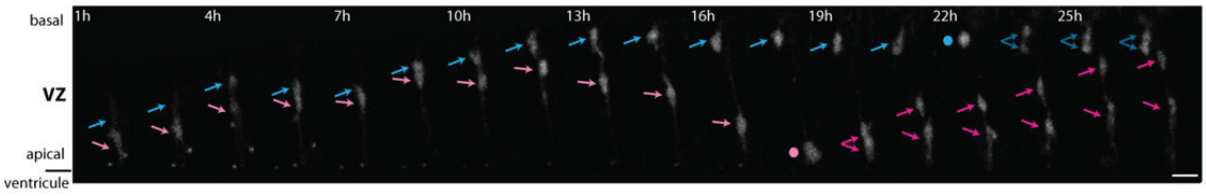

Fig. 12: Two-photon videomicroscopy acquisitions showing the division of an AP (pink arrow) and a BP (blue arrow).
The AP and the BP are daughter cells produced from a division that occurred a t 0. Both progenitor cells undergo a basal movement away from the ventricular surface, remaining close to each other. 12 h after division, the AP begins its apical movement towards the ventricule, to divide about 18 h after its birth (pink dot). Note that the basal process is very narrow during mitosis. On the contrary, the BP remains in the basal part of the VZ and divides about 22h after its birth (blue dot). Note the complete retraction of its processes during division, during which it adopts a spherical morphology. After this second round of division, both daughter cells of the AP display a basal movement, one going faster than the other, whereas the BP daughter cells stay rather static and close to each other. Scale bar: 20µm

	cont	p27 shRNA #3	GOF p27 WT	GOF p27 WT Nter	GOF p27 WT Cter	GOF p27 CK-	GOF p27 CK- Nter
n total cells	1310	913	27	71	467	469	327
n divisions	466	350	0	0	165	166	112
n neurons	100	27	27	71	25	47	28
n slices	9	15	8	10	9	6	8
n embryos	5	7	4	4	5	3	5

Table 1: Number of experiments and observations in videomicroscopy analysis, after E14.5 in utero electroporation.

Observation at the single cell level in real time allows to measure the time period elapsing between two successive mitosis, which corresponds to the cell-cycle length. Here, only the second and third generations of cells, where the entire cell-cycle could be observed, have been taken into account. In control conditions, the BPs, predominantly giving rise to neurons, have a longer cell-cycle length than the APs (21.0h vs. 18.7 h, p=0.002) (Fig. 13A). After p27 DM, cell-cycle length of both APs and BPs is shorter than in control progenitors (15.6h vs. 18.7h for APs, 18.3h vs. 21.0h for BPs) (Fig. 13A). p27 WT Cter GOF and p27 CK- GOF do not exert a significant impact on cell-cycle length (Fig. 13B).

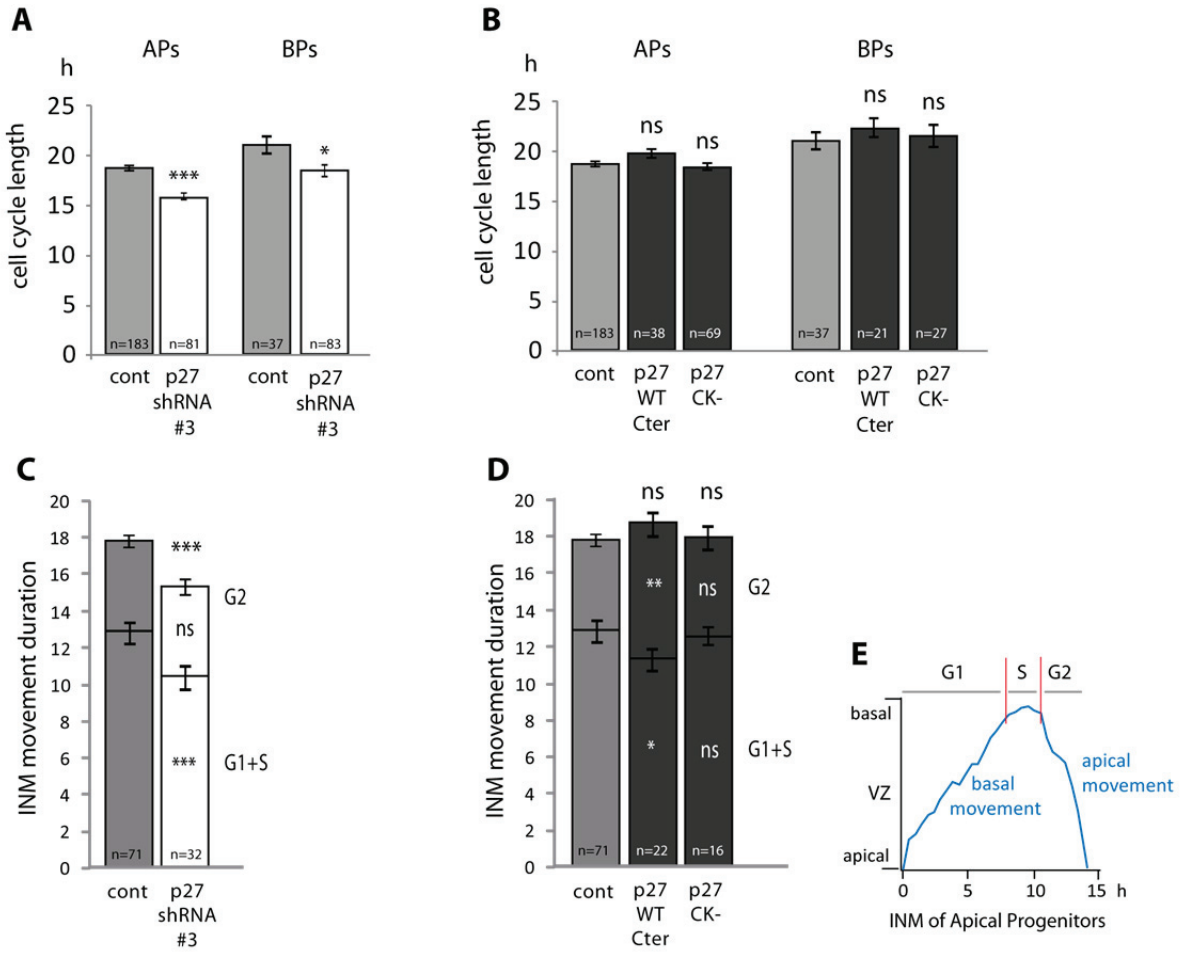

Fig. 13: Effect of p27 GOF and p27 DM on the cell-cycle length of AP and BP cells, measured on videomicroscopy recordings after E14.5 in utero electroporation.

A,B: Measurement of the number of hours elapsed between the birth of a precursor cell and its subsequent division, after p27 DM (A) or p27 GOF (B)

C,D: Duration of the movement associated with G1+S phase and G2 phase, during the INM of APs, after p27 DM (C) or p27 GOF (D)

C,D: Duration of the movement associated with G1+S phase and G2 phase, during the INM of APs, after p27 DM (C) or p27 GOF (D)

E: Spatiotemporal profile of the position of one apical progenitor cell nucleus, in the VZ thickness, during the INM movement. Correspondence between the cell-cycle phases (G1, S and G2) and the basal and apical nuclear movement is represented.

Measures are averaged on the total population of each progenitor type, for each condition. Error bars represent SEM.

n refers to the number of cells which have been analysed

GLM tests ; p values: < 0.05 *, < 0.01 **, < 0.005 ***, compared to control condition

In the VZ, nuclei of neural progenitors move up-and-down during the progression in the cell-cycle, undergoing the well characterized interkinetic nuclear movement (Sauer and Walker, 1959), [reviewed in (Reiner et al., 2011)]: during the G1 phase, the nuclei move to the basal surface and to the opposite (ventricular apical surface) side in G2. S phase occurs at the basal border of the VZ and mitosis takes place at the apical border, near the ventricule (Fig. 13E). This stereotypic cell-cycle related movement has been extensively characterised by several groups (Baye and Link, 2007; Kosodo et al., 2011; Tsai et al., 2010). This makes it

possible to estimate the relative length of G1/S phase and G2 phases by measuring the time period that precursors spend in the different fractions of the INM trajectory (Fig. 13E). In agreement with the published literature (Baye and Link, 2007; Kosodo et al., 2011; Tsai et al., 2010), we considered that G1 phase duration corresponds to the basally ascending movement, S phase to the time period when the precursor was located at the basal border of the VZ and undergoes minute stochastic movements. G2 duration was considered to correspond to the duration of the descending apically directed movement.

Our analysis shows that control APs undergo the classic basal- and apical-directed movements toward the VZ/SVZ border and the ventricule respectively (Fig. 12 and Movie 3). Precursors divide apically at the ventricular border to produce two daughter cells (Fig. 12). p27 WT GOF and p27 WT Nter GOF APs showed a strong impairment of the INM movement (Movie 4, Fig. 14 and S12). In these two GOF conditions, APs are unable to undergo a complete movement toward the ventricule. Instead they undergo a very slow random apically directed movement, which stops in the middle of the VZ. These precursors never reach the ventricular surface. They then resume a slow basally directed motion, to settle in the SVZ and become neurons (Movie 4, Fig. 14 and S12). By contrast, overexpression of the mutated forms of p27 (p27 CK-, WT Cter and CK- Nter) which do not interfere with the Cyclin/CDK complexes cell-cycle regulation, or p27 DM, did not alter the INM process. Under these conditions, the precursors undergo the complete basal- and apical-directed movement and divide at the ventricular surface like control precursors (Fig.14 and Movie 5).

Using this analytical procedure, we observe that control APs G2 phase is shorter than G1+S phase (4.9 h vs 13.0 h), confirming the published cell-cycle kinetics (Caviness et al., 2003) (Fig. 13 C). Except for the initial movement which pushes up the nucleus out of the ventricular surface right after division, the G1 basal movement is very slow, with a shallow slope, not easy to distinguish from the almost stationary behaviour observed in S phase nuclei (Fig. 13E). p27 DM shortens the duration of G1+S phase (10.4 h vs. 13.0 h for controls), but does not affect G2 phase length (Fig. 13C), confirming that p27 influences cell-cycle duration of APs, more precisely the G1+S phase (Lukaszewicz et al., 2005), consistent with the well-described p27 inhibitory action on the G1/S phase checkpoint (Sherr and Roberts, 1999). No significant differences in G1/S and G2 phases between control and CK- GOF were observed (Fig. 13D).

We observed that p27 WT Cter GOF induces a reduction in G1/S duration (11.3 h vs. 12.9 h for controls) and lengthens G2 phase (7.2 h vs. 4.9 h for controls) (Fig. 13C).

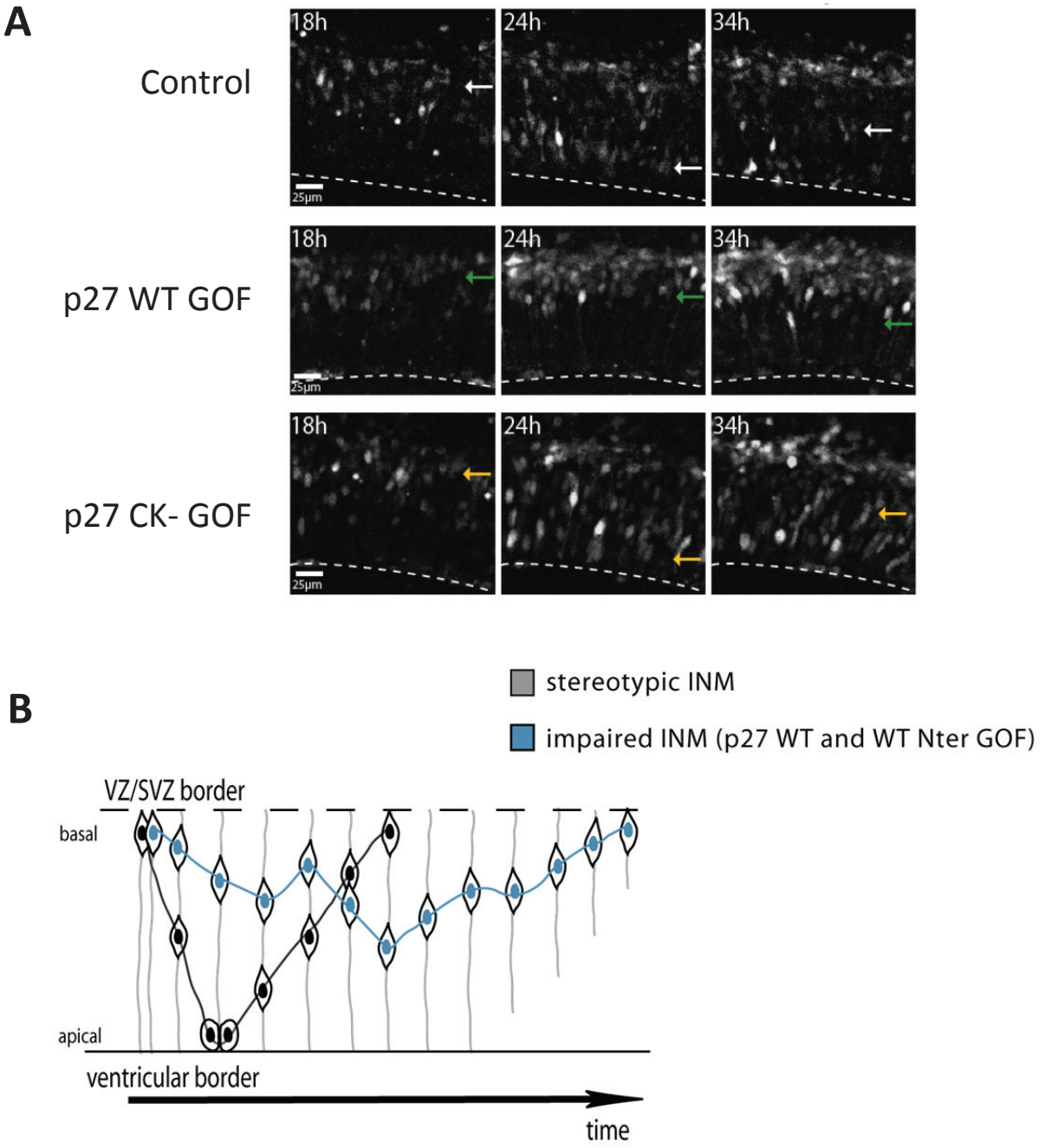

Fig. 14: Stereotypic INM movement and its impairment in p27 WT and WT Nter GOF AP cells.
A: Two-photon microphographs showing the apical movement occurring in G2 phase between 18h and 24h after electroporation of control vectors or p27 WT and CK- GOF vectors. Control and p27 CK- GOF cells manage to undergo divisions at the ventricular border (white and yellow arrows) whereas p27 WT GOF progenitor cells stay at the basal side of the VZ (green arrows).
B: Schematic view of the stereotypic INM movement observed in conditions that do not interfere with INM progression (control, p27 WT Cter / CK- / CK- Nter GOF,p27 shRNA), as well as impaired INM observed after p27 WT and WT Nter GOF.

p27 Cter affects INM dynamics

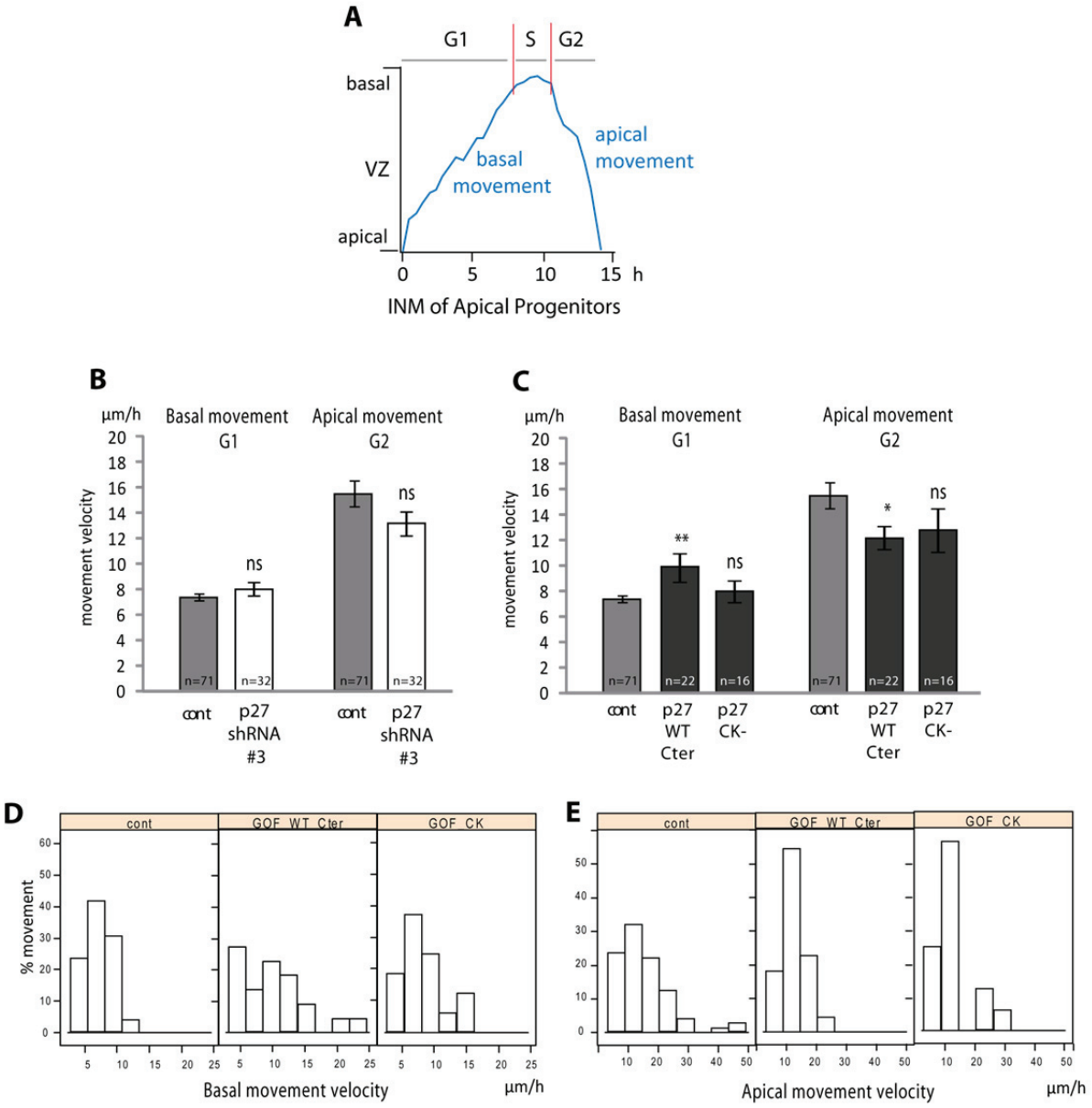

Fig. 15: Effect of p27 DM and p27 GOF on the kinetics of INM movements in the VZ, observed on videomicroscopy recordings after E14.5 in utero electroporation.

A: Spatiotemporal profile of the INM movement of APs

B,C: Velocity of INM basal and apical movement, after p27 DM (B) or p27 GOF (C)

Velocities are averaged on the total population of cells. Error bars represent s.e.m.

D,E: Distribution of the velocities among the p27 GOF AP cells, for the basal movement (D) and the apical movement (E)

GLM tests; p values: < 0.05 *, < 0.01 **, < 0.005 ***, compared to control conditions

The INM offers a unique model to study p27-related mechanisms that potentially correlate proliferation and migration of cycling APs. Here, we analysed the INM kinetics in E15 mouse cortical precursors.

We measured the kinetics of both basal and apical movements during APs cell-cycle in the GOF and DM conditions where the INM is maintained. Based on quantitative tracking of nuclear movements, the INM trajectory was broken up in three segments as follows (i) the basal movement in G1 phase, (ii) the stationary phase at the VZ/SVZ border in S phase (iii) and apical movement in G2 phase (Fig. 15A). The migration velocity was analysed in each of these INM segments (Fig. 15). Only complete INM movements, from one ventricular division to another, were taken into account. This allowed to distinguish the basal movements performed by cycling APs from the delamination movements performed by BPs or neurons, born at the ventricular border. Delamination movements are also followed by a stationary phase, either before a BP divides, or before a neuron migrates up to the CP (Movie 6).

In control APs, the INM basal movement is slower than the apical movement. This can be seen on the spatial profile representation (Fig. 15A), showing a steeper slope for the G2 phase associated -movement than for the G1 phase motion. Quantitative tracking of the movements reveals that the apical movement velocity (G2 phase) is more than twice as fast as the basal movement (G1 phase) (7.3 and 15.3 µm/h respectively) (Fig. 15B). After p27 DM, the velocity of INM movement is not modified, neither for the basal movement nor for the apical movement (Fig. 15B). After p27 WT Cterm, the velocity of the basal movement (G1) is significantly increased whereas the apical movement (G2) velocity is decreased (Fig. 15C). These observations are consistent with the observed changes in G1 and G2 duration which are respectively shortened and lengthened in p27 WT Cter GOF (cf Fig. 13D). After CK- GOF, the velocity of both the basal and the apical movements was also altered, although not significantly (Fig. 15B). Examination of the distribution profiles of velocities shows that whereas the maximum velocity during the basal movements of APs is 10µm/h, it reaches 15µm/h in CK-GOF, and even 25µm/h in WT Cter GOF. Conversely, velocities of CK-GOF APs did not exceed 30µm/h during the apical movement, whereas APs showed velocities up to 50µm/h. (Fig. 15D,E).

These results show that p27 Cter domain alters AP cell motility during G1 and G2 phases in different manners. Whereas p27 Cter promotes G1 movement velocity, it slows down G2 velocity.

p27 affects the type of divisions

Long-term two-photon recordings of clonally electroporated cells allowed us to reconstruct cell lineages, and to identify the type of divisions undergone by progenitors cells (Movie series 7).

Analysis of the successive rounds of divisions reveals that, in control conditions, AP cells are the most numerous progenitor type, outnumbering BPs, in agreement with their higher proliferative abilities (Noctor et al., 2004; Paschal et al., 1987) (Fig. S13).

In the control condition, more than 250 divisions have been classified in 8 categories (6 for APs and 2 for BPs) (Fig. 16). In AP divisions, all possible combinations of symmetric and asymmetric divisions were observed (Fig. 16 A,C). By contrast, BPs were never observed to undergo asymmetric divisions giving rise to one BP and one neuron, under any experimental condition (Fig. 16 A,B). Each division type is not equally represented in the control population. The three most frequent division types are (i) AP asymmetric differentiative divisions where an AP produces one AP and one neuron (AP>AP+N: 34.2%), (ii) AP symmetric differentiative divisions where an AP produces two neurons (AP>N+N: 22.4%),(iii) BP symmetric differentiative divisions producing two neurons (BP>N+N: 27.8%) (Fig. 16A). Other divisions types are less frequent: (iv) AP asymmetric differentiative division producing one BP plus one neuron (AP>BP+N: 3,8%), (v) AP asymmetric proliferative division producing two different precursors types (AP>AP+BP: 5.7%), (vi) AP symmetric proliferative division giving rise to two new progenitor cells, either AP or BP (AP>AP+AP: 2.7%; AP>BP+BP:2.7%) (Fig. 16A).The least frequent divisions are symmetric proliferative BP divisions where a BP gives rise to two BPs (BP>BP+BP: 0.8%) (Fig. 16A). (This represents only 2 cells among the nearly 200 progenitors observed to divide). BP symmetric divisions are nearly exclusively differentiative and give rise to two neurons (97.3% among BP divisions) (Fig. 16B), confirming previous observations (Noctor et al., 2008).

p27 DM significantly alters the distribution of the types of divisions by increasing the proliferative divisions and reducing the differentiative divisions. The symmetric and asymmetric differentiative AP division types, AP>AP+N and AP>N+N, are drastically reduced to 1.2% and 2.5% respectively (Fig. 16A). By contrast, the generation of BPs by APs is significantly increased -AP>AP+BP (going from 5.7% in control to 15.5% in DM condition) and AP>BP+BP (going from 2.7% in control to 9.3% in DM condition) (Fig. 16A). The number of symmetric proliferative divisions of BP, producing two new BPs, is also increased (BP>BP+BP: 3,1% after DM vs. 0.8% in controls) (Fig. 16A). This increase is BPs production is consistent with the increased proportion of Tbr2 expressing cycling precursors observed in the SVZ 48h after E15 in utero electroporation (Fig. S14C,D). Of note, Pax6 and Tbr2 are classic markers of AP and BPs, respectively (Paschal et al., 1987). Lastly, there is a doubling of the number of symmetric differentiative BP divisions (BP>N+N: 62.1% after DM vs. 27.8% in controls) (Fig. 16A). This is the consequence of the general increase of BPs production rather than a modification of the BP division type. Indeed, Fig. 16C shows that the AP divisions giving rise to at least one BP becomes predominant after p27 DM, whereas the frequency of the two BP division types is not modified (Fig. 16B).

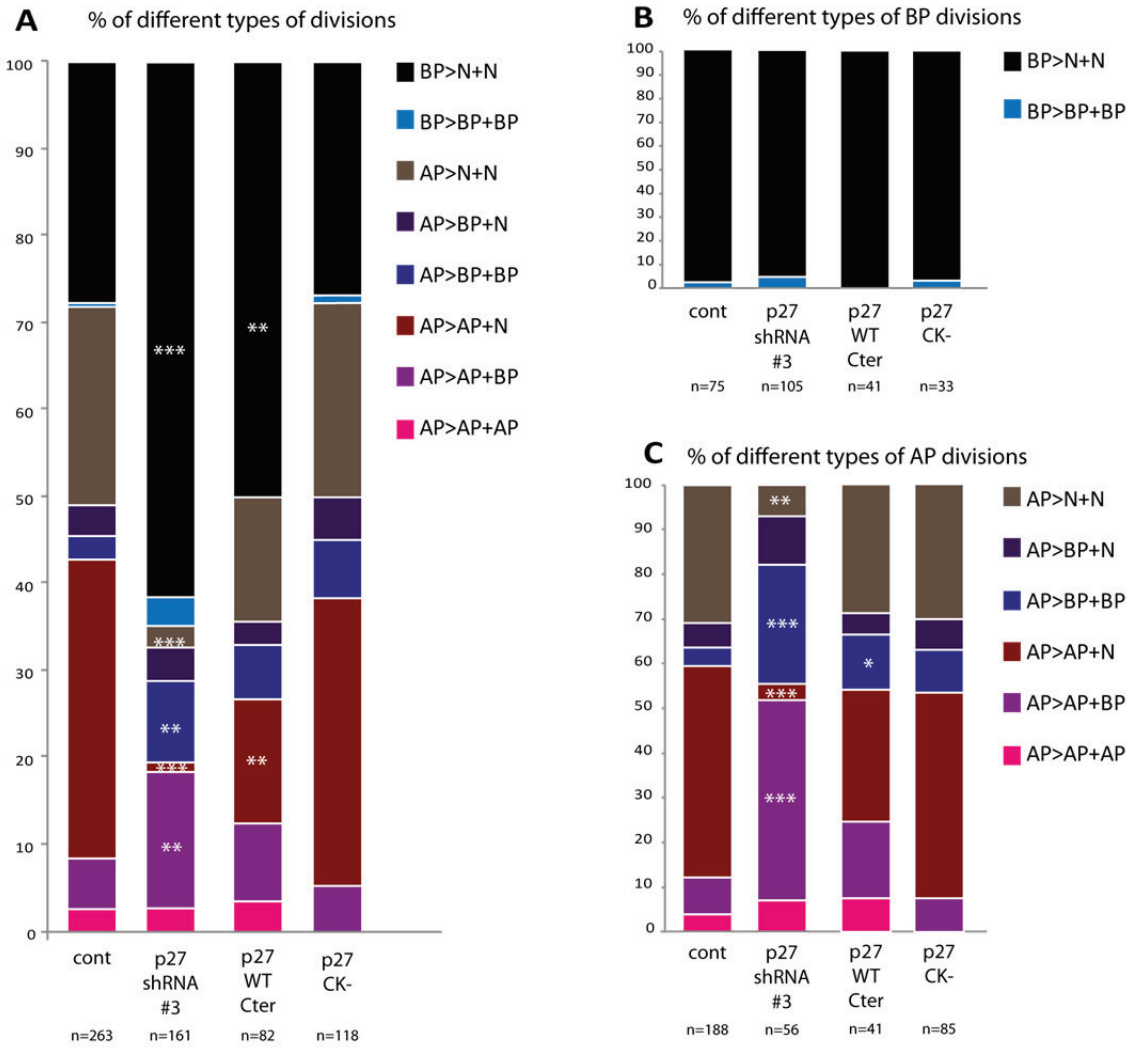

A'

	cont	p27 shRNA #3	GOF p27 WT Cter	GOF p27 CK-
BP>N+N	27,8	62,1	50,0	27,1
BP>BP+BP	0,8	3,1	0,0	0,8
AP>N+N	22,4	2,5	14,6	22,0
AP>BP+N	3,8	3,7	2,4	5,1
AP>BP+BP	2,7	9,3	6,1	6,8
AP>AP+N	34,2	1,2	14,6	33,1
AP>AP+BP	5,7	15,5	8,5	5,1
AP>AP+AP	2,7	2,5	3,7	0,0

B'

	cont	p27 shRNA #3	GOF p27 WT Cter	GOF p27 CK-
BP>N+N	97,3	95,2	100	97
BP>BP+BP	2,7	4,8	0	3

C'

	cont	p27 shRNA #3	GOF p27 WT Cter	GOF p27 CK-
AP>N+N	31,4	7,1	29,2	30,6
AP>BP+N	5,3	10,7	4,9	7,1
AP>BP+BP	3,7	26,8	12,2	9,4
AP>AP+N	47,9	3,6	29,3	45,8
AP>AP+BP	7,9	44,6	17,1	7,1
AP>AP+AP	3,7	7,1	7,3	0

Fig. 16: Effect of p27 GOF and p27 DM on the proportion of the different types of divisions, measured on videomicroscopy recordings after E14.5 in utero electroporation.

A: Proportions of the different types of divisions in the APs and BPs population.

B: Proportions of the different types of divisions in the BP population.

C: Proportions of the different types of divisions in the AP population.

A', B', C': Tables showing the numerical values for each type of division

Only divisions where both daughter cells have a known cell fate are considered.

n refers to the number of cells which have been analysed

Following p27 WT Cter GOF, AP still mainly give rise to one AP and one neuron (AP>AP+N: 14.6% vs. 34.2% in controls), or two neurons (AP>N+N: 14.6% vs. 22.4 % in controls) (Fig. 16A). However, there is an increase in the proportion of symmetric differentiative divisions of BP, producing two neurons (BP>N+N: 50.0% vs. 27.8% in controls) (Fig. 16A). Considering separately the divisions made by APs reveals an increase in the number of AP proliferative divisions giving birth to at least one BP (Fig. 16C). However, there is no significant modification of the frequency of the two BP division types (Fig. 16B). Of note, the absence of proliferative BP division (BP > BP+BP), already extremely rare in controls, can be explained by the overall lower number of progenitor cells analysed in the p27 WT Cter GOF condition.

p27 CK- GOF does not significantly modify the pattern of the different types of division (Fig. 16A,B,C).

p27 C-terminal domain seems to favor the production of BP. When p27 expression is reduced, APs first undergo more divisions at the ventricular border, and secondly produce more BPs to expand this secondary progenitor pool, at the expense of differentiated neurons

Discussion

Technical considerations

Our findings rely on the observation, in real-time, of the behaviour of progenitor cells in the mouse cortex, as well as their neuronal progeny. We have implemented a large scale electroporation strategy for the study of radial migration which makes it possible to track large cohorts of hundreds of neurons, progressively exiting the germinal zone through successive waves of radial migration toward the pial surface.

The analysis of the proliferative behaviour of precursors required an alternative strategy. Because large scale electroporation results in a high density of EGFP expressing precursors in the densely packed VZ and SVZ, this procedure does not allow a reliable identification of the cell divisions and relationships in a lineage. To overcome this difficulty, we have implemented the clonal electroporation strategy developed by Morin (Morin et al., 2007), enabling to target EGFP expression in a limited number of cells, resulting in high resolution images. This facilitates the tracking of progenitor cells lineages, allowing us to follow every successive division, as well as to determine the cell fate of both daughter cells.

Radial migration was analysed after *ex vivo* electroporation at E15.5, whereas cell lineages and INM studies were based on in utero electroporation at E14.5, followed by brain dissection and slicing at E15. In utero electroporation allowed us to keep embryos surviving in optimal conditions during 8 hours, the time period required for EGFP to be expressed in the cells. Freshly dissected brains could thus be imaged rapidly after slicing into organotypic slices. This greatly helped maintaining the tissue in optimal conditions. The VZ structural

integrity is crucial for the INM to be properly maintained, and it was largely improved using the in utero electroporation strategy.

In both massive and clonal electroporation, at E15.5 or E14.5, GOF or DM experiments led to significant changes in the level of p27 expression in the targeted population, throughout the duration of our observations (up to 72 hours).

p27 Cter domain promotes radial migration velocity of post-mitotic neurons, through action on the RhoA pathway

The present results showing that p27 promotes radial migration of post-mitotic neurons confirm and extend previous findings from Laurent Nguyen et al (Nguyen et al., 2006a). This pioneering and influential study uncovered the promigratory role of p27 by combining *in vivo* observations on p27-/- embryos and in utero electroporation of p27 mutant forms. This work demonstrated that p27 is required for both the differentiation and the normal migration of cortical neurons, via its C-terminal domain, independently from its role in promoting cell-cycle exit (Nguyen et al., 2006a). Importantly, they also showed that inactivation of the RhoA/ROCK1/2 signalling pathway is an important mechanism by which p27 regulates cortical neuron migration (Nguyen et al., 2006a).

In this study, the promigratory role of p27 and p27 Cter were inferred from static observations where the proportions of GFP cells were plotted in each of the three embryonic cortex compartments at E17.5: VZ/SVZ, IZ and CP, following electroporation at E14.5. It was considered that an increase in the proportions of GFP cells in the cortical plate with respect to the total GFP population (in GZ+IZ+CP) at E17.5 following electroporation at E14.5 was reflecting enhanced migration. However, because p27WT and p27 WT Cter GOF are shown to significantly increase precursors differentiation (eg Fig 3F,G and Fig7 A, B in (Nguyen et al., 2006a)), a higher proportions of GFP cells leave the germinal zones in GOF compared to control conditions. Consequently, this higher rate of differentiation induced at E14.5 would predictably lead to higher proportions of postmitotic neurons 3 days later in the CP, without necessarily requiring changes in migration kinetics. Conversely, in p27DM conditions, where siRNA reduces the rates of differentiation, a smaller fraction of GFP cells are observed 3 days later in the CP (Supp Fig2B in (Nguyen et al., 2006a)). Therefore, the static analysis does not allow to reliably dissect out the relative contribution from migration alteration and from changes in differentiation rates. Nor it does inform on the underlying cellular mechanisms involved in migration dynamics, such as intrinsic motility properties, occurrence and duration of pauses, time of migration initiation.

In the present study, videomicroscopy analysis of single neurons allowed to measure migration kinetics in real time. Observations were carried out on organotypic brain slices, two days after E15.5 *ex vivo* electroporation of bicistronic vectors (expressing both an EGFP reporter gene and different versions of the p27 protein), when precursor cells were seen to exit the germinal zones and initiate radial migration. No difference in migration initiation

time was observed. Our results show that p27kip does increase radial migration kinetics of postmitotic cortical neurons, through its C-terminal domain. This p27-induced increase in migration velocity results from both a significant increase in the motility index as well as from a reduction in pause duration.

The analysis of the spatial profile of the motility index revealed region specific kinetics in the depth of the post-mitotic compartments. Neurons exit the GZ with a relative slow motility, then reach their top speed in the middle of the IZ, and start decelerating upon entry in the CP. These variations could be linked to differences in cell density, which is higher in the CP and the lower IZ than in the upper IZ (Fig. S1 and S3). These regional differences in motility could also be due to regional differences in the components of the extracellular matrix. The extracellular matrix and surrounding cellular architecture provides an environment rich in signalling molecules, which migrating neurons must sort out if they are to arrive at their proper destination [reviewed in (Ayala et al., 2007)]. For instance, fibronectin is distributed along radial glial processes and is also produced by migrating neurons moving into specific cortical domains, helping neurons destined for specific targets to discriminate between adjacent glial guides [reviewed in (Pearlman and Sheppard, 1996)]. Chondroitin sulfate proteoglycans, such as neurocan, have roles in cell-cell and cell-substrate interactions and are unequally distributed in the post-mitotic compartments [reviewed in (Pearlman and Sheppard, 1996)]. Lastly, the glycoprotein Reelin is produced by marginal zone cells, forming a gradient into the cortical wall thickness, and has a well known role as a stop signal for migrating neurons, but has also a multifaceted role affecting many aspects of radial migration [reviewed in (Zhao and Frotscher, 2010)]. Thus, modifications of the neuronal motility index could be the consequence of modifications of the balance between cell contraction and adhesion strength on the substrate. Modulating p27 expression level counteracts these specific patterns of motility, suggesting that p27 acts on the finely balanced cytoskeleton remodelling allowing neuronal migration into a complex environment.

Regulation of fibroblast migration by p27 is mediated by the inactivation of the small GTPase RhoA (Besson et al., 2004b). Several studies suggest that downregulation of RhoA activity is required for the radial migration of neurons (Hand et al., 2005; Kholmanskikh et al., 2003). Electroporation of the VZ of embryonic mouse cortex with RhoA or DN RhoA shows that ectopic expression of RhoA blocks radial migration, whereas interfering with RhoA function promotes migration (Nguyen et al., 2006a). Loss of a negative regulator of Rho, p190 RhoGAP, causes defects in forebrain development, including impaired layering of the cerebral cortex (Brouns et al., 2000). Besides p27WT, we found that only the CK- and WT Cter mutants were able to promote radial migration, confirming that the C-terminal region of p27 mediates this migration promoting action. Nguyen et al, showed that inactivation of the RhoA/ROCK1/2 signalling pathway is an important mechanism by which p27 regulates radial neuron migration in the developing cortex. In agreement with these findings, our results show that RhoA pathway inhibition is sufficient to rescue both the motility index and

the pauses duration values which were respectively decreased and lengthened in p27 DM neurons.

By inactivating the RhoA pathway, p27 signalling can modulate F-actin in migrating neurons. In fibroblasts, p27 has been shown to decreases cofilin phosphorylation via the inactivation of the RhoA/Rho-kinase pathway (Besson et al., 2004b). Similar mechanisms appear to operate in cortical neurons. p27 deficient cortical neurons contain less F-actin than control cells (Kawauchi et al., 2006). *In vitro* experiments have shown that p27 DM -via p27 shRNA transfection- results in an increase in cofilin phosphorylation in cortical neurons. This p27 induced cofilin phosphorylation is suppressed via expression of DN Rho-kinase or DN RhoAN19 (Kawauchi et al., 2006). Electroporation of a phosphorylation deficient cofilin mutant leads to an arrest of newborn neurons in the IZ, underlining the crucial role of cofilin phosphorylation in radial migration (Kawauchi et al., 2006).

p27 Cter contrasting effect on the velocity of the apical and basal movements of INM

Time-lapse videomicroscopy recording of cycling APs on E15 organotypic slices showed that overexpression of p27 forms that interfere with cell-cycle progression -through the p27 N-terminal domain- strongly interferes with INM: APs are no longer able to undergo INM and division at the apical ventricular border, leading to the accumulation of the nuclei in the basal VZ. This shows that cell-cycle progression blockade impairs INM, in agreement with previous observations (Baye and Link, 2007, 2008; Pearson et al., 2005; Ueno et al., 2006). Of note, blocking the G1 to S phase progression by overexpressing another CKI, p18Ink4c, also lead to INM interruption (Kosodo et al., 2011).

Recordings in zebrafish retina have shown that that nuclei undergo rapid movements soon after division (transporting nuclei on 40% of the epithelium thickness) and prior to division (transporting nuclei on 30% to 70% of the epithelium) (Norden et al., 2009).In mouse neocortex, we were able to observe a similar behaviour. Indeed, just after division at the ventricular surface, nuclei go up rapidly during about one hour, and then slow down while moving basally. Then, nuclei undergo a rapid apical movement, during G2, to divide again at the ventricular border.

Using time-lapse videomicroscopy recording of cycling APs on E15 organotypic slices, we found that p27 Cter domain alters AP cell motility during INM. Specifically, we observed that p27 Cter alters G1 and G2 phases motions in different ways: p27 Cter increases G1 movement velocity whereas it slows down G2 velocity.

The basally directed G1 movement and the apically directed G2 movement have been shown to rely on distinct components of the cytoskeleton. The apical G2 motion has been shown to mostly rely on microtubule reorganization by Tpx2 (Kosodo et al., 2011) and dynein motor activity (Del Bene et al., 2008; Gambello et al., 2003; Tsai et al., 2005)(Tsai et

al., 2010). The basal nuclear migration is controlled by both microtubule/kinesin –mediated mechanisms (Tsai et al., 2010) and actomyosin (Schenk et al., 2009). The increase in velocity during the G1 movement following p27 WT Cter GOF is reminiscent of the observed p27 Cter domain promigratory effect in postmitotic neurons (Kawauchi et al., 2006; Nguyen et al., 2006a). In radially migrating neurons, this effect of p27Cterhas been shown to be mediated via inactivation on the Rho pathway which results in actin cytoskeleton remodelling (Kawauchi et al., 2006; Nguyen et al., 2006a). In cycling APs, one can hypothetise that a similar mechanism is operating. This is supported by the observations showing thatp27 can interact with RhoA in the VZ of the primate (see Chapter 1 Fig. 6 page 76) and in the mouse (Laurent Nguyen, personal communication).

The basal G1 movement has also been shown to rely at least partly on passive mechanisms: the nuclei basal movement would be determined by mechanical forces generated by the crowding of apically migrating nuclei (Kosodo et al., 2011). According to this view, a slowing down of the G2 apical movement would result in a slower G1 basal migration, which is not what we observe. This suggests that the above mentioned putative effect on actin remodelling is able to counteract the passive forces.

During G2 phase, p27 Cter induces a decrease in motility. Rho-GTPase have been shown to induce microtubule stabilization which is necessary for directional migration [reviewed in (Watanabe et al., 2005)]. p27 mediated inactivation of the Rho pathway will decrease microtubule stabilization and therefore impair migration. However, the precise underlying mechanisms remain to be deciphered. Together with the demonstration that Rho stabilizes microtubules, evidence suggests that microtubules locally modulate the activity of Rho-GTPases. These complex interactions [reviewed in (Watanabe et al., 2005)] point to the need of a finely regulated balance between Rho and microtubules dynamics which may have been perturbed by WT Cter GOF.

p27 could also alter microtubule dynamics during INM, independently of its action on the Rho pathway, via its newly discovered MAP function which is harboured by the Cter domain (Laurent Nguyen, personal communication, Thomas et al submitted). p27 is also able to interact with stathmin, a microtubule-destabilizing protein. Via its Cter domain, p27, restrain stathmin activity, leading to MT stabilization which negatively affects cell migration (Baldassarre et al., 2005; Belletti et al., 2010).

Further experiments will be necessary to validate these putative roles of p27 on actin and microtubules during INM. The actin polymerisation status can be examined in electroporated precursors using a fusion protein between EGFP and the actin-binding domain of the Utrophin protein (EGFP-UTRCH-ABD) (Norden et al., 2009; Pacary et al., 2011). This assay has been shown to faithfully report the presence of F-actin without altering F-actin concentrations in cells expressing the probe (Burkel et al., 2007). Activated myosinII can be immunolabelled thanks to Phospho-Myosin Light Chain 2 antibodies (Norden et al., 2009). This would allow to visualise actin fibres contractile activity during INM of precursors and the subsequent radial migration of their progeny. Microtubules could be examined by

immunolabelling of stable (acetylated) Tubulin versus α-tubulin (Norden et al., 2009) or after electroporation with a GFP tubulin (Kosodo et al., 2011; Tsai et al., 2010; Yingling et al., 2008) or GFP-EB3(Mimori-Kiyosue and Tsukita, 2003), a microtubule plus end-binding protein marker for polymerizing MT tips (Kosodo et al., 2011; Norden et al., 2009). Observations of the cytoskeleton could be coupled to the strategies allowing to label cells in each cell-cycle phase (cf (Sakaue-Sawano et al., 2008), see section below)

In parallel, RhoA activity could be measured on cortical slices by fluorescence resonance energy transfer (FRET) analysis (Pacary et al., 2011). This would entail electroporation of a FRET probe for RhoA (Nakamura et al., 2005) with p27 shRNA or GOF vectors, followed by FRET analysis on slices or in dissociated cortical cells. This will provide a high spatial resolution, required for the subcellular analysis, and which is not provided by in situ binding assay (Causeret et al., 2004).Importantly, this will inform about the subcellular location of RhoA activity in the polarised APs. It has been shown that RhoA activation is differentially modulated in distinct subcellular compartments in postmitotic neurons, either the plasma membrane or the soma and processes (Pacary et al., 2011). This differential and dynamic modulation of RhoA activity controls different aspects of the cell remodelling during migration (Pacary et al., 2011). Moreover, Rho-GTPases have been shown to interact with different effectors and to trigger different cellular responses when located in different cell compartments (Pertz, 2010). In the highly polarised APs, RhoA activity may also be spatially modulated, at the apical pole or basal pole or in the processes. This could impact differentially the nuclear movement towards or away from the centrosome.

So as to prove that RhoA mediates the induced cytoskeletal changes, inactivation of RhoA, via specific inhibitors (Y27632, (Besson et al., 2004b; Nguyen et al., 2006a)), co-electroporation of RhoA shRNA constructs (Pacary et al., 2011) or dominant-negative forms of RhoA (Hand et al., 2005; Nguyen et al., 2006a; Olson et al., 1995) as well as constitutively active forms of RhoA (McAllister et al., 2003), will have to be implemented in p27 DM and p27 GOF respectively.

p27 Cter may influence cell-cycle progression through INM regulation

Interestingly, these alterations in G1 and G2 associated migration velocities appear to influence G1 and G2 phases duration: the increased velocity during the basal movement is associated with a reduced G1/S phase duration whereas the slowing down in the apical movement is correlated with a lengthened G2 phase. The total duration of the cell-cycle remains however unaltered. These observations suggest that p27, in addition to its well-characterised canonical role on cyclinE/CDK2 exerted by its Nter domain during G1 progression may also alter cell-cycle kinetics of APs via novel mechanisms mediated by its Cter domain. Although the mechanisms remain to be elucidated, our observations raise the possibility that the Cter domain-known to interact with the Rho pathway (Besson et al.,

2004b; Nguyen et al., 2006a)- controls positively G1 and negatively G2 progression in APs. Although speculative, this hypothesis fits with observations showing that that Rho can negatively regulate the levels of the p27 protein (Hu et al., 1999; Olson et al., 1998; Vidal et al., 2002; Weber et al., 1997). In this way, Rho and p27 could be part of a negative feedback loop: while p27 may negatively regulate the Rho pathway, Rho signalling induces the down-regulation of p27. This complex crosstalk between a CDK inhibitor and components of the Rho pathway could provide a mechanism for coordinating cytoskeletal functions with cell-cycle progression.

One limitation of the videomicroscopy analysis of INM of EGFP expressing precursors is the difficulty to reliably extract individual cell-cycle phase durations from the movements kinetics. For instance, distinguishing the transition between G1 and S phase and between S and G2 phase relies on the changes in motion direction and velocity. These criterion are based on in situ observations on fixed tissue showing that nuclei undergo a prolonged static phase during S phase in the basal VZ (Schenk et al., 2009; Takahashi et al., 1993; Tamai et al., 2007; Zhang et al., 2009). The precise duration of each phase during INM would require being able to label the different cell-cycle phases via the fucci system which allows to distinguish G1 phase nuclei from S/G2/M phases nuclei (Sakaue-Sawano et al., 2008). Nuclei in each cell-cycle phase can also be labelled using a GFP-tagged version of PCNA, that displays a cell-cycle specific localization pattern (Leung et al., 2011). However, the precise time point, during both basal and apical movements, corresponding to the entry in S and G2 phase respectively, were not defined in this study.

p27 Cter and mode of division: promotion of BPs production

In control precursors, we observed numerous symmetric neurogenic divisions of APs, giving rise to two neurons. This type of divisions has not been described in substantial proportions for RGCs (Miyata et al., 2004; Noctor et al., 2004). In our experiments, the proportion of symmetric neurogenic divisions for APs increases with the rounds of divisions, becoming more predominant for the third round of division (Fig S13C). Hence, studies looking at only one or two rounds of division after progenitor cells labelling might have missed such divisions. Another possibility is that these divisions do not arise from RGC but from SNP cells. Indeed, SNPs were described as bipolar cells that possess a ventricular end-foot and a basal process of variable length, not connected to the pia, and that is retracted during mitotic division (Gal et al., 2006; Stancik et al., 2010). A few divisions with such a process retraction were seen at the ventricular surface (Kowalczyk et al., 2009; Noctor et al., 2008). SNPs have a longer cell-cycle length, attributable specifically to a lengthened G1-phase, and are highly neurogenic, mainly producing two neurons (Stancik et al., 2010). SNP progeny generally produce postmitotic neurons directly from the VZ.

However, SNP progenitors are not detected in other studies, looking with a higher resolution to the morphology of precursor cells (Noctor et al., 2008). These authors argue

that the fine pial processes does not always follow a direct course to the pial surface and instead can have a curving trajectory, making it difficult to claim that SNP are not just RGCs with a nearly indictable pial process. In our experiments, we cannot exclude that the symmetric differentiative divisions observed for apical divisions do not correspond to SNPs, because we followed INM of APs cells irrespectively of whether they displayed or not a complete pial process. In our experiments, all the cells dividing at the ventricular border undergo a complete INM movement, which has never been reported for SNPs (Gal et al., 2006).

Of note, some oRG cells were detected in the mouse VZ (Shitamukai et al., 2011; Wang et al., 2011). These oRG progenitors lack contact with the ventricular (apical) surface, but they maintain their tail-like pial (basal) processes and thus appear to be 'hanging' from the pial surface (Molnar et al., 2011). They undergo asymmetric divisions generating one oRG and one neuron. They divide basally but display a specific nuclear translocation before division. In our experiments, we detected a couple of cells similar to these progenitors, which we consider to be BPs because they undergo their division basally. Further observations will be needed to decipher between all these new types of progenitors. Looking more precisely at our recordings and performing some marker analysis will help us to detect some differences in the type of divisions for each type of precursor cells.

Our data as well as observations from other studies (Nguyen et al., 2006a) show that, acting through its N-terminal domain, p27 induces the exit of the cell-cycle and promotes the differentiation of cortical precursors into neurons. p27 WT GOF leads to a complete blockade of INM, which is linked to cell-cycle progression (Ueno et al., 2006). In the p27WT GOF condition, there is no more apical division at the ventricular border, which results in an altered progenitor fate.

By contrast, slight modifications of INM do not interfere with the progression of cell-cycle, but modify the progenitors cell fate. The p27 C-terminal domain favors the production of BPs. When p27 expression is reduced or in the case of WT Cter GOF, APs produce more BPs, expanding this secondary progenitor pool, at the expense of differentiated neurons. This is reminiscent of the situation observed after Cyclin D1 and Cyclin E expression (Pilaz et al., 2009). Modification of the type of division have been linked to modifications in the cell-cycle length and more specifically to G1 duration (Calegari et al., 2005; Calegari and Huttner, 2003; Lukaszewicz et al., 2005; Lukaszewicz et al., 2002; Pilaz et al., 2009; Polleux et al., 1997b). Indeed, a short cell-cycle length is associated with proliferative divisions, whereas a longer cell-cycle leads to differentiative divisions (Pilaz et al., 2009). This is in agreement with our observations showing that WT Cter GOF reduces G1/S phases duration. Basally dividing progenitors generate intermediate progenitor cells, with a lower proliferative capacity than APs dividing at the ventricular border, in agreement with the lower proportion of cycling cells in the germinal zones after p27GOF. However, one cannot exclude that another mechanism, independent from the effect of p27 on the cell-cycle length, could impact on the progenitor fate.

Supplementary figures

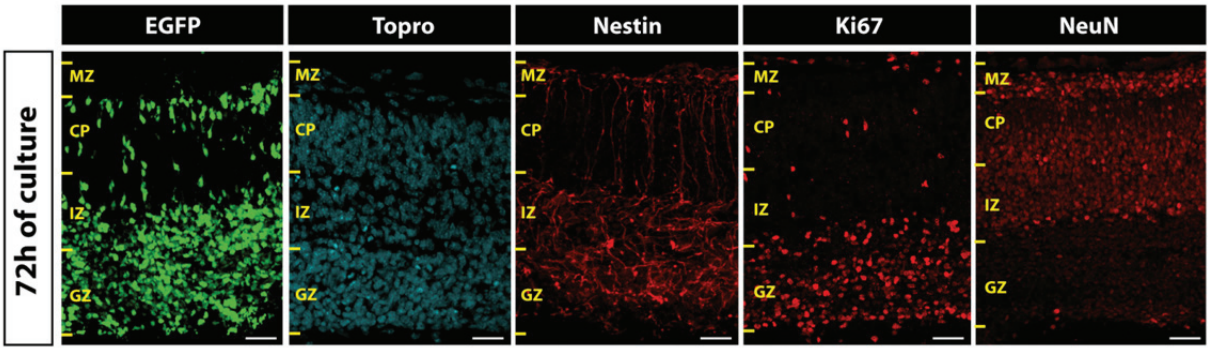

Fig. S1: Maintenance of the integrity of brain organotypic slices, 72h after *ex vivo* electroporation at E15.

Confocal microphotographs of coronal sections showing GFP (in green), Nestin (RGCs fibres), Ki67 (cycling cells) and NeuN (neurons) immunolabelling (in red), as well as nuclear staining with Topro (cyan). Electroporated cells and their labelled progeny are found in the germinal zones (GZ) as well as migrating in the IZ towards the CP. (scale bars: 40µm)

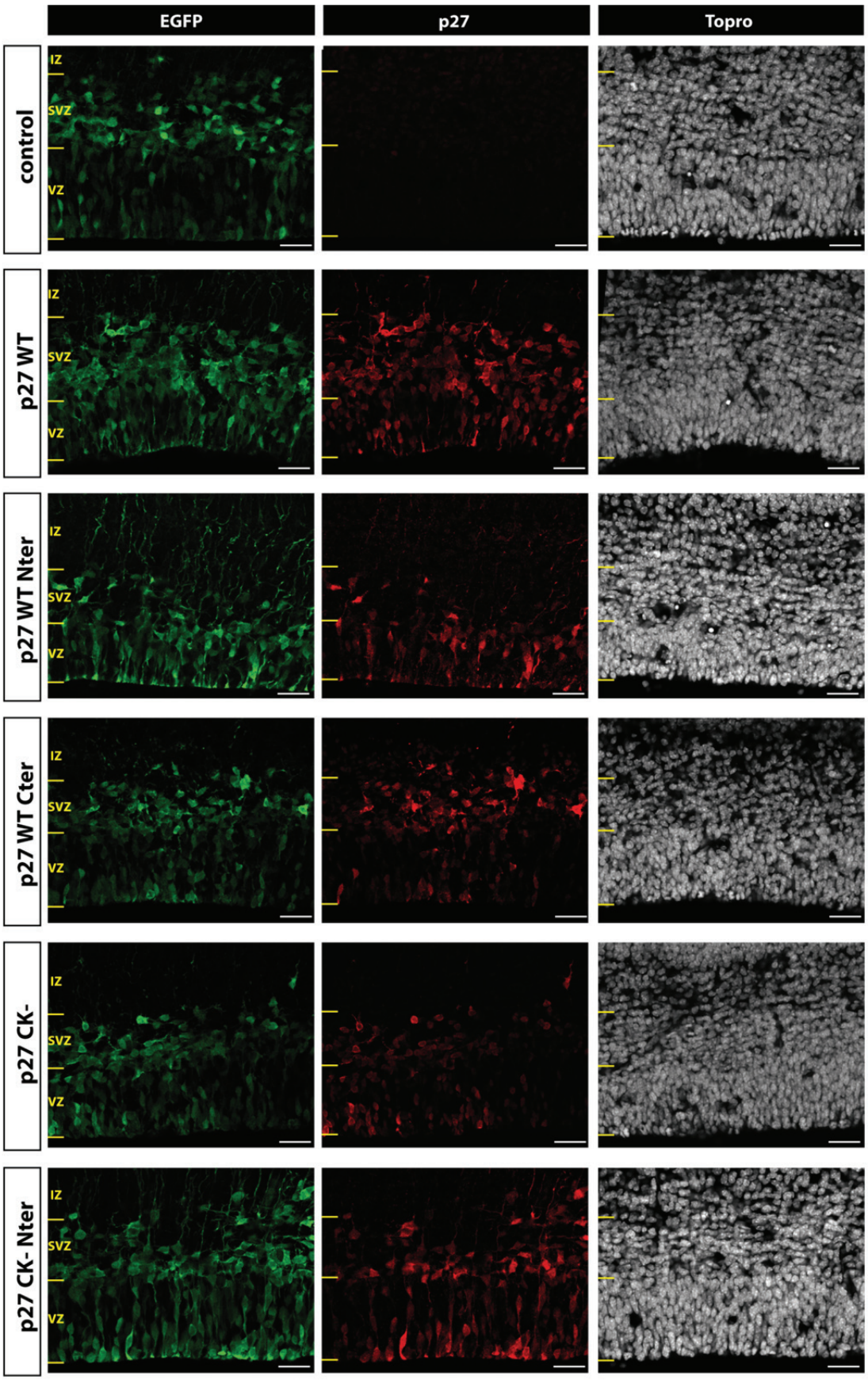

Fig. S2: p27 GOF 24h after in utero electroporation of bicistronic expression vector
Confocal microphotograph of EGFP (green) and p27 immunolabelling (red), with nuclear staining (grey), showing both nuclear and cytoplasmic overexpression of p27 protein in different GOF conditions. (scale bars: 30µm).

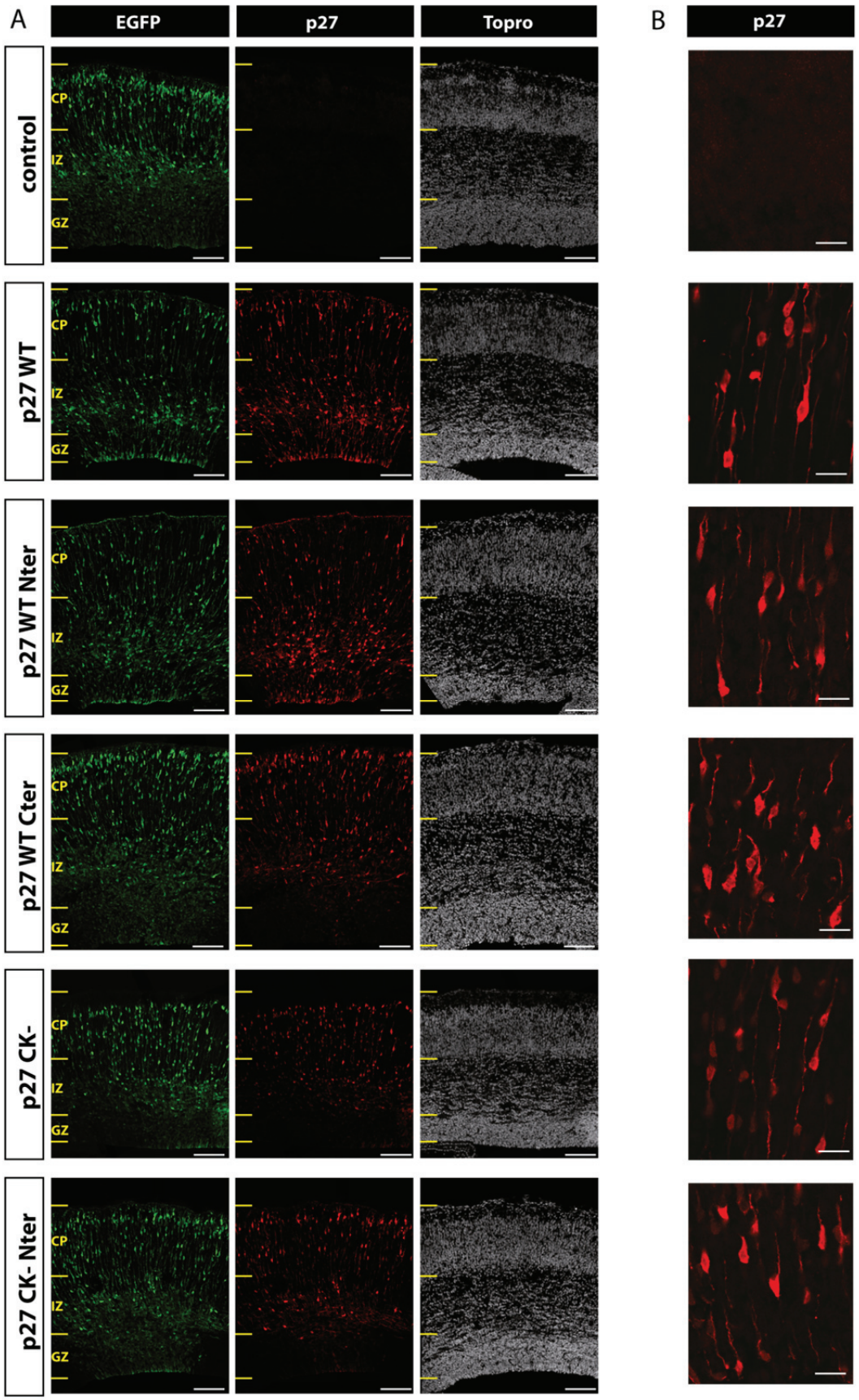

Fig. S3: p27 GOF 72h after in utero electroporation of bicistronic expression vectors

A: Confocal microphotograph of EGFP (green) and p27 immunolabelling (red), with nuclear staining (grey), showing both nuclear and cytoplasmic overexpression of p27 protein in different GOF conditions. (scale bars: 100µm)

B: Higher magnification of the p27 stainning in migrating neurons (scale bars: 20µm)

A

GOF / cont difference 24h		p27 WT	p27 WT Nter	p27 WT Cter	p27 CK-	p27 CK- Nter
VZ/SVZ	Soma	+362 % ***	+91 % **	+359 % ***	+396 % ***	+169 % ***
	n cells	2358	2853	2373	1630	3822
n slices, embryos		3sl, 3e	4sl, 4e	3sl, 3e	2sl, 2e	4sl, 4e

B

GOF / cont difference 72h		p27 WT	p27 WT Nter	p27 WT Cter	p27 CK-	p27 CK- Nter
VZ/SVZ	Soma	+202 % ***	+208 % ***	+80 % *	+171 % ***	+40 % *
	n cells	674	701	2150	1956	1687
IZ/CP	Soma	+491 % ***	+421 % ***	+370 % ***	+598 % ***	+304 % ***
	n cells	2373	2779	1975	2053	2943
n slices, embryos		4sl, 3e	3sl, 3e	3sl, 2e	4sl, 2e	3sl, 3e

C

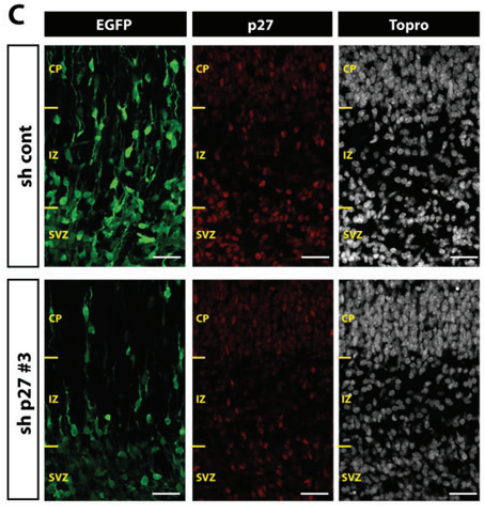

D

DM / cont shRNA difference 24h		p27 shRNA #2	p27 shRNA #3
VZ	Nucleus	-15 % ***	-27 % ***
	Cytoplasm	-21 % ***	-9 % *
	n cells	76	73
SVZ	Nucleus	-17 % *	-26 % ***
	Cytoplasm	-18 % *	-14 % ***
	n cells	39	52
n slices, embryos		2sl, 2e	3sl, 3e

E

DM / cont shRNA difference 72h		p27 shRNA #1	p27 shRNA #2	p27 shRNA #3
VZ/SVZ	Nucleus	-38 % ***	-17 % *	-62 % *
	Cytoplasm	-28 % ***	-23 % *	-49 % ***
	n cells	24	46	84
IZ	Nucleus	-27 % ***	-39 % ***	-73 % ***
	Cytoplasm	-14 % **	-28 % ***	-43 % ***
	n cells	39	177	114
CP	Nucleus	-30 % ***	-34 % ***	-71 % **
	Cytoplasm	-1 ns	-14 % ***	-45 % ***
	n cells	13	62	47
n slices, embryos		1sl, 1e	3sl, 3e	3sl, 3e

DM / cont siRNA difference 72h		p27 siRNA
VZ/SVZ	Nucleus	-22 % ***
	Cytoplasm	-16 % ***
	n cells	129
IZ	Nucleus	-32 % ***
	Cytoplasm	-31 % ***
	n cells	58
CP	Nucleus	-40 % ***
	Cytoplasm	-49 % ***
	n cells	45
n slices, embryos		2sl, 1e

Fig. S4: Quantification of p27 GOF and DM, 24 and 72 h after E14.5 in utero electroporation.
Confocal microscopy quantification of the intensity of the fluorescent immunolabelling against p27, in the EGFP+ precursor cells. Measurement of p27 subcellular expression level in the nucleus, -delineated thanks to nuclear staining- and in the cytoplasm, delineated thanks to EGFP staining.
A,B: p27 level increase in the VZ/SVZ and IZ/CP, 24h (A) and 72h (B) after in utero electroporation of p27 GOF vectors, compared to control.
C: Confocal microphotograph of EGFP (green) showing p27 (red) and nuclear staining (grey), in p27 shRNA condition compared to control shRNA condition. The downmodulation of p27 expression level is barely visible, and requires automatic quantification to be assessed. scale bars: 30µm
D,E,F: p27 level decrease in the VZ, SVZ, IZ and CP, 24h (D) and 72h (E,F) after in utero electroporation of p27 shRNA vectors (D,E) or siRNA (F), compared to control shRNA or siRNA.
Student's t tests ; p values: < 0.05 *, < 0.01 **, < 0.005 ***, compared to control, control siRNA or control shRNA conditions.

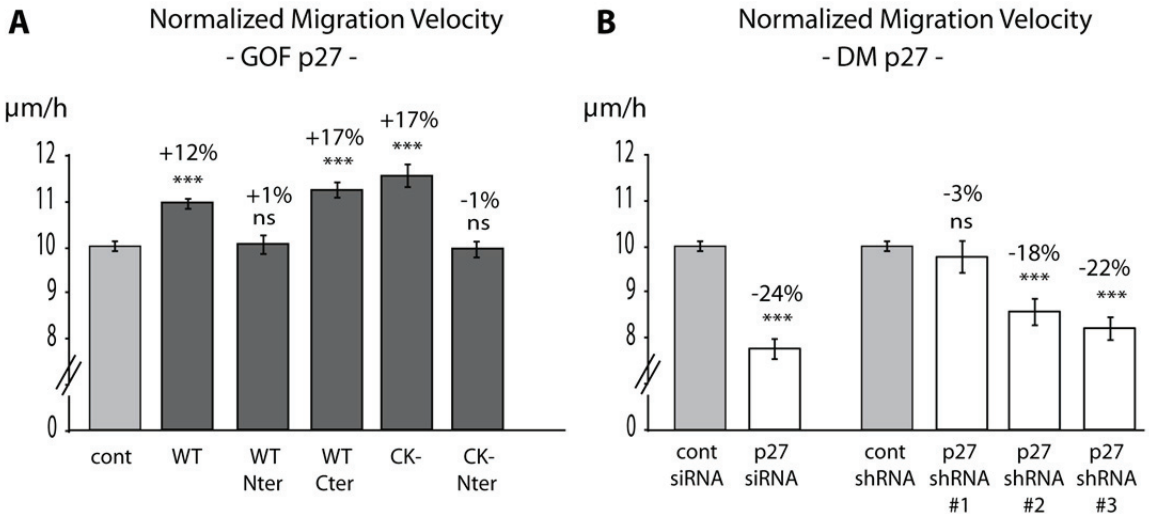

C

	cont	WT	WT Nter	WT Cter	CK-	CK-Nter
n neurons	626	505	143	228	223	158
n slices	7	6	1	2	3	1
n embryos	5	5	1	2	1	1

D

	cont siRNA	p27 siRNA	cont shRNA	p27 shRNA #1	p27 shRNA #2	p27 shRNA #3
n neurons	250	212	165	78	67	87
n slices	7	9	3	3	3	4
n embryos	5	5	2	2	2	3

Fig. S5: p27 promotes radial migration of post-mitotic cells at E15.5.

A,B: Migration velocity (µm/h) calculated on radially migrating cells after GOF of different forms of p27 (A), or after p27DM by RNAi (B). Control migration velocity was normalized to 10µm/h.

C,D: Tables listing the number of embryos, brain slices and neurons analysed in each conditions, after GOF of different forms of p27 (E), or after p27DM by RNAi (F).

Kinetics values are averaged on the total population of neurons. Error bars represent SEM.

Student's t tests ; p values: < 0.05 *, < 0.01 **, < 0.005 ***, compared to control, control siRNA or control shRNA conditions.

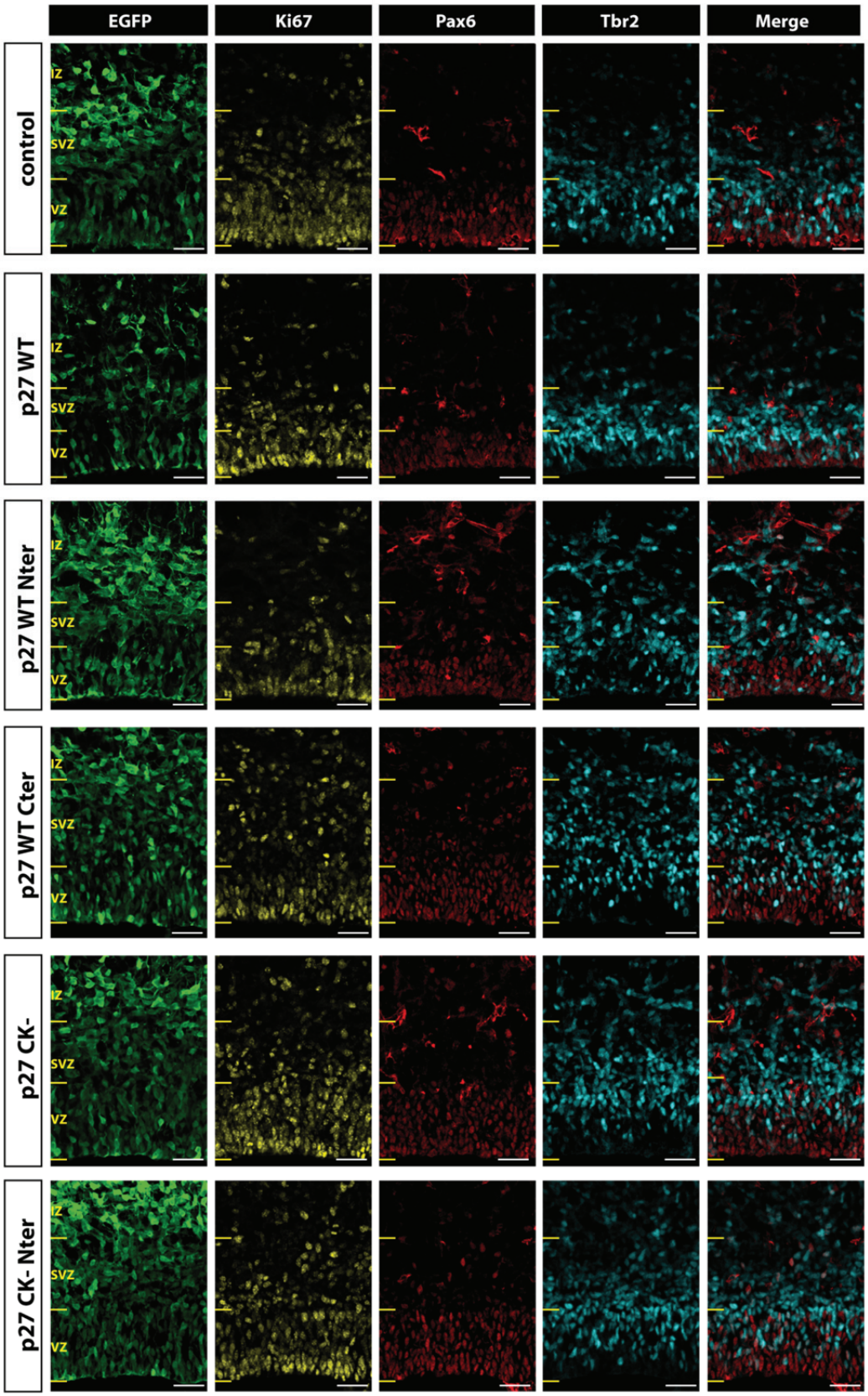

Fig. S6: Consequence of p27 GOF on precursor pools markers, 48h after in utero electroporation at E15.5.

Confocal microphotographs of coronal sections showing Ki67 (in yellow), Pax6 (in red) and Tbr2 (in cyan) stained cells in the VZ and SVZ, 48h after electroporation of different forms of p27 at E15.5. (scale bars: 30µm)

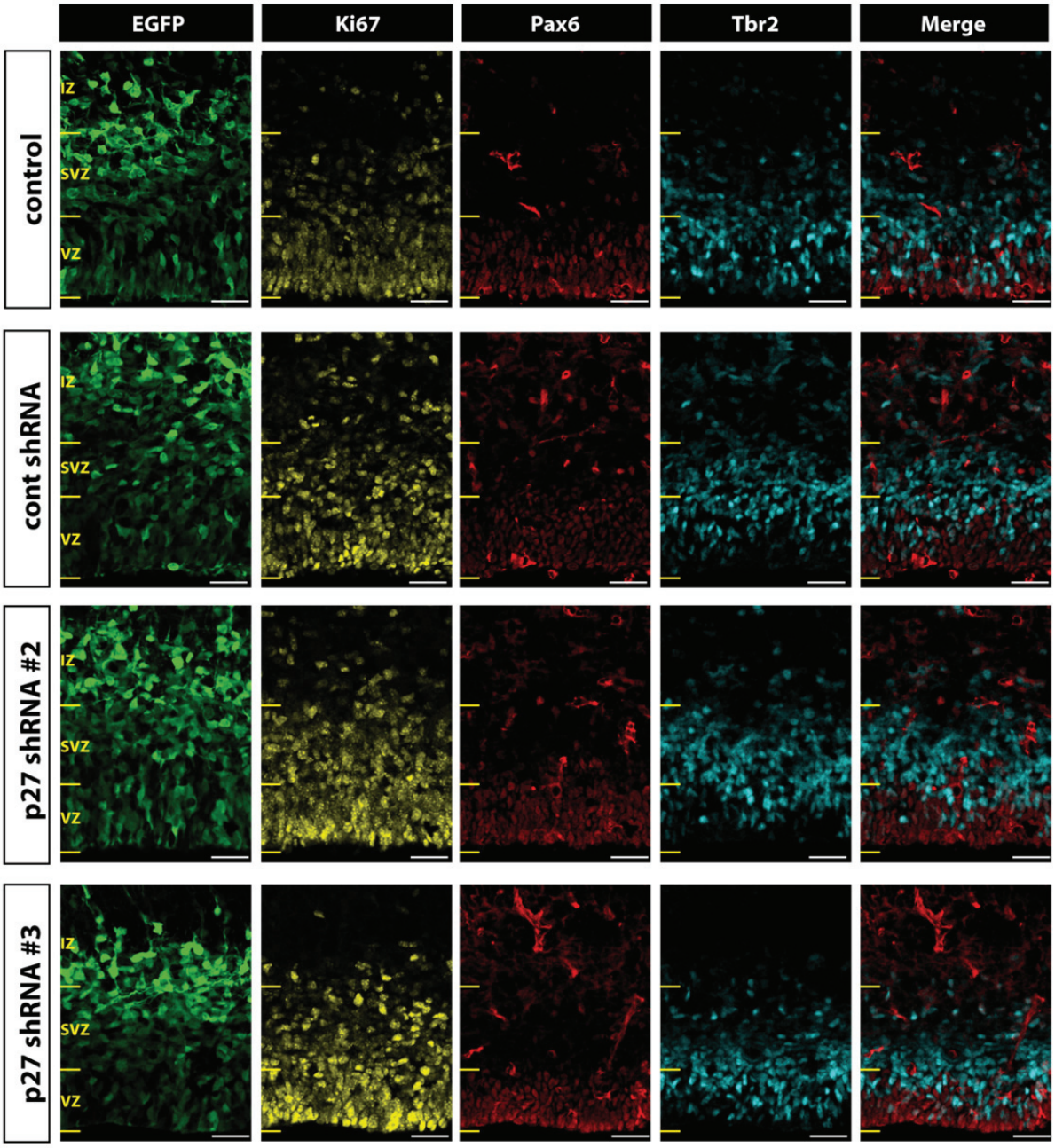

Fig. S7: Consequence of p27 DM on precursor pools, 48h after in utero electroporation at E15.5.
Confocal microphotographs of coronal sections showing Ki67 (in yellow), Pax6 (in red) and Tbr2 (in cyan) stained cells in the VZ and SVZ, 48h after electroporation of different p27 shRNA at E15.5. (scale bars: 30µm)

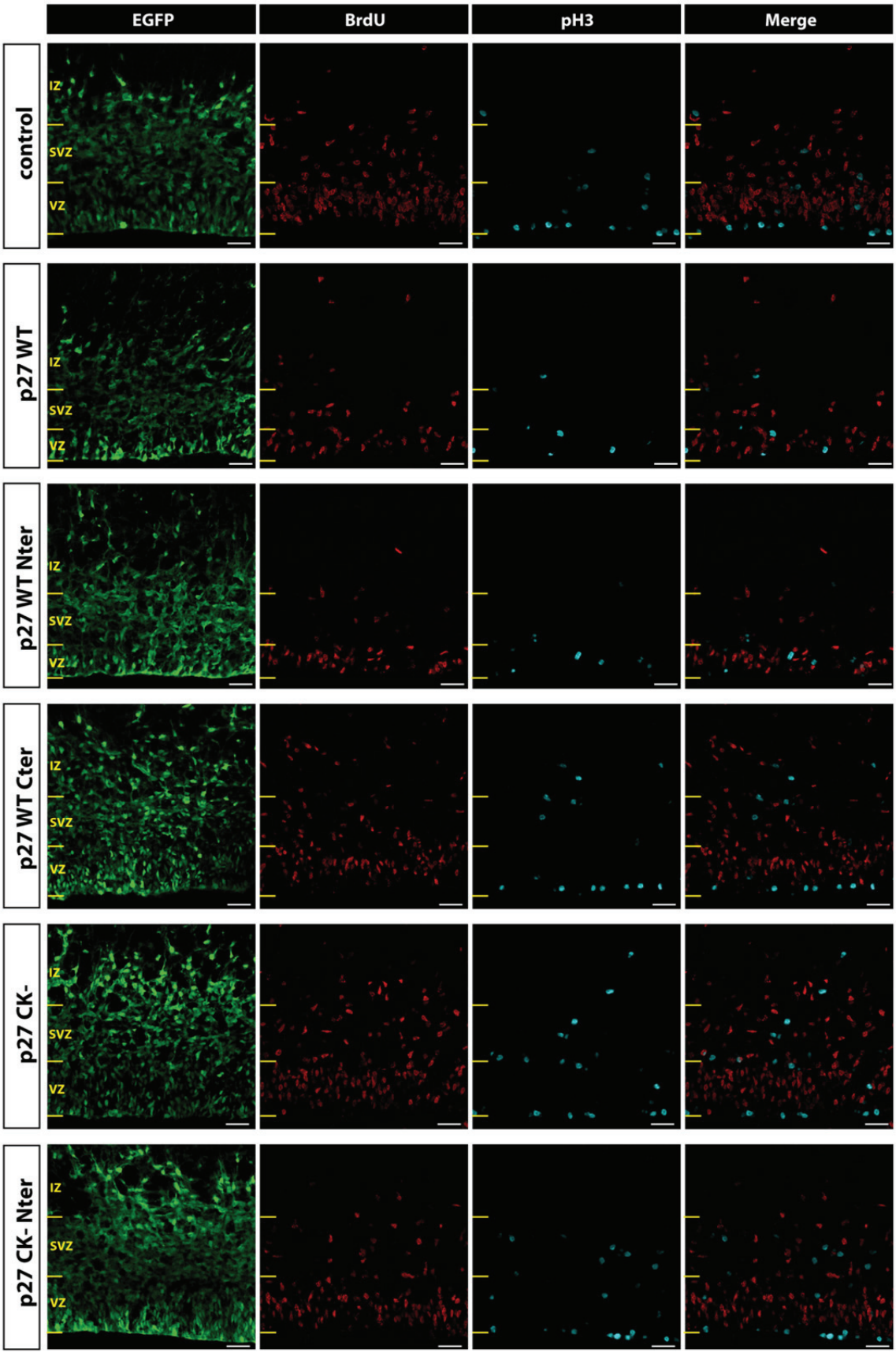

Fig. S8: Consequence of p27 GOF on S-phase and M-phase proportions, 48h after in utero electroporation at E15.5.

Confocal microphotographs of coronal sections showing BrdU (in red) and pH3 (in blue) stained precursors in the VZ and SVZ, 48h after electroporation of different forms of p27 at E15.5. A 30-min BrdU pulse was performed before sacrifice at E17.5. (scale bars: 30µm)

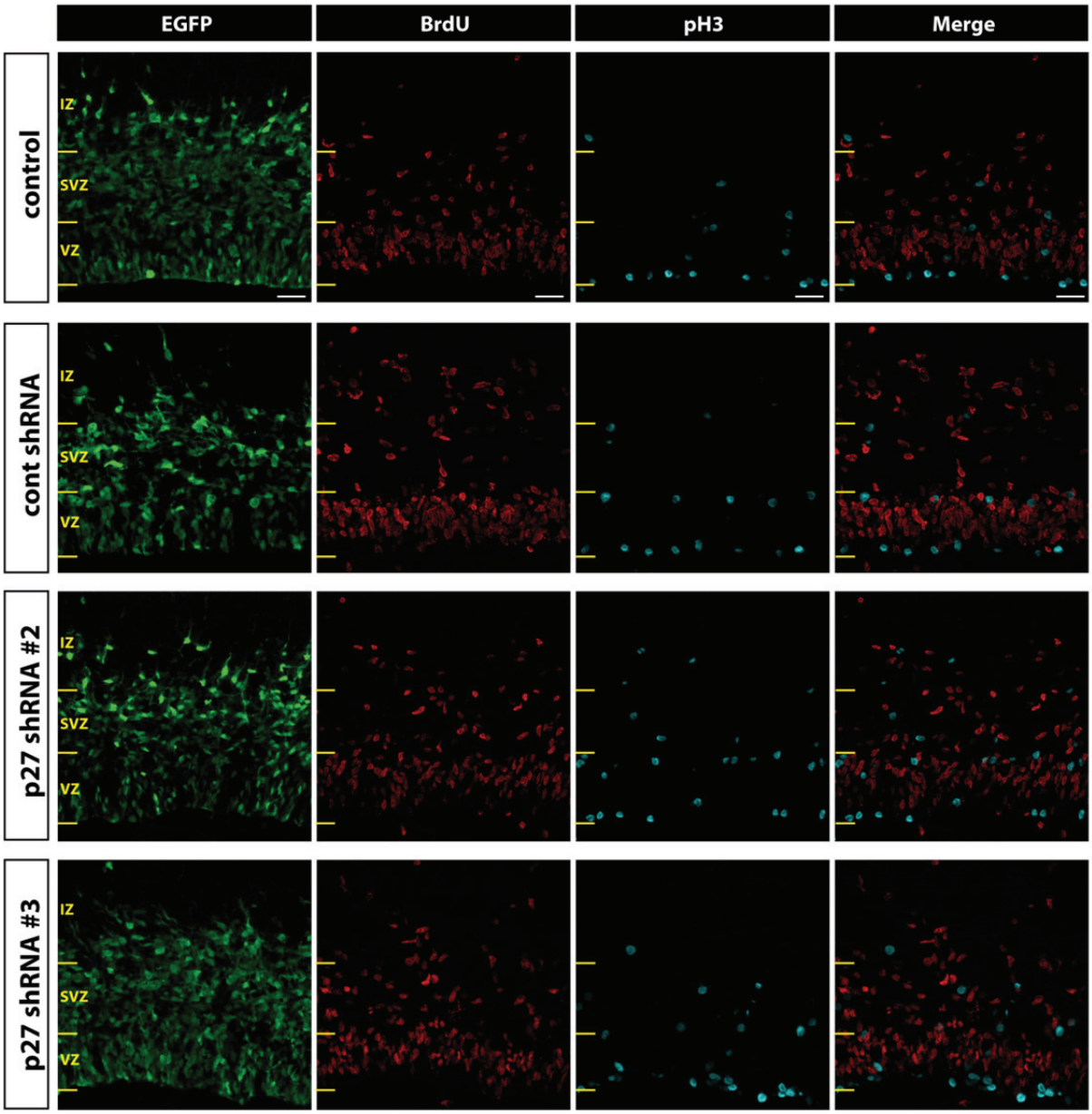

Fig. S9: Consequence of p27 DM on S-phase and M-phase proportions, 48h after in utero electroporation at E15.5.

Confocal microphotographs of coronal sections showing BrdU (in red) and pH3 (in blue) stained precursors in the VZ and SVZ, 48h after electroporation of different p27 shRNA at E15.5. A 30-min BrdU pulse was performed before sacrifice at E17.5. (scale bars: 30µm)

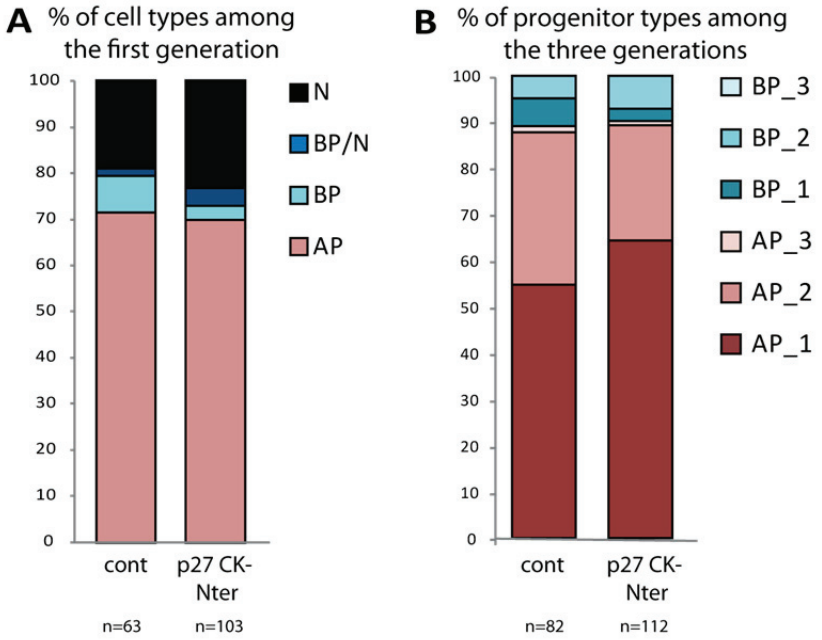

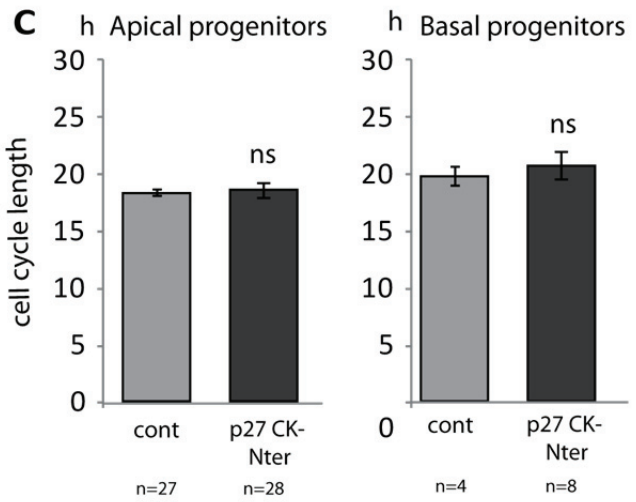

D

	cont	GOF p27 CK- Nter
n total cells	227	327
n divisions	82	112
n neurons	13	28
n slices	3	4
n embryos	1	1

Fig. S10: p27 CK- Nter GOF does not affect the proportion of different progenitor types nor the cell-cycle length of AP and BP cells.

A: Proportion of APs, BPs and Neurons (N) observed in the first daughter cells generated after electroporation. BP/N are cells that delaminate away from the ventricular border, but that are not observed long enough to determine whether they divide again or not.

B: Proportion of APs and BPs dividing at first, second and third rounds of division, with respect to the total number of divisions.

C: Measurement of the cell-cycle length (number of hours elapsed between the birth of a precursor cell and its subsequent division). Measures are averaged on the total population of each progenitor type, for each condition. Error bars represent SEM.

Student's t tests were performed with p values denoted as follows: < 0.05 *, < 0.01 **, < 0.005 ***, compared to control.

D: Number of experiments and observations in videomicroscopy analysis

n refers to the number of cells which have been analysed

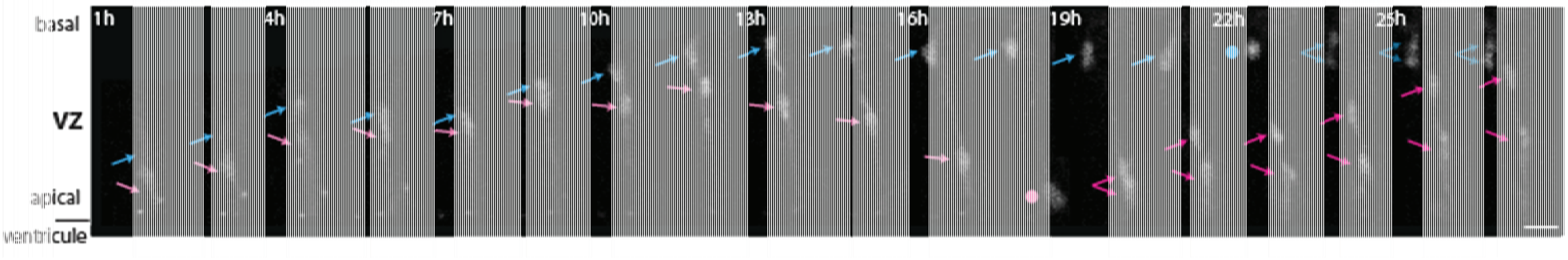

Fig. S11: Two-photon videomicroscopy acquisitions showing the division of an AP (pink arrow) and a BP (blue arrow).
The AP and the BP are daughter cells produced from a division that occurred a t 0. Both progenitor cells undergo a basal move ventricular surface, remaining close to each other. 12 h after division, the AP begins its apical movement towards the ventricule, after its birth (pink dot). Note that the basal process is very narrow during mitosis. On the contrary, the BP remains in the basal part about 22h after its birth (blue dot). Note the complete retraction of its processes during division, during which it adopts a spheri this second round of division, both daughter cells of the AP display a basal movement, one going faster than the other, whereas stay rather static and close to each other. Scale bar: 20µm

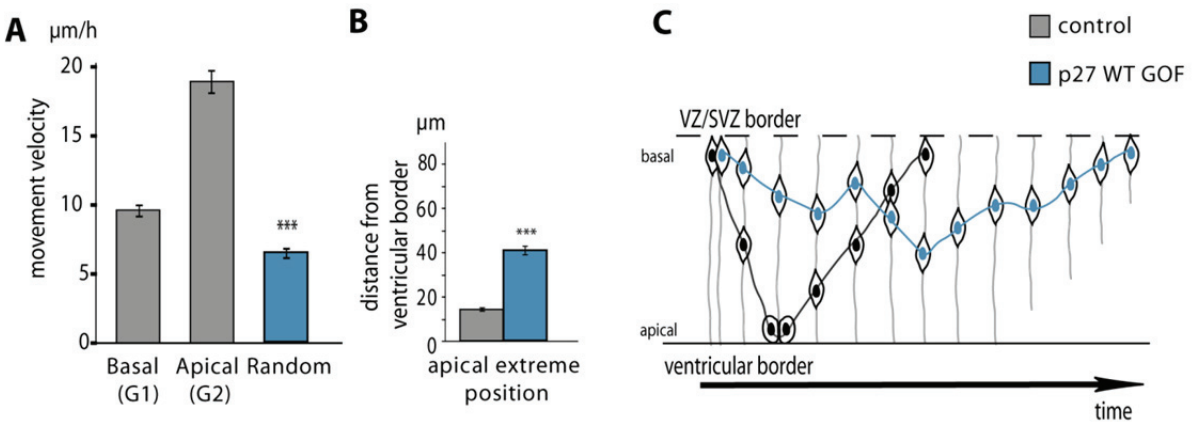

Fig. S12: Effect of p27 WT GOF on INM.

A: Velocity of the basal and apical movement in control condition and p27WTGOF.

B: Distance between the ventricular border and the apical extreme position of APs performing INM.

C: Schematic view of the INM movement in control condition or after p27 WT GOF.

Student's t tests were performed; p values: < 0.05 *, < 0.01 **, < 0.005 ***, compared to control.

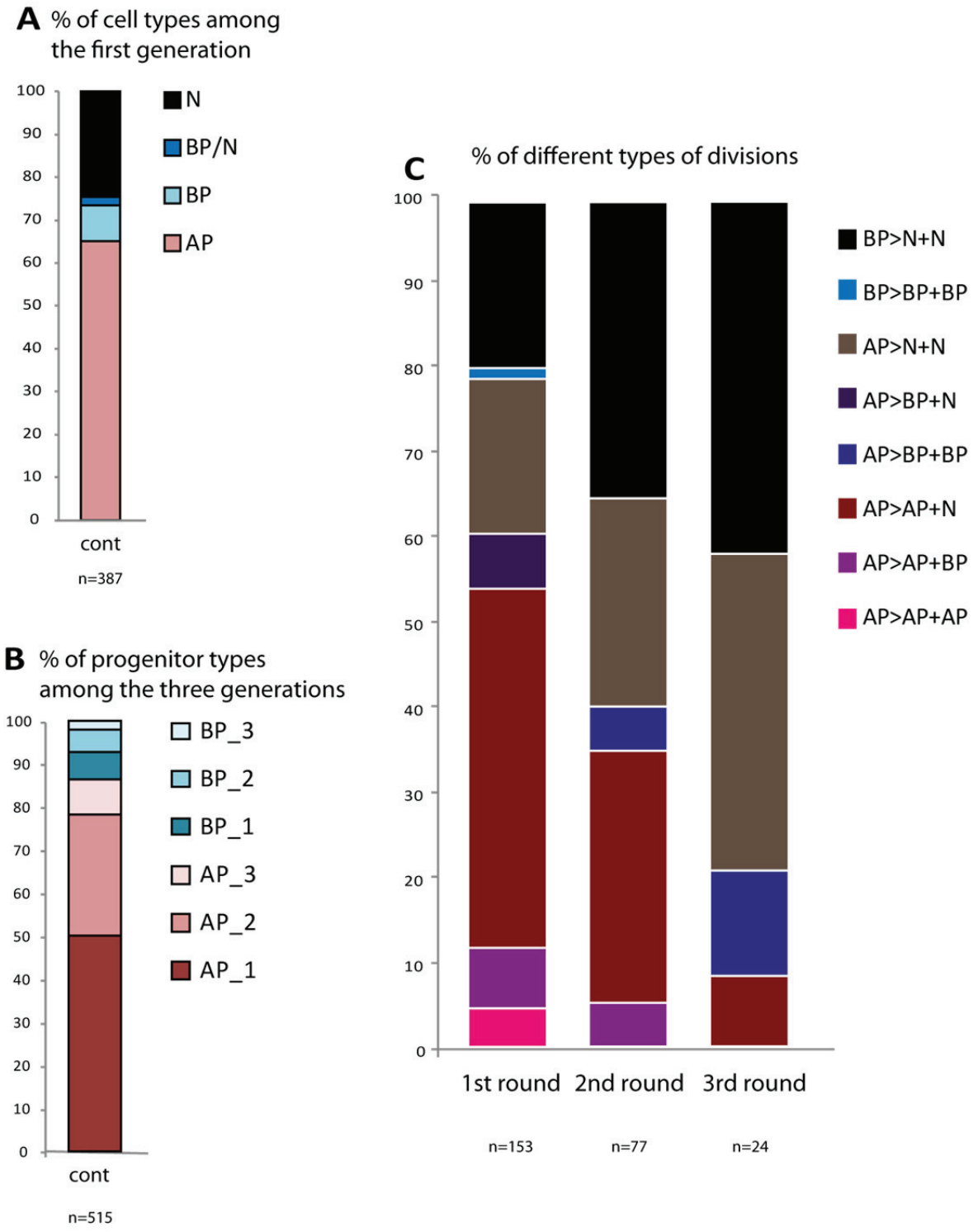

Fig. S13: Proportions of different progenitor cells and types of divisions in control conditions.
A: Proportions of APs, BPs and Neurons (N) observed in the first cell generation after electroporation. BP/N are cells that delaminate away from the ventricular border, but that are not observed long enough to determine whether they divide again or not.
B: Proportion of APs and BPs dividing at first, second and third rounds of division, with respect to the total number of divisions observed.
C: Proportions of the different types of divisions in the APs and BPs population, during the first, second and third round of division.

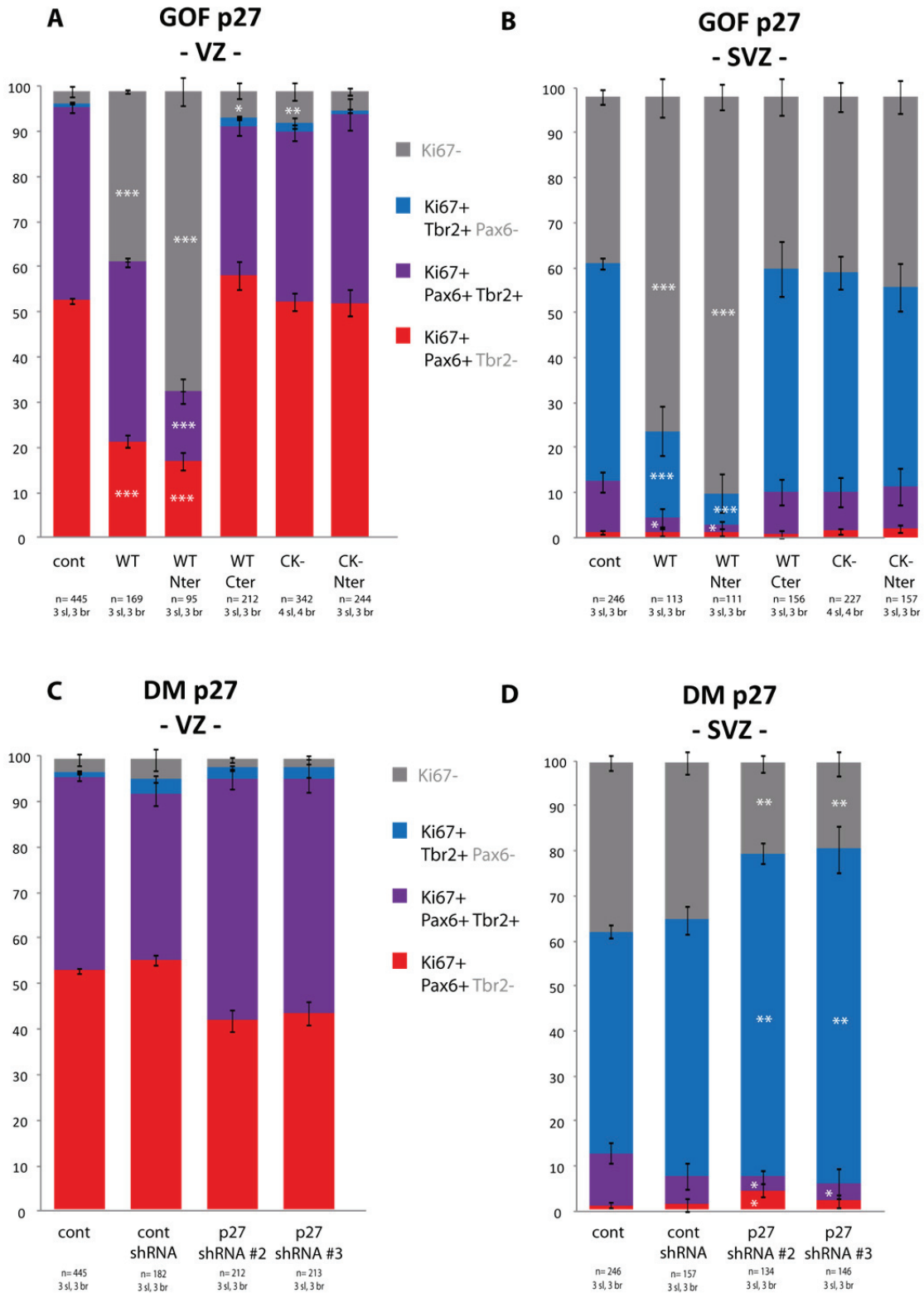

Fig. S14: Effect of p27 GOF and p27DM on the proportions of different types of precursor cells, in the VZ and the SVZ, 48h after in utero electroporation at E15.5.

A,B: Proportion of precursors cells expressing Pax6 and / or Tbr2, among the EGFP+ cells of the VZ (A) and the SVZ (B) after p27 GOF

C,D: Proportion of precursors cells expressing Pax6 and / or Tbr2, among the EGFP+ cells of the VZ (A) and the SVZ (B) after p27 DM

Proportion values are averaged on the total number of repeated observations (number of EGFP cells (n), brain slices (sl) and embryos (e) analyzed). Error bars represent SEM.

GLM tests ; p values: < 0.05 *, < 0.01 **, < 0.005 ***, compared to control.

References

Ayala, R., Shu, T., and Tsai, L.H. (2007). Trekking across the brain: the journey of neuronal migration. Cell *128*, 29-43.

Baldassarre, G., Belletti, B., Nicoloso, M.S., Schiappacassi, M., Vecchione, A., Spessotto, P., Morrione, A., Canzonieri, V., and Colombatti, A. (2005). p27(Kip1)-stathmin interaction influences sarcoma cell migration and invasion. Cancer cell *7*, 51-63.

Baye, L.M., and Link, B.A. (2007). Interkinetic nuclear migration and the selection of neurogenic cell divisions during vertebrate retinogenesis. J Neurosci *27*, 10143-10152.

Baye, L.M., and Link, B.A. (2008). Nuclear migration during retinal development. Brain Res *1192*, 29-36.

Belletti, B., Pellizzari, I., Berton, S., Fabris, L., Wolf, K., Lovat, F., Schiappacassi, M., D'Andrea, S., Nicoloso, M.S., Lovisa, S.*, et al.*(2010). p27kip1 controls cell morphology and motility by regulating microtubule-dependent lipid raft recycling. Mol Cell Biol *30*, 2229-2240.

Besson, A., Assoian, R.K., and Roberts, J.M. (2004a). Regulation of the cytoskeleton: an oncogenic function for CDK inhibitors? Nature reviews Cancer *4*, 948-955.

Besson, A., Gurian-West, M., Schmidt, A., Hall, A., and Roberts, J.M. (2004b). p27Kip1 modulates cell migration through the regulation of RhoA activation. Genes & development *18*, 862-876.

Brouns, M.R., Matheson, S.F., Hu, K.Q., Delalle, I., Caviness, V.S., Silver, J., Bronson, R.T., and Settleman, J. (2000). The adhesion signaling molecule p190 RhoGAP is required for morphogenetic processes in neural development. Development *127*, 4891-4903.

Burkel, B.M., von Dassow, G., and Bement, W.M. (2007). Versatile fluorescent probes for actin filaments based on the actin-binding domain of utrophin. Cell Motil Cytoskeleton *64*, 822-832.

Calegari, F., Haubensak, W., Haffner, C., and Huttner, W.B. (2005). Selective lengthening of the cell cycle in the neurogenic subpopulation of neural progenitor cells during mouse brain development. J Neurosci *25*, 6533-6538.

Calegari, F., and Huttner, W.B. (2003). An inhibition of cyclin-dependent kinases that lengthens, but does not arrest, neuroepithelial cell cycle induces premature neurogenesis. Journal of cell science *116*, 4947-4955.

Causeret, F., Hidalgo-Sanchez, M., Fort, P., Backer, S., Popoff, M.R., Gauthier-Rouviere, C., and Bloch-Gallego, E. (2004). Distinct roles of Rac1/Cdc42 and Rho/Rock for axon outgrowth and nucleokinesis of precerebellar neurons toward netrin 1. Development *131*, 2841-2852.

Caviness, V.S., Goto, T., Tarui, T., Takahashi, T., Bhide, P.G., and Nowakowski, R.S. (2003). Cell output, cell cycle duration and neuronal specification: a model of integrated mechanisms of the neocortical proliferative process. Cerebral cortex (New York, NY : 1991) *13*, 592-598.

Del Bene, F., Wehman, A.M., Link, B.A., and Baier, H. (2008). Regulation of neurogenesis by interkinetic nuclear migration through an apical-basal notch gradient. Cell *134*, 1055-1065.

Diez-Juan, A., and Andres, V. (2003). Coordinate control of proliferation and migration by the p27Kip1/cyclin-dependent kinase/Retinoblastoma pathway in vascular smooth muscle cells and fibroblasts. Circ Res *92*, 402-410.

Durand, B., Gao, F.B., and Raff, M. (1997). Accumulation of the cyclin-dependent kinase inhibitor p27/Kip1 and the timing of oligodendrocyte differentiation. Embo J *16*, 306-317.

Gal, J.S., Morozov, Y.M., Ayoub, A.E., Chatterjee, M., Rakic, P., and Haydar, T.F. (2006). Molecular and morphological heterogeneity of neural precursors in the mouse neocortical proliferative zones. J Neurosci *26*, 1045-1056.

Gambello, M.J., Darling, D.L., Yingling, J., Tanaka, T., Gleeson, J.G., and Wynshaw-Boris, A. (2003). Multiple dose-dependent effects of Lis1 on cerebral cortical development. J Neurosci *23*, 1719-1729.

Gautier E, C.V., Betizeau M, Doerflinger N, Kennedy H, Dehay C. (2010a). Area-specific dynamics of proliferation and migration during primate corticogenesis: role of the modular protein p27kip1. 18th ISDN (International Society for Development Neuroscience) Meeting, Estoril, Portugal.

Gautier E, C.V., Betizeau M, Doerflinger N, Patti D, Kennedy H, Dehay C (2010b). Area-specific dynamics of proliferation and migration during primate corticogenesis: role of the modular protein p27kip1. 40th SFN (Society for Neuroscience) Meeting, San Diego, USA.

Goto, T., Mitsuhashi, T., and Takahashi, T. (2004). Altered patterns of neuron production in the p27 knockout mouse. Dev Neurosci *26*, 208-217.

Goukassian, D., Díez-Juan, a., Asahara, T., Schratzberger, P., Silver, M., Murayama, T., Isner, J.M., and Andrés, V. (2001). Overexpression of p27(Kip1) by doxycycline-regulated adenoviral vectors inhibits endothelial cell proliferation and migration and impairs angiogenesis. The FASEB journal : official publication of the Federation of American Societies for Experimental Biology *15*, 1877-1885.

Hand, R., Bortone, D., Mattar, P., Nguyen, L., Heng, J.I.-T., Guerrier, S., Boutt, E., Peters, E., Barnes, A.P., Parras, C.*, et al.* (2005). Phosphorylation of Neurogenin2 specifies the migration properties and the dendritic morphology of pyramidal neurons in the neocortex. Neuron *48*, 45-62.

Hu, W., Bellone, C.J., and Baldassare, J.J. (1999). RhoA stimulates p27(Kip) degradation through its regulation of cyclin E/CDK2 activity. J Biol Chem *274*, 3396-3401.

Kawauchi, T., Chihama, K., Nabeshima, Y., and Hoshino, M. (2006). Cdk5 phosphorylates and stabilizes p27kip1 contributing to actin organization and cortical neuronal migration. Nat Cell Biol *8*, 17-26.

Kholmanskikh, S.S., Dobrin, J.S., Wynshaw-Boris, A., Letourneau, P.C., and Ross, M.E. (2003). Disregulated RhoGTPases and actin cytoskeleton contribute to the migration defect in Lis1-deficient neurons. J Neurosci *23*, 8673-8681.

Kosodo, Y., Suetsugu, T., Suda, M., Mimori-Kiyosue, Y., Toida, K., Baba, S.A., Kimura, A., and Matsuzaki, F. (2011). Regulation of interkinetic nuclear migration by cell cycle-coupled active and passive mechanisms in the developing brain. Embo J *30*, 1690-1704.

Kowalczyk, T., Pontious, A., Englund, C., Daza, R.A., Bedogni, F., Hodge, R., Attardo, A., Bell, C., Huttner, W.B., and Hevner, R.F. (2009). Intermediate neuronal progenitors (basal progenitors) produce pyramidal-projection neurons for all layers of cerebral cortex. Cereb Cortex *19*, 2439-2450.

Leung, L., Klopper, A.V., Grill, S.W., Harris, W.A., and Norden, C. (2011). Apical migration of nuclei during G2 is a prerequisite for all nuclear motion in zebrafish neuroepithelia. Development *138*, 5003-5013.

Lukaszewicz, A., Savatier, P., Cortay, V., Giroud, P., Huissoud, C., Berland, M., Kennedy, H., and Dehay, C. (2005). G1 phase regulation, area-specific cell cycle control, and cytoarchitectonics in the primate cortex. Neuron *47*, 353-364.

Lukaszewicz, A., Savatier, P., Cortay, V., Kennedy, H., and Dehay, C. (2002). Contrasting effects of basic fibroblast growth factor and neurotrophin 3 on cell cycle kinetics of mouse cortical stem cells. J Neurosci *22*, 6610-6622.

Mcallister, S.S., Becker-hapak, M., Pintucci, G., Pagano, M., and Dowdy, S.F. (2003). Novel p27 kip1 C-Terminal Scatter Domain Mediates Rac-Dependent Cell Migration Independent of Cell Cycle Arrest Functions. Society *23*, 216-228.

Mimori-Kiyosue, Y., and Tsukita, S. (2003). "Search-and-capture" of microtubules through plus-end-binding proteins (+TIPs). J Biochem *134*, 321-326.

Miyata, T., Kawaguchi, A., Saito, K., Kawano, M., Muto, T., and Ogawa, M. (2004). Asymmetric production of surface-dividing and non-surface-dividing cortical progenitor cells. Development *131*, 3133-3145.

Molnar, Z., Vasistha, N.A., and Garcia-Moreno, F. (2011). Hanging by the tail: progenitor populations proliferate. Nat Neurosci *14*, 538-540.

Morin, X., Jaouen, F., and Durbec, P. (2007). Control of planar divisions by the G-protein regulator LGN maintains progenitors in the chick neuroepithelium. Nature neuroscience *10*, 1440-1448.

Nadarajah, B., Brunstrom, J.E., Grutzendler, J., Wong, R.O., and Pearlman, A.L. (2001). Two modes of radial migration in early development of the cerebral cortex. Nat Neurosci *4*, 143-150.

Nadarajah, B., and Parnavelas, J.G. (2002). Modes of neuronal migration in the developing cerebral cortex. Nat Rev Neurosci *3*, 423-432.

Nakamura, T., Aoki, K., and Matsuda, M. (2005). Monitoring spatio-temporal regulation of Ras and Rho GTPase with GFP-based FRET probes. Methods *37*, 146-153.

Narumiya, S., Ishizaki, T., and Uehata, M. (2000). Use and properties of ROCK-specific inhibitor Y-27632. Methods Enzymol 325, 273-284.

Nguyen, L., Besson, A., Heng, J.I., Schuurmans, C., Teboul, L., Parras, C., Philpott, A., Roberts, J.M., and Guillemot, F. (2006a). p27kip1 independently promotes neuronal differentiation and migration in the cerebral cortex. Genes Dev 20, 1511-1524.

Nguyen, L., Besson, A., Roberts, J.M., and Guillemot, F. (2006b). Coupling cell cycle exit, neuronal differentiation and migration in cortical neurogenesis. Cell cycle (Georgetown, Tex) 5, 2314-2318.

Niwa, H., Burdon, T., Chambers, I., and Smith, A. (1998). Self-renewal of pluripotent embryonic stem cells is mediated via activation of STAT3. Genes Dev 12, 2048-2060.

Noctor, S.C., Martinez-Cerdeno, V., Ivic, L., and Kriegstein, A.R. (2004). Cortical neurons arise in symmetric and asymmetric division zones and migrate through specific phases. Nat Neurosci *7*, 136-144.

Noctor, S.C., Martinez-Cerdeno, V., and Kriegstein, A.R. (2008). Distinct behaviors of neural stem and progenitor cells underlie cortical neurogenesis. J Comp Neurol *508*, 28-44.

Norden, C., Young, S., Link, B.A., and Harris, W.A. (2009). Actomyosin is the main driver of interkinetic nuclear migration in the retina. Cell *138*, 1195-1208.

Olson, M.F., Ashworth, A., and Hall, A. (1995). An essential role for Rho, Rac, and Cdc42 GTPases in cell cycle progression through G1. Science *269*, 1270-1272.

Olson, M.F., Paterson, H.F., and Marshall, C.J. (1998). Signals from Ras and Rho GTPases interact to regulate expression of p21Waf1/Cip1. Nature *394*, 295-299.

Pacary, E., Heng, J., Azzarelli, R., Riou, P., Castro, D., Lebel-Potter, M., Parras, C., Bell, D.M., Ridley, A.J., Parsons, M.*, et al.* (2011). Proneural transcription factors regulate different steps of cortical neuron migration through Rnd-mediated inhibition of RhoA signaling. Neuron *69*, 1069-1084.

Paschal, B.M., Shpetner, H.S., and Vallee, R.B. (1987). MAP 1C is a microtubule-activated ATPase which translocates microtubules in vitro and has dynein-like properties. J Cell Biol *105*, 1273-1282.

Pearlman, A.L., and Sheppard, A.M. (1996). Extracellular matrix in early cortical development. Prog Brain Res *108*, 117-134.

Pearson, R.A., Luneborg, N.L., Becker, D.L., and Mobbs, P. (2005). Gap junctions modulate interkinetic nuclear movement in retinal progenitor cells. J Neurosci *25*, 10803-10814.

Pertz, O. (2010). Spatio-temporal Rho GTPase signaling - where are we now? Journal of cell science 123, 1841-1850.

Pilaz, L.J., Patti, D., Marcy, G., Ollier, E., Pfister, S., Douglas, R.J., Betizeau, M., Gautier, E., Cortay, V., Doerflinger, N., et al. (2009). Forced G1-phase reduction alters mode of division, neuron number, and laminar phenotype in the cerebral cortex. Proc Natl Acad Sci U S A 106, 21924-21929.

Polleux, F., Dehay, C., Moraillon, B., and Kennedy, H. (1997). Regulation of neuroblast cell-cycle kinetics plays a crucial role in the generation of unique features of neocortical areas. J Neurosci *17*, 7763-7783.

Rakic, P. (1972). Mode of cell migration to the superficial layers of fetal monkey neocortex. J Comp Neurol *145*, 61-83.

Reiner, O., Sapir, T., and Gerlitz, G. (2011). Interkinetic Nuclear Movement in the Ventricular Zone of the Cortex. J Mol Neurosci.

Sakaue-Sawano, A., Kurokawa, H., Morimura, T., Hanyu, A., Hama, H., Osawa, H., Kashiwagi, S., Fukami, K., Miyata, T., Miyoshi, H*., et al.* (2008). Visualizing spatiotemporal dynamics of multicellular cell-cycle progression. Cell *132*, 487-498.

Sauer, M.E., and Walker, B.E. (1959). Radioautographic study of interkinetic nuclear migration in the neural tube. Proc Soc Exp Biol Med *101*, 557-560.

Schenk, J., Wilsch-Brauninger, M., Calegari, F., and Huttner, W.B. (2009). Myosin II is required for interkinetic nuclear migration of neural progenitors. Proc Natl Acad Sci U S A *106*, 16487-16492.

Sherr, C.J., and Roberts, J.M. (1999). CDK inhibitors: positive and negative regulators of G1-phase progression. Genes & Development *13*, 1501-1512.

Shitamukai, A., Konno, D., and Matsuzaki, F. (2011). Oblique radial glial divisions in the developing mouse neocortex induce self-renewing progenitors outside the germinal zone that resemble primate outer subventricular zone progenitors. J Neurosci *31*, 3683-3695.

Stancik, E.K., Navarro-Quiroga, I., Sellke, R., and Haydar, T.F. (2010). Heterogeneity in ventricular zone neural precursors contributes to neuronal fate diversity in the postnatal neocortex. J Neurosci *30*, 7028-7036.

Sun, J., Marx, S.O., Chen, H.-j., Poon, M., Marks, A.R., and E, L. (2001). Role for p27 Kip1 in Vascular Smooth Muscle Cell Migration Ji Sun, Steven O. Marx, Hong-Jun Chen, Michael Poon, Andrew R. Marks and LeRoy E. Rabbani Circulation 2001;103;2967-2972. World Wide Web Internet And Web Information Systems.

Tabata, H., and Nakajima, K. (2003). Multipolar migration: the third mode of radial neuronal migration in the developing cerebral cortex. J Neurosci *23*, 9996-10001.

Takahashi, T., Nowakowski, R.S., and Caviness, V.S. (1996). Interkinetic and migratory behavior of a cohort of neocortical neurons arising in the early embryonic murine cerebral wall. The Journal of neuroscience : the official journal of the Society for Neuroscience *16*, 5762-5776.

Takahashi, T., Nowakowski, R.S., and Caviness, V.S., Jr. (1993). Cell cycle parameters and patterns of nuclear movement in the neocortical proliferative zone of the fetal mouse. J Neurosci *13*, 820-833.

Tamai, H., Shinohara, H., Miyata, T., Saito, K., Nishizawa, Y., Nomura, T., and Osumi, N. (2007). Pax6 transcription factor is required for the interkinetic nuclear movement of neuroepithelial cells. Genes Cells *12*, 983-996.

Tarui, T., Takahashi, T., Nowakowski, R.S., Hayes, N.L., Bhide, P.G., and Caviness, V.S. (2005). Overexpression of p27 Kip 1, probability of cell cycle exit, and laminar destination of neocortical neurons. Cerebral cortex (New York, NY : 1991) *15*, 1343-1355.

Tokumoto, M., Tsuruya, K., Fukuda, K., Kanai, H., Kuroki, S., and Hirakata, H. (2002). Reduced p21, p27 and vitamin D receptor in the nodular hyperplasia in patients with advanced secondary hyperparathyroidism. Kidney Int *62*, 1196-1207.

Tsai, J.W., Chen, Y., Kriegstein, A.R., and Vallee, R.B. (2005). LIS1 RNA interference blocks neural stem cell division, morphogenesis, and motility at multiple stages. J Cell Biol *170*, 935-945.

Tsai, J.W., Lian, W.N., Kemal, S., Kriegstein, A.R., and Vallee, R.B. (2010). Kinesin 3 and cytoplasmic dynein mediate interkinetic nuclear migration in neural stem cells. Nat Neurosci *13*, 1463-1471.

Ueno, M., Katayama, K., Yamauchi, H., Nakayama, H., and Doi, K. (2006). Cell cycle progression is required for nuclear migration of neural progenitor cells. Brain Res *1088*, 57-67.

Vidal, A., Millard, S.S., Miller, J.P., and Koff, A. (2002). Rho activity can alter the translation of p27 mRNA and is important for RasV12-induced transformation in a manner dependent on p27 status. J Biol Chem *277*, 16433-16440.

Vlach, J., Hennecke, S., and Amati, B. (1997). Phosphorylation-dependent degradation of the cyclin-dependent kinase inhibitor p27. The EMBO journal *16*, 5334-5344.

Wang, X., Tsai, J.W., LaMonica, B., and Kriegstein, A.R. (2011). A new subtype of progenitor cell in the mouse embryonic neocortex. Nat Neurosci *14*, 555-561.

Watanabe, T., Noritake, J., and Kaibuchi, K. (2005). Regulation of microtubules in cell migration. Trends Cell Biol *15*, 76-83.

Weber, J.D., Hu, W., Jefcoat, S.C., Jr., Raben, D.M., and Baldassare, J.J. (1997). Ras-stimulated extracellular signal-related kinase 1 and RhoA activities coordinate platelet-derived growth factor-induced G1 progression through the independent regulation of cyclin D1 and p27. J Biol Chem *272*, 32966-32971.

Yingling, J., Youn, Y.H., Darling, D., Toyo-Oka, K., Pramparo, T., Hirotsune, S., and Wynshaw-Boris, A. (2008). Neuroepithelial stem cell proliferation requires LIS1 for precise spindle orientation and symmetric division. Cell *132*, 474-486.

Zhang, X., Lei, K., Yuan, X., Wu, X., Zhuang, Y., Xu, T., Xu, R., and Han, M. (2009). SUN1/2 and Syne/Nesprin-1/2 complexes connect centrosome to the nucleus during neurogenesis and neuronal migration in mice. Neuron *64*, 173-187.

Zhao, S., and Frotscher, M. (2010). Go or stop? Divergent roles of Reelin in radial neuronal migration. Neuroscientist *16*, 421-434.

General Conclusion

Corticogenesis a highly dynamic process that requires the spatial and temporal coordination of multiple cell types as they proliferate, migrate, and differentiate. An important, yet unresolved issue is the coupling between proliferation/ neuron production rates and migration rates in the developing cortex.

This thesis work largely relies *ex vivo* organotypic culture methods combined with high-resolution imaging which provides a strong platform for resolving the cellular dynamics in a spatiotemporal fashion. Real-time videomicroscopy analysis made it possible to finely analyse the kinetics of the successive events taking place during corticogenesis: INM, progenitor cell divisions and subsequent post-mitotic radial migration. Our results in the mouse point to cell-cycle progression, proliferation, INM, mode of division and post-mitotic radial migration being coordinated through p27 modular action on both cell-cycle and cytoskeleton pathways, as summarized on the cartoon below.

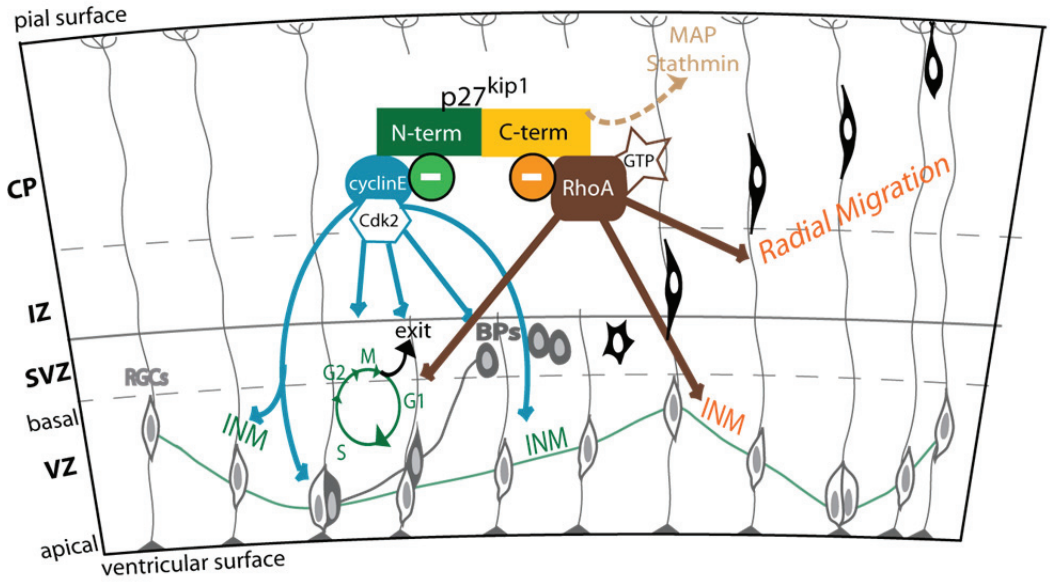

p27 mode of action to coordinate proliferation and migration

LEGENDE: When located into the nucleus, p27 interact and inhibits CyclinE/CDK complexes through its N-terminal domain [reviewed in (Sherr and Roberts, 1999)]. This interferes with the progression of the cell-cycle from G1 phase to S phase. INM progression is thus affected, as well as the cell fate of precursor cells, either giving rise to BPs or differentiating into neurons. After exit from the cell-cycle, post-mitotic neurons leave the germinal zone to undergo radial migration towards the CP. This locomotion is promoted by p27 inhibitory binding to the GTPase RhoA, into the cytoplasm. Inhibition of the RhoA pathway by p27 helps actin cytoskeleton remodelling necessary for progression of neurons into their extracellular space ((Kawauchi et al., 2006; Nguyen et al., 2006a)). Finally, p27 action through the RhoA pathway also affects INM progression, another type of nuclear migration during cortical development, which may also be important to tune the proportion of proliferative vs. differentiative divisions. Furthermore p27 harbours a newly discovered MAP function in its Cter domain (Laurent Nguyen, personal communication, Thomas et al

submitted), that could be implicated, in conjunction with its role on stathmin (Baldassarre et al., 2005; Belletti et al., 2010), in the regulation of the microtubule cytoskeleton. This could have an impact on both INM movement and radial migration.

Our study in the primate shed light on the relevance of these findings for corticogenesis. Using the primate embryonic area 17 and area 18 as a model system, we uncovered for the first time a concerted regulation of rates of proliferation and neuronal production with radial migration kinetics, in a stage-specific and area-specific manner. Specifically, we found that postmitotic neurons issued from precursors pool showing a high rate of proliferation exhibit increased radial migration kinetics compared to neurons generated by precursors with lower proliferation rates. One hypothesis is that these coordinated area-specific variations in proliferation and migration could serve to prevent overcrowding in regions of high neuron production. We provide evidence that p27 could play a key role in this coordination: (i) its nuclear and cytoplasmic expression level varies in a congruent way with kinetics of proliferation and migration, (ii) p27 is able to interact with RhoA in the GZ and the postmitotic compartments of the primate embryonic cortex. Thus, p27 is an evolutionary conserved protein which is a likely candidate to contribute to the coordination of cytoskeletal changes that occur during cell-cycle, cell division and migration during mammalian corticogenesis.

Perspectives: gaining an integrated understanding of p27-mediated interactions impact during corticogenesis via simulation.

The impact of these complex p27-mediated interactions on area formation and cortical cytoarchitecture can be best approached by modelling. The group of R. Douglas at the Institute of Neuroinformatics in Zurich has developed the CX3D software (Zubler and Douglas, 2009), a dynamic model of corticogenesis. CX3D makes it possible to integrate experimentally observed proliferation and migration parameters so as to quantitatively and dynamically simulate corticogenesis. Modelling has already been implemented to explore how differences in rates of proliferation between area 3 and area 6 of the mouse ((Polleux et al., 1997a; Polleux et al., 1997b)) translate into distinct cytoarchitectural features (Cx3D modelling: http://www.youtube.com/watch?v=6gtscHN6dyE&feature=related). Modelling of the proliferation and migration data observed in primate area 17 and area 18 will provide an integrated understanding of the impact of these coordinated processes in the emergence of cytoarchitecturally distinct areas, the establishment of areal boundaries and tangential expansion.

Future development of CX3D will also allow to assess p27 impact on the coordination of INM, proliferation and radial migration. Building upon the flexibility of CX3D, preliminary work has made it possible to independently modify several parameters related to p27 expression level, subcellular localisation, active domains, impact on cell-cycle phases duration, INM kinetics, types of division, as well as radial migration dynamics (Gautier and Zubler, unpublished).

References

Adnane, J., Bizouarn, F.A., Qian, Y., Hamilton, A.D., and Sebti, S.M. (1998). p21(WAF1/CIP1) is upregulated by the geranylgeranyltransferase I inhibitor GGTI-298 through a transforming growth factor beta- and Sp1-responsive element: involvement of the small GTPase rhoA. Mol Cell Biol *18*, 6962-6970.

Altar, C.A., Cai, N., Bliven, T., Juhasz, M., Conner, J.M., Acheson, A.L., Lindsay, R.M., and Wiegand, S.J. (1997). Anterograde transport of brain-derived neurotrophic factor and its role in the brain. Nature *389*, 856-860.

Altman, J., and Bayer, S.A. (1990). Vertical compartmentation and cellular transformations in the germinal matrices of the embryonic rat cerebral cortex. Experimental neurology *107*, 23-35.

Amano, M., Chihara, K., Kimura, K., Fukata, Y., Nakamura, N., Matsuura, Y., and Kaibuchi, K. (1997). Formation of actin stress fibres and focal adhesions enhanced by Rho-kinase. Science *275*, 1308-1311.

Amano, M., Ito, M., Kimura, K., Fukata, Y., Chihara, K., Nakano, T., Matsuura, Y., and Kaibuchi, K. (1996). Phosphorylation and activation of myosin by Rho-associated kinase (Rho-kinase). J Biol Chem *271*, 20246-20249.

Angevine, J.B., Jr., and Sidman, R.L. (1961). Autoradiographic study of cell migration during histogenesis of cerebral cortex in the mouse. Nature *192*, 766-768.

Arnold, S.J., Huang, G.J., Cheung, A.F., Era, T., Nishikawa, S., Bikoff, E.K., Molnar, Z., Robertson, E.J., and Groszer, M. (2008). The T-box transcription factor Eomes/Tbr2 regulates neurogenesis in the cortical subventricular zone. Genes Dev *22*, 2479-2484.

Arthur, W.T., and Burridge, K. (2001). RhoA inactivation by p190RhoGAP regulates cell spreading and migration by promoting membrane protrusion and polarity. Mol Biol Cell *12*, 2711-2720.

Astrom, K.E., and Webster, H.D. (1991). The early development of the neopallial wall and area choroidea in fetal rats. A light and electron microscopic study. Adv Anat Embryol Cell Biol *123*, 1-76.

Attardo, A., Calegari, F., Haubensak, W., Wilsch-Brauninger, M., and Huttner, W.B. (2008). Live imaging at the onset of cortical neurogenesis reveals differential appearance of the neuronal phenotype in apical versus basal progenitor progeny. PloS one *3*, e2388.

Ayala, R., Shu, T., and Tsai, L.H. (2007). Trekking across the brain: the journey of neuronal migration. Cell *128*, 29-43.

Bakal, C.J., Finan, D., LaRose, J., Wells, C.D., Gish, G., Kulkarni, S., DeSepulveda, P., Wilde, A., and Rottapel, R. (2005). The Rho GTP exchange factor Lfc promotes spindle assembly in early mitosis. Proc Natl Acad Sci U S A *102*, 9529-9534.

Baldassarre, G., Barone, M.V., Belletti, B., Sandomenico, C., Bruni, P., Spiezia, S., Boccia, A., Vento, M.T., Romano, A., Pepe, S.*, et al.* (1999). Key role of the cyclin-dependent kinase inhibitor p27 for embryonal carcinoma cell survival and differentiation. Oncogene *18*, 6241-6251.

Baldassarre, G., Belletti, B., Nicoloso, M.S., Schiappacassi, M., Vecchione, A., Spessotto, P., Morrione, A., Canzonieri, V., and Colombatti, A. (2005). p27(Kip1)-stathmin interaction influences sarcoma cell migration and invasion. Cancer cell *7*, 51-63.

Baye, L.M., and Link, B.A. (2007). Interkinetic nuclear migration and the selection of neurogenic cell divisions during vertebrate retinogenesis. J Neurosci *27*, 10143-10152.

Baye, L.M., and Link, B.A. (2008). Nuclear migration during retinal development. Brain Res *1192*, 29-36.

Behar, T.N., Dugich-Djordjevic, M.M., Li, Y.X., Ma, W., Somogyi, R., Wen, X., Brown, E., Scott, C., McKay, R.D., and Barker, J.L. (1997). Neurotrophins stimulate chemotaxis of embryonic cortical neurons. Eur J Neurosci *9*, 2561-2570.

Bellanger, J.M., and Gonczy, P. (2003). TAC-1 and ZYG-9 form a complex that promotes microtubule assembly in C. elegans embryos. Curr Biol *13*, 1488-1498.

Belletti, B., Pellizzari, I., Berton, S., Fabris, L., Wolf, K., Lovat, F., Schiappacassi, M., D'Andrea, S., Nicoloso, M.S., Lovisa, S*., et al.* (2010). p27 controls cell morphology and motility by regulating microtubule-dependent lipid raft recycling. Mol Cell Biol *30*, 2229-2240.

Benais-Pont, G., Punn, A., Flores-Maldonado, C., Eckert, J., Raposo, G., Fleming, T.P., Cereijido, M., Balda, M.S., and Matter, K. (2003). Identification of a tight junction-associated guanine nucleotide exchange factor that activates Rho and regulates paracellular permeability. J Cell Biol *160*, 729-740.

Benjelloun-Touimi, S., Jacque, C.M., Derer, P., De Vitry, F., Maunoury, R., and Dupouey, P. (1985). Evidence that mouse astrocytes may be derived from the radial glia. An immunohistochemical study of the cerebellum in the normal and reeler mouse. J Neuroimmunol *9*, 87-97.

Bernards, A., and Settleman, J. (2004). GAP control: regulating the regulators of small GTPases. Trends Cell Biol *14*, 377-385.

Berton, S., Belletti, B., Wolf, K., Canzonieri, V., Lovat, F., Vecchione, A., Colombatti, A., Friedl, P., and Baldassarre, G. (2009). The tumor suppressor functions of p27(kip1) include control of the mesenchymal/amoeboid transition. Mol Cell Biol *29*, 5031-5045.

Besson, A., Assoian, R.K., and Roberts, J.M. (2004a). Regulation of the cytoskeleton: an oncogenic function for CDK inhibitors? Nat Rev Cancer *4*, 948-955.

Besson, A., Gurian-West, M., Chen, X., Kelly-Spratt, K.S., Kemp, C.J., and Roberts, J.M. (2006). A pathway in quiescent cells that controls p27 stability, subcellular localization, and tumor suppression. Genes Dev *20*, 47-64.

Besson, A., Gurian-West, M., Schmidt, A., Hall, A., and Roberts, J. (2004b). p27 modulates cell migration through the regulation of RhoA activation. Genes Dev *18*, 862-876.

Bittman, K., Owens, D.F., Kriegstein, A.R., and LoTurco, J.J. (1997). Cell coupling and uncoupling in the ventricular zone of developing neocortex. J Neurosci *17*, 7037-7044.

Bloom, J., and Pagano, M. (2003). Deregulated degradation of the cdk inhibitor p27 and malignant transformation. Semin Cancer Biol *13*, 41-47.

Boehm, M., Yoshimoto, T., Crook, M.F., Nallamshetty, S., True, A., Nabel, G.J., and Nabel, E.G. (2002). A growth factor-dependent nuclear kinase phosphorylates p27(Kip1) and regulates cell cycle progression. Embo J *21*, 3390-3401.

Bort, R., Signore, M., Tremblay, K., Martinez Barbera, J.P., and Zaret, K.S. (2006). Hex homeobox gene controls the transition of the endoderm to a pseudostratified, cell emergent epithelium for liver bud development. Dev Biol *290*, 44-56.

Boyer, L., Travaglione, S., Falzano, L., Gauthier, N.C., Popoff, M.R., Lemichez, E., Fiorentini, C., and Fabbri, A. (2004). Rac GTPase instructs nuclear factor-kappaB activation by conveying the SCF complex and IkBalpha to the ruffling membranes. Mol Biol Cell *15*, 1124-1133.

Brouns, M.R., Matheson, S.F., Hu, K.Q., Delalle, I., Caviness, V.S., Silver, J., Bronson, R.T., and Settleman, J. (2000). The adhesion signaling molecule p190 RhoGAP is required for morphogenetic processes in neural development. Development *127*, 4891-4903.

Burkel, B.M., von Dassow, G., and Bement, W.M. (2007). Versatile fluorescent probes for actin filaments based on the actin-binding domain of utrophin. Cell Motil Cytoskeleton *64*, 822-832.

Burridge, K., and Wennerberg, K. (2004). Rho and Rac take center stage. Cell *116*, 167-179.

Calegari, F., Haubensak, W., Haffner, C., and Huttner, W.B. (2005). Selective lengthening of the cell cycle in the neurogenic subpopulation of neural progenitor cells during mouse brain development. J Neurosci *25*, 6533-6538.

Calegari, F., and Huttner, W.B. (2003). An inhibition of cyclin-dependent kinases that lengthens, but does not arrest, neuroepithelial cell cycle induces premature neurogenesis. Journal of cell science *116*, 4947-4955.

Carrano, A.C., Eytan, E., Hershko, A., and Pagano, M. (1999). SKP2 is required for ubiquitin-mediated degradation of the CDK inhibitor p27. Nat Cell Biol *1*, 193-199.

Causeret, F., Hidalgo-Sanchez, M., Fort, P., Backer, S., Popoff, M.R., Gauthier-Rouviere, C., and Bloch-Gallego, E. (2004). Distinct roles of Rac1/Cdc42 and Rho/Rock for axon outgrowth and nucleokinesis of precerebellar neurons toward netrin 1. Development *131*, 2841-2852.

Caviness, V.S., Goto, T., Tarui, T., Takahashi, T., Bhide, P.G., and Nowakowski, R.S. (2003). Cell output, cell cycle duration and neuronal specification: a model of integrated mechanisms of the neocortical proliferative process. Cerebral cortex (New York, NY: 1991) *13*, 592-598.

Caviness, V.S., Jr. (1982). Neocortical histogenesis in normal and reeler mice: a developmental study based upon [3H]thymidine autoradiography. Brain Res *256*, 293-302.

Caviness, V.S., Jr., Takahashi, T., and Nowakowski, R.S. (1995). Numbers, time and neocortical neuronogenesis: a general developmental and evolutionary model. Trends Neurosci *18*, 379-383.

Cheng, M., Olivier, P., Diehl, J.A., Fero, M., Roussel, M.F., Roberts, J.M., and Sherr, C.J. (1999). The p21(Cip1) and p27(Kip1) CDK 'inhibitors' are essential activators of cyclin D-dependent kinases in murine fibroblasts. Embo J *18*, 1571-1583.

Chenn, A., and McConnell, S.K. (1995). Cleavage orientation and the asymmetric inheritance of Notch1 immunoreactivity in mammalian neurogenesis. Cell *82*, 631-641.

Chu, I., Sun, J., Arnaout, A., Kahn, H., Hanna, W., Narod, S., Sun, P., Tan, C.K., Hengst, L., and Slingerland, J. (2007). p27 phosphorylation by Src regulates inhibition of cyclin E-Cdk2. Cell *128*, 281-294.

Connor, M.K., Kotchetkov, R., Cariou, S., Resch, A., Lupetti, R., Beniston, R.G., Melchior, F., Hengst, L., and Slingerland, J.M. (2003). CRM1/Ran-mediated nuclear export of p27(Kip1) involves a nuclear export signal and links p27 export and proteolysis. Mol Biol Cell *14*, 201-213.

Cory, G.O., and Ridley, A.J. (2002). Cell motility: braking WAVEs. Nature *418*, 732-733.

Cox, E.A., Sastry, S.K., and Huttenlocher, A. (2001). Integrin-mediated adhesion regulates cell polarity and membrane protrusion through the Rho family of GTPases. Mol Biol Cell *12*, 265-277.

Cunningham, J.J., and Roussel, M.F. (2001). Cyclin-dependent kinase inhibitors in the development of the central nervous system. Cell Growth Differ *12*, 387-396.

Danen, E.H., Sonneveld, P., Sonnenberg, A., and Yamada, K.M. (2000). Dual stimulation of Ras/mitogen-activated protein kinase and RhoA by cell adhesion to fibronectin supports growth factor-stimulated cell cycle progression. J Cell Biol *151*, 1413-1422.

Daniel, C., Pippin, J., Shankland, S.J., and Hugo, C. (2004). The rapamycin derivative RAD inhibits mesangial cell migration through the CDK-inhibitor p27. Lab Invest *84*, 588-596.

Dehay, C., Giroud, P., Berland, M., Smart, I., and Kennedy, H. (1993). Modulation of the cell cycle contributes to the parcellation of the primate visual cortex. Nature *366*, 464-466.

Dehay, C., and Kennedy, H. (2007). Cell-cycle control and cortical development. Nat Rev Neurosci *8*, 438-450.

Dehay, C., Savatier, P., Cortay, V., and Kennedy, H. (2001). Cell-cycle kinetics of neocortical precursors are influenced by embryonic thalamic axons. J Neurosci *21*, 201-214.

Del Bene, F., Wehman, A.M., Link, B.A., and Baier, H. (2008). Regulation of neurogenesis by interkinetic nuclear migration through an apical-basal notch gradient. Cell *134*, 1055-1065.

Deng, X., Mercer, S.E., Shah, S., Ewton, D.Z., and Friedman, E. (2004). The cyclin-dependent kinase inhibitor p27 is stabilized in G(0) by Mirk/dyrk1B kinase. J Biol Chem *279*, 22498-22504.

Denicourt, C., Saenz, C.C., Datnow, B., Cui, X.S., and Dowdy, S.F. (2007). Relocalized p27 tumor suppressor functions as a cytoplasmic metastatic oncogene in melanoma. Cancer Res *67*, 9238-9243.

DerMardirossian, C., and Bokoch, G.M. (2005). GDIs: central regulatory molecules in Rho GTPase activation. Trends Cell Biol *15*, 356-363.

Dhavan, R., and Tsai, L.H. (2001). A decade of CDK5. Nat Rev Mol Cell Biol *2*, 749-759.

Diez-Juan, A., and Andres, V. (2003). Coordinate control of proliferation and migration by the p27/cyclin-dependent kinase/retinoblastoma pathway in vascular smooth muscle cells and fibroblasts. Circ Res *92*, 402-410.

Ding, Y., and Casagrande, V.A. (1998). Synaptic and neurochemical characterization of parallel pathways to the cytochrome oxidase blobs of primate visual cortex. J Comp Neurol *391*, 429-443.

Dubreuil, V., Marzesco, A.M., Corbeil, D., Huttner, W.B., and Wilsch-Brauninger, M. (2007). Midbody and primary cilium of neural progenitors release extracellular membrane particles enriched in the stem cell marker prominin-1. J Cell Biol *176*, 483-495.

Durand, B., Gao, F.B., and Raff, M. (1997). Accumulation of the cyclin-dependent kinase inhibitor p27/Kip1 and the timing of oligodendrocyte differentiation. Embo J *16*, 306-317.

Edgar, J.M., and Price, D.J. (2001). Radial migration in the cerebral cortex is enhanced by signals from thalamus. Eur J Neurosci *13*, 1745-1754.

Elias, L.A., Wang, D.D., and Kriegstein, A.R. (2007). Gap junction adhesion is necessary for radial migration in the neocortex. Nature *448*, 901-907.

Elledge, S.J., and Harper, J.W. (1994). Cdk inhibitors: on the threshold of checkpoints and development. Curr Opin Cell Biol *6*, 847-852.

Englund, C., Fink, A., Lau, C., Pham, D., Daza, R.A., Bulfone, A., Kowalczyk, T., and Hevner, R.F. (2005). Pax6, Tbr2, and Tbr1 are expressed sequentially by radial glia, intermediate progenitor cells, and postmitotic neurons in developing neocortex. J Neurosci *25*, 247-251.

Estivill-Torrus, G., Pearson, H., van Heyningen, V., Price, D.J., and Rashbass, P. (2002). Pax6 is required to regulate the cell cycle and the rate of progression from symmetrical to asymmetrical division in mammalian cortical progenitors. Development *129*, 455-466.

Etienne-Manneville, S., and Hall, A. (2002). Rho GTPases in cell biology. Nature *420*, 629-635.

Farah, M.H., Olson, J.M., Sucic, H.B., Hume, R.I., Tapscott, S.J., and Turner, D.L. (2000). Generation of neurons by transient expression of neural bHLH proteins in mammalian cells. Development *127*, 693-702.

Farkas, L.M., and Huttner, W.B. (2008). The cell biology of neural stem and progenitor cells and its significance for their proliferation versus differentiation during mammalian brain development. Curr Opin Cell Biol *20*, 707-715.

Faulkner, N.E., Dujardin, D.L., Tai, C.Y., Vaughan, K.T., O'Connell, C.B., Wang, Y., and Vallee, R.B. (2000). A role for the lissencephaly gene LIS1 in mitosis and cytoplasmic dynein function. Nat Cell Biol *2*, 784-791.

Ferguson, K.L., Vanderluit, J.L., Hebert, J.M., McIntosh, W.C., Tibbo, E., MacLaurin, J.G., Park, D.S., Wallace, V.A., Vooijs, M., McConnell, S.K.*, et al.* (2002). Telencephalon-specific Rb knockouts reveal enhanced neurogenesis, survival and abnormal cortical development. Embo J *21*, 3337-3346.

Fero, M.L., Randel, E., Gurley, K.E., Roberts, J.M., and Kemp, C.J. (1998). The murine gene p27 is haplo-insufficient for tumour suppression. Nature *396*, 177-180.

Fero, M.L., Rivkin, M., Tasch, M., Porter, P., Carow, C.E., Firpo, E., Polyak, K., Tsai, L.H., Broudy, V., Perlmutter, R.M.*, et al.* (1996). A syndrome of multiorgan hyperplasia with features of gigantism, tumorigenesis, and female sterility in p27(Kip1)-deficient mice. Cell *85*, 733-744.

Fietz, S.A., Kelava, I., Vogt, J., Wilsch-Brauninger, M., Stenzel, D., Fish, J.L., Corbeil, D., Riehn, A., Distler, W., Nitsch, R.*, et al.* (2010). OSVZ progenitors of human and ferret neocortex are epithelial-like and expand by integrin signaling. Nat Neurosci *13*, 690-699.

Fish, J.L., Dehay, C., Kennedy, H., and Huttner, W.B. (2008). Making bigger brains-the evolution of neural-progenitor-cell division. Journal of cell science *121*, 2783-2793.

Fishell, G. (1995). Striatal precursors adopt cortical identities in response to local cues. Development *121*, 803-812.

Fode, C., Ma, Q., Casarosa, S., Ang, S.L., Anderson, D.J., and Guillemot, F. (2000). A role for neural determination genes in specifying the dorsoventral identity of telencephalic neurons. Genes Dev *14*, 67-80.

Frade, J.M. (2002). Interkinetic nuclear movement in the vertebrate neuroepithelium: encounters with an old acquaintance. Prog Brain Res *136*, 67-71.

Francis, F., Koulakoff, A., Boucher, D., Chafey, P., Schaar, B., Vinet, M.C., Friocourt, G., McDonnell, N., Reiner, O., Kahn, A*., et al.*(1999). Doublecortin is a developmentally regulated, microtubule-associated protein expressed in migrating and differentiating neurons. Neuron *23*, 247-256.

Frank, C.L., and Tsai, L.H. (2009). Alternative functions of core cell cycle regulators in neuronal migration, neuronal maturation, and synaptic plasticity. Neuron *62*, 312-326.

Friocourt, G., Liu, J.S., Antypa, M., Rakic, S., Walsh, C.A., and Parnavelas, J.G. (2007). Both doublecortin and doublecortin-like kinase play a role in cortical interneuron migration. J Neurosci *27*, 3875-3883.

Frost, J.A., Khokhlatchev, A., Stippec, S., White, M.A., and Cobb, M.H. (1998). Differential effects of PAK1-activating mutations reveal activity-dependent and -independent effects on cytoskeletal regulation. J Biol Chem *273*, 28191-28198.

Fujita, N., Sato, S., Katayama, K., and Tsuruo, T. (2002). Akt-dependent phosphorylation of p27 promotes binding to 14-3-3 and cytoplasmic localization. J Biol Chem *277*, 28706-28713.

Fujita, S. (1960). Mitotic pattern and histogenesis of the central nervous system. Nature *185*, 702-703.

Fukuda, T., Kawano, H., Osumi, N., Eto, K., and Kawamura, K. (2000). Histogenesis of the cerebral cortex in rat fetuses with a mutation in the Pax-6 gene. Brain Res Dev Brain Res *120*, 65-75.

Gal, J.S., Morozov, Y.M., Ayoub, A.E., Chatterjee, M., Rakic, P., and Haydar, T.F. (2006). Molecular and morphological heterogeneity of neural precursors in the mouse neocortical proliferative zones. J Neurosci *26*, 1045-1056.

Gambello, M.J., Darling, D.L., Yingling, J., Tanaka, T., Gleeson, J.G., and Wynshaw-Boris, A. (2003). Multiple dose-dependent effects of Lis1 on cerebral cortical development. J Neurosci *23*, 1719-1729.

Garcia-Moreno, F., Lopez-Mascaraque, L., and De Carlos, J.A. (2007). Origins and migratory routes of murine Cajal-Retzius cells. J Comp Neurol *500*, 419-432.

Gautier E, C.V., Betizeau M, Doerflinger N, Kennedy H, Dehay C. (2010a). Area-specific dynamics of proliferation and migration during primate corticogenesis: role of the modular protein p27. 18th ISDN (International Society for Development Neuroscience) Meeting, Estoril, Portugal.

Gautier E, C.V., Betizeau M, Doerflinger N, Patti D, Kennedy H, Dehay C (2010b). Area-specific dynamics of proliferation and migration during primate corticogenesis: role of the modular protein p27. 40th SFN (Society for Neuroscience) Meeting, San Diego, USA.

Ge, W., He, F., Kim, K.J., Blanchi, B., Coskun, V., Nguyen, L., Wu, X., Zhao, J., Heng, J.I., Martinowich, K*., et al.* (2006). Coupling of cell migration with neurogenesis by proneural bHLH factors. Proc Natl Acad Sci U S A *103*, 1319-1324.

Gergely, F. (2002). Centrosomal TACCtics. Bioessays *24*, 915-925.

Gergely, F., Kidd, D., Jeffers, K., Wakefield, J.G., and Raff, J.W. (2000). D-TACC: a novel centrosomal protein required for normal spindle function in the early Drosophila embryo. Embo J *19*, 241-252.

Gille, H., and Downward, J. (1999). Multiple ras effector pathways contribute to G(1) cell cycle progression. J Biol Chem *274*, 22033-22040.

Gillies, J.K., and Lorimer, I.A. (2007). Regulation of p27 by miRNA 221/222 in glioblastoma. Cell Cycle *6*, 2005-2009.

Goode, B.L., and Eck, M.J. (2007). Mechanism and function of formins in the control of actin assembly. Annu Rev Biochem *76*, 593-627.

Gorski, J.A., Talley, T., Qiu, M., Puelles, L., Rubenstein, J.L., and Jones, K.R. (2002). Cortical excitatory neurons and glia, but not GABAergic neurons, are produced in the Emx1-expressing lineage. J Neurosci *22*, 6309-6314.

Goto, T., Mitsuhashi, T., and Takahashi, T. (2004). Altered patterns of neuron production in the p27 knockout mouse. Dev Neurosci *26*, 208-217.

Gotz, M., and Barde, Y.A. (2005). Radial glial cells defined and major intermediates between embryonic stem cells and CNS neurons. Neuron *46*, 369-372.

Gotz, M., and Huttner, W.B. (2005). The cell biology of neurogenesis. Nat Rev Mol Cell Biol *6*, 777-788.

Gotz, M., Stoykova, A., and Gruss, P. (1998). Pax6 controls radial glia differentiation in the cerebral cortex. Neuron *21*, 1031-1044.

Goukassian, D., Diez-Juan, A., Asahara, T., Schratzberger, P., Silver, M., Murayama, T., Isner, J.M., and Andres, V. (2001a). Overexpression of p27(Kip1) by doxycycline-regulated adenoviral vectors inhibits endothelial cell proliferation and migration and impairs angiogenesis. Faseb J *15*, 1877-1885.

Govek, E.E., Hatten, M.E., and Van Aelst, L. (2010). The role of Rho GTPase proteins in CNS neuronal migration. Dev Neurobiol.

Grimmler, M., Wang, Y., Mund, T., Cilensek, Z., Keidel, E.M., Waddell, M.B., Jakel, H., Kullmann, M., Kriwacki, R.W., and Hengst, L. (2007). Cdk-inhibitory activity and stability of p27 are directly regulated by oncogenic tyrosine kinases. Cell *128*, 269-280.

Gruss, O.J., Wittmann, M., Yokoyama, H., Pepperkok, R., Kufer, T., Sillje, H., Karsenti, E., Mattaj, I.W., and Vernos, I. (2002). Chromosome-induced microtubule assembly mediated by TPX2 is required for spindle formation in HeLa cells. Nat Cell Biol *4*, 871-879.

Guillemot, F., Molnar, Z., Tarabykin, V., and Stoykova, A. (2006). Molecular mechanisms of cortical differentiation. Eur J Neurosci *23*, 857-868.

Gupta, A., Tsai, L.H., and Wynshaw-Boris, A. (2002). Life is a journey: a genetic look at neocortical development. Nat Rev Genet *3*, 342-355.

Hammond, J.W., Cai, D., Blasius, T.L., Li, Z., Jiang, Y., Jih, G.T., Meyhofer, E., and Verhey, K.J. (2009). Mammalian Kinesin-3 motors are dimeric in vivo and move by processive motility upon release of autoinhibition. PLoS Biol *7*, e72.

Hand, R., Bortone, D., Mattar, P., Nguyen, L., Heng, J.I.-T., Guerrier, S., Boutt, E., Peters, E., Barnes, A.P., Parras, C*., et al.* (2005). Phosphorylation of Neurogenin2 specifies the migration properties and the dendritic morphology of pyramidal neurons in the neocortex. Neuron *48*, 45-62.

Hansen, D.V., Lui, J.H., Parker, P.R., and Kriegstein, A.R. (2010). Neurogenic radial glia in the outer subventricular zone of human neocortex. Nature *464*, 554-561.

Hatten, M.E. (1990). Riding the glial monorail: a common mechanism for glial-guided neuronal migration in different regions of the developing mammalian brain. Trends Neurosci *13*, 179-184.

Haubensak, W., Attardo, A., Denk, W., and Huttner, W.B. (2004). Neurons arise in the basal neuroepithelium of the early mammalian telencephalon: a major site of neurogenesis. Proc Natl Acad Sci U S A *101*, 3196-3201.

Hayes, N.L., and Nowakowski, R.S. (2000). Exploiting the dynamics of S-phase tracers in developing brain: interkinetic nuclear migration for cells entering versus leaving the S-phase. Dev Neurosci *22*, 44-55.

Heins, N., Malatesta, P., Cecconi, F., Nakafuku, M., Tucker, K.L., Hack, M.A., Chapouton, P., Barde, Y.A., and Gotz, M. (2002). Glial cells generate neurons: the role of the transcription factor Pax6. Nat Neurosci *5*, 308-315.

Heng, J.I., Chariot, A., and Nguyen, L. (2010). Molecular layers underlying cytoskeletal remodelling during cortical development. Trends Neurosci *33*, 38-47.

Hengst, L., and Reed, S.I. (1996). Translational control of p27 accumulation during the cell cycle. Science *271*, 1861-1864.

Hevner, R.F. (2006). From radial glia to pyramidal-projection neuron: transcription factor cascades in cerebral cortex development. Mol Neurobiol *33*, 33-50.

Hevner, R.F., Daza, R.A., Rubenstein, J.L., Stunnenberg, H., Olavarria, J.F., and Englund, C. (2003). Beyond laminar fate: toward a molecular classification of cortical projection/pyramidal neurons. Dev Neurosci *25*, 139-151.

Higashida, C., Miyoshi, T., Fujita, A., Oceguera-Yanez, F., Monypenny, J., Andou, Y., Narumiya, S., and Watanabe, N. (2004). Actin polymerization-driven molecular movement of mDia1 in living cells. Science *303*, 2007-2010.

Higginbotham, H.R., and Gleeson, J.G. (2007). The centrosome in neuronal development. Trends Neurosci *30*, 276-283.

Hinds, J.W., and Ruffett, T.L. (1971). Cell proliferation in the neural tube: an electron microscopic and golgi analysis in the mouse cerebral vesicle. Z Zellforsch Mikrosk Anat *115*, 226-264.

Hoerder-Suabedissen, A., Wang, W.Z., Lee, S., Davies, K.E., Goffinet, A.M., Rakic, S., Parnavelas, J., Reim, K., Nicolic, M., Paulsen, O*., et al.* (2009). Novel markers reveal subpopulations of subplate neurons in the murine cerebral cortex. Cereb Cortex *19*, 1738-1750.

Hong, F., Larrea, M.D., Doughty, C., Kwiatkowski, D.J., Squillace, R., and Slingerland, J.M. (2008). mTOR-raptor binds and activates SGK1 to regulate p27 phosphorylation. Mol Cell *30*, 701-711.

Hu, W., Bellone, C.J., and Baldassare, J.J. (1999). RhoA stimulates p27(Kip) degradation through its regulation of cyclin E/CDK2 activity. J Biol Chem *274*, 3396-3401.

Huang, Z. (2009). Molecular regulation of neuronal migration during neocortical development. Mol Cell Neurosci *42*, 11-22.

Huttner, W.B., and Brand, M. (1997). Asymmetric division and polarity of neuroepithelial cells. Current opinion in neurobiology *7*, 29-39.

Huttner, W.B., and Kosodo, Y. (2005). Symmetric versus asymmetric cell division during neurogenesis in the developing vertebrate central nervous system. Curr Opin Cell Biol *17*, 648-657.

Ishida, N., Hara, T., Kamura, T., Yoshida, M., Nakayama, K., and Nakayama, K.I. (2002). Phosphorylation of p27 on serine 10 is required for its binding to CRM1 and nuclear export. J Biol Chem *277*, 14355-14358.

Ishida, N., Kitagawa, M., Hatakeyama, S., and Nakayama, K. (2000). Phosphorylation at serine 10, a major phosphorylation site of p27(Kip1), increases its protein stability. J Biol Chem *275*, 25146-25154.

Ishizaki, T., Maekawa, M., Fujisawa, K., Okawa, K., Iwamatsu, A., Fujita, A., Watanabe, N., Saito, Y., Kakizuka, A., Morii, N*., et al.* (1996). The small GTP-binding protein Rho binds to and activates a 160 kDa Ser/Thr protein kinase homologous to myotonic dystrophy kinase. Embo J *15*, 1885-1893.

Ishizaki, T., Morishima, Y., Okamoto, M., Furuyashiki, T., Kato, T., and Narumiya, S. (2001). Coordination of microtubules and the actin cytoskeleton by the Rho effector mDia1. Nat Cell Biol *3*, 8-14.

Itoh, R.E., Kurokawa, K., Ohba, Y., Yoshizaki, H., Mochizuki, N., and Matsuda, M. (2002). Activation of rac and cdc42 video imaged by fluorescent resonance energy transfer-based single-molecule probes in the membrane of living cells. Mol Cell Biol *22*, 6582-6591.

Itoh, Y., Masuyama, N., Nakayama, K., Nakayama, K.I., and Gotoh, Y. (2007). The cyclin-dependent kinase inhibitors p57 and p27 regulate neuronal migration in the developing mouse neocortex. J Biol Chem *282*, 390-396.

Jaffe, A.B., and Hall, A. (2005). Rho GTPases: biochemistry and biology. Annu Rev Cell Dev Biol *21*, 247-269.

James, M.K., Ray, A., Leznova, D., and Blain, S.W. (2008). Differential modification of p27 controls its cyclin D-cdk4 inhibitory activity. Mol Cell Biol *28*, 498-510.

Jones, E.G. (2009). The origins of cortical interneurons: mouse versus monkey and human. Cereb Cortex *19*, 1953-1956.

Kallen, B. (1962). Mitotic patterning in the central nervous system of chick embryos; studied by a colchicine method. Z Anat Entwicklungsgesch *123*, 309-319.

Kawaguchi, A., Ogawa, M., Saito, K., Matsuzaki, F., Okano, H., and Miyata, T. (2004). Differential expression of Pax6 and Ngn2 between pair-generated cortical neurons. J Neurosci Res *78*, 784-795.

Kawaguchi, D., Yoshimatsu, T., Hozumi, K., and Gotoh, Y. (2008). Selection of differentiating cells by different levels of delta-like 1 among neural precursor cells in the developing mouse telencephalon. Development *135*, 3849-3858.

Kawauchi, T., Chihama, K., Nabeshima, Y., and Hoshino, M. (2006). Cdk5 phosphorylates and stabilizes p27 contributing to actin organization and cortical neuronal migration. Nat Cell Biol *8*, 17-26.

Kawauchi, T., and Hoshino, M. (2008). Molecular pathways regulating cytoskeletal organization and morphological changes in migrating neurons. Dev Neurosci *30*, 36-46.

Kennedy, H., Douglas, R.J., Knoblauch, K., and Dehay, C. (2007). Self-organization and pattern formation in primate cortical networks. In Novartis Found Symp.

Kholmanskikh, S.S., Dobrin, J.S., Wynshaw-Boris, A., Letourneau, P.C., and Ross, M.E. (2003). Disregulated RhoGTPases and actin cytoskeleton contribute to the migration defect in Lis1-deficient neurons. J Neurosci *23*, 8673-8681.

Kimura, K., Ito, M., Amano, M., Chihara, K., Fukata, Y., Nakafuku, M., Yamamori, B., Feng, J., Nakano, T., Okawa, K*., et al.* (1996). Regulation of myosin phosphatase by Rho and Rho-associated kinase (Rho-kinase). Science *273*, 245-248.

King, S.J., and Schroer, T.A. (2000). Dynactin increases the processivity of the cytoplasmic dynein motor. Nat Cell Biol *2*, 20-24.

Klopfenstein, D.R., and Vale, R.D. (2004). The lipid binding pleckstrin homology domain in UNC-104 kinesin is necessary for synaptic vesicle transport in Caenorhabditis elegans. Mol Biol Cell *15*, 3729-3739.

Koizumi, H., and Gleeson, J.G. (2009). Sun proteins enlighten nuclear movement in development. Neuron *64*, 147-149.

Komuro, H., and Rakic, P. (1996). Intracellular Ca2+ fluctuations modulate the rate of neuronal migration. Neuron *17*, 275-285.

Kornack, D.R., and Rakic, P. (1998). Changes in cell-cycle kinetics during the development and evolution of primate neocortex. Proc Natl Acad Sci U S A *95*, 1242-1246.

Kosako, H., Yoshida, T., Matsumura, F., Ishizaki, T., Narumiya, S., and Inagaki, M. (2000). Rho-kinase/ROCK is involved in cytokinesis through the phosphorylation of myosin light chain and not ezrin/radixin/moesin proteins at the cleavage furrow. Oncogene *19*, 6059-6064.

Kosodo, Y., Suetsugu, T., Suda, M., Mimori-Kiyosue, Y., Toida, K., Baba, S.A., Kimura, A., and Matsuzaki, F. (2011). Regulation of interkinetic nuclear migration by cell cycle-coupled active and passive mechanisms in the developing brain. Embo J *30*, 1690-1704.

Kossatz, U., Vervoorts, J., Nickeleit, I., Sundberg, H.A., Arthur, J.S., Manns, M.P., and Malek, N.P. (2006). C-terminal phosphorylation controls the stability and function of p27. Embo J *25*, 5159-5170.

Kostovic, I., and Rakic, P. (1990). Developmental history of the transient subplate zone in the visual and somatosensory cortex of the macaque monkey and human brain. J Comp Neurol *297*, 441-470.

Kowalczyk, T., Pontious, A., Englund, C., Daza, R.A., Bedogni, F., Hodge, R., Attardo, A., Bell, C., Huttner, W.B., and Hevner, R.F. (2009). Intermediate neuronal progenitors (basal progenitors) produce pyramidal-projection neurons for all layers of cerebral cortex. Cereb Cortex *19*, 2439-2450.

Kriegstein, A., Noctor, S., and Martinez-Cerdeno, V. (2006). Patterns of neural stem and progenitor cell division may underlie evolutionary cortical expansion. Nat Rev Neurosci *7*, 883-890.

Kriegstein, A.R., and Noctor, S.C. (2004). Patterns of neuronal migration in the embryonic cortex. Trends Neurosci *27*, 392-399.

LaBaer, J., Garrett, M.D., Stevenson, L.F., Slingerland, J.M., Sandhu, C., Chou, H.S., Fattaey, A., and Harlow, E. (1997). New functional activities for the p21 family of CDK inhibitors. Genes Dev *11*, 847-862.

Laman, H., Funes, J.M., Ye, H., Henderson, S., Galinanes-Garcia, L., Hara, E., Knowles, P., McDonald, N., and Boshoff, C. (2005). Transforming activity of Fbxo7 is mediated specifically through regulation of cyclin D/cdk6. Embo J *24*, 3104-3116.

Langman, J., Guerrant, R.L., and Freeman, B.G. (1966). Behavior of neuro-epithelial cells during closure of the neural tube. J Comp Neurol *127*, 399-411.

Larrea, M.D., Hong, F., Wander, S.A., da Silva, T.G., Helfman, D., Lannigan, D., Smith, J.A., and Slingerland, J.M. (2009a). RSK1 drives p27 phosphorylation at T198 to promote RhoA inhibition and increase cell motility. Proc Natl Acad Sci U S A *106*, 9268-9273.

Larrea, M.D., Liang, J., Da Silva, T., Hong, F., Shao, S.H., Han, K., Dumont, D., and Slingerland, J.M. (2008). Phosphorylation of p27 regulates assembly and activation of cyclin D1-Cdk4. Mol Cell Biol *28*, 6462-6472.

Larrea, M.D., Wander, S.A., and Slingerland, J.M. (2009b). p27 as Jekyll and Hyde: regulation of cell cycle and cell motility. Cell Cycle *8*, 3455-3461.

Latasa, M.J., Cisneros, E., and Frade, J.M. (2009). Cell cycle control of Notch signaling and the functional regionalization of the neuroepithelium during vertebrate neurogenesis. Int J Dev Biol *53*, 895-908.

Lee, S., and Helfman, D.M. (2004). Cytoplasmic p21Cip1 is involved in Ras-induced inhibition of the ROCK/LIMK/cofilin pathway. J Biol Chem *279*, 1885-1891.

Lein, E.S., Hohn, A., and Shatz, C.J. (2000). Dynamic regulation of BDNF and NT-3 expression during visual system development. J Comp Neurol *420*, 1-18.

Letinic, K., Zoncu, R., and Rakic, P. (2002). Origin of GABAergic neurons in the human neocortex. Nature *417*, 645-649.

Leung, L., Klopper, A.V., Grill, S.W., Harris, W.A., and Norden, C. (2011). Apical migration of nuclei during G2 is a prerequisite for all nuclear motion in zebrafish neuroepithelia. Development *138*, 5003-5013.

Leung, T., Chen, X.Q., Tan, I., Manser, E., and Lim, L. (1998). Myotonic dystrophy kinase-related Cdc42-binding kinase acts as a Cdc42 effector in promoting cytoskeletal reorganization. Mol Cell Biol *18*, 130-140.

Leung, T., Manser, E., Tan, L., and Lim, L. (1995). A novel serine/threonine kinase binding the Ras-related RhoA GTPase which translocates the kinase to peripheral membranes. J Biol Chem *270*, 29051-29054.

Li, F., and Higgs, H.N. (2003). The mouse Formin mDia1 is a potent actin nucleation factor regulated by autoinhibition. Curr Biol *13*, 1335-1340.

Liang, J., Shao, S.H., Xu, Z.X., Hennessy, B., Ding, Z., Larrea, M., Kondo, S., Dumont, D.J., Gutterman, J.U., Walker, C.L.*, et al.* (2007). The energy sensing LKB1-AMPK pathway regulates p27(kip1) phosphorylation mediating the decision to enter autophagy or apoptosis. Nat Cell Biol *9*, 218-224.

Liang, J., Zubovitz, J., Petrocelli, T., Kotchetkov, R., Connor, M.K., Han, K., Lee, J.H., Ciarallo, S., Catzavelos, C., Beniston, R.*, et al.* (2002). PKB/Akt phosphorylates p27, impairs nuclear import of p27 and opposes p27-mediated G1 arrest. Nat Med *8*, 1153-1160.

Liberto, M., Cobrinik, D., and Minden, A. (2002). Rho regulates p21(CIP1), cyclin D1, and checkpoint control in mammary epithelial cells. Oncogene *21*, 1590-1599.

Liu, H., Di Cunto, F., Imarisio, S., and Reid, L.M. (2003). Citron kinase is a cell cycle-dependent, nuclear protein required for G2/M transition of hepatocytes. J Biol Chem *278*, 2541-2548.

Liu, X., Hashimoto-Torii, K., Torii, M., Ding, C., and Rakic, P. (2010). Gap junctions/hemichannels modulate interkinetic nuclear migration in the forebrain precursors. J Neurosci *30*, 4197-4209.

Lopez-Bendito, G., Cautinat, A., Sanchez, J.A., Bielle, F., Flames, N., Garratt, A.N., Talmage, D.A., Role, L.W., Charnay, P., Marin, O*., et al.*(2006). Tangential neuronal migration controls axon guidance: a role for neuregulin-1 in thalamocortical axon navigation. Cell *125*, 127-142.

Lukaszewicz, A., Cortay, V., Giroud, P., Berland, M., Smart, I., Kennedy, H., and Dehay, C. (2006). The concerted modulation of proliferation and migration contributes to the specification of the cytoarchitecture and dimensions of cortical areas. Cereb Cortex *16 Suppl 1*, i26-34.

Lukaszewicz, A., Savatier, P., Cortay, V., Giroud, P., Huissoud, C., Berland, M., Kennedy, H., and Dehay, C. (2005). G1 phase regulation, area-specific cell cycle control, and cytoarchitectonics in the primate cortex. Neuron *47*, 353-364.

Lukaszewicz, A., Savatier, P., Cortay, V., Kennedy, H., and Dehay, C. (2002). Contrasting effects of basic fibroblast growth factor and neurotrophin 3 on cell cycle kinetics of mouse cortical stem cells. J Neurosci *22*, 6610-6622.

Maekawa, M., Ishizaki, T., Boku, S., Watanabe, N., Fujita, A., Iwamatsu, A., Obinata, T., Ohashi, K., Mizuno, K., and Narumiya, S. (1999). Signaling from Rho to the actin cytoskeleton through protein kinases ROCK and LIM-kinase. Science *285*, 895-898.

Malatesta, P., Hartfuss, E., and Gotz, M. (2000). Isolation of radial glial cells by fluorescent-activated cell sorting reveals a neuronal lineage. Development *127*, 5253-5263.

Malek, N.P., Sundberg, H., McGrew, S., Nakayama, K., Kyriakides, T.R., and Roberts, J.M. (2001). A mouse knock-in model exposes sequential proteolytic pathways that regulate p27 in G1 and S phase. Nature *413*, 323-327.

Malliri, A., and Collard, J.G. (2003). Role of Rho-family proteins in cell adhesion and cancer. Curr Opin Cell Biol *15*, 583-589.

Mammoto, A., Huang, S., Moore, K., Oh, P., and Ingber, D.E. (2004). Role of RhoA, mDia, and ROCK in cell shape-dependent control of the Skp2-p27 pathway and the G1/S transition. J Biol Chem *279*, 26323-26330.

Manser, E., Huang, H.Y., Loo, T.H., Chen, X.Q., Dong, J.M., Leung, T., and Lim, L. (1997). Expression of constitutively active alpha-PAK reveals effects of the kinase on actin and focal complexes. Mol Cell Biol *17*, 1129-1143.

Marin-Padilla, M. (1978). Dual origin of the mammalian neocortex and evolution of the cortical plate. Anat Embryol (Berl) *152*, 109-126.

Marin, O., Valdeolmillos, M., and Moya, F. (2006). Neurons in motion: same principles for different shapes? Trends Neurosci *29*, 655-661.

Marston, S. (1995). Ca(2+)-dependent protein switches in actomyosin based contractile systems. Int J Biochem Cell Biol *27*, 97-108.

Matsui, T., Amano, M., Yamamoto, T., Chihara, K., Nakafuku, M., Ito, M., Nakano, T., Okawa, K., Iwamatsu, A., and Kaibuchi, K. (1996). Rho-associated kinase, a novel serine/threonine kinase, as a putative target for small GTP binding protein Rho. Embo J *15*, 2208-2216.

Mcallister, S.S., Becker-hapak, M., Pintucci, G., Pagano, M., and Dowdy, S.F. (2003). Novel p27 kip1 C-Terminal Scatter Domain Mediates Rac-Dependent Cell Migration Independent of Cell Cycle Arrest Functions. Society *23*, 216-228.

McClellan, K.A., and Slack, R.S. (2006). Novel functions for cell cycle genes in nervous system development. Cell Cycle *5*, 1506-1513.

McConnell, S.K., and Kaznowski, C.E. (1991). Cell cycle dependence of laminar determination in developing neocortex. Science *254*, 282-285.

Mettouchi, A., Klein, S., Guo, W., Lopez-Lago, M., Lemichez, E., Westwick, J.K., and Giancotti, F.G. (2001). Integrin-specific activation of Rac controls progression through the G(1) phase of the cell cycle. Mol Cell *8*, 115-127.

Meyer, E.J., Ikmi, A., and Gibson, M.C. (2011). Interkinetic nuclear migration is a broadly conserved feature of cell division in pseudostratified epithelia. Curr Biol *21*, 485-491.

Meyer, G., Schaaps, J.P., Moreau, L., and Goffinet, A.M. (2000). Embryonic and early fetal development of the human neocortex. J Neurosci *20*, 1858-1868.

Miki, H., Suetsugu, S., and Takenawa, T. (1998). WAVE, a novel WASP-family protein involved in actin reorganization induced by Rac. Embo J *17*, 6932-6941.

Miller, M.W. (1985). Cogeneration of retrogradely labeled corticocortical projection and GABA-immunoreactive local circuit neurons in cerebral cortex. Brain Res *355*, 187-192.

Mimori-Kiyosue, Y., and Tsukita, S. (2003). "Search-and-capture" of microtubules through plus-end-binding proteins (+TIPs). J Biochem *134*, 321-326.

Mitsuhashi, T., Aoki, Y., Eksioglu, Y.Z., Takahashi, T., Bhide, P.G., Reeves, S.A., and Caviness, V.S., Jr. (2001). Overexpression of p27 lengthens the G1 phase in a mouse model that targets inducible gene expression to central nervous system progenitor cells. Proc Natl Acad Sci U S A *98*, 6435-6440.

Miyata, T. (2008). Development of three-dimensional architecture of the neuroepithelium: role of pseudostratification and cellular 'community'. Dev Growth Differ *50 Suppl 1*, S105-112.

Miyata, T., Kawaguchi, A., Okano, H., and Ogawa, M. (2001). Asymmetric inheritance of radial glial fibres by cortical neurons. Neuron *31*, 727-741.

Miyata, T., Kawaguchi, A., Saito, K., Kawano, M., Muto, T., and Ogawa, M. (2004). Asymmetric production of surface-dividing and non-surface-dividing cortical progenitor cells. Development *131*, 3133-3145.

Mizutani, K., Yoon, K., Dang, L., Tokunaga, A., and Gaiano, N. (2007). Differential Notch signalling distinguishes neural stem cells from intermediate progenitors. Nature *449*, 351-355.

Molnar, Z., and Cheung, A.F. (2006). Towards the classification of subpopulations of layer V pyramidal projection neurons. Neurosci Res *55*, 105-115.

Molnar, Z., Metin, C., Stoykova, A., Tarabykin, V., Price, D.J., Francis, F., Meyer, G., Dehay, C., and Kennedy, H. (2006). Comparative aspects of cerebral cortical development. Eur J Neurosci *23*, 921-934.

Molnar, Z., Vasistha, N.A., and Garcia-Moreno, F. (2011). Hanging by the tail: progenitor populations proliferate. Nat Neurosci *14*, 538-540.

Montero, V.M. (1990). Quantitative immunogold analysis reveals high glutamate levels in synaptic terminals of retino-geniculate, cortico-geniculate, and geniculo-cortical axons in the cat. Vis Neurosci *4*, 437-443.

Moon, S.Y., and Zheng, Y. (2003). Rho GTPase-activating proteins in cell regulation. Trends Cell Biol *13*, 13-22.

Moore, K.A., Sethi, R., Doanes, A.M., Johnson, T.M., Pracyk, J.B., Kirby, M., Irani, K., Goldschmidt-Clermont, P.J., and Finkel, T. (1997). Rac1 is required for cell proliferation and G2/M progression. Biochem J *326 (Pt 1)*, 17-20.

Morin, X., Jaouen, F., and Durbec, P. (2007). Control of planar divisions by the G-protein regulator LGN maintains progenitors in the chick neuroepithelium. Nature neuroscience *10*, 1440-1448.

Morris, N.R., Efimov, V.P., and Xiang, X. (1998). Nuclear migration, nucleokinesis and lissencephaly. Trends Cell Biol *8*, 467-470.

Mummery, C.L., van den Brink, C.E., and de Laat, S.W. (1987). Commitment to differentiation induced by retinoic acid in P19 embryonal carcinoma cells is cell cycle dependent. Dev Biol *121*, 10-19.

Munoz-Alonso, M.J., Acosta, J.C., Richard, C., Delgado, M.D., Sedivy, J., and Leon, J. (2005). p21Cip1 and p27 induce distinct cell cycle effects and differentiation programs in myeloid leukemia cells. J Biol Chem *280*, 18120-18129.

Murciano, A., Zamora, J., Lopez-Sanchez, J., and Frade, J.M. (2002). Interkinetic nuclear movement may provide spatial clues to the regulation of neurogenesis. Mol Cell Neurosci *21*, 285-300.

Murray, A.W. (2004). Recycling the cell cycle: cyclins revisited. Cell *116*, 221-234.

Murthy, K., and Wadsworth, P. (2005). Myosin-II-dependent localization and dynamics of F-actin during cytokinesis. Curr Biol *15*, 724-731.

Nadarajah, B. (2003). Radial glia and somal translocation of radial neurons in the developing cerebral cortex. Glia *43*, 33-36.

Nadarajah, B., Alifragis, P., Wong, R.O., and Parnavelas, J.G. (2003). Neuronal migration in the developing cerebral cortex: observations based on real-time imaging. Cereb Cortex *13*, 607-611.

Nadarajah, B., Brunstrom, J.E., Grutzendler, J., Wong, R.O., and Pearlman, A.L. (2001). Two modes of radial migration in early development of the cerebral cortex. Nat Neurosci *4*, 143-150.

Nadarajah, B., and Parnavelas, J.G. (2002). Modes of neuronal migration in the developing cerebral cortex. Nat Rev Neurosci *3*, 423-432.

Nagahara, H., Vocero-Akbani, A.M., Snyder, E.L., Ho, A., Latham, D.G., Lissy, N.A., Becker-Hapak, M., Ezhevsky, S.A., and Dowdy, S.F. (1998). Transduction of full-length TAT fusion proteins into mammalian cells: TAT-p27 induces cell migration. Nat Med *4*, 1449-1452.

Nakajima, K. (2007). Control of tangential/non-radial migration of neurons in the developing cerebral cortex. Neurochemistry international *51*, 121-131.

Nakamura, T., Aoki, K., and Matsuda, M. (2005). Monitoring spatio-temporal regulation of Ras and Rho GTPase with GFP-based FRET probes. Methods *37*, 146-153.

Nakayama, K., Ishida, N., Shirane, M., Inomata, A., Inoue, T., Shishido, N., Horii, I., and Loh, D.Y. (1996). Mice lacking p27(Kip1) display increased body size, multiple organ hyperplasia, retinal dysplasia, and pituitary tumors. Cell *85*, 707-720.

Nakayama, K.I., and Nakayama, K. (2006). Ubiquitin ligases: cell-cycle control and cancer. Nat Rev Cancer *6*, 369-381.

Narumiya, S., Ishizaki, T., and Uehata, M. (2000). Use and properties of ROCK-specific inhibitor Y-27632. Methods Enzymol *325*, 273-284.

Narumiya, S., Tanji, M., and Ishizaki, T. (2009). Rho signaling, ROCK and mDia1, in transformation, metastasis and invasion. Cancer Metastasis Rev *28*, 65-76.

Narumiya, S., and Yasuda, S. (2006). Rho GTPases in animal cell mitosis. Curr Opin Cell Biol *18*, 199-205.

Nguyen, L., Besson, A., Heng, J.I.-T., Schuurmans, C., Teboul, L., Parras, C., Philpott, A., Roberts, J.M., and Guillemot, F. (2006a). P27 Independently Promotes Neuronal Differentiation and Migration in the Cerebral Cortex. Genes & development *20*, 1511-1524.

Nguyen, L., Besson, A., Roberts, J.M., and Guillemot, F. (2006b). Coupling Cell Cycle Exit, Neuronal Differentiation and Migration in Cortical Neurogenesis. Cell Cycle *5*.

Niwa, H., Burdon, T., Chambers, I., and Smith, A. (1998). Self-renewal of pluripotent embryonic stem cells is mediated via activation of STAT3. Genes Dev *12*, 2048-2060.

Nobes, C.D., and Hall, A. (1999). Rho GTPases control polarity, protrusion, and adhesion during cell movement. J Cell Biol *144*, 1235-1244.

Noctor, S.C., Flint, A.C., Weissman, T.A., Dammerman, R.S., and Kriegstein, A.R. (2001). Neurons derived from radial glial cells establish radial units in neocortex. Nature *409*, 714-720.

Noctor, S.C., Martinez-Cerdeno, V., Ivic, L., and Kriegstein, A.R. (2004). Cortical neurons arise in symmetric and asymmetric division zones and migrate through specific phases. Nat Neurosci *7*, 136-144.

Noctor, S.C., Martinez-Cerdeno, V., and Kriegstein, A.R. (2008). Distinct behaviors of neural stem and progenitor cells underlie cortical neurogenesis. J Comp Neurol *508*, 28-44.

Norden, C., Young, S., Link, B.A., and Harris, W.A. (2009). Actomyosin is the main driver of interkinetic nuclear migration in the retina. Cell *138*, 1195-1208.

Nourse, J., Firpo, E., Flanagan, W.M., Coats, S., Polyak, K., Lee, M.H., Massague, J., Crabtree, G.R., and Roberts, J.M. (1994). Interleukin-2-mediated elimination of the p27 cyclin-dependent kinase inhibitor prevented by rapamycin. Nature *372*, 570-573.

Ohnuma, S., Philpott, A., and Harris, W.A. (2001). Cell cycle and cell fate in the nervous system. Current opinion in neurobiology *11*, 66-73.

Ohnuma, S., Philpott, A., Wang, K., Holt, C.E., and Harris, W.A. (1999). p27Xic1, a Cdk inhibitor, promotes the determination of glial cells in Xenopus retina. Cell *99*, 499-510.

Okada, Y., and Hirokawa, N. (1999). A processive single-headed motor: kinesin superfamily protein KIF1A. Science *283*, 1152-1157.

Olenik, C., Aktories, K., and Meyer, D.K. (1999). Differential expression of the small GTP-binding proteins RhoA, RhoB, Cdc42u and Cdc42b in developing rat neocortex. Brain Res Mol Brain Res *70*, 9-17.

Olson, M.F., Ashworth, A., and Hall, A. (1995). An essential role for Rho, Rac, and Cdc42 GTPases in cell cycle progression through G1. Science *269*, 1270-1272.

Olson, M.F., Paterson, H.F., and Marshall, C.J. (1998). Signals from Ras and Rho GTPases interact to regulate expression of p21Waf1/Cip1. Nature *394*, 295-299.

Owens, D.F., and Kriegstein, A.R. (1998). Patterns of intracellular calcium fluctuation in precursor cells of the neocortical ventricular zone. J Neurosci *18*, 5374-5388.

Oyamada, M., Oyamada, Y., and Takamatsu, T. (2005). Regulation of connexin expression. Biochim Biophys Acta *1719*, 6-23.

Pacary, E., Heng, J., Azzarelli, R., Riou, P., Castro, D., Lebel-Potter, M., Parras, C., Bell, D.M., Ridley, A.J., Parsons, M.*, et al.* (2011). Proneural transcription factors regulate different steps of cortical neuron migration through Rnd-mediated inhibition of RhoA signaling. Neuron *69*, 1069-1084.

Pagano, M., Tam, S.W., Theodoras, A.M., Beer-Romero, P., Del Sal, G., Chau, V., Yew, P.R., Draetta, G.F., and Rolfe, M. (1995). Role of the ubiquitin-proteasome pathway in regulating abundance of the cyclin-dependent kinase inhibitor p27. Science *269*, 682-685.

Palazzo, A.F., Cook, T.A., Alberts, A.S., and Gundersen, G.G. (2001). mDia mediates Rho-regulated formation and orientation of stable microtubules. Nat Cell Biol *3*, 723-729.

Parras, C.M., Schuurmans, C., Scardigli, R., Kim, J., Anderson, D.J., and Guillemot, F. (2002). Divergent functions of the proneural genes Mash1 and Ngn2 in the specification of neuronal subtype identity. Genes Dev *16*, 324-338.

Paschal, B.M., Shpetner, H.S., and Vallee, R.B. (1987). MAP 1C is a microtubule-activated ATPase which translocates microtubules in vitro and has dynein-like properties. J Cell Biol *105*, 1273-1282.

Pearlman, A.L., and Sheppard, A.M. (1996). Extracellular matrix in early cortical development. Prog Brain Res *108*, 117-134.

Pearson, R.A., Luneborg, N.L., Becker, D.L., and Mobbs, P. (2005). Gap junctions modulate interkinetic nuclear movement in retinal progenitor cells. J Neurosci *25*, 10803-10814.

Pertz, O. (2010). Spatio-temporal Rho GTPase signaling - where are we now? Journal of cell science *123*, 1841-1850.

Petanjek, Z., Kostovic, I., and Esclapez, M. (2009). Primate-specific origins and migration of cortical GABAergic neurons. Front Neuroanat *3*, 26.

Peters and Jones (1985). Cerebral cortex, comparative structure and evolution of cerebral cortex, Part 1. *8A*.

Philipp-Staheli, J., Payne, S.R., and Kemp, C.J. (2001). p27(Kip1): regulation and function of a haploinsufficient tumor suppressor and its misregulation in cancer. Exp Cell Res *264*, 148-168.

Pilaz, L.J., Patti, D., Marcy, G., Ollier, E., Pfister, S., Douglas, R.J., Betizeau, M., Gautier, E., Cortay, V., Doerflinger, N.*, et al.*(2009). Forced G1-phase reduction alters mode of division, neuron number, and laminar phenotype in the cerebral cortex. Proc Natl Acad Sci U S A *106*, 21924-21929.

Polleux, F., Dehay, C., Goffinet, A., and Kennedy, H. (2001). Pre- and post-mitotic events contribute to the progressive acquisition of area-specific connectional fate in the neocortex. Cereb Cortex *11*, 1027-1039.

Polleux, F., Dehay, C., and Kennedy, H. (1997a). The timetable of laminar neurogenesis contributes to the specification of cortical areas in mouse isocortex. J Comp Neurol *385*, 95-116.

Polleux, F., Dehay, C., Moraillon, B., and Kennedy, H. (1997b). Regulation of neuroblast cell-cycle kinetics plays a crucial role in the generation of unique features of neocortical areas. J Neurosci *17*, 7763-7783.

Polyak, K., Lee, M.H., Erdjument-Bromage, H., Koff, A., Roberts, J.M., Tempst, P., and Massague, J. (1994). Cloning of p27, a cyclin-dependent kinase inhibitor and a potential mediator of extracellular antimitogenic signals. Cell *78*, 59-66.

Ponce-Castaneda, M.V., Lee, M.H., Latres, E., Polyak, K., Lacombe, L., Montgomery, K., Mathew, S., Krauter, K., Sheinfeld, J., Massague, J*., et al.* (1995). p27: chromosomal mapping to 12p12-12p13.1 and absence of mutations in human tumors. Cancer Res *55*, 1211-1214.

Quinn, J.C., Molinek, M., Martynoga, B.S., Zaki, P.A., Faedo, A., Bulfone, A., Hevner, R.F., West, J.D., and Price, D.J. (2007). Pax6 controls cerebral cortical cell number by regulating exit from the cell cycle and specifies cortical cell identity by a cell autonomous mechanism. Dev Biol *302*, 50-65.

Rakic, P. (1971). Guidance of neurons migrating to the fetal monkey neocortex. Brain Res *33*, 471-476.

Rakic, P. (1972). Mode of cell migration to the superficial layers of fetal monkey neocortex. J Comp Neurol *145*, 61-83.

Rakic, P. (1974). Neurons in rhesus monkey visual cortex: systematic relation between time of origin and eventual disposition. Science *183*, 425-427.

Rakic, P. (1978). Neuronal migration and contact guidance in the primate telencephalon. Postgrad Med J *54 Suppl 1*, 25-40.

Rakic, P. (1988). Specification of cerebral cortical areas. Science *241*, 170-176.

Rakic, P. (1995). A small step for the cell, a giant leap for mankind: a hypothesis of neocortical expansion during evolution. Trends Neurosci *18*, 383-388.

Rakic, P. (2005). Vive la difference! Neuron *47*, 323-325.

Rash, B.G., and Grove, E.A. (2006). Area and layer patterning in the developing cerebral cortex. Current opinion in neurobiology *16*, 25-34.

Reiner, O., Sapir, T., and Gerlitz, G. (2011). Interkinetic Nuclear Movement in the Ventricular Zone of the Cortex. J Mol Neurosci.

Reinsch, S., and Gonczy, P. (1998). Mechanisms of nuclear positioning. Journal of cell science *111 (Pt 16)*, 2283-2295.

Ren, X.D., Kiosses, W.B., and Schwartz, M.A. (1999). Regulation of the small GTP-binding protein Rho by cell adhesion and the cytoskeleton. Embo J *18*, 578-585.

Reynaud, E.G., Leibovitch, M.P., Tintignac, L.A., Pelpel, K., Guillier, M., and Leibovitch, S.A. (2000). Stabilization of MyoD by direct binding to p57(Kip2). J Biol Chem *275*, 18767-18776.

Reynisdottir, I., Polyak, K., Iavarone, A., and Massague, J. (1995). Kip/Cip and Ink4 Cdk inhibitors cooperate to induce cell cycle arrest in response to TGF-beta. Genes Dev *9*, 1831-1845.

Reznikov, K., Acklin, S.E., and van der Kooy, D. (1997). Clonal heterogeneity in the early embryonic rodent cortical germinal zone and the separation of subventricular from ventricular zone lineages. Dev Dyn *210*, 328-343.

Ridley, A.J., Schwartz, M.A., Burridge, K., Firtel, R.A., Ginsberg, M.H., Borisy, G., Parsons, J.T., and Horwitz, A.R. (2003). Cell migration: integrating signals from front to back. Science *302*, 1704-1709.

Riento, K., and Ridley, A.J. (2003). Rocks: multifunctional kinases in cell behaviour. Nat Rev Mol Cell Biol *4*, 446-456.

Rockel, A.J., Hiorns, R.W., and Powell, T.P. (1980). The basic uniformity in structure of the neocortex. Brain *103*, 221-244.

Rodier, G., Montagnoli, A., Di Marcotullio, L., Coulombe, P., Draetta, G.F., Pagano, M., and Meloche, S. (2001). p27 cytoplasmic localization is regulated by phosphorylation on Ser10 and is not a prerequisite for its proteolysis. Embo J *20*, 6672-6682.

Roovers, K., and Assoian, R.K. (2000). Integrating the MAP kinase signal into the G1 phase cell cycle machinery. Bioessays *22*, 818-826.

Roovers, K., and Assoian, R.K. (2003). Effects of rho kinase and actin stress fibres on sustained extracellular signal-regulated kinase activity and activation of G(1) phase cyclin-dependent kinases. Mol Cell Biol *23*, 4283-4294.

Roovers, K., Klein, E.A., Castagnino, P., and Assoian, R.K. (2003). Nuclear translocation of LIM kinase mediates Rho-Rho kinase regulation of cyclin D1 expression. Developmental cell *5*, 273-284.

Rosenblatt, J., Cramer, L.P., Baum, B., and McGee, K.M. (2004). Myosin II-dependent cortical movement is required for centrosome separation and positioning during mitotic spindle assembly. Cell *117*, 361-372.

Ross, J.L., Ali, M.Y., and Warshaw, D.M. (2008). Cargo transport: molecular motors navigate a complex cytoskeleton. Curr Opin Cell Biol *20*, 41-47.

Russo, A.A., Jeffrey, P.D., Patten, A.K., Massague, J., and Pavletich, N.P. (1996). Crystal structure of the p27 cyclin-dependent-kinase inhibitor bound to the cyclin A-Cdk2 complex. Nature *382*, 325-331.

Sahai, E., and Marshall, C.J. (2003). Differing modes of tumour cell invasion have distinct requirements for Rho/ROCK signalling and extracellular proteolysis. Nat Cell Biol *5*, 711-719.

Sahai, E., Olson, M.F., and Marshall, C.J. (2001). Cross-talk between Ras and Rho signalling pathways in transformation favours proliferation and increased motility. Embo J *20*, 755-766.

Sakaue-Sawano, A., Kurokawa, H., Morimura, T., Hanyu, A., Hama, H., Osawa, H., Kashiwagi, S., Fukami, K., Miyata, T., Miyoshi, H*., et al.* (2008). Visualizing spatiotemporal dynamics of multicellular cell-cycle progression. Cell *132*, 487-498.

Sansom, S.N., Griffiths, D.S., Faedo, A., Kleinjan, D.J., Ruan, Y., Smith, J., van Heyningen, V., Rubenstein, J.L., and Livesey, F.J. (2009). The level of the transcription factor Pax6 is essential for controlling the balance between neural stem cell self-renewal and neurogenesis. PLoS Genet *5*, e1000511.

Sasaki, K., Tamura, S., Tachibana, H., Sugita, M., Gao, Y., Furuyama, J., Kakishita, E., Sakai, T., Tamaoki, T., and Hashimoto-Tamaoki, T. (2000). Expression and role of p27(kip1) in neuronal differentiation of embryonal carcinoma cells. Brain Res Mol Brain Res *77*, 209-221.

Sauer, F. (1935). Mitosis in the neural tube. J Comp Neurol, 377–405.

Sauer, M.E., and Walker, B.E. (1959). Radioautographic study of interkinetic nuclear migration in the neural tube. Proc Soc Exp Biol Med *101*, 557-560.

Schaar, B.T., and McConnell, S.K. (2005). Cytoskeletal coordination during neuronal migration. Proc Natl Acad Sci U S A *102*, 13652-13657.

Schaper A (1897). The earliest differentiatian in the central nervous system of the vertebrates. Science 430–431.

Schatz, C.A., Santarella, R., Hoenger, A., Karsenti, E., Mattaj, I.W., Gruss, O.J., and Carazo-Salas, R.E. (2003). Importin alpha-regulated nucleation of microtubules by TPX2. Embo J *22*, 2060-2070.

Schenk, J., Wilsch-Brauninger, M., Calegari, F., and Huttner, W.B. (2009). Myosin II is required for interkinetic nuclear migration of neural progenitors. Proc Natl Acad Sci U S A *106*, 16487-16492.

Schmechel, D.E., Rakic, P. (1979). A Golgi study of radial glial cells in developing monkey telencephalon:morphogenesis and transformation into astrocytes. Anat Embryol (Berl)Jun 5;156(2):115-52.

Schmidt, A., and Hall, A. (2002). Guanine nucleotide exchange factors for Rho GTPases: turning on the switch. Genes Dev *16*, 1587-1609.

Schuurmans, C., Armant, O., Nieto, M., Stenman, J.M., Britz, O., Klenin, N., Brown, C., Langevin, L.M., Seibt, J., Tang, H.*, et al.* (2004). Sequential phases of cortical specification involve Neurogenin-dependent and -independent pathways. Embo J *23*, 2892-2902.

Sessa, A., Mao, C.A., Hadjantonakis, A.K., Klein, W.H., and Broccoli, V. (2008). Tbr2 directs conversion of radial glia into basal precursors and guides neuronal amplification by indirect neurogenesis in the developing neocortex. Neuron *60*, 56-69.

Sheaff, R.J., Groudine, M., Gordon, M., Roberts, J.M., and Clurman, B.E. (1997). Cyclin E-CDK2 is a regulator of p27. Genes Dev *11*, 1464-1478.

Shen, Q., Wang, Y., Dimos, J.T., Fasano, C.A., Phoenix, T.N., Lemischka, I.R., Ivanova, N.B., Stifani, S., Morrisey, E.E., and Temple, S. (2006). The timing of cortical neurogenesis is encoded within lineages of individual progenitor cells. Nat Neurosci *9*, 743-751.

Sherr, C.J., and Roberts, J.M. (1999). CDK inhibitors: positive and negative regulators of G1-phase progression. Genes Dev *13*, 1501-1512.

Shin, I., Yakes, F.M., Rojo, F., Shin, N.Y., Bakin, A.V., Baselga, J., and Arteaga, C.L. (2002). PKB/Akt mediates cell-cycle progression by phosphorylation of p27(Kip1) at threonine 157 and modulation of its cellular localization. Nat Med *8*, 1145-1152.

Shitamukai, A., Konno, D., and Matsuzaki, F. (2011). Oblique radial glial divisions in the developing mouse neocortex induce self-renewing progenitors outside the germinal zone that resemble primate outer subventricular zone progenitors. J Neurosci *31*, 3683-3695.

Shu, T., Ayala, R., Nguyen, M.D., Xie, Z., Gleeson, J.G., and Tsai, L.H. (2004). Ndel1 operates in a common pathway with LIS1 and cytoplasmic dynein to regulate cortical neuronal positioning. Neuron *44*, 263-277.

Sidman, R.L., Miale, I.L., and Feder, N. (1959). Cell proliferation and migration in the primitive ependymal zone: an autoradiographic study of histogenesis in the nervous system. Experimental neurology *1*, 322-333.

Sidman, R.L., and Rakic, P. (1973). Neuronal migration, with special reference to developing human brain: a review. Brain Res *62*, 1-35.

Skoglund, T.S., Pascher, R., and Berthold, C.H. (1996). Heterogeneity in the columnar number of neurons in different neocortical areas in the rat. Neuroscience letters *208*, 97-100.

Slingerland, J., and Pagano, M. (2000). Regulation of the cdk inhibitor p27 and its deregulation in cancer. J Cell Physiol *183*, 10-17.

Slingerland, J.M., Hengst, L., Pan, C.H., Alexander, D., Stampfer, M.R., and Reed, S.I. (1994). A novel inhibitor of cyclin-Cdk activity detected in transforming growth factor beta-arrested epithelial cells. Mol Cell Biol *14*, 3683-3694.

Smart, I.H. (1973). Proliferative characteristics of the ependymal layer during the early development of the mouse neocortex: a pilot study based on recording the number, location and plane of cleavage of mitotic figures. Journal of anatomy *116*, 67-91.

Smart, I.H. (1984). Histogenesis of the mesocortical area of the mouse telencephalon. Journal of anatomy *138 (Pt 3)*, 537-552.

Smart, I.H., Dehay, C., Giroud, P., Berland, M., and Kennedy, H. (2002). Unique morphological features of the proliferative zones and postmitotic compartments of the neural epithelium giving rise to striate and extrastriate cortex in the monkey. Cereb Cortex 12, 37-53.

Smith, D.S., Niethammer, M., Ayala, R., Zhou, Y., Gambello, M.J., Wynshaw-Boris, A., and Tsai, L.H. (2000). Regulation of cytoplasmic dynein behaviour and microtubule organization by mammalian Lis1. Nat Cell Biol *2*, 767-775.

Solecki, D.J., Model, L., Gaetz, J., Kapoor, T.M., and Hatten, M.E. (2004). Par6alpha signaling controls glial-guided neuronal migration. Nat Neurosci *7*, 1195-1203.

Solecki, D.J., Trivedi, N., Govek, E.E., Kerekes, R.A., Gleason, S.S., and Hatten, M.E. (2009). Myosin II motors and F-actin dynamics drive the coordinated movement of the centrosome and soma during CNS glial-guided neuronal migration. Neuron *63*, 63-80.

Srayko, M., Quintin, S., Schwager, A., and Hyman, A.A. (2003). Caenorhabditis elegans TAC-1 and ZYG-9 form a complex that is essential for long astral and spindle microtubules. Curr Biol *13*, 1506-1511.

Stancik, E.K., Navarro-Quiroga, I., Sellke, R., and Haydar, T.F. (2010). Heterogeneity in ventricular zone neural precursors contributes to neuronal fate diversity in the postnatal neocortex. J Neurosci *30*, 7028-7036.

Starr, D.A., and Fischer, J.A. (2005). KASH 'n Karry: the KASH domain family of cargo-specific cytoskeletal adaptor proteins. Bioessays *27*, 1136-1146.

Starr, D.A., and Han, M. (2003). ANChors away: an actin based mechanism of nuclear positioning. Journal of cell science *116*, 211-216.

Sun, J., Marx, S.O., Chen, H.J., Poon, M., Marks, A.R., and Rabbani, L.E. (2001). Role for p27(Kip1) in Vascular Smooth Muscle Cell Migration. Circulation *103*, 2967-2972.

Supriatno, Harada, K., Kawaguchi, S., Yoshida, H., and Sato, M. (2003). Effect of p27 on the ability of invasion and metastasis of an oral cancer cell line. Oncol Rep *10*, 527-532.

Sutterluty, H., Chatelain, E., Marti, A., Wirbelauer, C., Senften, M., Muller, U., and Krek, W. (1999). p45SKP2 promotes p27 degradation and induces S phase in quiescent cells. Nat Cell Biol *1*, 207-214.

Swant, J.D., Rendon, B.E., Symons, M., and Mitchell, R.A. (2005). Rho GTPase-dependent signaling is required for macrophage migration inhibitory factor-mediated expression of cyclin D1. J Biol Chem *280*, 23066-23072.

Tabata, H., and Nakajima, K. (2003). Multipolar migration: the third mode of radial neuronal migration in the developing cerebral cortex. J Neurosci *23*, 9996-10001.

Takahashi, T., Bhide, P.G., Goto, T., Miyama, S., and Caviness, V.S., Jr. (1999). Proliferative behavior of the murine cerebral wall in tissue culture: cell cycle kinetics and checkpoints. Experimental neurology *156*, 407-417.

Takahashi, T., Nowakowski, R.S., and Caviness, V.S., Jr. (1993). Cell cycle parameters and patterns of nuclear movement in the neocortical proliferative zone of the fetal mouse. J Neurosci *13*, 820-833.

Takahashi, T., Nowakowski, R.S., and Caviness, V.S., Jr. (1995a). The cell cycle of the pseudostratified ventricular epithelium of the embryonic murine cerebral wall. J Neurosci *15*, 6046-6057.

Takahashi, T., Nowakowski, R.S., and Caviness, V.S., Jr. (1995b). Early ontogeny of the secondary proliferative population of the embryonic murine cerebral wall. J Neurosci *15*, 6058-6068.

Takahashi, T., Nowakowski, R.S., and Caviness, V.S., Jr. (1996). Interkinetic and migratory behavior of a cohort of neocortical neurons arising in the early embryonic murine cerebral wall. J Neurosci *16*, 5762-5776.

Tamai, H., Shinohara, H., Miyata, T., Saito, K., Nishizawa, Y., Nomura, T., and Osumi, N. (2007). Pax6 transcription factor is required for the interkinetic nuclear movement of neuroepithelial cells. Genes Cells *12*, 983-996.

Tanaka, H., Yamashita, T., Asada, M., Mizutani, S., Yoshikawa, H., and Tohyama, M. (2002). Cytoplasmic p21(Cip1/WAF1) regulates neurite remodeling by inhibiting Rho-kinase activity. J Cell Biol *158*, 321-329.

Tanaka, T., Serneo, F.F., Higgins, C., Gambello, M.J., Wynshaw-Boris, A., and Gleeson, J.G. (2004). Lis1 and doublecortin function with dynein to mediate coupling of the nucleus to the centrosome in neuronal migration. J Cell Biol *165*, 709-721.

Tarui, T., Takahashi, T., Nowakowski, R.S., Hayes, N.L., Bhide, P.G., and Caviness, V.S. (2005). Overexpression of p27 Kip 1, probability of cell cycle exit, and laminar destination of neocortical neurons. Cereb Cortex *15*, 1343-1355.

Taverna, E., and Huttner, W.B. (2010). Neural progenitor nuclei IN motion. Neuron *67*, 906-914.

Tokumoto, M., Tsuruya, K., Fukuda, K., Kanai, H., Kuroki, S., and Hirakata, H. (2002). Reduced p21, p27 and vitamin D receptor in the nodular hyperplasia in patients with advanced secondary hyperparathyroidism. Kidney Int *62*, 1196-1207.

Toyoshima, H., and Hunter, T. (1994). p27, a novel inhibitor of G1 cyclin-Cdk protein kinase activity, is related to p21. Cell *78*, 67-74.

Tran, P.T., Marsh, L., Doye, V., Inoue, S., and Chang, F. (2001). A mechanism for nuclear positioning in fission yeast based on microtubule pushing. J Cell Biol *153*, 397-411.

Tsai, J.W., Bremner, K.H., and Vallee, R.B. (2007). Dual subcellular roles for LIS1 and dynein in radial neuronal migration in live brain tissue. Nat Neurosci *10*, 970-979.

Tsai, J.W., Chen, Y., Kriegstein, A.R., and Vallee, R.B. (2005). LIS1 RNA interference blocks neural stem cell division, morphogenesis, and motility at multiple stages. J Cell Biol *170*, 935-945.

Tsai, J.W., Lian, W.N., Kemal, S., Kriegstein, A.R., and Vallee, R.B. (2010). Kinesin 3 and cytoplasmic dynein mediate interkinetic nuclear migration in neural stem cells. Nat Neurosci *13*, 1463-1471.

Tsai, L.H., and Gleeson, J.G. (2005). Nucleokinesis in neuronal migration. Neuron *46*, 383-388.

Tsvetkov, L.M., Yeh, K.H., Lee, S.J., Sun, H., and Zhang, H. (1999). p27(Kip1) ubiquitination and degradation is regulated by the SCF(Skp2) complex through phosphorylated Thr187 in p27. Curr Biol *9*, 661-664.

Uehata, M., Ishizaki, T., Satoh, H., Ono, T., Kawahara, T., Morishita, T., Tamakawa, H., Yamagami, K., Inui, J., Maekawa, M*., et al.* (1997). Calcium sensitization of smooth muscle mediated by a Rho-associated protein kinase in hypertension. Nature *389*, 990-994.

Ueno, M., Katayama, K., Yamauchi, H., Nakayama, H., and Doi, K. (2006). Cell cycle progression is required for nuclear migration of neural progenitor cells. Brain Res *1088*, 57-67.

Vallee, R.B., Seale, G.E., and Tsai, J.W. (2009). Emerging roles for myosin II and cytoplasmic dynein in migrating neurons and growth cones. Trends Cell Biol *19*, 347-355.

Vallee, R.B., Tai, C., and Faulkner, N.E. (2001). LIS1: cellular function of a disease-causing gene. Trends Cell Biol *11*, 155-160.

Vernon, A.E., Devine, C., and Philpott, A. (2003). The cdk inhibitor p27Xic1 is required for differentiation of primary neurones in Xenopus. Development *130*, 85-92.

Vicente-Manzanares, M., Ma, X., Adelstein, R.S., and Horwitz, A.R. (2009). Non-muscle myosin II takes centre stage in cell adhesion and migration. Nat Rev Mol Cell Biol *10*, 778-790.

Vidal, A., Millard, S.S., Miller, J.P., and Koff, A. (2002). Rho activity can alter the translation of p27 mRNA and is important for RasV12-induced transformation in a manner dependent on p27 status. J Biol Chem *277*, 16433-16440.

Viglietto, G., Motti, M.L., Bruni, P., Melillo, R.M., D'Alessio, A., Califano, D., Vinci, F., Chiappetta, G., Tsichlis, P., Bellacosa, A*., et al.* (2002). Cytoplasmic relocalization and inhibition of the cyclin-dependent kinase inhibitor p27(Kip1) by PKB/Akt-mediated phosphorylation in breast cancer. Nat Med *8*, 1136-1144.

Villalonga, P., Guasch, R.M., Riento, K., and Ridley, A.J. (2004). RhoE inhibits cell cycle progression and Ras-induced transformation. Mol Cell Biol *24*, 7829-7840.

Villalonga, P., and Ridley, A.J. (2006). Rho GTPases and cell cycle control. Growth Factors *24*, 159-164.

Vlach, J., Hennecke, S., and Amati, B. (1997). Phosphorylation-dependent degradation of the cyclin-dependent kinase inhibitor p27. Embo J *16*, 5334-5344.

Vreugdenhil, E., Kolk, S.M., Boekhoorn, K., Fitzsimons, C.P., Schaaf, M., Schouten, T., Sarabdjitsingh, A., Sibug, R., and Lucassen, P.J. (2007). Doublecortin-like, a microtubule-associated protein expressed in radial glia, is crucial for neuronal precursor division and radial process stability. Eur J Neurosci *25*, 635-648.

Wang, W.Z., Hoerder-Suabedissen, A., Oeschger, F.M., Bayatti, N., Ip, B.K., Lindsay, S., Supramaniam, V., Srinivasan, L., Rutherford, M., Mollgard, K*., et al.* (2010). Subplate in the developing cortex of mouse and human. Journal of anatomy *217*, 368-380.

Wang, X., Tsai, J.W., LaMonica, B., and Kriegstein, A.R. (2011). A new subtype of progenitor cell in the mouse embryonic neocortex. Nat Neurosci *14*, 555-561.

Wang, X.Q., Lui, E.L., Cai, Q., Ching, W.Y., Liu, K.S., Poon, R.T., and Fan, S.T. (2008). p27 promotes migration of metastatic hepatocellular carcinoma cells. Tumour Biol *29*, 217-223.

Watanabe, N., Madaule, P., Reid, T., Ishizaki, T., Watanabe, G., Kakizuka, A., Saito, Y., Nakao, K., Jockusch, B.M., and Narumiya, S. (1997). p140mDia, a mammalian homolog of Drosophila diaphanous, is a target protein for Rho small GTPase and is a ligand for profilin. Embo J *16*, 3044-3056.

Watanabe, S., Ando, Y., Yasuda, S., Hosoya, H., Watanabe, N., Ishizaki, T., and Narumiya, S. (2008). mDia2 induces the actin scaffold for the contractile ring and stabilizes its position during cytokinesis in NIH 3T3 cells. Mol Biol Cell *19*, 2328-2338.

Watanabe, T., Noritake, J., and Kaibuchi, K. (2005). Regulation of microtubules in cell migration. Trends Cell Biol *15*, 76-83.

Watterson RL, V.P., Bartha A, (1956). Absence of a true germinal zone in neural tubes of young chick embryos as demonstrated by the colchicine technique. Anat Rec 124:379.

Weber, J.D., Hu, W., Jefcoat, S.C., Jr., Raben, D.M., and Baldassare, J.J. (1997). Ras-stimulated extracellular signal-related kinase 1 and RhoA activities coordinate platelet-derived growth factor-induced G1 progression through the independent regulation of cyclin D1 and p27. J Biol Chem *272*, 32966-32971.

Webster, W., and Langman, J. (1978). The effect of cytochalasin B on the neuroepithelial cells of the mouse embryo. Am J Anat *152*, 209-221.

Weissman, T.A., Riquelme, P.A., Ivic, L., Flint, A.C., and Kriegstein, A.R. (2004). Calcium waves propagate through radial glial cells and modulate proliferation in the developing neocortex. Neuron *43*, 647-661.

Welsh, C.F., and Assoian, R.K. (2000). A growing role for Rho family GTPases as intermediaries in growth factor- and adhesion-dependent cell cycle progression. Biochim Biophys Acta *1471*, M21-29.

Welsh, C.F., Roovers, K., Villanueva, J., Liu, Y., Schwartz, M.A., and Assoian, R.K. (2001). Timing of cyclin D1 expression within G1 phase is controlled by Rho. Nat Cell Biol *3*, 950-957.

Whited, J.L., Cassell, A., Brouillette, M., and Garrity, P.A. (2004). Dynactin is required to maintain nuclear position within postmitotic Drosophila photoreceptor neurons. Development *131*, 4677-4686.

Worman, H.J., and Gundersen, G.G. (2006). Here come the SUNs: a nucleocytoskeletal missing link. Trends Cell Biol *16*, 67-69.

Worthylake, R.A., and Burridge, K. (2003). RhoA and ROCK promote migration by limiting membrane protrusions. J Biol Chem *278*, 13578-13584.

Worthylake, R.A., Lemoine, S., Watson, J.M., and Burridge, K. (2001). RhoA is required for monocyte tail retraction during transendothelial migration. J Cell Biol *154*, 147-160.

Wu, F.Y., Wang, S.E., Sanders, M.E., Shin, I., Rojo, F., Baselga, J., and Arteaga, C.L. (2006). Reduction of cytosolic p27(Kip1) inhibits cancer cell motility, survival, and tumorigenicity. Cancer Res *66*, 2162-2172.

Wu, S.X., Goebbels, S., Nakamura, K., Kometani, K., Minato, N., Kaneko, T., Nave, K.A., and Tamamaki, N. (2005). Pyramidal neurons of upper cortical layers generated by NEX-positive progenitor cells in the subventricular zone. Proc Natl Acad Sci U S A *102*, 17172-17177.

Xiang, X., Osmani, A.H., Osmani, S.A., Xin, M., and Morris, N.R. (1995). NudF, a nuclear migration gene in Aspergillus nidulans, is similar to the human LIS-1 gene required for neuronal migration. Mol Biol Cell *6*, 297-310.

Xie, Z., Moy, L.Y., Sanada, K., Zhou, Y., Buchman, J.J., and Tsai, L.H. (2007). Cep120 and TACCs control interkinetic nuclear migration and the neural progenitor pool. Neuron *56*, 79-93.

Xie, Z., Sanada, K., Samuels, B.A., Shih, H., and Tsai, L.H. (2003). Serine 732 phosphorylation of FAK by Cdk5 is important for microtubule organization, nuclear movement, and neuronal migration. Cell *114*, 469-482.

Yamamoto, M., Marui, N., Sakai, T., Morii, N., Kozaki, S., Ikai, K., Imamura, S., and Narumiya, S. (1993). ADP-ribosylation of the rhoA gene product by botulinum C3 exoenzyme causes Swiss 3T3 cells to accumulate in the G1 phase of the cell cycle. Oncogene *8*, 1449-1455.

Yasuda, S., Oceguera-Yanez, F., Kato, T., Okamoto, M., Yonemura, S., Terada, Y., Ishizaki, T., and Narumiya, S. (2004). Cdc42 and mDia3 regulate microtubule attachment to kinetochores. Nature *428*, 767-771.

Yingling, J., Youn, Y.H., Darling, D., Toyo-Oka, K., Pramparo, T., Hirotsune, S., and Wynshaw-Boris, A. (2008). Neuroepithelial stem cell proliferation requires LIS1 for precise spindle orientation and symmetric division. Cell *132*, 474-486.

Yokoo, T., Toyoshima, H., Miura, M., Wang, Y., Iida, K.T., Suzuki, H., Sone, H., Shimano, H., Gotoda, T., Nishimori, S*., et al.* (2003). p57Kip2 regulates actin dynamics by binding and translocating LIM-kinase 1 to the nucleus. J Biol Chem *278*, 52919-52923.

Zalcman, G., Dorseuil, O., Garcia-Ranea, J.A., Gacon, G., and Camonis, J. (1999). RhoGAPs and RhoGDIs, (His)stories of two families. Prog Mol Subcell Biol *22*, 85-113.

Zecevic, N., Chen, Y., and Filipovic, R. (2005). Contributions of cortical subventricular zone to the development of the human cerebral cortex. J Comp Neurol *491*, 109-122.

Zecevic, N., Hu, F., and Jakovcevski, I. (2011). Interneurons in the developing human neocortex. Dev Neurobiol *71*, 18-33.

Zeng, Y., Hirano, K., Hirano, M., Nishimura, J., and Kanaide, H. (2000). Minimal requirements for the nuclear localization of p27(Kip1), a cyclin-dependent kinase inhibitor. Biochem Biophys Res Commun *274*, 37-42.

Zetterberg, A., Larsson, O., and Wiman, K.G. (1995). What is the restriction point? Curr Opin Cell Biol *7*, 835-842.

Zhang, X., Lei, K., Yuan, X., Wu, X., Zhuang, Y., Xu, T., Xu, R., and Han, M. (2009). SUN1/2 and Syne/Nesprin-1/2 complexes connect centrosome to the nucleus during neurogenesis and neuronal migration in mice. Neuron *64*, 173-187.

Zhao, S., and Frotscher, M. (2010). Go or stop? Divergent roles of Reelin in radial neuronal migration. Neuroscientist *16*, 421-434.

Zheng, Y. (2001). Dbl family guanine nucleotide exchange factors. Trends Biochem Sci *26*, 724-732.

Zubler, F., and Douglas, R. (2009). A framework for modeling the growth and development of neurons and networks. Front Comput Neurosci *3*, 25.

Zwaan, J., Bryan, P.R., Jr., and Pearce, T.L. (1969). Interkinetic nuclear migration during the early stages of lens formation in the chicken embryo. J Embryol Exp Morphol *21*, 71-83.